n-76-01
II A-786

Mechanical Vibration and Shock Measurements

BRÜEL & KJÆR

The Application of the Brüel & Kjær Measuring Systems
to

MECHANICAL VIBRATION AND SHOCK MEASUREMENTS

by
Professor, Jens Trampe Broch
Dipl.ing. E.T.H.

Revised Edition
May 1972
Reprint June 1973

CONTENTS

3

4

MECHANICAL VIBRATION AND
SHOCK MEASUREMENTS

INTRODUCTION

Mechanical vibrations and shocks are *dynamic* phenomena, — i.e. their intensity varies with time. Both the maximum intensity, however, and the rate of change in intensity with time, spread over wide measurement ranges and often require highly specialized equipment for their precise determination. Ground motions caused by far-off earthquakes (or explosions) may, for instance, be barely detectable while vibrations caused by large combustion engines can cause severe mechanical fatigue damage.

Although in most cases mechanical shocks and vibrations are undesired byproducts of otherwise useful processes, and great efforts are spent to reduce their effects, some vibrations are produced on purpose. Typical examples are the vibrations produced by conveying and screening machines, mechanical hammers, ultrasonic cleaning baths, etc., while desirable shock-effects are built into riveting hammers and pile-drivers.

As the same methods of description and measurement apply, in general, whether the vibrations or shocks being characterized are wanted or unwanted no clear distinction has been made throughout this book. The various chapters have been laid out with a view mainly to descr;ibe measurement data and techniques necessary to characterize vibrations and shocks and to evaluate their effects on a responding medium. For more comprehensive treatments of theoretical aspects the reader is referred to standard textbooks and to literature cited in the bibliography.

1. PRÉCIS

In this précis it is intended to give a brief extract of the main subjects dealt with in the succeeding chapters. This should allow the more experienced vibration measurement engineer to rapidly find the charts and data that he might need, and help the less experienced engineer to easily find the text that he would want to study a little closer.

Chapter 2 reviews briefly the basic characteristics of mechanical vibra- tions and shocks, and various quantities characterizing their magnitudes are defined. With regard to *stationary vibrations*, periodic as well as random, the most important single quantity to determine is the RMS (root mean square) value, because of its relation to the energy content of the vibrations:

$$X_{RMS} = \sqrt{\frac{1}{T} \int_o^T x^2(t)\, dt}$$

For the characterization of *shocks* there seems to be no single quantity of similar importance although quantities such as the peak acceleration and the total velocity change (acceleration vs. time integral) represent useful and descriptive data. However, it is practically impossible from any of the single quantities mentioned above to predict with reasonable accuracy all the various effects that vibrations and shocks may cause in mechanical systems. To do so additional descriptive means must be utilized, and one of the most powerful methods in use today is the technique of *frequency analysis* (Fourier transformation).

Frequency analysis of *periodic signals* is briefly outlined in section 2.1, and in section 2.2 is shown how the technique can be used to also describe *random vibrations*. While the frequency spectrum of a periodic signal con- sists of discrete harmonically related vibration components which may be characterized by their individual RMS-values, the frequency spectra of random vibrations are continuous and a description is best made in terms of mean square spectral density (power spectral density):

$$w(f) = \lim_{\Delta f \to 0} \lim_{T \to \infty} \frac{1}{\Delta f\, T} \int_o^T x^2_{\Delta f}(t)\, dt$$

Section 2.3 describes how the Fourier transform technique can be applied also to *transient phenomena and shocks*, and some examples of this kind of analysis are shown in Figs. 2.13 and 2.14.

In section 2.4 the description of *nonstationary random vibrations* is briefly discussed and certain types of nonstationarity are exemplified in Fig.2.16. Chapter 3 deals with the response of mechanical systems to vibrations and shocks, and in section 3.1 the response of *linear systems* to deterministic vibrations is discussed. Use is made of the general principle of superposition and the phenomenon of *resonance* is described (Figs.3.3 and 3.4).

Section 3.2 outlines some response properties of *nonlinear systems* and some nonlinear spring characteristics are shown in Fig.3.6. Fig.3.7 illustrates how these kinds of nonlinear springs affect resonances of which they may be part. Typical nonlinear phenomena such as instabilities and the production of subharmonics are also mentioned, and a physical explanation for their occurrence is given.

A brief outline of the theory of rotational and torsional vibrations in lumped parameter systems is presented in section 3.3, stating that while rectilinear motions are governed by force equations rotational motions are governed by torque equations.

In section 3.4 the response of mechanical systems to stationary random vibrations is derived, while section 3.5 deals with shock responses and introduces the concept of *shock response spectra*. This is a rather specific type of "spectrum" and should not be confused with the Fourier spectrum of the forcing shock pulse. Various quantities connected with the shock response spectrum are defined, and a mathematical relationship between the undamped residual shock spectrum and the Fourier spectrum of the shock pulse is given.

Section 3.6 discusses briefly the response of *structures* to mechanical vibrations. It is shown that the response is here no longer a function of time only, but also of space, and a description may best be made in terms of natural modes. While "simple" compressional vibrations (waves) in linear structures can be mathematically treated by means of a second order differential equation, transverse vibrations need a fourth order differential equation for their proper description.

Some examples of typical mode shapes are given in Figs.3.19 (beams) and 3.20 (square plates).

Chapter 4 describes some effects of vibration and shock on mechanical systems and man. In section 4.1 the damaging effects of vibrations in terms of mechanical fatigue are discussed to some length, both with respect to

7

periodic vibrations and with respect to random vibrations, while section 4.2
deals with balance quality of rotating machines. In Fig.4.9 curves indicating
the maximum residual unbalance corresponding to various balancing grades
are given.

The last section of Chapter 4, section 4.3, summarises some effects of
vibration and shock on man. Vibration exposure criteria curves are shown in
Fig.4.14 and curves indicating the tolerance of human subjects to impact
pulses are indicated in Fig.4.15.

Chapter 5 discusses some practical and theoretical aspects of vibration
measurement instrumentation and techniques. In section 5.1 some general
measurement considerations are made and section 5.2 introduces some basic
measurement systems. It is shown how the Brüel & Kjær Impulse Precision
Sound Level Meter Type 2204 can be used as *a direct reading, battery
operated vibration meter* and that the addition of an external Filter Set
enables the vibration spectrum to also be frequency analyzed. Further types
of *frequency analysis,* using constant bandwidth, as well as constant
percentage bandwidth, analyzing equipment are also outlined. When very
low frequency vibrations are to be analyzed the use of *frequency transform-
ations* by means of the FM (frequency modulated) magnetic Tape Recorder
Type 7001 is recommended.

Section 5.3 describes some of the most important properties of modern
accelerometers, and typical frequency characteristics for Brüel & Kjær
Accelerometers are shown in Fig.5.20. Furthermore, as the selection of the
most suitable accelerometer in some cases may be a little complicated the
chart given in Fig.5.21 has been prepared. Apart from indicating the main
fields of application for the various accelerometers, other pertinent data
relating to their overall performance are also stated in the chart. Finally the
interconnection between the *voltage sensitivity* and the *charge sensitivity* of
an accelerometer is mentioned.

The use of the two "types" of sensitivity is further discussed in section
5.4 in conjunction with the selection of the appropriate accelerometer
preamplifier. Again a chart has been prepared in an attempt to assist the
reader in his selection, and the chart is presented in Fig.5.29.

In section 5.5 the use of various types of analyzers and read-outs is more
thoroughly described, and the importance of the *phase characteristic* of the
measurement system mentioned. Examples of phase distortion are shown in
Fig.5.30 while Fig.5.31 indicates the range of "ideal" operation of a typical
vibration measurement system. Even though the phase distortion of the

8

measuring equipment is important, if measurements are to be made directly on the vibration signal waveform, it may be neglected when the problem consists in a determination of RMS-values and frequency spectra only. Here, on the other hand, the problem of *statistical errors* becomes significant in conjunction with the analysis of random vibrations. The statistical error in an RMS-measurement is then given by the expression:

$$\epsilon = \frac{1}{2\sqrt{\Delta f\,T}}$$

where Δf is the measurement bandwidth (or the resonant bandwidth) in Hz and T is the *effective averaging time* of the detecting equipment. This relationship is demonstrated in Figs.5.38, 5.39 and 5.40.

Section 5.6 deals with the calibration and performance checks of the measuring arrangement. While the "simple" calibrator built into the Preamplifier Type 4292 may be used for a quick performance check, considerably more accurate calibration can be made by means of the Calibrators Type 4291 and 4801+4815. Furthermore, a special Calibrator, Type 4290, is available mainly for frequency response calibration.

In section 5.7 some practical *accelerometer mounting methods* are discussed, and six methods of mounting are shown in Fig.5.46. The influence of the mounting method upon the frequency characteristic of the accelerometer is demonstrated in Fig.5.48. Also other practical accelerometer application problems, such as the formation of undesired ground loops (Fig.5.50), and the problem of cable noise and microphonics, are mentioned.

The Chapter concludes with the suggestion of a general measurement scheme in section 5.8. This scheme is meant as a help to remember the most important factors in the setting up and use of a vibration measurement system, and it is recommended that this section is read in full.

In Chapter 6 the practical *measurement and analysis of shock pulses* are treated, and in section 6.1 some general measurement considerations are outlined. The importance of linear *frequency and phase responses* of the measuring equipment is emphasized. Typical effects of limitations in the frequency response are shown in Figs.6.1, 6.2, 6.3, 6.4, 6.5 and 6.6, while the chart, Fig.6.7, allows an estimate to be made of the frequency response required in particular shock measurement situations.

Section 6.2 describes briefly some typical shock measurement systems and points out the advantages obtained by *recording the shock pulse on magnetic tape*.

9

In section 6.3 the practical frequency (Fourier) *analysis of tape recorded shock pulses* is discussed in some detail. There are, generally speaking, two different ways of performing such analysis in practice. One way consists in applying the pulse to the analyzing filters once per filter, while the second way consists in repeating the pulse periodically by the use of a very short, closed, tape loop containing the pulse. Various practical aspects involved are outlined, and results obtained according to both methods of analysis are exemplified in Fig.6.12.

Chapter 7 deals with some methods of shock and vibration control. As one of the most important methods of control is the *isolation of vibration and shocks* this is discussed to some extent in section 7.1. Even though the principles involved in the isolation of both vibrations and shocks are similar, certain distinct differences exist. It has, therefore, been found convenient to split the section into a) Vibration isolation, and b) Shock isolation. The basic principle of *vibration isolation* consists in selecting a spring mounting for the equipment (machine) to be isolated so that the natural frequency of the spring mass system is considerably lower than (say less than three times) the lowest frequency component to be isolated. Typical resonance curves for spring-mass systems with various damping ratios are shown in Fig.7.2, and Figs.7.6, 7.7 and 7.8 illustrate the measurements necessary to solve a practical vibration isolation case.

With regard to *shock isolation* this is treated on the basis of the shock response spectrum and the choice of proper damping in the isolation system is emphasized. It is shown that an effective *shock force* isolation can only be obtained by transforming the force into *motion*.

In section 7.2 the theory and application of the *dynamic vibration absorber* and the use of *vibration damping treatments* are outlined. The results of applying a dynamic vibration absorber to a resonant system are sketched in Figs.7.21, 7.22 and 7.23, while useful design curves are shown in Figs.7.24 and 7.25.

When it comes to the application of vibration damping treatments this may be done in several ways, the simplest of which is to spray a layer of *viscoelastic material with high internal losses* over the surface of the vibrating structure, Fig.7.30. Other methods consist in the design of various types of *sandwich structures* as illustrated in Fig.7.31. The section concludes with a description of different methods of measuring the internal losses in damping materials, the most important one seeming to be one suggested by Dr. H. Oberst et. al. which utilizes the Brüel & Kjær Complex Modulus Apparatus Type 3930.

10

Section 7.3 describes several methods of *vibration testing* of mechanical equipment. This kind of testing and investigating the effects of internal equipment resonances has become quite popular and powerful over the past years and brief descriptions are given of the *frequency sweep test* as well as the *wide band random* and the *sweep random vibration tests.*

In section 7.4 another kind of mechanical testing, *the shock test,* is discussed to some extent. Even though most of the shock testing performed today is made on specially designed shock machines, the techniques of utilizing electrodynamic vibration machines in shock spectrum testing seems to attain increasing popularity in shock and vibration laboratories. Both kinds of shock testing are briefly outlined.

Section 7.5 describes the basic aspects of the *balancing of rotating machines.* Both static and dynamic balancing are discussed and some simple balancing methods are pointed out.

In the last Chapter of the book, Chapter 8, an outline is given on the concept of mechanical *impedance* and *mobility, correlation* and *cross-spectral density* measurements as well as on the determination of *probability density data* for random vibrations.

While section 8.1 (mechanical impedance and mobility) and section 8.2 (cross-correlation and cross-spectral density measurements) describe the use of two channel type measurements, the final section, 8.3, (probability density measurements) is based, primarily, on the use of single channel measurements. The applicability as well as the limitations of the various methods are pointed out and examples of their practical use given.

General References

Books:

BISHOP, R.E.D. and   Mechanics of Vibration. Cambridge University
JOHNSON, D.C.:   Press, 1960.

CREMER, L. and   Körperschall. Springer Verlag. Berlin/Heidelberg/
HECKL, M.:   New York 1967.

Den HARTOG, J.P.:   Mechanical Vibrations, McGraw-Hill Book Com-
                           pany, Inc. 1956.

11

HARRIS, C.M. and CREDE, C.E.:	Shock and Vibration Handbook. McGraw-Hill Book Company, Inc. 1961.
JACOBSEN, L.S. and AYRE, R.S.:	Engineering Vibrations. McGraw-Hill Book Company, Inc. 1958.
MORROW, C.T.:	Shock and Vibration Engineering. John Wiley and Sons, Inc. 1963.
MORSE, P.M.:	Vibration and Sound. McGraw-Hill Book Company, Inc. 1948.
SNOWDON, J.C.:	Vibration and Shock in Damped Mechanical Systems. John Wiley and Sons, Inc. 1968.
TIMOSHENKO, S.:	Vibration Problems in Engineering. D. Van Nostrand Company, Inc. Princeton, N.J. 1955.
Van SANTEN, G.W.:	Mechanical Vibration. Philips Technical Library, Eindhoven 1953.

Journals:

Acustica.	Hirzel Verlag, Stuttgart.
Akusticheskii Zhurnal.	Published by the Academy of Science of the U.S.S.R. Moscow. (Also translated and published by the American Institute of Physics as: Soviet Physics, Acoustics.)
Experimental Mechanics.	Published by the Society of Experimental Stress Analysis, U.S.A.
J.A.S.A.	(Journal of the Acoustical Society of America.) Published by the American Institute of Physics, New York.
Journal of Sound and Vibration.	Published by Academic Press, Inc. London.
Journal of the Acoustical Society of Japan.	(Japanese) Published by the Acoustical Society of Japan, University of Tokyo, Tokyo.

Kampf dem Lärm.	Published by Deutschen Arbeitsring für Lärmbekämpfung, E. V. Düsseldorf.
Lärmbekämpfung.	Verlag für angewandte Wissenschaften GmbH. Baden-Baden.
Noise Control.	Published by the American Institute of Physics, New York.
Sound and Vibration.	Published monthly by Acoustical Publications, Inc., Ohio, U.S.A.
Shock, Vibration and Associated Environments.	Published by the Office of the Director of Defense Research and Engineering, Washington, D.C.

2. CHARACTERISTICS OF VIBRATION AND SHOCK

2.1. Periodic Vibration

Periodic vibration may be looked upon as an oscillating motion of a particle, or body, about a reference position, the motion repeating itself exactly after certain periods of time. The simplest form of periodic vibrations is the socalled harmonic motion which when plotted as a function of time, is represented by a sinusoidal curve, Fig.2.1. Here T is the period of vibration, i.e. the time elapsed between two successive, exactly equal conditions of motion.
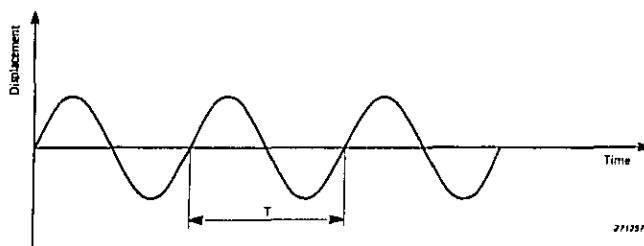
Fig.2.1. Example of a pure harmonic (sinusoidal) vibration signal

The *frequency* of the vibration is

$$f = \frac{1}{T}$$

Turning to the magnitude of the vibration this may be characterized by different quantities, all of which have definite mathematical relationships to each other *as long as harmonic motion is considered.*

If the vibration has the form of a pure translational oscillation along one axis (x) only, the instantaneous *displacement* of the particle (or body) from

14

the reference position can be mathematically described by means of the equation:

$$x = X_{peak} \sin (2 \pi \frac{t}{T}) = X_{peak} \sin (2 \pi ft) = X_{peak} \sin (\omega t)$$

where $\omega = 2 \pi f = $ angular frequency

$X_{peak} = $ Maximum displacement from the reference position

$t = $ time

As the *velocity* of a moving particle (or body) is the time rate of change of the displacement, the motion can also be described in terms of velocity (v):

$$v = \frac{dx}{dt} = \omega X_{peak} \cos (\omega t) = V_{peak} \cos (\omega t) = V_{peak} \sin (\omega t + \frac{\pi}{2})$$

Finally, the *acceleration* (a) of the motion is the time rate of change of the velocity:

$$a = \frac{dv}{dt} = \frac{d^2 x}{dt^2} = -\omega^2 X_{peak} \sin (\omega t) = -A_{peak} \sin (\omega t) = A_{peak} \sin (\omega t + \pi)$$

From the above equations it can be seen that the form and period of vibration remain the same whether it is the displacement, the velocity or the acceleration that is being studied. However, the velocity leads the displacement by a phase angle of 90° ($\frac{\pi}{2}$) and the acceleration again leads the velocity by a phase angle of 90° ($\frac{\pi}{2}$). As characterizing values for the magnitude the peak values have been used, i.e. X_{peak}, V_{peak} and A_{peak}. The magnitude description in terms of peak values is quite useful as long as pure harmonic vibration is considered because it applies directly in the equations given above. If, on the other hand, more complex vibrations are being studied other descriptive quatities may be preferred. One of the reasons for this is that the peak value describes the vibration in terms of a quantity which depends only upon an instantaneous vibration magnitude regardless of the time history producing it.

A further descriptive quantity, which does take the time history into account, is the *average absolute* value, defined as (see also Fig.2.2):

$$X_{|Average|} = \frac{1}{T} \int_0^T |x| \, dt$$

15
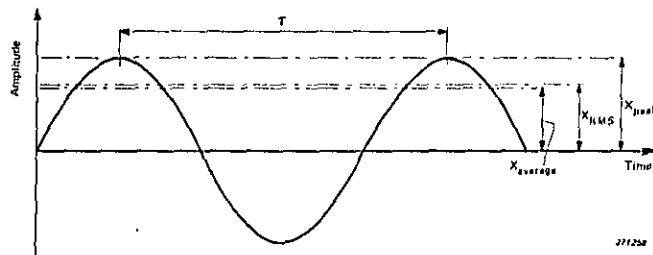
Fig.2.2. Example of a harmonic vibration signal with indication of the peak, the RMS and the average absolute value

Even though this quantity takes into account the time history of the vibration over one period (T) it has been found to be of limited practical interest. A much more useful descriptive quantity which also takes the time history into account, is the *RMS (root mean square)* value (Fig.2.2):

$$X_{RMS} = \sqrt{\frac{1}{T} \int_0^T x^2 (t) \, dt}$$

The major reason for the importance of the RMS-value as a descriptive quantity is its direct relationship to the energy content of the vibrations.

For a *pure harmonic motion* the relationship between the various values is:

$$X_{RMS} = \frac{\pi}{2\sqrt{2}} X_{|Average|} = \frac{1}{\sqrt{2}} X_{peak}$$

A more general form of these relationships may be given by:

$$X_{RMS} = F_f X_{|Average|} = \frac{1}{F_c} X_{peak}$$

or: $F_f = \frac{X_{RMS}}{X_{|Average|}}$; $F_c = \frac{X_{peak}}{X_{RMS}}$

The factors F_f and F_c are called "form-factor" and "crest-factor", respectively, and give some indication of the waveshape of the vibrations being studied.

16
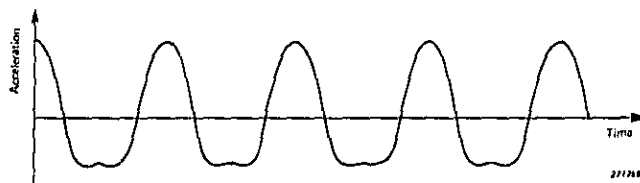
Fig.2.3. Example of a non-harmonic periodic motion (piston acceleration
of a combustion engine)

For pure harmonic motion:

$$F_f = \frac{\pi}{2\sqrt{2}} = 1.11 \ (\approx 1 \ dB) \ \text{and} \ F_c = \sqrt{2} = 1.414 \ (= 3 \ dB)$$

Most of the vibrations encountered in daily life are not pure harmonic
motions even though many of them may be characterized as periodic. A
typical non-harmonic periodic motion is shown in Fig.2.3 (piston accelera-
tion of a combustion engine). By determining the peak, average absolute
and RMS-value of this vibration as well as the form-factor and crest-factor a
lot of useful information is obtained, and it can be clearly concluded that
the motion is not harmonic. However, it will be practically impossible, on
the basis of this information, to predict all the various effects that the
vibration might produce in connected structural elements. Other methods of
description must therefore be used.

One of the most powerful descriptive methods is the method of frequen-
cy analysis. This is based on a mathematical theorem, first formulated by
FOURIER, which states that any periodic curve, no matter how complex,
may be looked upon as a combination of a number of pure sinusoidal curves
with harmonically related frequencies:

$$F(t) = X_o + X_1 \sin(\omega t + \varphi_1) + X_2 \sin(2\omega t + \varphi_2)$$
$$+ X_3 \sin(3\omega t + \varphi_3) + \ldots + X_n \sin(n\omega t + \varphi_n)$$

As the number of elements in the series increase it becomes an increasing-
ly better approximation to the original curve. The various elements con-
stitute the *vibration frequency spectrum*. In Fig.2.4 the nonharmonic
periodic motion of Fig.2.3 is redrawn together with the two most important
harmonic curves representing its frequency spectrum. A somewhat more

17
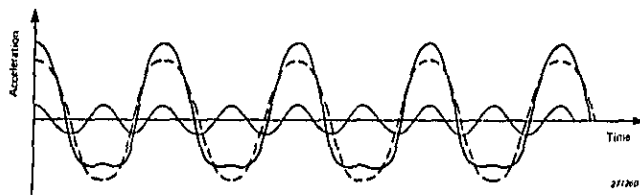
Fig.2.4. *Illustration of how the waveform shown in Fig.2.3 can be "broken up" into a sum of harmonically related sinewaves*

convenient method of representing this spectrum is shown in Fig.2.5b, while Fig.2.6 shows some further examples of periodic time functions and their frequency spectra. A specific feature of periodic vibrations, which becomes clear by looking at Fig.2.5 and 2.6 is that their spectra consists of *discrete lines* when presented in the so-called frequency domain (Figs.2.5b and 2.6b). This is in contrast to random vibrations which show continuous frequency spectra (section 2.2, Fig.2.12).


a)   b)
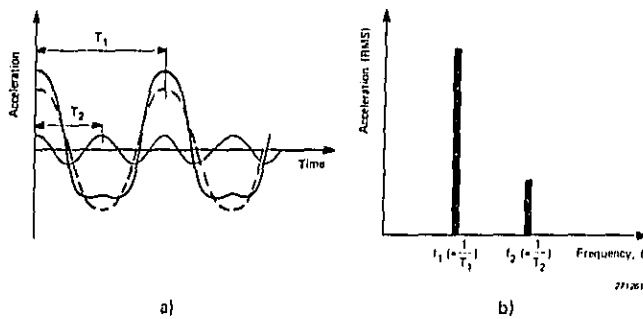
Fig.2.5. *Illustration of how the signal, Fig.2.3 can be described in terms of a frequency spectrum*
   a) Description in the time domain
   b) Description in the frequency domain

18
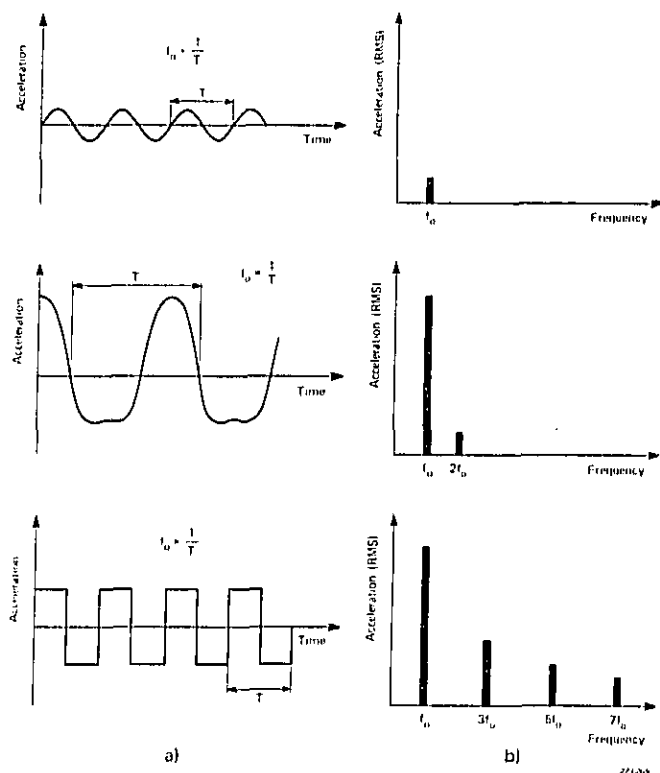
Fig.2.6. Examples of periodic signals and their frequency spectra
    a) Descriptions in the time domain
    b) Descriptions in the frequency domain

19

2.2. Stationary Random Vibration

Random vibrations are met rather frequently in nature and may be characterized as vibratory processes in which the vibrating particles undergo irregular motion cycles that never repeat themselves exactly, see Fig.2.7. To obtain a complete description of the vibrations, an infinitely long time record is thus theoretically necessary. This is of course an impossible requirement, and finite time records would have to be used in practice. Even so, if the time record becomes too long it will also become a very inconvenient means of description and other methods have therefore been devised and are commonly used. These methods have their origin in statistical mechanics and communication theory and involve concepts such as amplitude *probability distributions in terms of probability densities* and *continuous vibration frequency spectra in terms of mean square spectral densities* *).
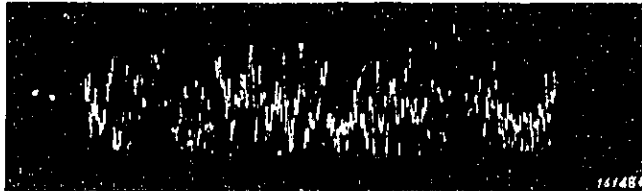

Fig.2.7. Example of a random vibration signal

Without going into too much mathematical detail the meaning of the above concepts should be briefly reviewed because of their importance in relation to practical vibration measurements.

The concept of probability is of a mathematical origin and denotes the chance of a particular event happening. If the event in question is absolutely certain to happen the probability of occurrence of the event is said to be 1. On the other hand, if the event in question is certain *not* to happen the probability of occurrence is said to be 0. Thus probabilities are, in the sense used here, positive real numbers between 1 and 0.

---

*) Mean square spectral density is also often termed "Power Spectral Density" (P.S.D.) because the mean square is a quantity proportional to power.

20

In the study of continuous processes such as stationary[**] random vibra-
tions it is often convenient to use the concept of probability *density* instead
of probability. Physically the probability density can be defined as the
probability of finding instantaneous amplitude values within a certain ampli-
tude interval, Δx, divided by the size of that interval (thus: density), see
Fig.2.8. This means that while probabilities are dimensionless quantities the
probability density is a quantity having a certain dimension.
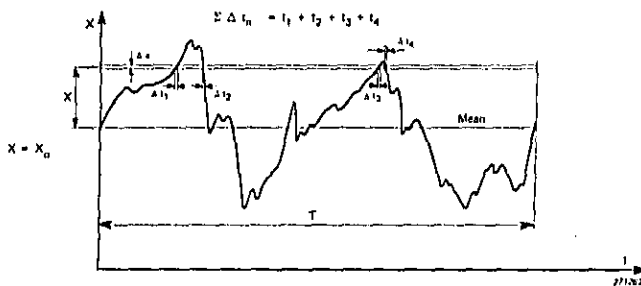
*Fig.2.8. Sketch illustrating the concepts of probability and probability
density*

Mathematically formulated the probability density at some specified
amplitude level, x, is:

$$p\,(x) = \lim_{\Delta x \to 0} \frac{P\,(x) - P\,(x + \Delta x)}{\Delta x}$$

Here p(x) designates the probability density while P(x) is the probability
that any instantaneous amplitude value exceeds the level x and P $(x + \Delta x)$ is
the probability of occurrence of instantaneous amplitude values exceeding
the level $x + \Delta x$. By plotting the value of p(x) for all values of x a probabili-
ty density curve is obtained which has the feature that an integration of the
curve from a value x_1 to a value x_2 immediately tells the probability of
occurrence of instantaneous amplitude values within the interval $(x_2 - x_1)$,
independent of the actual magnitude of x_1 and x_2. The presentation of

[**]Stationary random vibrations are defined as random vibrations whose *statistical*
characteristics do not change with time.

experimental probability data in terms of probability density curves bears some advantages because it allows for a direct comparison of data between experiments (and between experimenters) independent of the width of the amplitude interval, Δx, used in the experiment. Finally, theoretical probability data are commonly presented in the form of probability density curves and this method of presentation must therefore be considered the most generally acceptable one.

From the definition of probability density it follows that by integrating the probability density curve over all possible amplitude values the magnitude of the integral will be 1 (because the probability of finding a certain amplitude value within all possible amplitude values is 1). The practical procedure involved in converting experimental and/or theoretical data into probability density data ensuring that the area under the probability density curve is 1, is called normalization, and the most commonly known normalized probability density curve, the normal (Gaussian) curve, is shown in Fig.2.9.

Probability density function

$$p(x) = \frac{1}{\sigma \sqrt{2\pi}} \exp\left(-\frac{1}{2}\frac{x^2}{\sigma^2}\right)$$
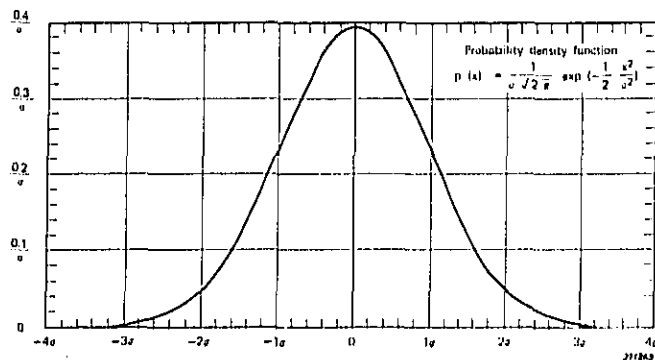
Fig.2.9. The normalized Gaussian probability density curve

Even though probability density data are very useful signal descriptions and give excellent information on how, on the average, the instantaneous amplitudes in a vibratory signal are distributed, they give little or no information as to the time history or frequency content of the process being studied. To try and remedy this, and to obtain further descriptive data, statistical physicists introduced a function called the *autocorrelation func-*

22

tion, $\psi(\tau)$. This function describes (on the average) how a particular instantaneous amplitude value depends upon previously occurring instantaneous amplitude values in that $\psi(\tau)$ is defined as:

$$\psi(\tau) = \lim_{T \to \infty} \frac{1}{T} \int_0^T f(t) \, f(t + \tau) \, dt$$

where $f(t)$ is the magnitude of the vibratory process at an arbitrary instant of time, t, and $f(t + \tau)$ designates the magnitude of the same process observed at a time, τ, later, see Fig.2.10.
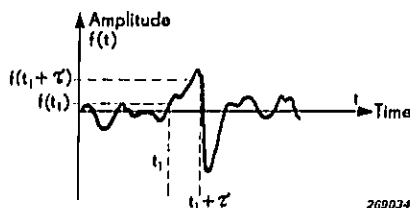
*Fig.2.10. Basic concepts involved in deriving the autocorrelation function*

In the case of an "ideal" stationary random process the autocorrelation function would consist of an infinitely narrow impulse-function around zero ($\tau = 0$), see Fig.2.11a), as in such a process each instantaneous amplitude value should be completely independent of all other instantaneous amplitude values.

However, in practice the autocorrelation functions associated with stationary random vibrations cluster around $\tau = 0$, but are never "infinitely narrow" impulse-functions, Fig.2.11b) and c). The reason for this spreading out of the curve around zero is that all practical random processes are frequency limited, and the narrower the frequency limits are the more spread-out are the corresponding autocorrelation functions.

From the autocorrelation function another, very important function in practice, can be deduced, which has a certain resemblance to the Fourier frequency spectra described in section 2.1 for periodic vibrations. This function has been termed the *mean square spectral density function* (power spectral density function) and can be derived from the autocorrelation function as follows: Assuming that the integral of $\psi(\tau)$ from $-\infty$ to $+\infty$ is finite (see Fig.2.11) one can write:

23
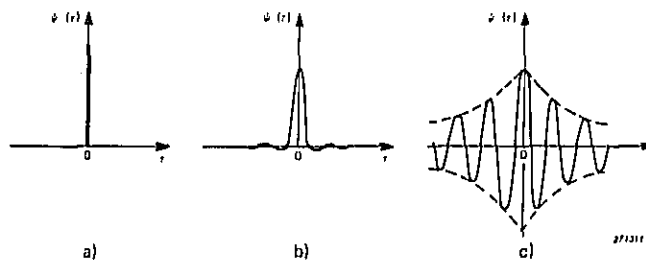
Fig.2.11. Example of autocorrelation functions
a) Autocorrelation function for an ideal stationary random process containing frequencies from 0 to ∞ (constant spectral density)
b) Autocorrelation function for a "practical" wide band stationary random process
c) Autocorrelation function for a narrow band stationary random process

$$w(\omega) = \int_{-\infty}^{\infty} \psi(\tau) e^{-j\omega t} d\tau$$

where $\omega = 2\pi f$ and f is frequency.

From the theory of Fourier integrals it is furthermore known that $\psi(\tau)$ can also be found from the above integral by inversion:

$$\psi(\tau) = \frac{1}{2\pi} \int_{-\infty}^{\infty} w(\omega) e^{j\omega\tau} d\omega = \int_{-\infty}^{\infty} w(\omega) e^{j2\pi f\tau} df$$

The Fourier integral relations between $\psi(\tau)$ and $w(\omega)$ are often called the Wiener-Kintchine relations and play a very important role in the theory of random processes.

In physically realizable stationary processes one operates with positive frequencies only and $\psi(\tau) = \psi(-\tau)$ whereby the integral for $\psi(\tau)$ becomes:

$$\psi(\tau) = 2 \int_{0}^{\infty} w(\omega) \cos(\omega\tau) df$$

or, if a function w (f) is defined so that

$$w(f) = 2 w(\omega)$$

24

then $\quad \psi(\tau) = \int\limits_0^\infty w(f) \cos(2\pi f \tau)\, df$

To interpret the function $w(f)$ consider the case where $\tau = 0$:

$$\psi(0) = \lim_{T\to\infty} \frac{1}{T}\int\limits_0^T f(t)\, f(t+0)\, dt = \lim_{T\to\infty} \frac{1}{T}\int\limits_0^T f^2(t)\, dt$$

and $\quad \psi(0) = \int\limits_0^\infty w(f)\, df$

thus $\quad \lim_{T\to\infty} \frac{1}{T}\int\limits_0^T f^2(t)\, dt = \int\limits_0^\infty w(f)\, df$

Both of these integrals are measures of the power involved in the process, one in terms of the process time function, $F(t)$, and the other in terms of a frequency function, $w(f)$. Because of the squaring involved in the above time function description, $w(f)$ has been designated as the *mean square spectral density function* (or power spectral density function).

Analytically, it is sometimes more convenient to start an investigation by studying the autocorrelation function associated with the problem and then, by means of the above relation, calculate the mean square spectral density function. On the other hand, experimentally it is generally easier to measure the mean square spectral density function directly by means of analog frequency analyzers as explained in the following.

An ideal analog frequency analyzer will allow only that part of the signal to be measured which has frequency components within a narrow frequency band, Δf, see Fig.2.12. Assuming that no attenuation or amplification of
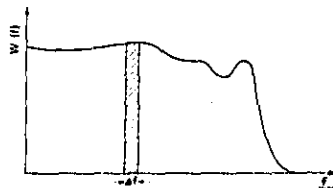

Fig.2.12. *Determination of the mean square spectral density by means of ideal filters*

25

these frequency components takes place in the analyzer the signal which is passed onto its indicating arrangement is:

$$\int_0^\infty w(f)\, df = \int_f^{f+\Delta f} w(f)\, df = \lim_{T \to \infty} \frac{1}{T} \int_0^T f^2_{\Delta f}(t)\, dt$$

Here $f_{\Delta f}(t)$ is the above mentioned part of the complete signal, $f(t)$, which has frequency components within Δf. If now Δf is made so small that $w(f)$ can be considered constant within this frequency range then

$$\int_f^{f+\Delta f} w(f)\, df \approx w(f)\, \Delta f$$

thus, in the limiting case when $\Delta f \to 0$, one obtains:

$$w(f) = \lim_{\Delta f \to 0} \lim_{T \to \infty} \frac{1}{\Delta f\, T} \int_0^T f^2_{\Delta f}(t)\, dt$$

This equation forms the basis of most analog experimental techniques used in the mean square spectral density analysis of random signals.

Before closing the discussion on methods used to describe and analyse random vibration phenomena some important "practical" facts should be pointed out:

Returning to the equation

$$\lim_{T \to \infty} \frac{1}{T} \int_0^T f^2(t)\, dt = \int_0^\infty w(f)\, df$$

it can be seen that the expression on the left hand side of this equation has a certain resemblance to the square of the expression previously used to define the RMS-value of a periodic vibration signal (section 2.1). Actually if the limiting operation is carried out the expressions would be identical. This means that *the description of a complex signal in terms of its overall RMS-value is equally meaningful whether the signal has a periodic or a random character.* (A further discussion of this statement in terms of statistical quantities is carried out in Appendix A).

When it comes to *spectral* description, however, *a periodic signal* may well be described in terms of *the RMS-values of its various frequency components* (its frequency spectrum), while *random vibration signals* are best described in terms of *mean square spectral density functions.* This is due to the fact that random signals produce continuous frequency spectra and the RMS-value measured within a certain frequency band will therefore depend

upon the width of the band. The detailed measurement evaluation techniques will, in view of the above normally also differ, a fact which is more specially discussed in Chapter 4 of this book and in a separate publication*).

2.3. Transient Phenomena and Shocks

Transient phenomena and mechanical shocks are, like random vibrations encountered relatively often in daily life. They may originate from such widely different releases of energy as rough handling of equipment, explosions and supersonic motion. However, common for this type of energy release is its short duration and sudden occurrence.

A simple shock may be defined as a transmission of kinetic energy to a system which takes place in a relatively short time compared with the natural period of oscillation of the system, while transient phenomena (also termed complex shocks) may last for several periods of vibration of the system.

Shocks and transient vibrations may be described in terms of force, acceleration, velocity or displacement and for a complete description it is necessary to obtain an exact time history record of the quantity in question.

In many cases the ultimate goal is not the waveform itself, but rather a means to estimate the effect that the corresponding shock or transient vibration would have on a certain mechanical system. A more useful method of description might then again be found in the form of Fourier analysis. If the time function for a shock is F (t) then its Fourier transform is given by:

$$F(f) = \int_{-\infty}^{\infty} F(t)\, e^{-j\omega t}\, dt$$

The analogy between this expression and the mean square spectral density function for stationary random vibrations (section 2.2) is readily seen. There is, however, a very distinct difference in that the mean square spectral density function for stationary random vibrations is the Fourier transform of an already time-averaged, even function, the autocorrelation function. In the above Fourier integral for shock (impulse) function no

---

27

a)

$$|F(f)| = AT \left| \frac{\sin \pi f t}{\pi f t} \right|$$

b)

$$F(f) = \frac{AT}{2} \left[\frac{1}{\pi f t} \sqrt{1 - \frac{1}{\pi f t} \sin 2 \pi f T + (\frac{1}{\pi f T} \sin \pi f t)} \right]$$

c)

$$F(f) = \frac{2 AT}{\pi} \left| \frac{\cos \pi f T}{1 - 4 f^2 T^2} \right|$$

Impulse time functions   Fourier spectra
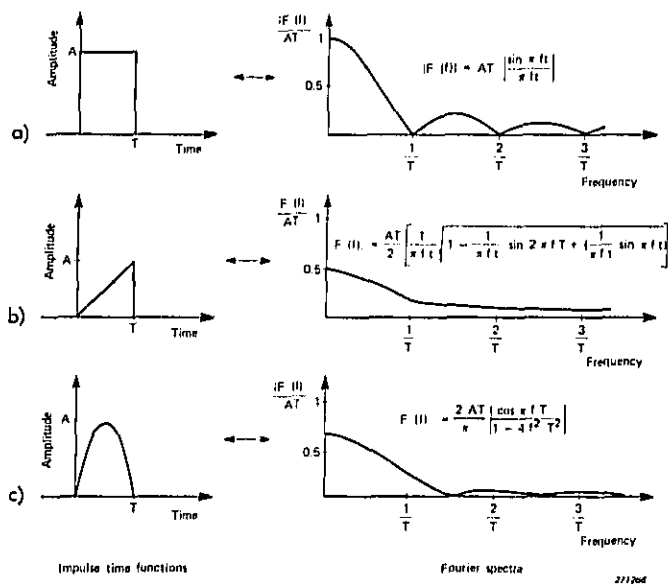
Fig.2.13.   *Example of shock time functions and their Fourier transform*
         (spectra)
         a) A rectangular shock pulse
         b) A final peak sawtooth shock pulse
         c) A half-sine shock pulse

time-averaging is involved, which, to a certain extent, complicates the meas-
urement technique necessary to evaluate the integral. This is further
discussed in Chapter 5 of this book. Mathematically, on the other hand,
these difficulties do not exist and in Fig.2.13 various shock time functions
and their Fourier spectra are given. It is seen from the figure that in general
a shock pulse contains energy spread over all frequencies from zero to
infinity, and that the spectra are continuous with no discrete frequency
components.

In the expressions for F (f) given in the figure all the expressions within
the parallel brackets approach unity as f goes to zero, so that at very low

28

$$F(t) = e^{-\beta t} \cos(\omega_0 t + \varphi)$$

$$\varphi = \tan^{-1}\left(\frac{\beta}{\omega_0}\right)$$

$$F(\omega) = \frac{\omega}{\sqrt{[(\omega_0^2 + \beta^2) - \omega^2]^2 + (2\beta\omega)^2}}$$

Transient time function   Fourier spectra
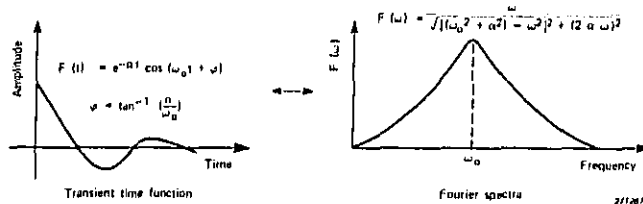
Fig.2.14.   Example of an oscillating transient and its Fourier spectrum function

frequencies the magnitude of the spectrum component is equal to the area (amplitude-time integral) of the shock pulse, irrespective of the pulse shape. This fundamental relationship is of considerable practical importance, for example in shock testing. It means that so long as the shock pulse is short compared with the natural period of the mechanical system on which it acts, the severity of the shock is determined by the area of the shock pulse alone (see also Fig.3.12.b II).

In the case of transient phenomena the situation is somewhat different. Such phenomena, in the sense used in this book may consist either of a single period "shock-wave", or of an oscillating transient. The Fourier spectrum function of an oscillating transient is shown in Fig.2.14 above and it is seen that the magnitude of the spectrum components in this special case tends towards zero as the frequency $f = \frac{\omega}{2\pi}$ goes to zero. Also, a maximum magnitude of the spectrum is reached around $f_o = \frac{\omega_0}{2\pi}$ where f_o corresponds roughly to the frequency of oscillation of the transient. This maximum is broader the quicker the transient phenomenon ceases.

If the "transient" does not cease at all, i.e. when the "transient" is no longer a transient but a periodic phenomenon (in this case an harmonic vibration), the frequency spectrum degenerates into a discrete spectral line (infinitely narrow maximum at $f_o = \frac{\omega_0}{2\pi}$).

2.4. Non-Stationary Random Vibration

Theoretically all kinds of random vibrations encountered in practice are non-stationary because their statistical properties vary with time. However,

29
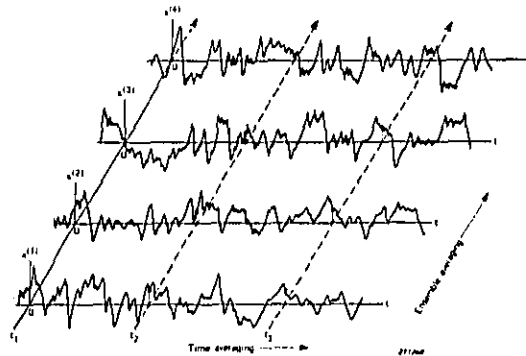
Fig.2.15.   Illustration of an ensemble of random functions

from an engineering point of view this variation in statistical properties may
be so slow, or of such a character, that many of the phenomena studied can
be considered stationary in a practical sense.

*Non-stationary random vibrations may therefore, in practice, be defined
as random vibrations whose statistical properties vary with time within time
intervals considered essential for their proper description.* To analyze and
describe such vibration data it is thus necessary to take their variation in
statistical properties with time into account. A typical example of seriously
non-stationary random vibrations is the vibrations induced in space vehicles
during launch and re-entry.

To theoretically analyze non-stationary random vibrations properly it is
necessary to introduce the concept of *ensemble averaging.* An ensemble
average is an average taken over a large number (an ensemble) of repeated
experiments, see Fig.2.15. As can be seen from the figure an ensemble
average can be taken at any particular instant of time t_1, t_2, t_3 etc., and
when the average values are plotted against time a more or less complete
description of the vibration is obtained. There are, on the other hand,
several reasons why this method of description is not very useful in practice.
Firstly, it requires that the non-stationary process can be repeated a very
large number of times. In the case of space vehicle launch and re-entry for
instance this is not possible due to the cost of such experiments. Secondly,
the amount of data necessary for a thorough description is so large that
their proper measurement will pose serious problems.

30
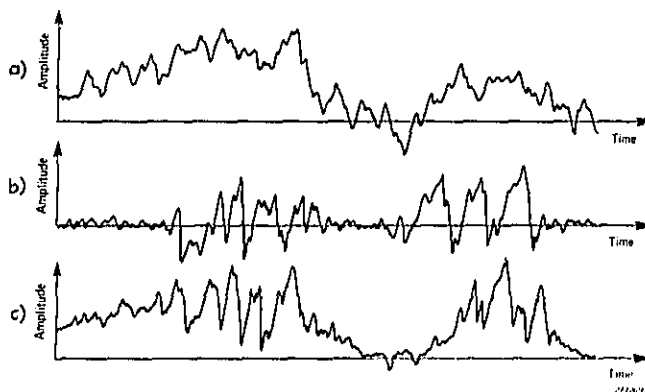
Fig.2.16. *Examples of some basic types of nonstationary random vibra-*
tions
a) Time-varying mean value
b) Time-varying mean square value
c) Time-varying mean and mean square value

It is therefore normally necessary to seek other methods of description,
and in general some sort of time averaging is used. There are, however,
certain limitations imposed upon this kind of time averaging in that the
response and averaging time of the measurement equipment employed
should preferably be small relative to important time trends in the non-
stationary data. This again may lead to considerable statistical uncertainties
in the measurements, see also Chapter 4, section 4.4.

Fig.2.16 illustrates some basic and important types of non-stationary
random vibrations.

2.5. Selected Bibliography

ANSI: S2, 10—1971 Analysis and Presentation of Shock
                     and Vibration Data. A.S.A. 335 East 45th St.,
                     New York. 10017.

BENDAT, J.S.:   Principles and Applications of Random Noise
                     Theory. John Wiley and Sons, Inc. New York,
                     1958.

BENDAT, J.S. and
PIERSOL, A.G.:
Measurement and Analysis of Random Data
John Wiley and Sons, Inc. New York 1965.

BLACKMAN, R.B. and
TUKEY, J.W.:
The Measurement of Power Spectra. Dover
Publication, Inc. New York 1958.

CRANDALL, S.H. and
MARK, W.D.:
Random Vibrations in Mechanical Systems.
Academic Press, New York 1963.

DIN:
DIN 1311. (February 1970) Schwingungslehre
Kinematische Begriffe. Beuth-Vertrieb GmbH,
Berlin 30 und Köln.

KHARKEVICH, A.A.:
Spectra and Analysis. Fitzmatgiz, Moscow 1960
(in Russian). Also available in English translation
published by Consultants Bureau, New York
1957.

MORROW, C.T.:
Shock and Vibration Engineering. John Wiley
and Sons, Inc. New York 1963.

PIERSOL, A.G.:
The Measurement and Interpretation of Ordinary
Power Spectra for Vibration Problems. NASA
CR-90, Washington D.C. and MAC-305-1, Los
Angeles, 1964.

PIERSOL, A.G.:
Spectral Analysis of Non-Stationary Spacecraft
Vibration Data. NASA CR-341, Washington,
D.C. December 1965.

RICE, S.O.:
Mathematical Analysis of Random Noise. Bell
System Tech. Journ. 23 (1944) and 24 (1945).
Also contained in N. Wax: "Selected Papers on
Noise and Stochastic Processes". Dover Publica-
tions, Inc. New York 1954.

RUZICKA, J.E.:
Characteristics of Mechanical Vibration and
Shock. Sound and Vibration. April 1967.

SHARMAN, R.V.:
Vibrations and Waves. Butterworth, London
1963.

THRALL, G.P. and BENDAT, J.S.:

Mean and Mean Square Measurements of Non-stationary Random Processes. NASA CR-226, Washington D.C., May 1965.

VIGNESS, I.:

The Fundamental Nature of Shock and Vibration, Electrical Manufacturing, pp. 89-108, June 1959.

3. RESPONSE OF MECHANICAL SYSTEMS TO
VIBRATIONS AND SHOCKS

3.1. Response of Linear Mechanical Systems to Vibrations. Resonance

The motion of a mechanical system subjected to external forces is commonly termed the *response* of the system to the particular forces in question. Similarly, the external forces acting upon the system are termed the *exciting* forces, or simply the excitation. These terms are general and have to be specified closer when the behaviour of a particular system is being investigated.

To aid such specifications it is normally necessary to construct a somewhat simplified mechanical model and, on the basis of the model to formulate the equations of motion for the system. This model can then be used as a basis for a further analysis.
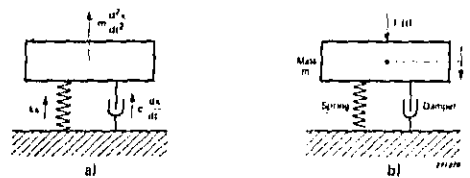
Fig.3.1. Models of a single degree-of-freedom system
a) System in free vibrations
b) System in forced vibrations

One of the simplest models of a vibrating system is shown in Fig.3.1a), and consists of a mass, a spring and a damper. If the system behaves linearly (and time-invariant) the equation of motion of the mass is (no external force applied):

$$m \frac{d^2x}{dt^2} + c \frac{dx}{dt} + kx = 0$$

34

This system is called a *single degree-of-freedom system* in that it consists of *one* mass only, which moves along *one* axis only and its motion can thus be described by a single second order differential equation.

By applying an external force f (t) to the system as indicated in Fig.3.1b) the equation of motion becomes:

$$m \frac{d^2x}{dt^2} + c \frac{dx}{dt} + kx = f(t)$$

The solution of this equation gives directly the *displacement* response, x (t), of the mass, m, produced by the excitation, f (t). Other response quantities such as the *velocity response* or the *acceleration response* can be found from the well known relationships between the displacement, velocity and acceleration (see also Appendix B):

$$v(t) = \frac{dx}{dt} \qquad \text{and} \qquad a(t) = \frac{d^2x}{dt^2}$$

where v (t) = velocity and a (t) = acceleration of the mass, m, Fig.3.1b).

The force f (t), can have any dependency on time, and as long as the motion of the mass can be described by a linear differential equation of the type given above, it is, in principle, possible to obtain exact solutions for x (t), v (t) and a (t). A very powerful tool in obtaining the required solutions is the *superposition principle*, which is applicable to linear differential equations. It states that *the effect of simultaneously super-imposed actions is equal to the sum of the effects of each individual action.*

Utilization of this principle can be made for instance by considering the function f (t) as consisting of an infinite number of impulses, each with an infinitesimal width, $\Delta\tau$, and a height f (τ) and superimposing the responses produced by the action of each of these impulses, see Fig.3.2.

Mathematically this application of the superposition principle can be written:

$$x(t) = \int_{-\infty}^{t} f(\tau) h(t - \tau) d\tau$$

where h (t − τ) is the response of the system, (Fig.3.1,) at the time t to a unit impulse excitation acting at time τ. A unit impulse excitation is characterized by a force which is zero except at t = τ where it is infinite and encloses unit area:

$$\lim_{\epsilon \to 0} \int_{-\epsilon}^{\epsilon} \delta(\tau) d\tau = 1$$

35
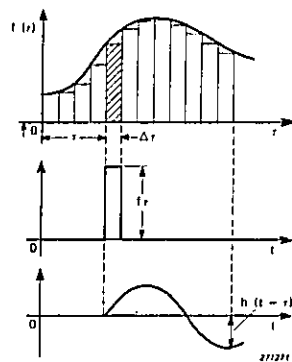
Fig.3.2. Illustration of the concepts involved in time domain superposition

Another method of utilizing the superposition principle is to determine
the Fourier transform $f(\omega)$ of $f(t)$ and study the response of the system to
each Fourier component separately. The impulse response function $h(t - \tau)$
defined above, then transforms into a complex *frequency response function,*
$H(\omega)$ and $x(t)$ is obtained in terms of its Fourier transform, $X(\omega)$:

$$X(\omega) \quad = \int_{-\infty}^{\infty} x(t) e^{-j\omega t} dt = \int_{-\infty}^{\infty} e^{-j\omega t} dt \int_{-\infty}^{t} f(\tau) h(t - \tau) d\tau$$

$$= \int_{-\infty}^{\infty} dt \int_{-\infty}^{t} e^{-j\omega(t-\tau)} h(t - \tau) e^{-j\omega\tau} f(\tau) d\tau$$

By setting $t - \tau = \xi$ and expanding the regions of integration remember-
ing that $h(t - \tau) = 0$ when $\tau > t$ $X(\omega)$ can be written:

$$X(\omega) \quad = \int_{-\infty}^{\infty} d\tau \int_{-\infty}^{\infty} e^{-j\omega\xi} h(\xi) e^{-j\omega\tau} f(\tau) d\xi$$

$$= \int_{-\infty}^{\infty} h(\xi) e^{-j\omega\xi} d\xi \int_{-\infty}^{\infty} f(\tau) e^{-j\omega\tau} d\tau$$

Thus:
$$X(\omega) \quad = H(\omega) f(\omega)$$

36

The complex frequency response function H (ω) of the system shown in Fig.3.1 is found simply by solving the equation of motion for an arbitrary Fourier component, $F_o\, e^{j\omega \tau}$:

$$m \frac{d^2x}{dt^2} + c \frac{dx}{dt} + kx = F_o\, e^{j\omega t}$$

$$\omega = 2\pi f = \text{angular frequency.}$$

At this point the physical meaning of the *complex* frequency response function should be stated. A complex frequency response function means a response function which gives information on *both the absolute value of the response quantity and the phase lag between the response and the excitation*. The general solution to the above equation is:

$$X(\omega) = H(\omega)\, F_o\, e^{j\omega \tau}$$

Here

$$H(\omega) = \frac{1/m}{\omega_o^2 - \omega^2 + j \frac{\omega_o}{Q} \omega}$$

$\omega_o = \sqrt{\dfrac{k}{m}}$ the angular *resonant frequency* of the mechanical system and $Q = \dfrac{1}{c} \sqrt{km}$ is a measure of the system's damping. Q is normally called the
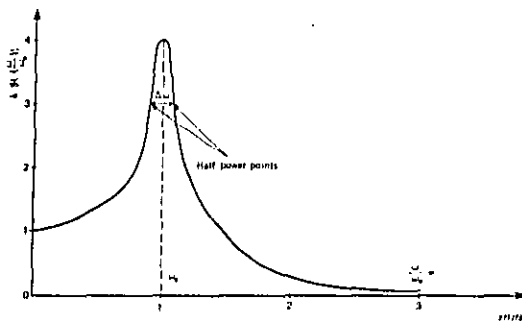
Fig.3.3. *Example of a resonance curve with indication of the half power points*

$$[|H(\omega)| = \sqrt{1/2\, |H(\omega_o)|^2} = 0.707\, |H(\omega_o)|]$$

37

quality factor of the system and the larger the value of Q the smaller is the damping. For a completely undamped system $Q = \infty$ while for a critically damped system $Q = 1/2$. An approximate measure of Q is obtained in practice by measuring the width of the response curve, $|H(\omega)|$, at the half power points, see Fig.3.3.

The half power points are the points on the curve where

$$|H(\omega)|^2 = \frac{1}{2} |H(\omega_0)|^2$$

If this width is $\Delta\omega$ then

$$Q = \frac{\omega_0}{\Delta\omega}$$

For Q-values larger than 5, the error inherent in the approximation is smaller than some 3% (actually, even when Q is as low as 2 the error is of the order of 10%, see also Fig.3.4. Because of its direct relationship to the damping the factor Q has become a very important quantity in the description of single degree-of-freedom linear systems.

The phase lag between the response and the excitation is given by the expression:

$$\varphi = \tan^{-1}\left[\frac{1}{Q\left(\frac{\omega}{\omega_0} - \frac{\omega_0}{\omega}\right)}\right]$$

and this function is plotted in Fig.3.4b) for various values of Q.

a)   b)
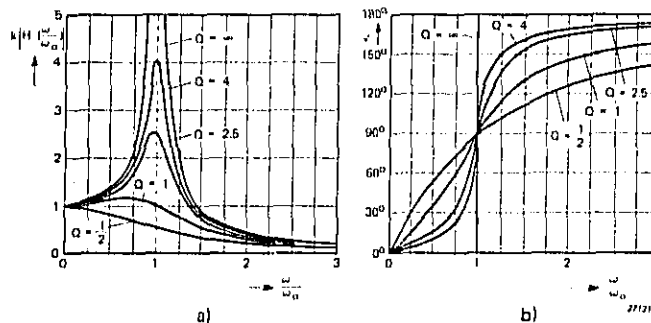
Fig.3.4. Examples of complex frequency response functions
a) Modulus (absolute value of the response)
b) Phase lag between response and excitation corresponding to a)

38

A number of interesting facts can be seen from these curves.

Firstly, in the case of no damping ($Q = \infty$) the response and the excitation are *in phase* ($\emptyset = 0$) *below* resonance, while *above* resonance they are 180° out of phase. Because $Q = \infty$ the change in phase takes place in the form of a discontinuous jump.

Secondly, when $Q \neq \infty$, i.e. damping is introduced in the system, the change in phase between response and excitation tends to take place gradually, and the larger the damping (the smaller Q) the slower is the phase change with frequency around resonance.

Thirdly, independent of the magnitude of the damping, the phase lag between the response and the excitation *at resonance* is 90°.

If the system being studied consists of several masses interconnected with spring and damper elements the approximate measure of Q stated above cannot be utilized unless the coupling between the different masses is so small that a unidirectional motion of one mass does not influence the motion of any of the others (or vice versa).

In general, however, some coupling always exists, even though it might, under certain circumstances be neglected in practice. Systems in which a single mass moves in more than one direction or systems which consist of several, elastically interconnected masses, are commonly termed *multi-degree-of-freedom systems.* A linear multi-degree-of-freedom system can be mathematically described by a set of coupled second-order linear differential equations and when the frequency response curve of the system is plotted it will normally show one resonance "peak" per degree-of-freedom. *Thus a two degree-of-freedom* system shows two resonance peaks, *a three degree-of-freedom system shows three resonance peaks, etc.,* see Fig.3.5.
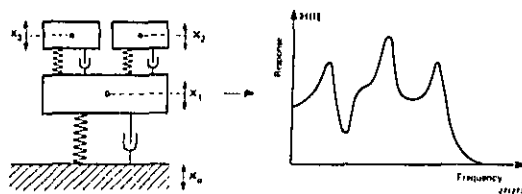
Fig.3.5. Example of a multi degree-of-freedom system (three degrees-of-freedom) and its frequency response function

3.2. Some Response Properties of Non-linear Systems

In the previous section (and in Appendix B) some important response characteristics of linear systems have been discussed, in particular their so-called frequency response functions. These functions can be derived mathematically from the linear differential equation of motion for the system. In the case of a single degree of freedom system this equation was given as

$$m \frac{d^2x}{dt^2} + c \frac{dx}{dt} + kx = f(t)$$

where m, c and k were considered constants, independent of x and t. This requirement is not always fulfilled in practice and the above equation may take the form:

$$m \frac{d^2x}{dt^2} + \beta \left(\frac{dx}{dt}\right) + F(x) = f(t)$$

where

m = mass of the vibrating system

$\beta \left(\frac{dx}{dt}\right)$ = velocity dependent "damping" term

$F(x)$ = displacement dependent "stiffness" term

$f(t)$ = forcing function (see Fig.3.1).

Because this differential equation is no longer linear the principle of superposition cannot be applied and the derivations outlined in section 3.1 are therefore no longer valid. In principle each particular non-linear vibration problem has to be solved on its own. However, certain general properties which are of considerable practical interest may be discussed without actually solving the equation.

Consider for instance the case where only the "stiffness"-term is non-linear. The motion of the mass m is then governed by the equation:

$$m \frac{d^2x}{dt^2} + c \frac{dx}{dt} + F(x) = f(t)$$

By comparing this equation with the one governing linear motion it is seen that the stiffness constant k in the linear equation is no longer constant but depends upon the vibration amplitude x in that k x has been substituted by F (x). As the angular resonant frequency of the linear system is given by

$$\omega_0 = \sqrt{\frac{k}{m}}$$

an obvious conclusion would be that the resonant frequency of the non-
linear system will now depend upon the vibration amplitude (x). That this
really is the case can be confirmed both theoretically and experimentally.
On the other hand, to obtain the exact relationship the non-linear differen-
tial equation has to be rigorously solved.

Fig.3.6 shows some examples of the possible dependency of F (x) upon
x. If the spring becomes "stiffer" by deflection it is normally termed a
"hardening" spring while if it becomes less stiff by deflection it is termed a
"softening" spring.
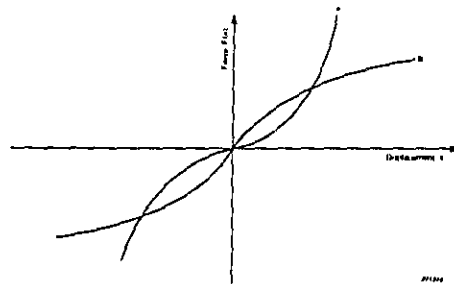
Fig.3.6. Force vs. displacement characteristics for some symmetrical spring
arrangements:
a) Hardening type spring
b) Softening type spring

In the case of a "hardening" spring k will increase with vibration ampli-
tude thus causing the resonance to move towards higher frequencies. Con-
versely, if k decreases with increasing vibration amplitude the resonance will
move towards lower frequencies. Fig.3.7 illustrates how the resonance curve
depends upon the spring characteristics and the vibration amplitude.

It is seen from the figure that resonance systems containing non-linear
stiffness show a bend in their resonance curves. This bend is, of course, only
theoretical as the vibrating system cannot "force" the frequency of the
driving force. In actual physical systems the bend therefore produces a
region of instability as indicated in Fig.3.8. When the frequency response
curve of such a system is measured by slowly sweeping the frequency of the
driving force past resonance, certain jumps in the response amplitude occur,
the frequency location of the jump being dependent both upon the magni-

41
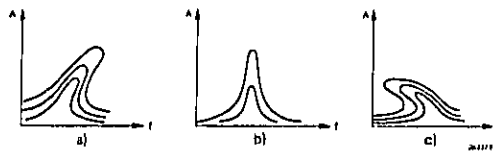
Fig.3.7. Typical resonance curves for various levels of excitation for:
a) A hardening spring type resonant system
b) A linear resonant system
c) A softening spring type resonant system
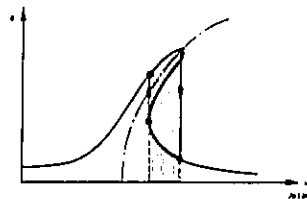
Fig.3.8. Theoretical frequency response curve for a hardening spring type resonant system. The hatched areas indicate the region of instability

tude of the driving force and upon the direction of the frequency sweep. Actual curves obtained from analog model studies are shown in Fig.3.9.

A further property of non-linear systems is that they distort the wave-shape of the response signal, i.e. even if the force driving the system is purely sinusoidal the wave-shape of the response will not be sinusoidal, see also Appendix C. Normally the response wave-shape will contain a number of frequency components harmonically related to the frequency of the driving force. This can be confirmed mathematically for instance, by approximating the solution to the non-linear differential equation by means of a series expansion, and experimentally by analyzing the response wave-shape by means of an analog frequency analyzer.

Under certain circumstances (very low damping) a very special
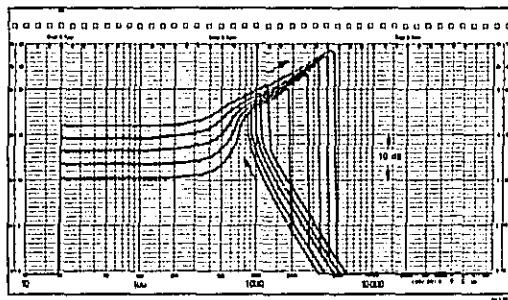
Fig.3.9. Frequency response curves for a hardening spring type resonant system. The curves were measured for various levels of excitation of an analog model system

phenomenon occurs in nonlinear resonance systems of the type described above. This is the phenomenon of subharmonics. A subharmonic is a response vibration occurring at 1/2, 1/3, 1/4, 1/5 etc. of the frequency of the driving force. A physical explanation for the occurrence of subharmonics may be given in that the driving force supplies energy to one of the harmonics of the non-linear system and when energy is supplied it will start to oscillate. The higher harmonic then pulls all the other harmonics with it, as the specifically excited harmonic is an integral part of the whole motion.

While the occurrence of subharmonics in practice is relatively rare, "ordinary" harmonics (sometimes called superharmonics) are present to a greater or lesser extent in all non-linear systems. Even if their amplitude values are rather small they may play an important role when the vibration of complex (multi-degree-of-freedom) mechanical systems are considered. An example readily illustrates this statement:

Consider for instance the case where a non-linear spring element in a multi-degree-of-freedom system produces a third harmonic of the order of 1%. If the frequency of this harmonic by chance coincides with the resonant frequency of another resonance in the system which happens to have a resonance amplification factor Q = 100 this specific resonance will respond with the same amplitude as the actually excited resonance even though its frequency did not exist in the wave-shape of the driving force!

43

Finally*), if the non-linearity is velocity-dependent only, i.e. the equation of motion for the system can be written:

$$m \frac{d^2x}{dt^2} + \beta \; (\frac{dx}{dt}) + kx = f(t)$$

a somewhat different situation exists.

Also in this case the production of harmonics varies with frequency and excitation level, but the resonant frequency itself remains practically constant. A special case occurs when the damping is negative, in that in this case the system oscillates. Examples of systems where these kinds of self-sustained oscillations may take place are the flutter of aeroplane wings, oscillations in electrical transmission lines due to the action of the wind and some cases of Coulomb friction. One of the most disastrous cases of damage caused by self-sustained oscillations is the failure of the Tacoma Bridge in 1940.

3.3. Rotational and Torsional Vibrations

In the previous sections of this Chapter the vibration responses considered have been of the so-called *translational type*, i.e. the vibrating masses have been oscillating rectilinearly along one (or more) axis only.

Another type of motion occurs when a body is forced to vibrate around one (or more) axis, such as is often the case for instance in rotating machinery or unsymmetrically loaded machine foundations. The simplest form of rotational vibrations may be that of torsional vibrations in a shaft, see Fig.3.10a). Assuming that the inertia of the shaft itself is negligible compared with the inertia of the mass, m, and that the elastic behaviour of the mass can be neglected in comparison with the torsional elasticity of the shaft, the equation of free rotational motion for the system can be written:

$$I \cdot \frac{d^2\varphi}{dt^2} + c' \frac{d\varphi}{dt} + k' \; \varphi = 0$$

Here I is the moment of inertia of the mass around its center of rotation, i.e. (around the shaft), φ is the angle of motion, c' is a damping constant and k' is the angular stiffness of the shaft, which depends upon the modulus of elasticity in shear and of the physical shaft configuration.

---

*) The case of non-linear masses in resonating systems have, to the authors knowledge, not seemed to be of any great interest in practice and is therefore not treated in this text.
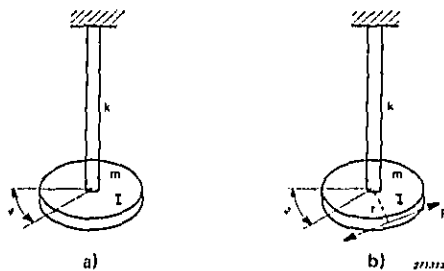
Fig.3.10. Examples of torsional vibration
a) Free vibration
b) Forced vibration

It can be seen that the differential equation governing the angular motion of the mass in Fig.3.10 has a completely analogous form to that governing rectilinear motion and which was given in section 3.1. This means that exactly the same mathematical treatment as discussed in section 3.1 can be applied to the rotational vibrations of the kind described above. The only differences are that the mass in section 3.1 must be substituted by the moment of inertia, and the (rectilinear) displacement, x, by the angle φ. If external forces are applied to the system their effects on the rotational motion are measured by the *torque*, M, that they produce Fig.3.10b). The corresponding equation of motion is:

$$I\frac{d^2\varphi}{dt^2}+c'\cdot\frac{d\varphi}{dt}+k'\cdot\varphi = M = F\cdot r$$

$I = \int_m r^2\,dm$
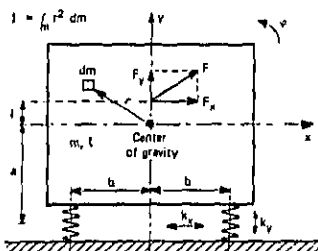
Force equations:

$$m\frac{d^2x}{dt^2} = -k_x\,x - k_x\,a\,\varphi + F_x$$

$$m\frac{d^2y}{dt^2} = -k_y\,y + F_y$$

Torque equation:

$$I\frac{d^2\varphi}{dt^2} = -k_x\,a\,x - k_x\,a^2\,\varphi - k_y\,b^2\,\varphi - F_x\,l$$

Fig.3.11. Model of an unsymmetrically loaded foundation, and the corresponding equations of motion

45

Thus, rotational motions are governed by torque equations, while recti-linear motions are gover^ :d by force equations.

A second example of rotational motion is, as mentioned above, that of an unsymmetrically loaded foundation. This case is illustrated in Fig.3.11, and plays an important role in the vibration and shock isolation of machines and equipment, see also Chapter 7, section 7.1.

3.4. Response of Mechanical Systems to Stationary Random Vibrations

In section 3.1 it was shown that the response of any linear system to a prescribed excitation can be determined from a knowledge of the system's impulse response function or its complex frequency response function. If now the excitation consists of a Gaussian random process characterized by means of its auto-correlation function (or, what may be more common in practice, by means of its mean square spectral density function) what would the relationship between the excitation and the response then be?

Starting with the auto-correlation function representation of the response this can be formulated in terms of the system's impulse response function:

$$x(t) \, x(t+\tau) = \int_{-\infty}^{\infty} f(t-\tau_1) \, h(\tau_1) \, d\tau_1 \int_{-\infty}^{\infty} f(t+\tau-\tau_2) \, h(\tau_2) \, d\tau_2$$

$$= \iint_{-\infty}^{\infty} f(t-\tau_1) \, f(t+\tau-\tau_2) \, h(\tau_1) \, h(\tau_2) \, d\tau_1 \, d\tau_2$$

(The formulation of the impulse response function is here slightly different from the one utilized previously. However, by studying Fig.3.2 and the connected mathematics it is easily seen that the two formulations are equivalent). As the auto-correlation function is by definition:

$$\psi_x(\tau) = \lim_{T \to \infty} \frac{1}{T} \int_0^T x(t) \, x(t+\tau) \, dt$$

$$= \lim_{T \to \infty} \frac{1}{T} \int_0^T \left[\iint_{-\infty}^{\infty} f(t-\tau_1) \, f(t+\tau-\tau_2) \, h(\tau_1) \, h(\tau_2) \, d\tau_1 \, d\tau_2 \right] dt$$

then

$$\psi_x(\tau) = \iint_{-\infty}^{\infty} \psi_f(\tau+\tau_1-\tau_2) \, h(\tau_1) \, h(\tau_2) \, d\tau_1 \, d\tau_2$$

which can be seen by setting $f(t+\tau-\tau_2) = f(t-\tau_1+\tau-\tau_2+\tau_1)$

where $\tau - \tau_2 + \tau_1$ represents time lag in the multiplication process used to obtain the auto-correlation function for the excitation. The response mean square spectral density function is found by taking the Fourier transform of $\psi_x(\tau)$:

$$w_x(\omega) = \int_{-\infty}^{\infty} \psi_x(\tau)\, e^{-j\omega\tau}\, d\tau$$

or what is the same:

$$w_x(\omega) = \int_{-\infty}^{\infty} \psi_x(\tau)\, e^{-j\omega(\tau+\tau_1-\tau_2)}\, e^{j\omega\tau_1}\, e^{-j\omega\tau_2}\, d\tau$$

and inserting the formula given above for $\psi_x(\tau)$ into this expression:

$$w_x(\omega) = \left[\int_{-\infty}^{\infty} h(\tau_1)\, e^{j\omega\tau_1}\, d\tau_1 \int_{-\infty}^{\infty} h(\tau_2)\, e^{-j\omega\tau_2}\, d\tau_2 \right] w_f(\omega)$$

as

$$w_f(\omega) = \int_{-\infty}^{\infty} \psi_f(\tau+\tau_1-\tau_2)\, e^{-j\omega(\tau+\tau_1-\tau_2)}\, d\tau$$

thus: $\quad w_x(\omega) = H^*(\omega)\, H(\omega)\, w_f(\omega) = |H(\omega)|^2\, w_f(\omega)$

where $H^*(\omega)$ is the complex conjugate of $H(\omega)$. This result is one of the most important ones in the theory of random processes and states that *the response mean square spectral density of a linear system at any frequency is equal to the excitation mean square spectral density times the square of the complex frequency response function at that frequency.* That a relationship of this kind was to be expected is also intuitively felt by considering the meaning of the mean square spectral density function and the relationship found in section 3.1 between the excitation and the response in terms of the complex frequency response function, $H(\omega)$.

The response mean square spectral density function may, from a measurement point of view, be considered either as a frequency *spectrum* or as a system *response function* depending upon the problem at hand.

If the system being considered is non-linear the relationships stated above do, of course, no longer hold as those relationships were built on the general superposition principle which is only valid for linear systems whose motion is governed by linear differential equations. The mean square spectral density function for the response is therefore no longer a unique function but changes with excitation level. Also the probability density function for instantaneous response amplitudes is no longer Gaussian and in general a

47

vast amount of data· is necessary to characterize the response of such systems to Gaussian random excitations.

If the non-linearity is situated in the stiffness element of the system considered, it is possible in some important cases to formulate and solve exactly the stochastic equations describing the probability density functions of the response. In general, however, some sort of linearization technique has to be used in a theoretical treatment. A considerable amount of theoretical and experimental work has been laid down in this area in the past decade or so and interested readers are referred to the literature listed at the end of this chapter for further studies.

3.5. Shock Response and Shock Spectra

In section 2.3 a shock was defined as a transmission of kinetic energy to a system, the transition taking place in a relatively short time compared with the natural period of oscillation of the system. A rectangular shock pulse may therefore constitute one or two shocks depending upon the natural period of oscillation of the system influenced by it and the duration of the pulse. This is illustrated in Fig.3.12 I and II), and it should be noted that the maximum system response may in the case of Fig.3.12 I reach a value which is twice the magnitude of the shock pulse.

A concept which has proved to be of considerable value with respect to the comparison of shock motions, to the design of equipment to withstand shocks, and to the formulation of laboratory tests as a means to simulate
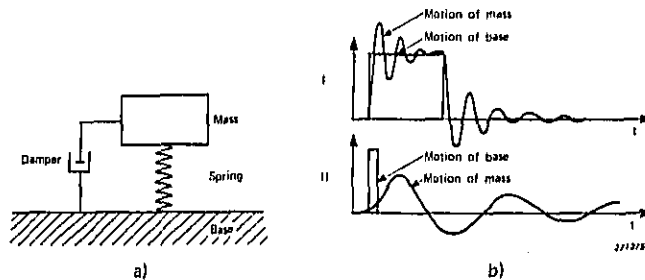
Fig.3.12. Response of a single degree-of-freedom system to shock excitation

48

environmental conditions is the *shock response spectrum,* or briefly the *shock spectrum* (Note: This is not to be confused with the Fourier spectrum of the forcing shock pulse). The shock spectrum is obtained by letting the shock pulse in question be applied to a linear, undamped single degree-of-freedom system and plotting for example the maximum response of the system as a function of the system's natural frequency.

Various types of shock spectra are used depending upon the intended application of the information obtained. These may be the initial shock spectrum which is obtained from the maximum response while the shock pulse is still acting, or the residual shock spectrum which is obtained from the maximum response after the pulse has occurred.

Other definitions may be the overall or maximax spectrum which is plotted on the basis of the maximum response without regard to time, and the overall negative maximum shock spectrum which is obtained by considering the maximum response of the single degree-of-freedom system in the negative direction.

In practical measurement systems the requirement of zero damping in the responding single degree-of-freedom system may be difficult to achieve. However, for relatively small amounts of damping the shock spectra will not be essentially different from the spectra obtained with no damping, since the response for the first few cycles will be virtually identical. The response of an undamped single degree-of-freedom system to a shock pulse can be calculated relatively easily for simple shock wave forms, using for example
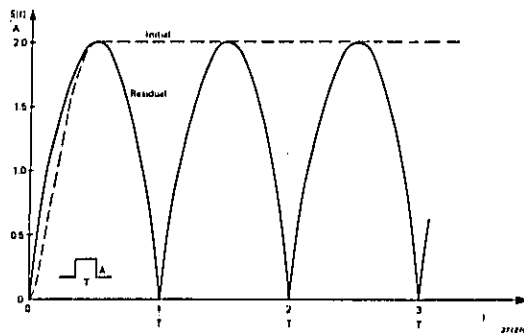
Fig. 3. 13.   Shock spectra for a rectangular shock pulse

49

Laplace transform methods. Figs.3.13, 3.14 and 3.15 illustrate shock spectra obtained for a rectangular, sawtooth and halfsine shock pulse of duration T. The maximax shock spectra are found simply by taking the highest of the two spectrum values at any frequency.

It may be worth while in connection with the discussion of shock spectra to point out an interesting fact, namely that the Fourier spectrum of the shock pulse and the undamped residual shock spectrum are related by the formula:

$$S(f) = 2 \pi f |F(f)|$$

where S (f) designates the residual shock spectrum and F (f) is the Fourier spectrum of the shock (see also Appendix D).
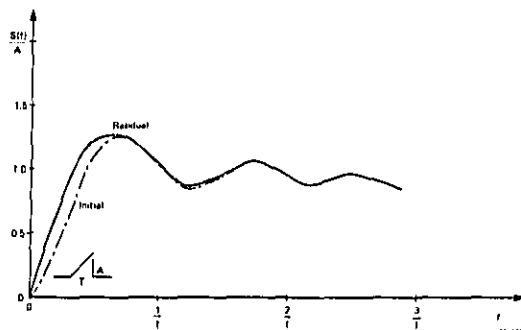
Fig.3.14. Shock spectra for a final peak sawtooth shock pulse
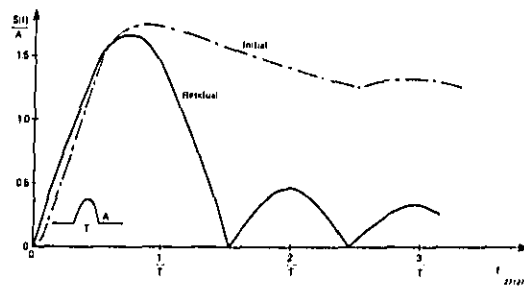
Fig.3.15. Shock spectra for a halfsine shock pulse

50

3.6. Vibrations in Structures. Mechanical Waves

The mechanical systems considered in the preceding text have been of the so-called idealized lumped parameter type, i.e. masses have been assumed to be rigid bodies where all points within the body move in phase, and elastic elements have been assumed to have no mass. In practice all masses have a certain elasticity and all spring elements have masses. For instance a beam or a plate is a continuous combination of masses and springs.

As the number of degrees-of-freedom of a mechanical system was defined as the number of elastic movements of masses (resonances, see section 3.1) it follows that structures like beams and plates *have an infinite number of degrees-of-freedom.* The infinite number of "resonances" resulting from the infinite number of degrees-of-freedom are in the case of structures normally termed *"natural modes"*, or simply "modes".

While in lumped parameter systems all points within a mass are supposed to move in phase, this is no longer true for structures. A simple example illustrates this clearly: In Fig.3.16 the vibration of a beam clamped at one end and acted upon by an oscillating force in the other is shown. When the frequency of the oscillating force coincides with one of the beam's modes, the vibration pattern of the beam forms a "standing wave", as shown in the figure. It is readily seen that the points within the beam at the place marked x_1 here move in opposite phase with respect to the points at the place marked x_2. One of the major differences between the motion of a lumped parameter system and a structure is thus that in the case of structures each resonance is associated with a *mode shape.*
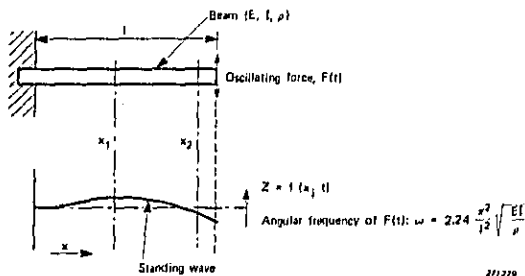
Fig.3.16. *Illustration of the response of a beam to an oscillating force the frequency of which coincides with one of the beam's natural vibration modes*

51

To describe for instance the motion of the beam in Fig.3.16 it is therefore not enough to describe the instantaneous vibration amplitude , z, as a function of t (time) only. It must also be described as a function of space coordinates, in this case x, i.e. z = f (x; t).

In deriving the differential equation governing this motion it is necessary to apply partial differentials and the equation becomes a *partial differential equation.* Similarly the equation of motion for a plate, Fig.3.17 will be of the type: z = f (x; y; t).
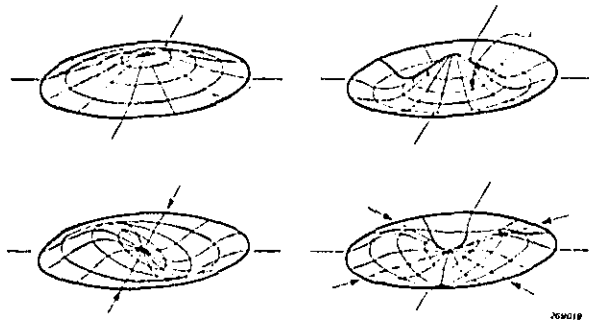
Fig.3.17. Shapes of a few of the normal modes of vibration of a circular plate clamped at its edge. (After Morse)

The examples shown in Fig.3.16 and 3.17 illustrate *transverse vibrations.* Also *compressional* and *torsional* vibrations may be excited in structures, Fig.3.18, and a combination of all three types of vibrations may take place. The vibrations in structures may therefore be exceedingly complex and exact solutions to the differential equations of motion exist only for a few types of simple structures and load configurations.

A more comprehensive theoretical treatment of structural vibrations is outside the scope of this book, but can be found in many excellent textbooks on the subject (see also the bibliography at the end of the Chapter). It has been deemed appropriate, however, to illustrate some typical mode shapes for transverse vibrations of simple beams and plates.

52
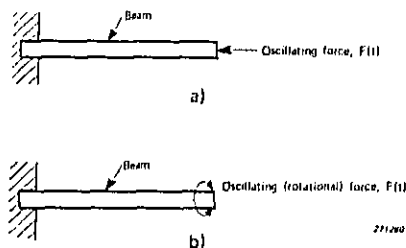
Fig.3.18. Illustration of compressional and torsional vibrations of a beam
a) Compressional vibration
b) Torsional vibration

From the theory of bending of beams and Newton's second law of motion the differential equation governing the free transverse vibrations of a beam can be found:

$$-\frac{\rho S}{g} \times \frac{\partial^2 z}{\partial t^2} + \frac{\partial^2}{\partial x^2}(E I \frac{\partial^2 z}{\partial x^2}) = 0$$

where: ρ = Mass density of the beam material
S = Cross-sectional area of the beam
g = Acceleration of gravity
E = Modulus of elasticity (Young's Modulus)
I = Moment of inertia of the cross-section

This is a *fourth-order partial differential equation* the solution of which depends upon the boundary conditions, i.e. the way in which the beam is fastened. Fig.3.19 shows some examples of boundary conditions and corresponding mode shapes for the first four natural vibration modes.

The infinite number of degrees-of-freedom mentioned above manifest themselves by the fact that there is an infinite number of higher natural vibration modes. In general, however, only a few of the lower modes seem to be of great practical interest.

In the case of free transverse vibrations of plates the equation of motion is again a fourth-order partial differential equation, still more complicated to solve than the one governing the vibration of beams:

$$\frac{\partial^4 z}{\partial x^4} + 2 \frac{\partial^4 z}{\partial x^2 \partial y^2} + \frac{\partial^4 z}{\partial y^4} + \frac{12 \rho (1 - \mu^2)}{E h^2 g} \frac{\partial^2 z}{\partial t^2} = 0$$

53

Clamped − free (Cantilever)	A = 3.52	0.774 A = 22.4	0.500 0.868 A = 61.7	0.356 0.644 0.906 A = 121.0
Hinged − hinged (Simple)	A = 9.87	0.500 A = 39.5	0.333 0.667 A = 88.9	0.25 0.50 0.75 A = 158
Clamped − clamped (Built-in)	A = 22.4	0.500 A = 61.7	0.359 0.641 A = 121	0.278 0.500 0.722 A = 200
Free − free	0.224 0.776 A = 22.4	0.132 0.500 0.868 A = 61.7	0.094 0.356 0.644 0.906 A = 121	0.073 0.277 0.500 0.723 0.927 A = 200
Clamped − hinged	A = 15.4	0.560 A = 50.0	0.384 0.692 A = 104	0.294 0.529 0.765 A = 178
Hinged − free	0.736 A = 15.4	0.446 0.853 A = 50.0	0.308 0.616 0.898 A = 104	0.235 0.471 0.707 0.922 A = 178

Fig.3.19. *Examples of boundary conditions and mode-shapes for various single uniform beam configurations*

where h is the thickness of the plate and μ is Poisson's ratio (about 0.3 for most engineering materials).

Fig.3.17 illustrates the shapes of some of the first normal modes of a circular plate clamped at its edges, while examples of modal lines of square plates with various edge conditions are shown in Fig.3.20. Note from Fig.3.19 and 3.20 that the frequencies of the normal modes in structural members are in general not harmonically related.

There are, however , other types of vibrations in structures which are, at least to a first approximation, harmonically related. These are compressional (longitudinal) vibrations, and in certain cases also torsional vibrations.

In setting up the equation of motion for compressional vibrations in a

	1st Mode	2nd Mode	3rd Mode	4th Mode	5th Mode	6th Mode
$\omega_n / \sqrt{Dg/\rho ha^4}$	3.494	8.547	21.44	27.46	31.17	
Nodal lines						
$\omega_n / \sqrt{Dg/\rho ha^4}$	35.99	73.41	108.27	131.64	132.25	165.15
Nodal lines						
$\omega_n / \sqrt{Dg/\rho ha^4}$	8.958	24.08	28.90	48.05	63.14	
Nodal lines						

$\omega_n = 2\pi f_n$ ρ = Weight density   a = Plate length

$D = Eh^3/12(1-\mu^2)$ h = Plate thickness

Fig. 3.20.   *Examples of modal line configurations for square plates under various edge conditions. (After D. Young)*

beam, Fig. 3.21, it is noted that the result is a *second order partial differential equation* of the type:

$$\frac{\partial^2 \xi}{\partial x^2} = \frac{\rho}{E\,g} \frac{\partial^2 \xi}{\partial t^2}$$

$d\xi = \frac{\partial \xi}{\partial x}\,dx \;\; = \epsilon = \frac{\sigma_x}{E}; \qquad \sigma_x = E\frac{\partial \xi}{\partial x}; \qquad \frac{\partial \sigma_x}{\partial x} = E\frac{\partial^2 \xi}{\partial x^2}$

$\sigma_x + \frac{\partial \sigma_x}{\partial x}\,dx \qquad d\sigma_x = \frac{\partial \sigma_x}{\partial x}\,dx$

Also: $d\sigma_x = dm\,\frac{\partial^2 \xi}{\partial t^2} = \frac{\rho}{g}\,dx\,\frac{\partial^2 \xi}{\partial t^2}$

Thus: $\frac{\partial \sigma_x}{\partial x}\,dx = \frac{\rho}{g}\,dx\,\frac{\partial^2 \xi}{\partial t^2}; \qquad \frac{\partial^2 \xi}{\partial x^2} = \frac{\rho}{E\,g}\,\frac{\partial^2 \xi}{\partial t^2}$
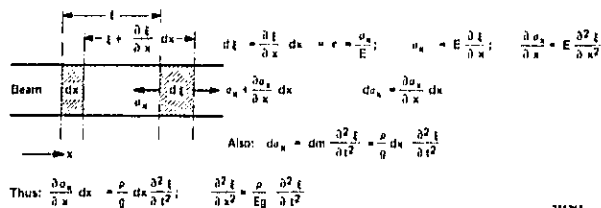
Fig. 3.21.   *Sketch showing the derivation of the equation of motion for compressional (longitudinal) vibrations in a beam*

55

This equation has the same form as the so-called wave-equation which governs various kinds of wave phenomena in theoretical physics. Compressional vibrations are therefore also often referred to as *mechanical waves* with a wave velocity (v) of:

$$\frac{1}{v^2} = \frac{\rho}{E\,g}; \qquad v = \sqrt{\frac{E\,g}{\rho}}$$

The main reason for the inclusion of this brief section on structural vibrations in the book has been to illustrate that *the actual vibrations measured on a complicated construction may be widely different from point to point even if the measuring points considered are situated a relatively short distance apart from each other.* Also, the direction in space of the vibrations may vary and for thorough investigations it is therefore necessary to measure the vibrations both as a function of frequency and as a function of space coordinates at each measuring point.

3.7. Selected Bibliography

BENDAT, J.S. and PIERSOL, A.G.:	Measurement and Analysis of Random Data. John Wiley and Sons, Inc. New York 1965.
BROCH, J.T.:	Non-Linear Amplitude Distortion in Vibrating Systems, Brüel & Kjær Tech. Rev. No. 4-1963.
BROCH, J.T.:	Random Vibration of Some Non-Linear Systems. Brüel & Kjær Tech. Rev. No. 3-1964.
CRANDALL, S.H. and MARK, W.D.:	Random Vibrations in Mechanical Systems. Academic Press. New York 1963.
CRANDALL, S.H. et al.:	Random Vibrations I and II. The M.I.T. Press and John Wiley and Sons, Inc. 1958 and 1963.
Den HARTOG, J.P.:	Mechanical Vibrations. McGraw-Hill Book Company, Inc. 1961.
HAYASHI, C.:	Forced Oscillations in Non-Linear Systems. Nippon Pub. Co., Osaka, Japan. 1953.
JACOBSEN, L.S. and AYRE, R.S.:	Engineering Vibrations. McGraw-Hill Book Company, Inc. 1958.
KARMAN, T. and BIOT, M.A.:	Mathematical Methods in Engineering. McGraw-Hill Book Company, Inc. 1940.

KER WILSON, W.:   Vibration Engineering. C. Griffin & Company,
                         Ltd., London 1959.

KITTELSEN, K.E.:   Measurement and Description of Shock. Brüel &
                         Kjær. Tech. Rev. No. 3-1966.

Mc LACHLAN, N.W.:   Ordinary Non-Linear Differential Equations in
                         Engineering and Physical Sciences. Oxford at the
                         Clarendon Press, 1958.

MINORSKY, N.:   Introduction to Non-Linear Mechanics. Edwards
                         Bros., Ann Arbor, Mich. 1947.

MORROW, C.T.:   The Shock Spectrum as a Criterion of Severity of
                         Shock Impulses. J.A.S.A. Vol.29, No. 5, May
                         1957.

MORROW, C.T.:   Shock and Vibration Engineering. John Wiley
                         and Sons, Inc. 1963.

MORSE, P.M.:   Vibration and Sound. McGraw-Hill Book
                         Company, Inc. 1948.

ROBSON, J.D.:   An Introduction to Random Vibration, Edin-
                         burgh University, Press 1963.

SALTER, J.P.:   Steady State Vibration, Kenneth Mason Book
                         Co., England 1969.

STOKER, J.J.:   Non-Linear Vibrations in Mechanical and Elec-
                         trical Systems. Interscience Publishers, Inc. New
                         York, 1950.

THOMSON, W.T. and   The Response of Mechanical Systems to Random
BARTON, M.V.:   Excitation. J. Appl. Mech. Vol. 24, p. 248 –
                         251, 1957.

VIGNESS, I.:   Elementary Considerations of Shock Spectra.
                         Shock, Vibration and Associated Environments,
                         Bulletin 34, 1965, Part 3.

YOUNG, D.:   Vibration of Rectangular Plates by the Ritz
                         Method. J. Appl. Mechanics. Vol. 17, p. 448,
                         1950.

4. EFFECTS OF VIBRATIONS AND SHOCK ON MECHANICAL SYSTEMS AND MAN

4.1. Damaging Effects of Vibrations. Mechanical Fatigue.

Even though mechanical failure due to material fatigue is by far the most commonly known deteriorating effect of vibrations, a vibrating mechanical construction may fail in practice for other reasons as well. Failure may, for instance, be caused by the occurrence of one, or a few, excessive vibration amplitudes (brittle materials, contact-failures in relays and switches, collisions between two vibrating systems etc.), — or by the fact that a certain vibration amplitude value is exceeded in too great a fraction of time.

However, the importance of mechanical fatiguing effects has initiated a considerable amount of research and testing around the world. It has therefore been deemed appropriate to include a section here which deals with this particular topic.

The fatigue phenomenon is today deemed to originate from local yield in the material or, in other words, from a *sliding of atomic layers.* This sliding is caused by a combination of so-called "dislocations" (irregularities in the crystalline structure of the material) and local stress concentrations. It is now assumed that each slip, no matter how small, is connected with a small deterioration of the material, independent of the direction of the slip. The deterioration stops only when the slip stops. Some definite proof for this hypothesis has, to the author's knowledge, not been established as yet (1971). It gives, however, a logical and reasonable explanation for the formation of the microscopic "slip bands" which is the first visible sign of material fatigue.

When slip bands have been formed they are, under continuous vibration loading, observed to progress and form minute cracks which eventually join together and produce major cracks. As soon as a crack has reached a certain size it will propagate through the material according to a mathematical law of the form:

$$\frac{dx}{dN} = c \, e_r^{m} \, x^{n}$$

where   x = crack length
          N = number of stress reversals
   c, m, n = constants dependent upon the material properties
               (a reasonable assumption seems in many cases to be
               $m = 2$, $n = 1$)
         e_r = relative strain

Finally the crack will become so large that the stress in the remaining material becomes too great, whereby the crack propagation becomes unstable, and fatigue failure occurs.

Even though it is possible to describe a certain part of the fatiguing process by means of a relatively simple mathematical expression (see formula above) both the formation of "slip bands" and the final crack instability stages are of a highly statistical nature. Taken as a whole, therefore, *fatigue failures must be regarded as statistical phenomena.*

The statistical nature of the phenomenon manifests itself as a considerable spread in the results of fatigue experiments. As an example of the result of such experiments Fig.4.1 shows a histogram made from investigations on the fatigue life of notched aluminium specimens. The results shown were obtained from tests at a single vibration stress level.

By making similar tests at a number of vibration stress levels, a curve, commonly termed the S-N curve (Wöhler-Kurve) can be obtained, which shows the relationship between *the average number of stress reversals to failure and the vibration stress level.*
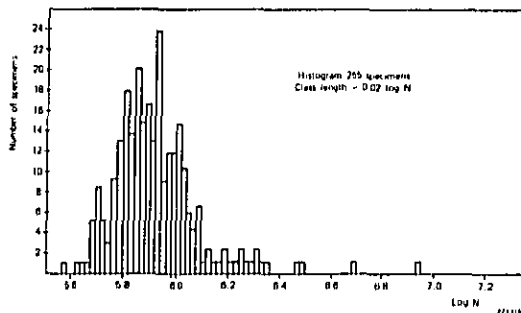

Fig.4.1. Typical histogram obtained from fatigue experiments (after Bloomer and Roylance)
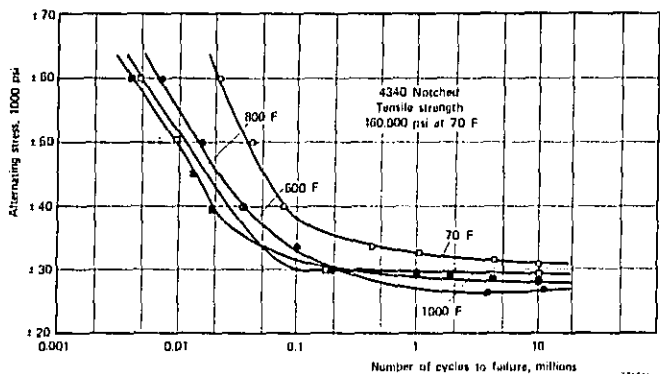
Fig.4.2. Fatigue strength curves for notched 4340 steel (from Metals Hand-book)

The actual S-N curve for a material does not only depend upon the vibrational effects, but is affected also by factors such as temperature, atmospheric conditions (corrosional effects), pre-treatment of the material, etc. Fig.4.2 illustrate a set of S-N curves valid for 4340 steel under normal atmospheric conditions. The curves shown are based on pure harmonic vibration loading only. In practice, however, a mechanical part, or material, is very rarely, if ever, subjected to pure harmonic vibrations of constant maximum amplitude during its complete "life".

To try and take varying amplitudes into account in theoretical estima-tions of the average fatigue life a "rule" of linear accumulation of damage has been suggested (Palmgren, Minor):

$$D = \Sigma \frac{n_i}{N_i}$$

Here n_i is the actual number of stress reversals at a vibration stress level which requires a total number of stress reversals, N_i, to failure. Failure should thus occur when $D = 1$. By using the above expression, and a mathematical approximation to the S-N curve of the form

$$NS^b = a$$

it is sometimes possible to establish a closed mathematical formula for D.

60

Two conditions which have to be fulfilled when use is to be made of the formulae for D and the S-N curve are, however, that each stress reversal has an approximately sinusoidal wave-shape and that the mean stress is zero. These conditions are fulfilled, for instance, by the vibrational stresses occurring in a linear single degree-of-freedom system excited by random vibrations see Fig.4.3.
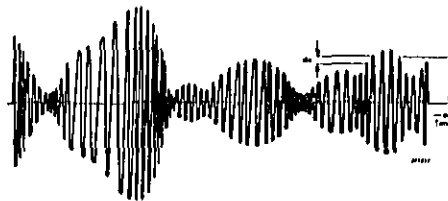
Fig.4.3. *Illustration of the stress-versus-time trace produced in a single degree-of-freedom system excited by random vibrations*

Furthermore, in such systems the statistical distribution of maximum vibration amplitudes (peaks) can be mathematically described by means of the so-called *Rayleigh-distribution*, Fig.4.4:

$$p\,(x)\,dx = \frac{x}{\sigma^2}\,e^{-\frac{x^2}{2\sigma^2}}\,dx$$

where $p\,(x)\,dx$ is the probability of occurrence of peaks within the infinitely small amplitude "window" dx (Figs.4.3 and 4.4). As the total number of peaks occurring within dx is $n(x) = f_o \cdot T \cdot p(x)dx$, and the partial fatigue damage caused by these stress reversals around the vibration level x is

$$Dx = \frac{n\,(x)}{N\,(x)} = f_o \cdot T \frac{p\,(x)\,dx}{N\,(x)}$$

the accumulated damage over all vibration peak levels during the period of time, T, is:

$$D = \Sigma \frac{n\,(x)}{N\,(x)} = f_o\,T\,\int_0^\infty \frac{p\,(x)\,dx}{N\,(x)}$$

Utilizing now the mathematical approximation to the S-N curve as well as the expression for the Rayleigh distribution of stress reversals given above, the total time to failure (D = 1) can be estimated by solving the integral in the formula for D:
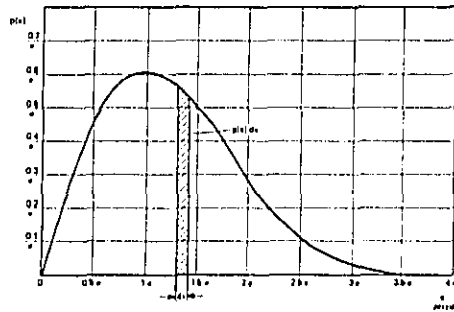
Fig.4.4. *Typical peak probability density curve for narrow band random vibrations (Rayleigh distribution)*

$$T = \frac{a}{f_o \, (\sqrt{2} \, \sigma)^b \cdot \Gamma \, (1 + \frac{b}{2})}$$

where Γ is the gamma-function tabulated in most reference books on mathematical functions.

In the case of common engineering materials b takes values between 3 and 8 (Steel b = 3.5; Tinbronze 80% Cu — 16% Sn — 10% Pb, b = 7.5.)

Even though the formula for T given above has been derived on the basis of stress vs. time histories of the kind shown in Fig.4.3 it may also be used to a first approximation in more complicated cases. If, for instance, the stress time history on a critical point in a construction looks somewhat like the trace shown in Fig.4.5 one could assign an "average frequency", f_o, to the vibrations based on the average number of zero-crossings per unit time. *Using this frequency in the above formula together with the overall RMS-value of the dynamic stress, the resulting average time to failure gives a conservative estimate.*

The problem of random load fatigue has been studied quite extensively over the past 15 to 20 years, and interested readers are referred to the selected bibliography cited at the end of the Chapter, in particular to the Brüel & Kjær Technical Reviews No. 1—1968 and No. 4-1968.
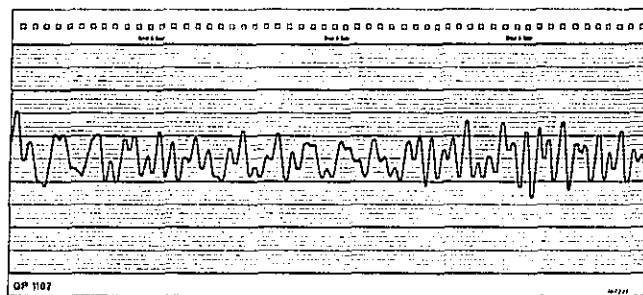
Fig.4.5. Typical stress-versus-time trace at a "critical point" on a complicated structure

4.2. Vibration of Rotating Bodies. Balance Quality

Unbalance in rotating machinery may be one of the most frequent causes of vibration. However, in many cases the vibrations caused by a small amount of unbalance may not be too serious.

On the other hand, in cases involving large machinery rotating at high speed the problem of unbalance becomes critical.

There are basically two different "kinds" of unbalance occurring in practice: Unbalance in one plane, so-called "static unbalance" and unbalance in two or more planes commonly termed "dynamic unbalance".

To illustrate the phenomenon of static unbalance consider Fig.4.6. The rotor is here assumed to consist of a rigid disc, for instance a fly-wheel. If the center of gravity of the "disc" does not coincide with the shaft center (center of rotation) the disc will vibrate during rotation and cause vibrational forces to be transmitted to the bearings. These vibrations can be eliminated by adding mass to the light side of the disc opposite to the mass-load causing the unbalance, see Fig.4.6. As the centrifugal forces acting on the added mass must be exactly equal in magnitude and opposite in direction to the centrifugal forces causing the original unbalance the following relationship holds (Fig.4.6).

$$m \times r = M \times e$$

63
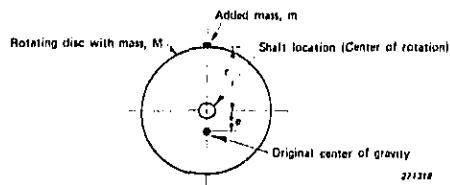
Fig.4.6. *Example of static unbalance and how it can be remedied*

The reason why this kind of unbalance is termed "static unbalance" is that the problem of determining the location of the balancing mass, m, is basically a problem of statics: When the disc is not rotating, and the axis of rotation is horizontal, the disc will place itself in a position where the center of gravity lies on a vertical line through the center of rotation, (Fig.4.7a). The correction mass (weight) can now be placed on top of the disc, the amount of mass necessary to achieve the required balance being that which brings the disc into indifferent equilibrium, Fig.4.7b).
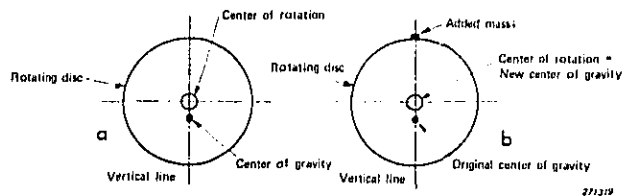

Fig.4.7. *Illustration of the simplest method of static balancing*
a) "Natural" position of the non-rotating unbalanced disc
b) Sketch illustrating the result of static balancing of the disc. (The center of gravity of the disc now coincides with the center of rotation)

If the rotor is no longer of the rigid *disc* type but rather a *rigid elongated body* as shown in Fig.4.8, not *only* a center-of-gravity-displacement kind of unbalance may be present, but also an unbalanced *couple* may affect the motion of the rotor, see Fig.4.8b). It is then required to carry out balancing in *two* planes, for instance the planes marked X and Y in the figure. This kind of unbalance is commonly termed *dynamic unbalance* because it is essential for its detection and correction that the rotor rotates.
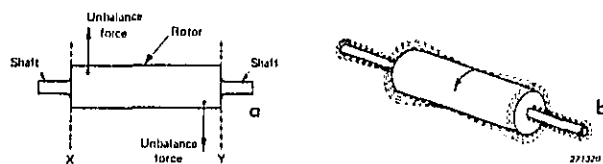
Fig.4.8. *Example of dynamic unbalance*
a) Sketch of a rotor where an unbalanced couple affects its motion
*b) Illustration of the effect caused by the unbalanced couple*

Although the ideal balance situation would be one where the rotating body, after being properly balanced, shows no unbalance at all, this is neither an economically nor practically achievable situation. Even after very careful balancing the rotor will always possess a certain residual unbalance.

In view of these facts the I.S.O. (International Standards Organisation) has proposed certain recommendations as to the "Balance Quality of Rotating Rigid Bodies". These recommendations relate all the permissible residual unbalance to the maximum operating speed of the rotor, and associate various types of representative rotors with ranges of recommended quality grades.

The curves showing the proposed acceptable residual unbalance as a function of the speed of the rotor, and the quality grade, are given in Fig.4.9, while the following table illustrates the connection between the quality grade and the type of rotor.
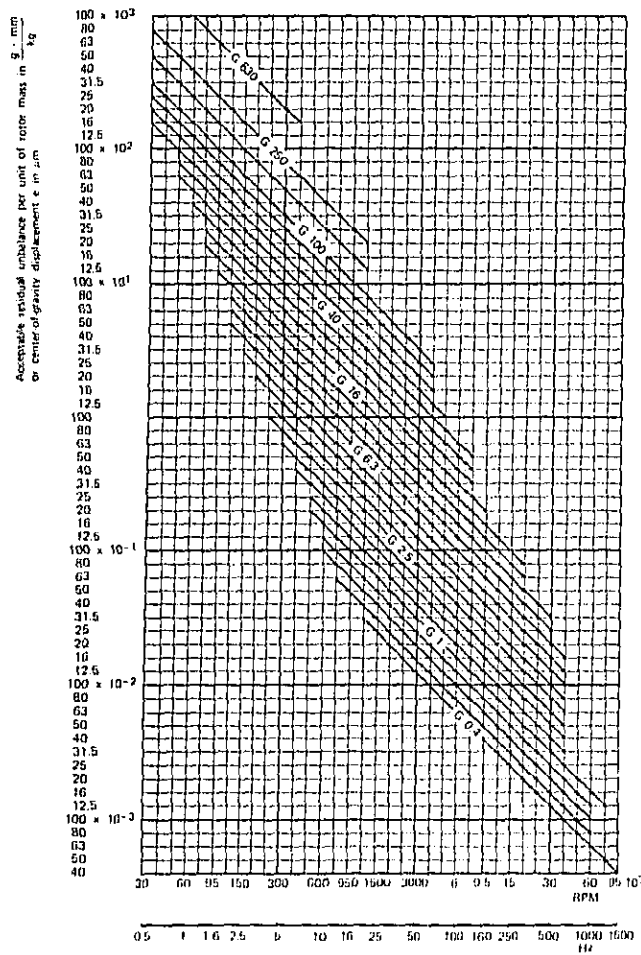
Fig.4.9. *Maximum residual unbalance corresponding to various balancing grades, G. (I.S.O.)*

Balancing Grades for Various Groups of Representative Rigid Rotors

Quality grade G	e_ω (1) (2) mm/sec	Rotor types — General examples
G 4000	4000	Crankshaft-drives (3) of rigidly mounted slow marine diesel engines with uneven number of cylinders (4).
G 1600	1600	Crankshaft-drives of rigidly mounted large two-cycle engines.
G 630	630	Crankshaft-drives of rigidly mounted large four-cycle engines. Crankshaft-drives of elastically mounted marine diesel engines.
G 250	250	Crankshaft-drives of rigidly mounted fast four-cylinder diesel engines (4).
G 100	100	Crankshaft-drives of fast diesel engines with six and more cylinders (4). Complete engines (gasoline or diesel) for cars, trucks and locomotives (5).
G 40	40	Car wheels, wheel rims, wheel sets, drive shafts. Crankshaft-drives of elastically mounted fast four-cycle engines (gasoline or diesel) with six and more cylinders (4). Crankshaft-drives for engines of cars, trucks and locomotives.
G 16	16	Drive shafts (propeller shafts, cardan shafts) with special requirements. Parts of crushing machinery. Parts of agricultural machinery. Individual components of engines (gasoline or diesel for cars, trucks and locomotives. Crankshaft-drives of engines with six and more cylinders under special requirements.
G 6.3	6.3	Parts of process plant machines. Marine main turbine gears (merchant service). Centrifuge drums. Fans. Assembled aircraft gas turbine rotors.

			Fly wheels. Pump impellers. Machine-tool and general machinery parts. Normal electrical armatures. Individual components of engines under special requirements.
G	2.5	2.5	Gas and steam turbines, including marine main turbines (merchant service). Rigid turbo-generator rotors. Rotors. Turbo-compressors. Machine-tool drives. Medium and large electrical armatures with special requirements. Small electrical armatures. Turbine-driven pumps.
G	1	1	Tape recorder and phonograph (gramophone) drives. Grinding-machine drives. Small electrical armatures with special requirements.
G	0.4	0.4	Spindles, discs, and armatures of precision grinders. Gyroscopes.

Notes:

1. $\omega = 2\pi n/60 \approx n/10$, if n is measured in revolutions per minute and ω in radians per second.

2. In general, for rigid rotors with two correction planes, one half of the recommended residual unbalance is to be taken for each plane; these values apply usually for any two arbitrarily chosen planes, but the state of unbalance may be improved upon at the bearings. For disc-shaped rotors the full recommended value holds for one plane.

3. A crankshaft-drive is an assembly which includes the crankshaft, a flywheel, clutch, pulley, vibration damper, rotating portion of connecting rod, etc.

4. For the present purposes, slow diesel engines are those with a piston velocity of less than 9 m/s; fast diesel engines are those with a piston velocity of greater than 9 m/s.

5. In complete engines the rotor mass comprises the sum of all masses belonging to the crankshaft-drive described in footnote 3 above.

4.3. Effects of Vibration and Shock on Man

The human body is both physically and biologically a "system" of an exceedingly complex nature. When looked upon as a mechanical system it contains a number of linear as well as non-linear "elements", and the mechanical properties are quite labile and different from person to person.

Biologically the situation is by no means simpler, especially when psychological effects are included. In considering the response of man to vibrations and shocks it is necessary, however, to take into account both mechanical and psychological effects.

Because experiments with human beings are difficult, time-consuming and in extreme cases unesthetical, much of the knowledge gained to date has been obtained from experiments on animals. It is, of course, not always possible to "scale" results obtained from animal experiments to reactions expected from man, but nevertheless such experiments often result in valuable information.

As the purpose of this Chapter is more to review some of the present knowledge than to discuss in detail particular experiments the following pages contain a brief description of some major facts which are presently known about man's response to vibrations and shocks. Most of the data presented have been obtained from a report by D.H. Goldman and H.E. von Gierke[*] and interested readers are referred to this report, or to Chapter 44 in the "Shock and Vibration Handbook"[**], for more detailed information.

Considering first the human body as a mechanical "system" it may, at low frequencies and low vibration levels, be roughly approximated by a linear lumped parameter system of the type shown in Fig.4.10. One of the most important "parts" of this system with respect to vibration and shock effect seems to be the part marked "thorax-abdomen system". This is due

[*] Goldman, D.E. and von Gierke, H.E.: The Effect of Shock and Vibration on Man. No.60—3, Lecture and Review Series, Naval Medical Research Institute, Bethesda, Maryland, U.S.A. 1960.

[**] "Shock and Vibration Handbook", Edited by C.M. Harris and C.E. Crede. McGraw-Hill Book Company, Inc. New York 1961.
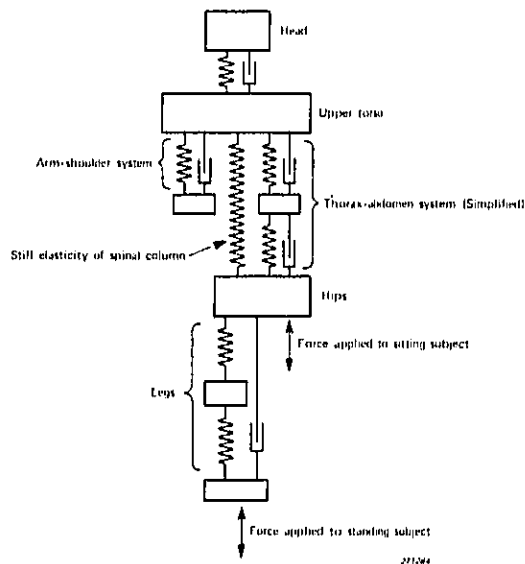
Fig.4.10. Simplified mechanical system representing the human body standing on a vertically vibrating platform. (After Coerman et al.)

to a distinct resonance effect occurring in the 3 — 6 Hz range as indicated on Figs.4.11 and 4.12 and which makes an efficient vibration isolation of a sitting or standing person very difficult. A further resonance effect is found in the 20 to 30 Hz region and is caused by the head-neck-shoulder system, Fig.4.12.

Also in the region 60 to 90 Hz disturbances are felt which suggest eyeball resonances, and a resonance effect in the lower jaw-scull system has been found between 100 and 200 Hz.

Above some 100 Hz simple lumped parameter models like that shown in Fig.4.10 are not very useful. It is then necessary to apply continuous structure analysis methods which readily become very complex. By such

70
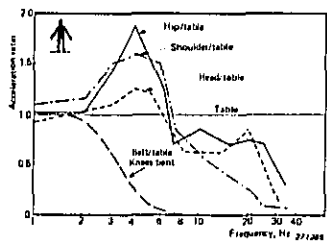
Fig.4.11. Transmissibility of vertical vibration from table to various parts
of the body of a standing human subject as a function of fre-
quency. (After Dieckmann; data for transmission to belt, after
Radke)

methods it has, however, been shown that for the scull itself the fundamen-
tal mode of vibration seems to be in the region of 300 – 400 Hz with
resonances for higher modes around 600 and 900 Hz. At still higher fre-
quencies use must be made of wave-theory both in the form of shear waves
and of compressional waves (sound waves).
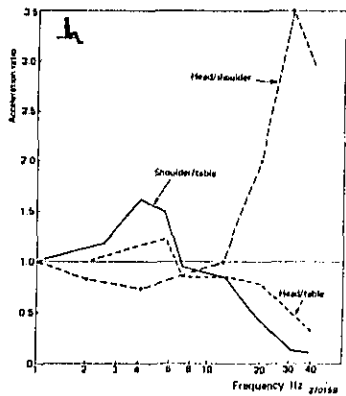
Fig.4.12. Transmissibility of vertical vibration from table to various parts
of a seated human subject as a function of frequency. (After
Dieckmann)

71

From a shock and vibration point of view the low frequency range may be considered most important. Some very interesting measurements have here been made by von Bekesy and concern the attenuation of vibration along the human body. In Fig.4.13 the results obtained at 50 Hz are reproduced and show that the attenuation from foot to head is of the order of 30 dB. Similarly the attenuation from hand to head is roughly 40 dB.
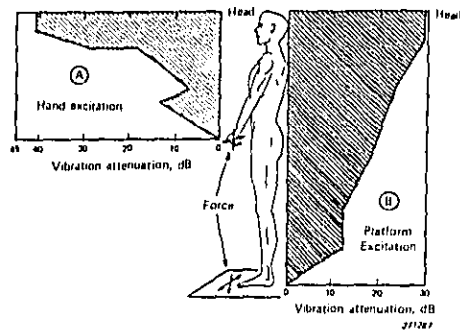
Fig.4.13.   Attenuation of vibration at 50 Hz along human body. The attenuation is expressed in decibels below values at the point of excitation. For excitation of (A) hand, and (B) platform on which subject stands. (After von Bekesy)

Apart from the mechanical responses mentioned above both physiological and psychological effects are observed. Although these effects are rather complex and difficult to measure it seems that physiological results obtained from animal experiments to a certain extent also apply to man. These experiments have been mostly concerned with changes in food assimilation, muscular activity, reproductive activity etc. as well as actual internal injury.

The psychological effects like perception, feelings of discomfort, and pain have been studied by several investigators but the data available seem to be rather limited. Some vibration exposure criteria curves have, however, been proposed in the I.S.O.*) for the vibration frequency range 1 Hz to 100 Hz.

---

*) I.S.O. = International Standards Organization.
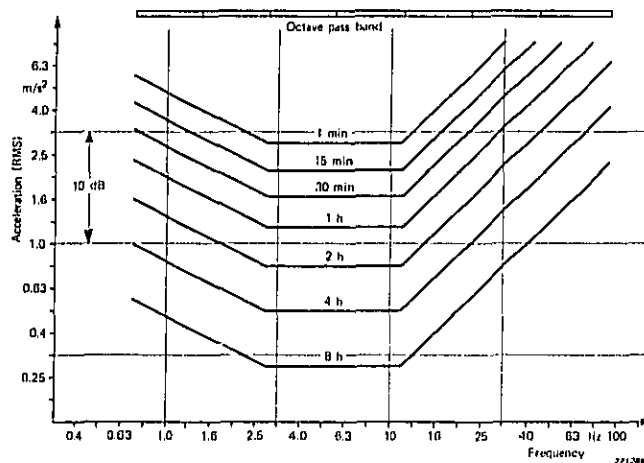
Fig.4.14. Vibration Exposure criteria curves

These are shown in Fig.4.14 and are valid for vibrations transmitted to the torso of a standing or sitting person.

Vibrations in the frequency range below about 1 Hz produce annoyances which are individually very different, for instance cinetosis (air sickness). For frequencies above 100 Hz the vibrational perceptions are mainly effective on the skin, and depend greatly upon the influenced body point and on the damping layers (e.g. shoes, clothes) at this point. It seems, therefore, to be practically impossible to state generally valid vibration exposure criteria for frequencies outside the above mentioned range (1 — 100 Hz).

The vibration levels indicated by the curves in Fig.4.14 are given in terms of *RMS acceleration levels which produce equal fatigue-decreased proficiency*. Exceeding the exposure specified by the curves will, in most situations cause noticeable fatigue and decreased job proficiency in most tasks. The degree of task interference depends on the subject and the complexity of the task but the curves indicate the general range for onset of such inter-ference and the time dependency observed.

73
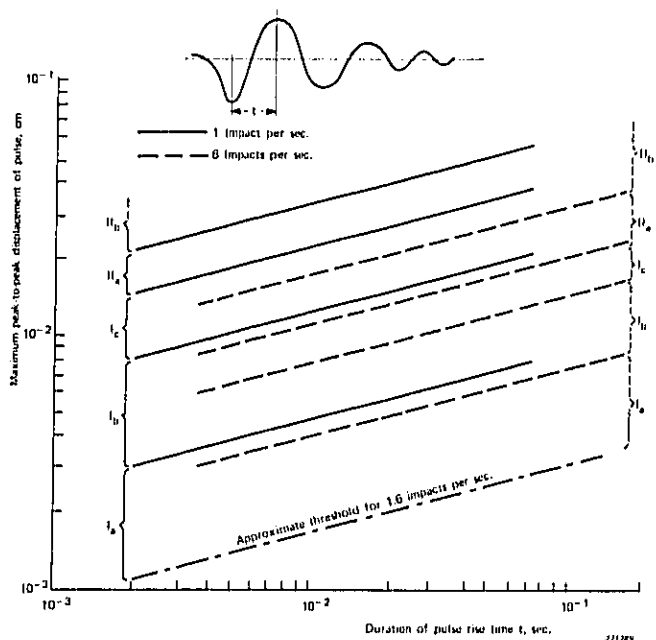
Fig.4.15. Tolerance of human subjects in the standing or supine position to repetitive vertical impact pulses representative of impacts from pile drivers, heavy tools, heavy traffic, etc. Subjective reaction is plotted as a function of the maximum displacement of the initial pulse and its rise time. The numbers indicate the following reactions for the areas between the lines: *I a,* thres-hold of perception; *I b,* of easy perception; *I c,* of strong perception, annoying; *II a,* very unpleasant, potential danger for long exposures; *II b,* extremely unpleasant, definitely danger-ous. The decay process of the impact pulses was found to be of little practical significance. (After Reiher and Meister)

An *upper bound to exposure* considered acceptable (hazard to health as well as performance) *is taken to be twice as high as (6 dB above)* the "fatigue-decreased proficiency" boundary shown in Fig.4.14, while the "reduced comfort boundary" is assumed to be about one third of (10 dB below) the stated levels.

These criteria are presented as recommended guidelines or trend curves rather than firm boudaries classifying quantitative biological or psychological limits. They are intended only for situations involving healthy, normal people considered fit for normal living routines and the stress of an average working day.

Finally, Fig.4.15 indicates the tolerance of human subjects to single shock acceleration pulses of the type produced in the floor near drop forges or similar equipment (results from a single study).

4.4. Selected Bibliography

BLOOMER, N.T. and   A Large Scale Fatigue Test of Aluminium
ROYLANCE, T.F.:   Specimens. The Aeronautical Quarterly, Vol.
                         XVI, Nov. 1965.

BROCH, J.T.:   Effects of Spectrum Non-Linearities upon the
                         Peak Distribution of Random Signals. Brüel &
                         Kjær Technical Review, No. 3—1963.

BROCH, J.T.:   Peak Distribution Effects In Random Load
                         Fatigue. Brüel & Kjær Technical Review, No. 1—
                         1968.

BROCH, J.T.:   On the Damaging Effects of Vibration. Brüel &
                         Kjær Technical Review No. 4—1968.

BUSSA, S.L.:   The Effect of RMS Stress Level, Irregularity
                         Factor and Power Spectrum Shape on the
                         Fatigue Life of SAE 1006 Notched Specimens
                         under Stochastic Loading Conditions. M.Sc.
                         Thesis, Wayne State University, Detroit, Michi-
                         gan 1967.

COERMANN, R. et al: The Passive Dynamic Mechanical Properties of
                      the Human Thorax — Abdomen System and of
                      the Whole Body System. Aerospace Med.
                      Vol. 31, p. 443, 1960.

COERMANN, R: Einwirkung stossförmiger Beschleunigungen auf
                      den Menschen. VDI-Berichte*) Nr. 135,1969.

CORTEN, H.T. and   Cumulative Fatigue Damage, Int. Conference on
DOLAN, T.J.:   Fatigue of Metals, Inst. of Mechanical Eng.
                      London 1956.

DIECKMANN, D.:   Einfluß vertikaler mechanischen Schwingungen
                      auf den Mensch. Arbeitsphysiol. Vol. 16, S. 519,
                      1957.

FEDERN, K.:   Unwuchttoleranzen rotierender Körper. Werk-
                      statt und Betrieb 86, S. 243, 1953.

FEDERN, K.:   Erfahrungswerte, Richtlinien und Gütemasstäbe
                      für die Beurteilung von Maschinenschwingungen,
                      Konstruktion, 10 Jg. Heft 8, S. 289 — 298, 1958.

FEDERN, K.:   Critère, Mesure et Elimination des Vibrations
                      en construction mécanique. Revue universelle des
                      Mines, 9; Serie, TXVIII, No. 2, Féurier 1962.

FORSYTH, P.J.E.:   A Two Stage Process of Fatigue Crack Growth.
                      Proceedings of the Crack Propagation Sympo-
                      sium, Cranfield 1961.

FREUDENTHAL, A.M.   On the Statistical interpretation of Fatigue Tests.
and GUMBEL: Proc. Roy Soc. (Mathm. and Phys. Sc.) 216
                      1953.

FREUDENTHAL, A.M.   On Stress Interaction in Fatigue and a Cumula-
and HELLER, R.A.:   tive Damage Rule. Journal of the Aeronautical
                      Sciences, Vol. 26, No. 7—1959.

GOLDMAN, D.E. and   The Effect of Shock and Vibration on Man.
VON GIERKE, H.E.:   No. 60—3, Lecture and Review Series. Naval

*) VDI = Verein Deutscher Ingenieure.

	Medical Research Institute, Bethesda, Maryland, U.S.A. 1960.
HEAD, A.K.:	The Propagation of Fatigue Cracks, J. Appl. Mech., ASME Vol. 23, September 1956.
LIU, H.W.:	Crack Propagation in Thin Metal Sheet Under Repeated Loading. Transactions ASME, Vol. 83, 1961.
LÜBCKE, E.:	Schaffung einer Güteklassifizierung für Elektromotoren. Berichtsheft 2, FokoMa; Maschinenmarkt, S. 143 – 144, 1955.
McCLINTOCK, F.A. and IRWIN, G.R.:	Plasticity Aspects of Fracture Mechanics, Fracture Toughness Testing and its Applications, ASTM STP 381.
McLEAN, D.:	Mechanical Properties of Metals. John Wiley & Sons, 1962.
MILES, J.W.:	On Structural Fatigue Under Random Loading. Journal of the Aeronautical Sciences, Vol. 21, Nov. 1965.
MINER, M.A.:	Cumulative Damage in Fatigue. Journ. of Appl. Mech. Vol 12–1945.
MIWA, T.:	Evaluation Methods for Vibration Effect (Part 1 – 9), Ind. Health (Japan) 1967 – 1969.
MUSTER, D. and FLORES, B.:	Balancing Criteria and their Relationship to Current American Practice. Journ. of Eng. for Ind. Trans. ASME, Series B, Vol. 91, 1969.
RATHBONE, T.C.:	Vibration Tolerance. Power Plant Engineering 43, p. 721 – 724, 1939.
REIHER, H. und MEISTER, F.J.:	Die Empfindlichkeit des Menchen gegen Stöße. Forschung auf dem Gebiete des Ingenieurwesen. Vol. 3, S. 177, 1932.

ROTHERT, H.:   Mechanische Schwingungen in Elektrischen Maschinen. VDI — Berichte, Bd. 4, S. 65 — 69, 1955.

ROVINDRAN, R.:   Statistical and Metallographic Aspects of Fatigue Failure Mechanisms in Metals. UTIAS*) Technical Note No. 123, University of Toronto 1968.

SWANSON, S.R.:   A Two Distribution Interpretation of Fatigue S-N Data. Canadian Aeronautical Journal, Vol. 6, No. 6, June 1960.

SWANSON, S.R., CICCI, F. and HOPPE, W.:   Crack Propagation in Clad 7079—T 6 Aluminium Alloy Sheet Under Constant and Random Amplitude Fatigue Loading. Paper 37, 69th Annual of the ASTM, June 1966.

VDI: Beurteilungsmaßstäbe für mechanische Schwingungen von Maschinen. VDI-Richtline 2056, Oktober 1964.

WEIBULL, W.:   A Statistical Representation of Fatigue Failures in Solids. Kungl. Tekniska Högskolans Handlingar, No. 27, Stockholm 1949.

WEIBULL, W.:   Fatigue Testing and Analysis of Results. AGARD-Publication by Pergamon Press. Oxford — London — New York — Paris 1961.

WOOD, W.A.:   Experimental Approach to Basic Study of Fatigue. Institute for the Study of Fatigue and Reliability Report, No. 24, Columbia University, August 1965.

---

*) UTIAS = University of Toronto, Institute of Aerospace Studies.

5. VIBRATION MEASUREMENT INSTRUMENTATION AND TECHNIQUES

5.1. General Measurement Considerations

While in the preceding chapters some basic theoretical aspects of mechanical vibrations and shocks have been outlined, it is the intention in this and the succeeding chapters to discuss the more practical aspects connected with actual vibration measurements. As indicated in section 2.3 there are, in general, three quantities which are of great interest in vibration studies: The displacement, the velocity and the acceleration. Because the quantities are interrelated by simple differentiating and integrating operations it does not normally matter which quantity is actually measured. In the early days of vibration measurements it was common to measure the velocity of the vibrations by means of, rather clumsy, velocity sensitive devices. During the last decade or so there has, however, been a distinct tendency to prefer the use of acceleration sensitive transducers, so-called accelerometers, for the measurements instead of velocity pick-ups.

Two of the reasons for this "transfer" in preference are that accelerometers can normally be made mechanically smaller than velocity pick-ups, and that their useful frequency range is wider. If the measured result is wanted in terms of velocity or displacement, rather than in terms of acceleration, use can be made of electronic integrators at the output of the accelerometer, see also Appendix E.

The requirement of mechanically small vibration transducers originates from the fact that the transducer should load the structural member on which it is placed as little as possible. Also, one often desires to measure the vibration at a *point* on a structure, not on an *"area"*.

With regard to the frequency range of interest in vibration measurements this has been continuously increasing over the past years. Not so long ago a common upper frequency limit was considered to be of the order of 50 Hz. Today many vibration measurements are carried out up to 5000 Hz, or even higher. The increased interest in higher frequencies has been caused mainly by the rapid development of fast moving vehicles, especially in the aircraft and space vehicle fields. Also the vibrations encountered in aircraft and

79

space vehicles are of a random rather than of a periodic nature. This again often calls for the use of more complicated measurement techniques than was common in earlier days. To be able to predict the effects of vibrations on mechanical structures and man, it is for instance normally necessary to *frequency analyze* the vibrations.

Various kinds of electronic frequency analyzers may be used for this purpose the main differences between them being their absolute bandwidth and their variation in bandwidth with frequency. However, very often in practical vibration work, it is necessary to use analyzers with an exceedingly narrow bandwidth as the structures excited by the vibrations may contain mechanical resonators with large Q-values (lightly damped resonances). What kind of instrumentation should be used in a particular measurement situation must actually be decided upon, in view of the ultimate use of the measured data and the measurement equipment available. In the following sections of this book some typical vibration measurement equipment and their uses are briefly discussed.

5.2. Some Basic Measurement Systems

As mentioned in the previous section it is almost inevitably necessary to frequency analyze the measured vibrations if the data are going to be used for predictive purposes. Nevertheless, use is sometimes still made of simple frequency-"independent" vibration measuring equipment to obtain an idea of the overall vibration level at a certain place. Such equipment consists in general of a vibration pick-up and an electronic amplifier with indicating meter calibrated in vibrational units (g, m/sec^2, m/sec, inches/sec, mm, μinches). The frequency response of the combined system (pick-up + amplifier) is then considered to be flat over a certain specified frequency range.
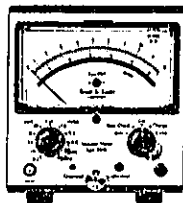
Fig.5.1. Photograph of the Vibration Meter Type 2510

Fig.5.1 shows an example of such an instrument, namely the *Brüel & Kjær Vibration Meter Type 2510.*

As can be seen from Fig.5.2 the frequency response of this instrument is flat from 10 Hz to 1000 Hz. It has been developed mainly for measurements on rotating electrical machinery (600 – 60000 r.p.m.), and measures the RMS-value of the vibration velocity*). A special feature of the instrument is that it can be powered either from the mains, or from selfcontained, rechargeable batteries.
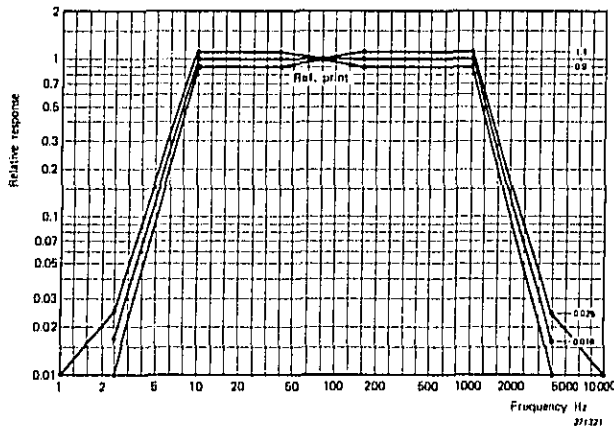
Fig.5.2. Standardized frequency response of the Vibration Meter

A second example of battery operated easily portable instrument is given in Fig.5.3.

Actually the instrument shown is an *Impulse Precision Sound Level Meter Type 2204* supplied with one of the Brüel & Kjær Accelerometers (see also section 5.3). This Sound Level Meter has, however, the advantage

---

*) The instrument fulfils the requirements of the German Standard DIN 45666 for measurements on rotating machinery (Richtlinie VDI 2056). Also, similar recommendation have been proposed internationally (ISO) as well as "locally" in Great Britain and the U.S.A.

of being delivered with interchangeable instrument meter scales which enables a meter reading to be made directly in vibrational units.

It may therefore, within its specified limits be used as well as a Vibration Meter as a Sound Level Meter. Also a specially designed integrator
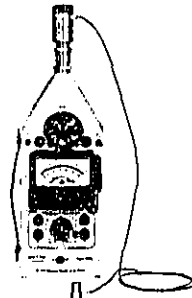
Fig.5.3. Photograph of a battery operated easily portable instrument designed for simple measurements of vibrations (and noise) in the field
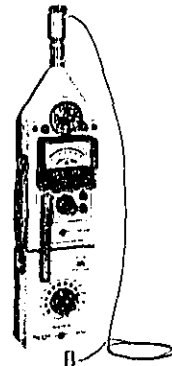
Fig.5.4. Photograph of the instrument, Fig.5.3, fitted with an Octave Filter Set Type 1613 for coarse frequency analysis of the vibrations

(ZR 0020) can be connected to the instrument whereby the vibrational quantity measured will be either displacement, velocity or acceleration, whichever is desired.

By fitting an *Octave Filter Set Type 1613* to the set-up, as shown in Fig.5.4 a coarse frequency analysis of the measured vibrations is possible. This arrangement may not be the "ideal" vibration analyzer; *it does, on the other hand, furnish the practicing sound and vibration engineer with an extremely versatile and useful general purpose instrument.* To further facilitate the use in the field of the instrumentation system a Carrying Case Type 3503 is available, containing the instruments (Type 2204 + Type 1613) as well as the necessary accessories, Fig.5.5.
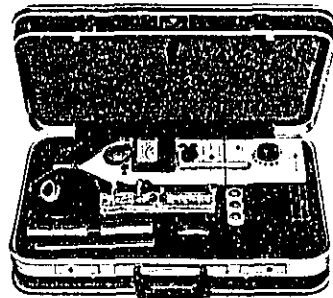
Fig.5.5. Carrying Case Type 3503 containing the instrumentation system Fig.5.4, and various accessories for specific measurement purposes

If battery-operation of the instruments is not required a somewhat more elaborate but also a more powerful, analysis system is obtained by means of the arrangement shown in Fig.5.6. It consists of an *Accelerometer, e.g. Brüel & Kjær Type 4339,* a *Preamplifier (for instance Type 2625),* a *Measuring Amplifier Type 2606,* an *Octave and Third Octave Filter Set Type 1614* and a *Level Recorder Type 2305.*

In this case it is possible to frequency analyze the vibration in terms of 1/3 octave frequency bands from 2 Hz to 160 kHz, and to *record the result of the analysis automatically on pre-printed recording paper,* see Fig.5.7.
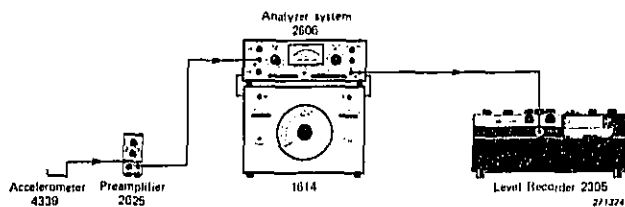
Fig.5.6. Arrangement suitable for the automatic frequency analysis of vibrations in terms of 1/1 octave or 1/3 octave frequency bands
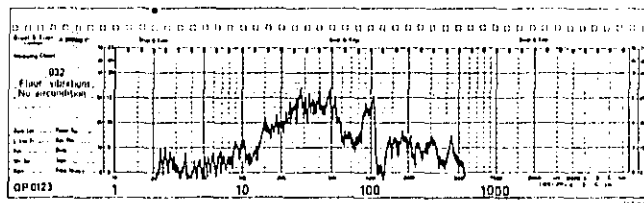
Fig.5.7. Example of an automatically recorded spectrogram

A somewhat similar measuring arrangement is sketched in Fig.5.8. Here the Measuring Amplifier Type 2606 and the Octave and Third Octave Filter Set Type 1614 have been substituted by the *Frequency Analyzer Type 2107*. Also in this case it is possible to record the result of the analysis automatically on pre-printed paper. However, the lowest frequency components which can be analyzed is here of the order of 20 Hz. This may be a disadvantage because in many cases vibration signals contain significant frequency components much below 20 Hz.

To overcome this difficulty use can be made of *frequency transformation by means of magnetic tape recording*. Such frequency transformations are made simply by recording the vibration signal on a precision FM (frequency modulated) tape recorder operating at low speed, and then playing back the signal for analysis at a considerably higher speed, see Fig.5.9. In Fig.5.9a) the vibration signal is recorded on the Brüel & Kjær *Tape Recorder Type 7001* at low speed, while Fig.5.9b) illustrates the play-back of the recorded signal for analysis at 40 times the speed used for recording. With a
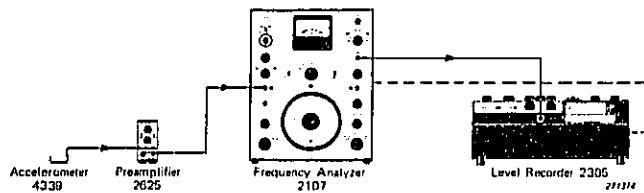
Fig.5.8. *Automatic frequency analysis arrangement utilizing the frequency Analyzer Type 2107*
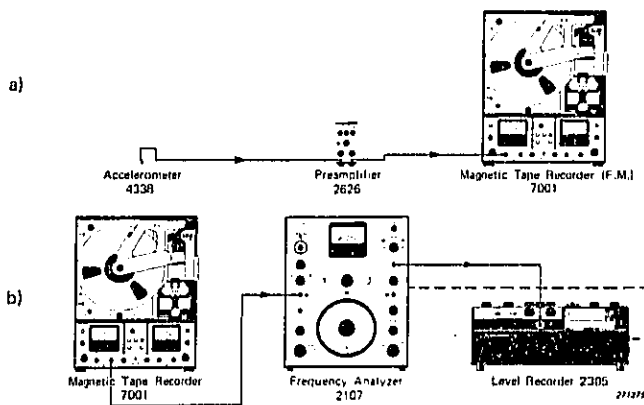
Fig.5.9. *Arrangements used for frequency transformation and analysis by means of magnetic tape recording*
a) Recording arrangement
b) Play-back and analysis arrangement

frequency transformation ratio of 1 : 40 a 0.5 Hz signal component is thus transformed up to the required 20 Hz! The result of a frequency analysis carried out according to the above described principles is shown in Fig.5.10 (response of a two degrees-of-freedom system excited by Gaussian random vibrations).

Actually, the use of precision magnetic tape recorders in practical vibra-

85
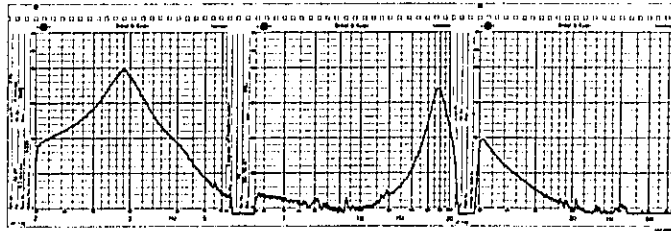
Fig.5.10. Result of a measurement made according to Fig.5.9
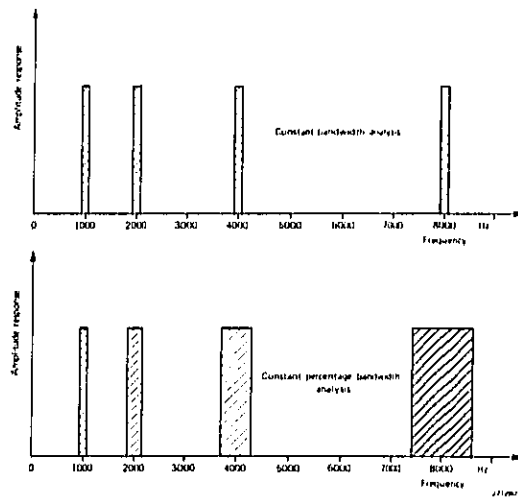
Fig.5.11. Sketch illustrating the difference in absolute resolution between constant bandwidth type of analysis and constant percentage bandwidth type analysis. Note: Use is here made of linear frequency scales

tion work is not uncommon. In many cases an arrangement of the type shown in Fig.5.9a) is taken out in the field and the vibrations recorded and stored for later analysis in the laboratory. The use of tape speed (and thus frequency) transformations does not furnish then any extra difficulties and instrumentation investments.

The Frequency Analyzer (Type 2107) shown in Fig.5.8 is a so-called narrow band frequency analyzer with bandwidth as narrow as 6% of the frequency to which it is tuned. Both the Filter Sets Type 1613 and Type 1614 mentioned above, and the Analyzer Type 2107, belong to a category of frequency analyzers called *constant percentage bandwidth analyzers*. This is due to the fact that their absolute bandwidths are directly proportional to the analysis frequency. A second type of commonly used frequency analyzers is called *constant bandwidth analyzers* because in this case the absolute bandwidth is *constant*, independent of the analysis frequency. Fig.5.11 illustrates the difference between the two types of analysis, and a measuring arrangement utilizing constant bandwidth analysis is shown in Fig.5.12.
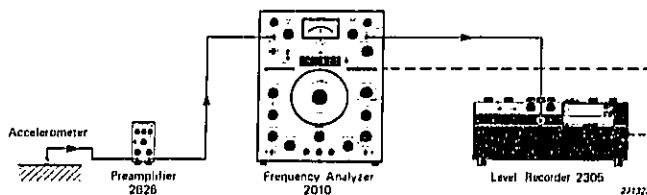
Fig.5.12. Measuring arrangement utilizing narrow band constant band-width analysis (Heterodyne Analyzer Type 2010)

The analyzing part of the set-up, Fig.5.12, consists of the *Heterodyne Analyzer Type 2010*. This instrument is a very versatile narrow band frequency analyzer particularly well suited for vibration analysis.

A second constant bandwidth type analysis arrangement is shown in Fig.5.14, and contains the *Heterodyne Slave Filter Type 2021*, controlled by the *Automatic Vibration Exciter Control Type 1025*. Actually, the main advantages obtained by using Heterodyne Slave Filters is thus not obvious from Fig.5.14, but consists in the fact that *several filters can be controlled to exactly the same frequency* from a single Beat Frequency Oscillator (which is often standard equipment in vibration laboratories). In

87
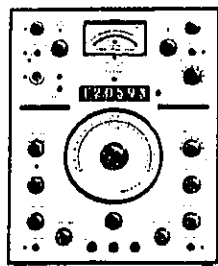
Fig.5.13. Photograph of the Heterodyne Analyzer Type 2010

this way many measuring points can be analyzed simultaneously and correct time-interdependency between the data be maintained. This is of great importance in advanced vibration measurement technology, see also Chapter 8.
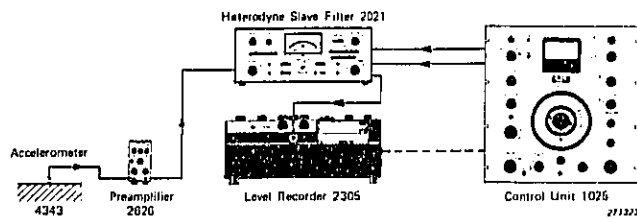
Fig.5.14. Example of use of the Heterodyne Slave Filter Type 2021 (Narrow band analysis)

The frequency analysis equipment described above have all been of a type where the output from frequency selective filters are presented, one at a time, to a single RMS-rectifier and read-out device. This kind of analysis is commonly termed *sequential analysis*. Even though it may be performed automatically it requires a certain amount of analysis time, and only relatively slow changes in the frequency spectrum with time can be easily detected. Another method of frequency analysis, termed *real time analysis (or parallel analysis)*, has therefore gained considerable interest in later years. Here the output from a number of "parallel" filters are fed

88
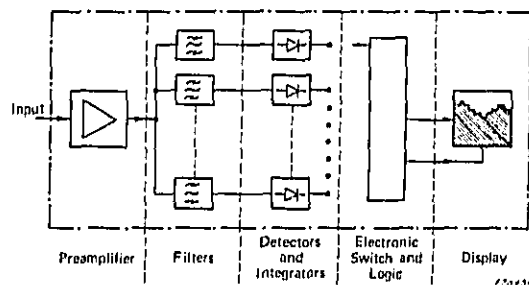
Fig.5.15.   Principle of operation of a real time (parallel) analyzer

Fig.5.16.   Photograph of the Real Time Analyzer Type 3347

89

simultaneously (or within fractions of a second) to the read-out, Fig.5.15. In this way the complete frequency spectrum can be presented "instantaneously", and even very rapid changes in the spectrum with time can be detected. An instrument capable of performing this type of frequency analysis is shown in Fig.5.16. As can be seen from the figure the complete 1/3 Octave frequency spectrum of the vibrations is here presented on the screen of a television type picture tube. Outputs are furthermore, also provided for analogue instrumentation, such.as X—Y or level recorders, and for digital data receivers, such as tape puncher, printer, or computer "on-line". Connecting the Analyzer to a suitably programmed computer thus forms a flexible and very rapid system for automatic data processing with the advantages of real time analysis.

Common to all vibration analysis systems, whether sequential or parallel, is that they consist of four basic "elements": a vibration pick-up (accelerometer), a preamplifier (in some newer texts also termed signal conditioner), an analyzer and a read-out recorder Fig.5.17.
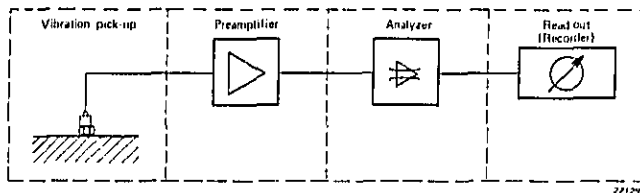
Fig.5.17.   Basic combination of "elements" in a vibration analysis system

In the following sections each of these "elements" are discussed separately in order to facilitate the selection of "elements" best suited for a particular measurement situation.

5.3. Selection of Accelerometer

An accelerometer is an electromechanical transducer which produces at its output terminals a voltage proportional to the acceleration to which it is subjected. The most commonly used accelerometers today are the so-called compression type piezoelectric accelerometers whose construction is illustrated schematically in Fig.5.18.

90
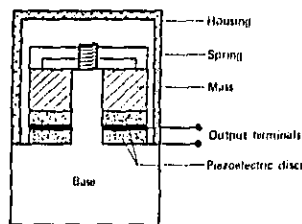
Fig.5.18. Sketch showing the basic construction of the Brüel & Kjær com-
          pression   type   piezo-electric   accelerometers   (single-ended
          version)

   In the Brüel & Kjær accelerometers the transducing element consists of
two piezoelectric discs on which is resting a heavy mass. The mass is pre-
loaded by a stiff spring and the whole assembly is mounted in a metal
housing with a thick base. When the accelerometer is subjected to vibration,
the mass will exert a variable force on the piezoelectric discs. This force is
exactly proportional to the acceleration of the mass. Due to the piezoelec-
tric effect a variable potential (voltage) will be developed across the two
discs, which is proportional to the force and therefore to the acceleration of
the mass. For frequencies much lower than the resonant frequency of the
mass and the stiffness of the whole accelerometer system the acceleration of
the mass will be virtually the same as the acceleration of the whole trans-
ducer and the voltage produced will therefore also be proportional to the
acceleration to which the transducer is subjected.
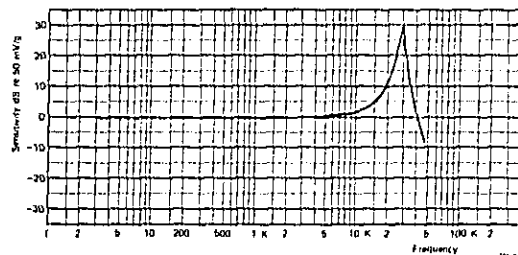
Fig.5.19. Typical frequency characteristic of a piezo-electric accelerome-
          ter (low frequencies not considered)

91

These relationships can be illustrated by means of the *accelerometer frequency characteristic* shown in Fig.5.19. Here the output voltage from an accelerometer is recorded as a function of frequency, the accelerometer being exposed to a constant, frequency independent, acceleration level. The effect of the above mentioned resonance is clearly noticed. Actually this resonance effect determines the upper limit of the accelerometer's useful frequency range, while the lower limit normally depends upon the properties of the connected amplifiers (Figs.5.17 and 5.31).

The *sensitivity* of the accelerometer, i.e. the magnitude of the voltage developed across its output terminals when subjected to a certain acceleration, depends partly upon the piezo-electric properties of the material used in the piezoelectric discs, and partly upon the weight of the mass, Fig.5.18. For a given piezo-electric material the mechanical size of the accelerometer is therefore important with respect to its sensitivity. The smaller the accelerometer is, the lower is the sensitivity. On the other hand, a decrease in mechanical size is also normally accompanied by an increase in frequency of the accelerometer resonance, i.e. a wider useful frequency range. Fig.5.20 shows some typical frequency characteristics for various Brüel & Kjær accelerometers, and in the table Fig.5.21 their main fields of application are indicated. Even if the *frequency response* and *sensitivity* may be the two most important properties to know for the selection of a suitable accelerometer there are many other factors to consider. One of those is the *accelerometer cross-axis or transverse sensitivity. The transverse sensitivity* is the
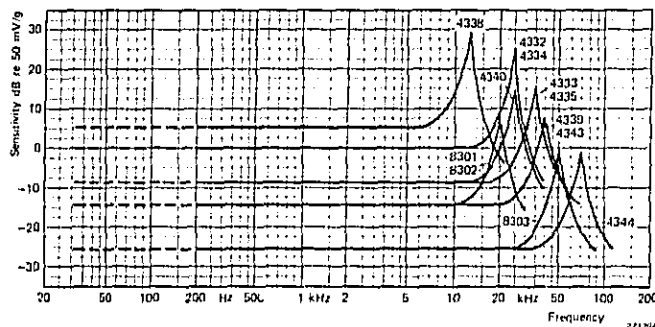
Fig.5.20. Typical frequency characteristics for various types of Brüel & Kjær Accelerometers. (Weight of Type 4338: 60 grams; Weight of Type 4339: 16 grams; Weight of Type 4344: 2 grams)

92

Accelerometer Type no.	Connection	Main Application	Suitable Preamplifier(s)*	Sensitivity Voltage (mV/g)	Sensitivity Charge (pC/g)	Mounted Resonance (kHz)	Transverse Sensitivity (%)	Maximum Shock (g)	Weight (grammes)	Special Features
4330	Side	General Vibration Measurements. Vibration Testing and Control.	Use with Voltage / Charge / Sensitive Voltage / Charge Electronics	(1606), 2616, 2623, (2622), 2623, 2624, 2624, 2626, 2626, 4292, 2624, (2204 + ZR 0020)	10 ± 0.2, ~10, 10 ± 0.2, ~10	~10, 10 ± 0.2, ~10, 10 ± 0.2	40, 40, 25, 25	< 3	10.000	16, 16, 21, 21	Uni Gain. All welded construction. Wide Frequency Range. Uni Gain. Low Base Strain Sensitivity. Provision for Water Cooling.
4343	Side										
8301	Top										
8302	Top										
4338	Top	Vibration Measurements On Heavy Structures. Measurements of Low Level, Low Frequency Vibrations. For use with Charge Sensitive Electronics.	2510, (1606), 2616, (2622), 2623, 2624, 2626, 2626, 4292, (2204 + ZR 0020)	~100	100 ± 2	12	< 3	1000	60	Uni Gain. Very High Sensitivity. Rugged Housing. Very Low Base Strain Sensitivity.
4344	Side	High Frequency (and high level) Vibration Measurements. Shock Measurements. Measurements on Light Weight Structures.	(1606), 2616, (2622), 2623, 2624, 2625, 2626, 4292, (2204 + ZR 0020)	1.7–2.6, ~3, 1.7–2.6, ~3	1.3–2.2, ~3, 1.3–2.2, ~3	70, 45	< 4	14.000, 10.000	2, 16	Titanium Housing. Low Weight. Very High Resonance Frequency. Titanium Housing. Low Weight. Rugged 10–32 UF Top Connector.
8303	Top										
4345	Side	Vibration Measurements in Extreme Temperature Environments. For use with Charge Sensitive Electronics.	(2622), 2624, 2626	~5	~6	30	< 3	3000	27	Max. Working Temperature 400°C. Rugged All Welded Hermetically Sealed Construction. Flat Temp. Response.
4340	Top	For Vibration Measurements in Three Mutually Perpendicular Directions.	3 × (1606), 3 × 2616 2 × (2622), 3 × 2623 3 × 2624, 2625 3 × 2626, 3 × 4292	14–24	14–20	23	< 4	500	36	Special Integral Titanium Housing, Giving Low Weight & High Resonance Frequency.
4332	Side	General Vibration Measurements.	(1606), 2616, (2622), 2623, 2624, 2625, 2626, 4292, (2204 + ZR 0020)	45–65	40–60	25	< 4	7000	30	High Sensitivity and Fairly Low Weight.
4334	Top										
4333	Side	Non-Critical Purposes.		14–24	14–20	36		10.000	13	Titanium Housing. Wide Frequency Range
4335	Top										
8304	Side	Very Low Freq. Long Shock Durations. Low Pyroelectric Effect. For use with Charge Sensitive Electronics.	(2622), 2624, 2626		~10	30	< 2	10.000	30	High Stability Quartz Sensitive Element. Extremely Flat Temp. Resp. to 260°C. Very Low Sens. to Temp. Transients.
8305	Side	Back-to-back Calibration of Accelerometers. For use with Charge Sensitive Electronics.	(2622), 2624, 2626		~10	30	< 1	1000	40	Identical to 8304 & Can Be Mounted Directly Between Shaker & Accelerometer.
8306	Side	Ultra-low Level, Low Freq. Measurements. e.g. Building Vibrations.		10.000 ± 200	10.000 ± 200	3	< 5	1	500	Uni Gain. Built-in preamplifier and filter. Requires 28 V DC Power Supply.

Production of Preamplifiers in parenthesis are discontinued.
* All Brüel & Kjær Accelerometers may also be used together with the Microphone Preamplifiers Type 2615, and 2619

Fig.5.21. Table indicating the main fields of application of the various Brüel & Kjær Accelerometers together with some pertinent data

93

sensitivity to accelerations in a plane perpendicular to the main accelerometer axis, Fig.5.22. It is normally expressed in percent of the reference (main axis) sensitivity and should be as small as possible. For a good accelerometer the maximum transverse sensitivity should be less than 3% of the main axis sensitivity at low frequencies.
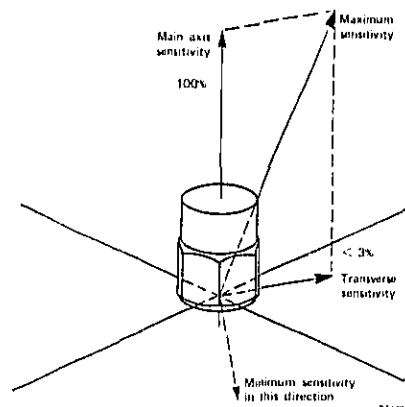

Fig.5.22. Graphical illustration of transverse sensitivity

The transverse sensitivity is normally caused by irregularities in the piezo-electric material, and limitations in the mechanical coupling between the piezo-electric discs and the metal parts. Careful mechanical machining helps to minimize transverse sensitivity. Fig.5.23 shows a typical frequency characteristic for the transverse sensitivity at frequencies up to 10.000 Hz.

Another factor which should be considered is the *environment* under which the accelerometer is supposed to be operating.

Accelerometers are often used to measure vibration in the field, or on specimens, subjected to severe environmental conditions. It is therefore important that *their sensitivity to environmental changes is as small as possible*. The factors that may influence an accelerometer's performance are primarily *temperature, humidity and rapidly varying ambient pressure (sound)*. The temperature effect causes a reduction in the voltage sensitivity of the accelerometer at higher temperatures, but if the accelerometer has

94
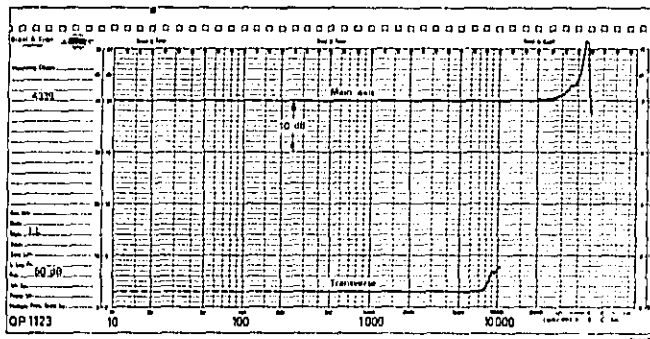
Fig.5.23. Example of frequency response data for transverse sensitivity of
an accelerometer

undergone a suitable temperature cycling process in the production stages,
the sensitivity will revert to its normal value when the temperature is
brought back to normal again. However, beyond a certain temperature (the
Curie point) the piezoelectric element is permanently damaged.

The Brüel & Kjær accelerometers are designed to be used for temper-
atures up to 260°C (500°F) without cooling. The sensitivity will be slightly
reduced at the higher temperatures, but the necessary heat cycling process
has been carried out, so that no permanent change will take place. It should
be noted that great care has been taken to use materials which will with-
stand high temperatures. The thermal coefficient of expansion of insulating
material and metal parts are carefully matched in order to maintain
humidity sealing.

Tests have also been conducted in order to find the influence of low
temperatures on accelerometer performance. The voltage sensitivity in-
creases steadily down to some −100°C and then levels out, while the
capacity undergoes a gradual decrease with decreasing temperature.

Typical performance characteristics are given in Fig.5.24 for the temper-
ature range −100 to + 250°C (−150 to + 500°F).

Effects due to acoustical excitation are unavoidable with piezoelectric
accelerometers, but may be reduced by careful design. Typical acoustic

95

sensitivities have been measured for the Brüel & Kjær accelerometers and found to be less than 0.5 μV/μbar for the smallest accelerometer.*)
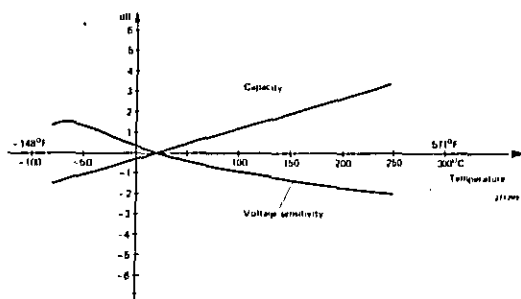
*Fig.5.24.   Typical performance characteristics for a Brüel & Kjær Acceler-
ometer in the temperature range −100 to + 260°C*

Also the *long term stability,* i.e. the calibration vs. time history, of the accelerometers has been followed for a number of representative units taken from production lots. The change in calibration data was found to be less than 2% per year.

In concluding this brief discussion on the selection of accelerometers it should be mentioned that very often two "types" of accelerometer sensitivities are stated by the manufacturer. They are the *voltage sensitivity* and the *charge sensitivity.*

The reason for this can be better understood by considering the equivalent electrical circuit of an accelerometer, Fig.5.25. At the frequencies of interest the accelerometer may be thought of as an electrical generator with a high internal capacity. As the charge on a capacitor is defined as

$$q = e \times C$$

where   q = electrical charge
e = voltage across the capacitor
C = capacitance of the capacitor

---

*) An acoustic sensitivity of 0.5 μV/μbar corresponds to an electric output of 1 mV
when the accelerometer is exposed to a sound pressure level of 140 dB.

96
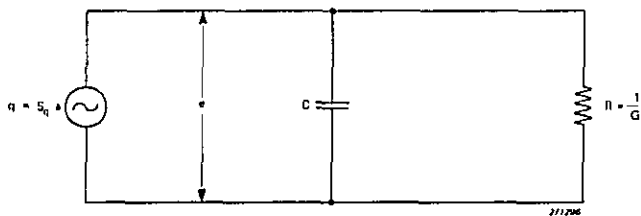
Fig.5.25. Equivalent electrical circuit of an accelerometer

it is clear that a certain acceleration, a, which produces a certain output voltage, e, also produces a charge, q, on the capacitor, C.

When the accelerometer is used in conjunction with charge measuring electronics it is thus of prime importance to know its charge sensitivity, while when it is used in conjunction with voltage measuring electronics the voltage sensitivity will be the most important "type" of sensitivity. This is further discussed in section 5.4.

5.4. Selection of Preamplifier

The *preamplifier*, Fig.5.17, is basically introduced in the measurement circuit for two reasons:

1. To amplify the relatively weak output signal from the accelerometer, and

2. to transform the high output impedance of the accelerometer to a lower value.

In Fig.5.25 the equivalent electrical circuit of an accelerometer is shown. By connecting the accelerometer to a preamplifier the electrical circuit of the combination will be of the type shown in Fig.5.26. Here q_a is the charge developed on the total capacitance $C_a + C_c + C_i$ (C_a = accelerometer internal capacitance, C_c = connecting cable capacity, C_i = input capacitance of the preamplifier), S_q is the charge sensitivity of the accelerometer and a is the acceleration to which the accelerometer is subjected. R_a is the leakage resistance of the accelerometer (can normally be neglected) and R_i is the input resistance of the preamplifier. The resistance R_i in combination with

97
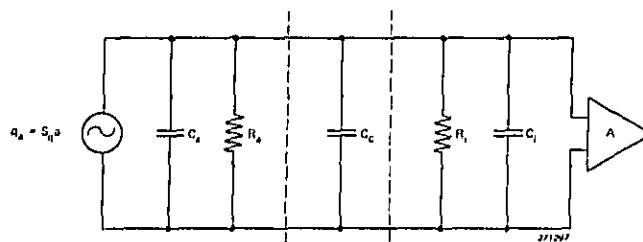
Fig.5.26. Equivalent electrical circuit for a combination of accelerometer, cable and preamplifier

the capacitances $C_a + C_c + C_i$ determines the lower frequency limit of operation for the combination accelerometer + preamplifier.

As mentioned in section 5.3 two "types" of accelerometer sensitivities are stated by the manufacturer, i.e. the charge sensitivity, S_q, and the voltage sensitivity, S_v. The charge sensitivity is defined as:

$$S_q = \frac{q_a}{a}$$

and the voltage sensitivity as:

$$S_v = \frac{e_a}{a}$$

where e_a is the open circuit output voltage from the accelerometer.

The sensitivities are furthermore interrelated via the accelerometer internal capacity, C_a, as this capacity is physically a part of the transducing element:

$$S_v = \frac{S_q}{C_a}$$

It is now possible to design the preamplifier in two ways, one in which the output voltage is directly proportional to the *input voltage*, and one in which the output voltage is proportional to the *input charge*. In the first case the preamplifier is called a *voltage amplifier*, in the second a *charge amplifier*.

The major operational difference between the two types of amplifiers is that *when a voltage amplifier is used the overall system is very sensitive to*

98

changes in cable capacitance, i.e. to changes in cable length between the accelerometer and the preamplifier, while *when a charge amplifier is used the effect of changes in cable length is negligible.*

This can also be readily seen mathematically. Consider first the *voltage amplifier.* The input voltage is here (neglecting the effects of R_a and R_i):

$$e_i = \frac{q_a}{C_a + C_c + C_i} = \frac{S_a\, a}{C_a + C_c + C_i} = \frac{S_v C_a\, a}{C_a + C_c + C_i} = \frac{C_a}{C_a + C_c + C_i}\, e_a$$

Thus the input voltage e_i is equal to the accelerometer open circuit voltage e_a multiplied by the factor $C_a/(C_a + C_c + C_i)$. By changing the cable capacity, C_c, the input voltage e_i is also changed. Since the output voltage from the preamplifiers $e_o = A\, e_i$, where A is the amplification factor of the amplifier, *the output voltage from the system, Fig.5.26 will depend upon the cable capacity.*
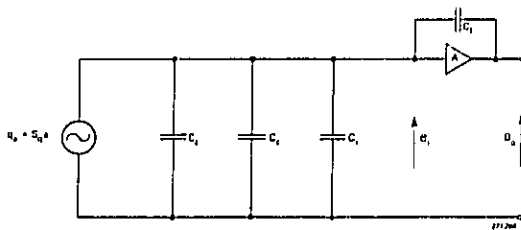
Fig.5.27. Equivalent electrical circuit for an accelerometer + cable + charge amplifier

In the case of the *charge amplifier,* Fig.5.27 should be consulted. Basically a charge amplifier consists of an high gain operational amplifier with a feedback capacitor, C_f, and it can be shown that the output voltage from the circuit is given by the expression:

$$e_o = \frac{q_a\, A}{C_a + C_c + C_i - C_f\, (A - 1)} = e_i\, A$$

Thus:

$$e_i = \frac{S_a\, a}{C_a + C_c + C_i - C_f\, (A - 1)} = \frac{C_a}{C_a + C_c + C_i - C_f\, (A - 1)}\, e_a$$

99
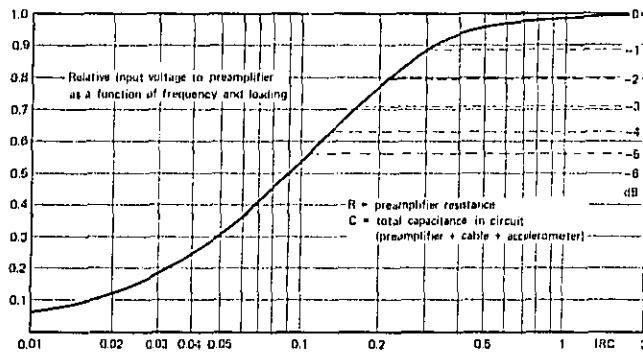
Fig.5.28. Chart which may be used to find the required input resistance, R_i, of a voltage preamplifier when the accelerometer + cable capacity, C, and the tolerable low frequency limit, f, of the measuring system are known

Examples:

a) If the −1 dB low frequency limit is f_{-1} then $R \approx \dfrac{0.31}{C f_{-1}}$

b) If the −3 dB low frequency limit is f_{-3} then $R \approx \dfrac{0.16}{C f_{-3}}$

As A is very large this expression becomes:

$$e_i \approx |\frac{C_a}{C_f A}| \quad e_a \approx |\frac{q_a}{C_f A}|$$

which is independent of the cable capacity C_c.

Another difference in performance between the voltage amplifier and the charge amplifier is that *the input resistance* of a voltage amplifier, R_i in Fig.5.26, cannot always be neglected, and will *affect the very low frequency response of the system*. This is illustrated in Fig.5.28 where the relative output voltage from the system is plotted vs. the expression *f R C (f=*frequency). Voltage amplifiers, or rather the voltage*pre*-amplifiers, are normally simpler in construction and contain less components than charge preamplifiers. They are therefore often less expensive and more reliable. On the other hand, cable length corrections and low frequency response considerations can be avoided by the use of charge preamplifiers. In selecting the appropriate preamplifier for vibration work the above arguments should be

100

Preamplifier Type	Features	Powered by	Frequency Range	Input			Output		Lowest Measurable Vibration Level
				Resistance	Capacitance	Max. Inp. voltage	Resistance	Max. Outp. voltage	
2616	Battery operated. Battery compartment removeable. Contains overload indicators and built in signal attenuator (−40 dB)	6–35 Volts DC (4–10 mA)	0.13 Hz–500 kHz	>1200 MΩ	10 pF	14 V peak (140 peak)	<180 Ω	14 V peak	
2623	For impedance transformation. Small, lightweight instrument, insensitive to mechanical vibrations. Powered from external DC source	2805 (28 Volts DC)	0.5 Hz–500 kHz	>2000 MΩ	3.5 pF	−10 V peak	<40 Ω	−10 V peak	
2624	Charge amplifier for the measurement of very low frequency vibrations and shocks. Eliminates influence of cable between accelerometer and preamplifier. Powered from external DC source	2805 (28 Volts DC)	0.003 Hz–30 kHz	−	−	−	<5 Ω	−10 V peak	
2625	Contains integrating networks for the measurement of velocity and displacement. Three suitable inputs with individual adjustments. Powered from DC. Built in battery compartment. Max. Amplification: 20 dB (10×)	2805 (28 Volts DC)	1 Hz–35 kHz (Acceleration)	>450 MΩ	14 pF	3 V peak at 0 dB gain	<50 Ω (from serial no 377905)	7 V peak	
2626	Conditioning charge amplifier for vibration testing and all kinds of vibration measurements. Built in, selectable high pass and low pass filters. Direct and transformer coupled output	Mains	0.3 Hz–100 kHz max.	−	−	10⁶ pC	<10 Ω	10 V peak	
4792	Contains integrating networks for the measurement of velocity and displacement. Max. amplification 20 dB (10×). Built in accelerometer calibrator.	2107, 2112, 2113, 2114, 2603, 2606, 2607, 2608	1 Hz–35 kHz (Acceleration)	>450 MΩ	8 pF	14 V peak (zero gain)	−	14 V peak	

Fig.5.29. Table indicating some important features and other relevant data for the various Brüel & Kjær Preamplifiers

duly considered. A number of preamplifiers are available from Brüel & Kjær. As all the preamplifiers can be used with all the Brüel & Kjær accelerometers the preamplifier may be selected purely according to its own merits. To assist the reader in the selection some important features of the various preamplifiers have been tabulated in Fig.5.29.

5.5. Selection of Analyzer and Read-out. Data Presentation

Even though all the basic "elements" in a vibration measuring arrangement (Fig.5.17) are equally essential, the one marked "analyzer" may be considered the "central" unit. It determines, in general what signal properties are being measured and what kind of data can be obtained in the form of numbers or curves.

The simplest "analyzer" consists of a linear amplifier and a detection device which makes it possible to measure some characteristic vibration signal values, for instance the peak value, the RMS-value or the average absolute value of either the acceleration, the velocity or the displacement (see also Chapter 2, section 2.1). In this connection it should be pointed out that if it is desired to measure signal peak values, not only the frequency response of the measuring system should be duly considered but its *phase response* must also be taken into account.

Although the frequency response of the system may indicate that all frequencies of interest are being passed on to the detection device without attenuation, considerable phase distortion can take place. If such distortion occurs, the relative phase shifts between the various frequency components in a complex signal change and the waveform of the signal reaching the
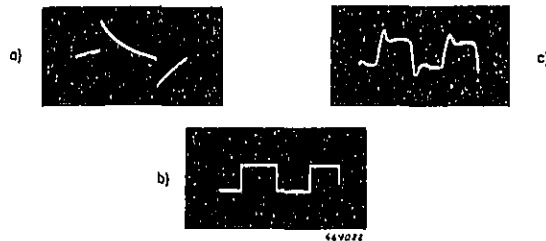

Fig.5.30.   Examples of waveform distortion due to phase non-linearity in the measuring system

102

detection device may look totally different from the waveform of the original vibration signal. Fig.5.30 exemplifies this with respect to a square-shaped vibration signal.

In Fig.5.30a) the input signal to the detection device is shown for the case where the fundamental frequency of the vibration corresponds to the *low* frequency limit of the measuring system, while Fig.5.30b) shows the undistorted signal. Finally, Fig.5.30c) indicates the signal waveshape at the detection device when the fundamental frequency of the vibration corresponds to the *high* frequency limit of the system. The changes in signal waveshape for the three cases are clearly noticed.

As a practical "rule of thumb" it may be stated that *serious waveshape distortion of the signal may be avoided when the fundamental vibration frequency is higher than 10 times the low frequency limit of the measuring system and the highest significant vibration frequency component has a frequency which is lower than 0.1 times the high frequency limit of the system, Fig.5.31.*

This "rule" should be applied with care, but may serve as a guideline in the selection of measuring equipment. In critical cases it is often advantageous to look at the signal waveshape at various points in the measurement system by means of an oscilloscope.

If, on the other hand, measurements are not made directly on the signal waveshape but on some kind of signal average value, for instance the RMS-value, phase relationships are no longer so critical. In the case of
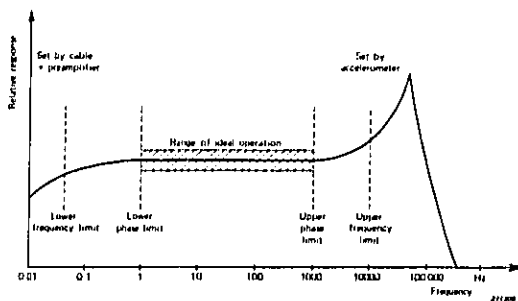
Fig.5.31. Sketch indicating how frequency non-linearity affects the range of "ideal" operation of a measurement system

RMS-measurements the phase relationships are actually of no importance at all, because of the squaring process involved.

Normally an "analyzer", or rather a detection device, of the type described above does not give the vibration engineer sufficient information about the signal he is studying. In most practical cases it will be necessary at least to be able to determine the frequency composition of the vibration signal. Use should then be made of a *frequency analyzer*.

Some basic frequency analysis arrangements were briefly described in section 5.2 and in the following some relevant considerations as to their practical use are outlined.

As mentioned in section 5.2 two types of frequency analyzers are commonly available, namely the *constant bandwidth* type analyzer and the *constant percentage bandwidth* type analyzer. The questions now arise. (1) When should the constant bandwidth analyzer be used and when should the constant percentage bandwidth analyzer be used? (2) Are there other possible and practical methods of analog vibration frequency analysis?

There is no unique answer to the first question, while the second one may be answered with a "yes". However, the two questions are best discussed in conjunction with each other.

When the measurement problem consists in analyzing a vibration signal containing a number of *completely stable, discrete frequency components* the constant bandwidth type analyzer may be preferred if the vibrations are of a *periodic* nature because in this case the various frequency components
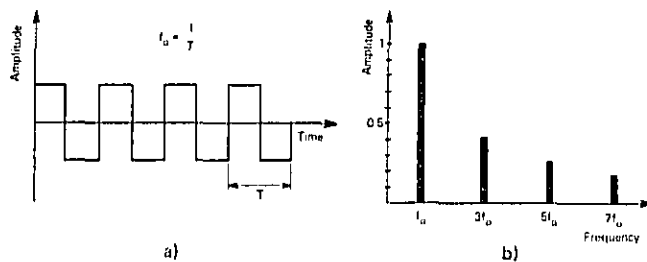
Fig.5.32. Example of the frequency spectrum of a periodic signal (square wave)

104

are harmonically related, Fig.5.32. By comparing Fig.5.32b) with Fig.5.11 it is readily seen that if constant percentage bandwidth analysis was used it might not be possible to measure the highest harmonic components of the signal separately, because more than one component could then be inside the analyzer bandwidth Fig.5.11b). On the other hand, if the percentage bandwidth of the analyzer is very small, say 6%, this phenomenon would in practice not become serious until one tried to measure the fifteenth harmonic!

If the (periodic) signal is not quite stable, and only the first few harmonics are of interest, a constant percentage bandwidth type analyzer is equally well suited for the measurement. Such cases may occur when vibration measurements are made on rotating machinery or internal combustion engines and, because the "unstable" operation causes a constant percentage type of frequency variation, the constant percentage bandwidth analyzer may even be preferable!

When the vibration signal to be analyzed is *of a stochastic nature (random vibrations)* which produce a continuous frequency spectrum the preferred type of analysis will depend not only upon the spectrum itself, but also upon the ultimate use of the measured data. If, for instance, the data are to be used in the preparation of vibration test specifications no detailed spectrum analysis is normally required because such specifications are, in general, derived by enveloping a number of measurement situations. Analysis in the form of 1/3 octave, or even 1/1 octave, frequency bands will therefore suffice.

On the other hand, if the data are to be used for the study of vibration transmission characteristics, or for possible failure predictions, very often an extremely detailed frequency analysis is required. Whether the analysis should be made in terms of constant bandwidth, constant percentage bandwidth, or some other bandwidth — versus — frequency type of analysis, may then often depend upon the amount of data to be analyzed and the analysis equipment available in the laboratory. Even though the constant percentage bandwidth type of analysis seems, also in this case, to offer many advantages, its resolving power may not be sufficient in practice. In some practical cases a frequency resolution of 0.5%, or better, is required, and this requirement is difficult to meet with practical analog constant percentage bandwidth analyzers. It may, however, be met by the constant bandwidth type analyzer, at least over a certain portion of the vibration frequency range.

A further discussion on the use of constant percentage bandwidth, constant bandwidth, and other bandwidth — versus — frequency types of

analysis of random vibrations is carried out in a separate publication[*]) and
interested readers are referred to this for detailed information.

In conjunction with the frequency analysis of stationary *random vibra-
tions* it should on the other hand be mentioned that the most efficient (and
common) method of presenting this kind of data is in terms of *mean square
(or power) spectral density* functions (see also Chapter 2, section 2.2). As
the mean square spectral density function has been defined as

$$w(f) = \lim_{\Delta f \to 0} \lim_{T \to \infty} \frac{1}{\Delta f\, T} \int_0^T f^2_{\Delta f}(t)\, dt = \lim_{\Delta f \to 0} \frac{x^2_{\Delta f}}{\Delta f}; x_{\Delta f} = \text{RMS-value}$$

this presentation involves the *division of the squared RMS-value, measured
in a narrow filter-band with bandwidth, Δf, by the bandwidth.*

If a *constant bandwidth* type analyzer is used for the measurements the
*resulting frequency spectrum is therefore directly proportional to the mean
square spectral density function.* In cases where a *constant percentage band-
width* analyzer is used, however, a certain, *frequency dependent correction*
has to be applied to the measured spectrum to obtain a measure for the
mean square spectral density function. Because here $\Delta f = \text{const.} \times f$, by
definition, this correction is very simple in that

$$w(f) = \left(\frac{x_{\Delta f}}{\sqrt{\text{const.} \times f}}\right)^2$$

The correction can be applied either graphically, Fig.5.33, or electrically
by means of a special filter, Fig.5.34 (it should be noted that the straight
line type of correction shown in Fig.5.33 is only valid when the frequency
spectra are plotted to logarithmic scales).

From the above discussion on the subject of frequency analysis it will be
clear that the techniques used, both with regard to the measurements them-
selves, and to the presentation of the measured data differ somewhat,
depending upon whether the vibrations are of a periodic or random nature.
If the *vibrations are periodic (or contain discrete frequency components
only) the spectra should be presented in terms of measured RMS-values
"independent" of the measurement bandwidth.* On the other hand, if the
vibrations are of the *random vibration type the spectra should be presented
in terms of mean square spectral density functions which do depend upon
the measurement bandwidth.* This is important to keep in mind because

---

[*]) "The Application of B & K Equipment to Frequency Analysis and Power Spectral
Density Measurements".

106
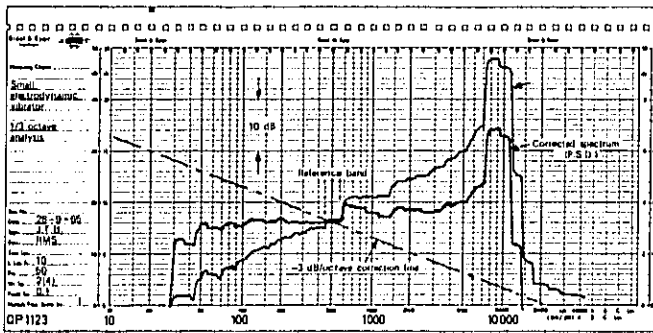
Fig.5.33. *Graphical transformation of constant percentage bandwidth data into mean square spectral density data using the 1/√T̄-correction*
a) Measured spectrum
b) Mean square spectral density diagram
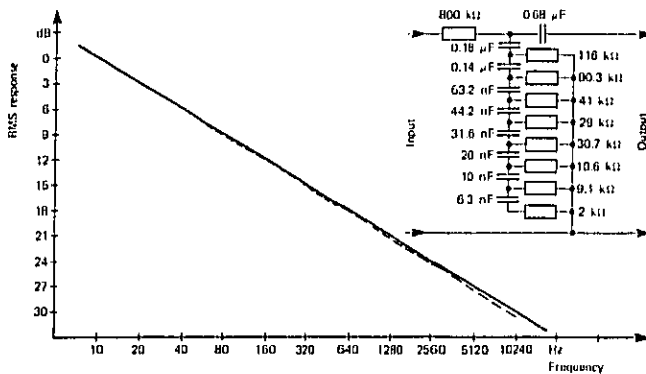
Fig.5.34. *Filter circuit producing a 1/√T̄ characteristic. The circuit should be loaded by an impedance higher than 0.5 MΩ. The generator impedance should preferably be low but is not critical (<50 kΩ)*

considerable confusion has been caused in the past due to misleading presentations and interpretations of frequency analysis data.

In some cases in practice the vibrations consist of a combination of random and periodic signals. If the machinery producing this kind of vibrations contains sharp (lightly damped) resonances a "peak" in the vibration frequency spectrum may indicate either a discrete frequency component or a lightly damped resonance. To be able to distinguish roughly between the two phenomena it is necessary to consider, for a moment, *the averaging time of the read-out device.*

Referring to Chapter 2, sections 2.1 and 2.2 the RMS-value of a vibration signal was defined mathematically as:

$$X_{RMS} = \sqrt{\frac{1}{T} \int_0^T x^2 (t)\, dt}$$

In this formula T *is the averaging time,* i.e. the time used to physically determine the RMS-value of the vibrations. Now, in cases of statistically varying vibrations (random vibrations) the *true* RMS-value is only obtained if T is infinitely great. Because T cannot in practice be made infinitely great, and because the time of observation (reading of the meter) in practical vibration measurements is normally considerably greater than the instrument averaging time, T, the observed RMS value of the vibrations fluctuates during measurements.
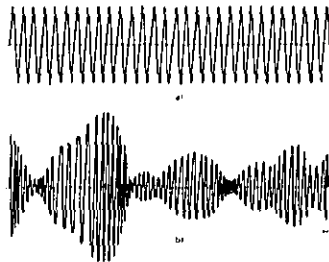

Fig.5.35.   *Illustration of the difference in character between a purely harmonic (sinusoidal) vibration and a narrow band random vibration signal*
a) Harmonic vibration
b) Narrow band random vibration. (Note the fluctuations in maximum amplitudes)

108

Implicit in the above formula is also the measurement bandwidth in that *the narrower the bandwidth the greater are the fluctuations, provided that T is kept constant.* On the other hand by selecting a greater T in the instrument meter circuit the fluctuations can be decreased. This relationship can be stated mathematically by means of the formula:

$$\epsilon = \frac{1}{2\sqrt{\Delta f\, T}}$$

where ϵ is a measure of the RMS fluctuations,[*] Δf the vibration frequency bandwidth (or measurement bandwidth, — whichever is the smallest), and T is the averaging time. Also, this relationship provides a "key" to determine whether a "peak" in the measured vibration frequency spectrum is caused by a discrete frequency component (purely periodic signal) or by a randomly excited, lightly damped resonance: *If the "peak" is caused by a discrete frequency component* the RMS value should show only small fluctuations ("instability" in the machinery) and *the fluctuations should not change greatly when T is decreased.* If, on the other hand, *the "peak" is caused by a randomly excited, lightly damped resonance a decrease in T will cause a considerable increase in the RMS fluctuations.* Fig.5.35 illustrates the difference in character between a purely periodic vibration signal and a randomly excited, lightly damped resonance.

The formula

$$\epsilon = \frac{1}{2\sqrt{\Delta f\, T}}$$

constitutes one of the essential "laws" in the field of frequency analysis of random vibrations and states that if, for a particular measurement situation, *it is desirable to increase the frequency resolution (decrease Δf), then T must be correspondingly increased to obtain the same measurement accuracy.*

Fig.5.36 shows a table of the various types of frequency analyzers which are available from Brüel & Kjær. Most of these analyzers may be swept automatically, the sweep being controlled from the Brüel & Kjær Level Recorder Type 2305, see also section 5.2.

The Level Recorder also constitutes a convenient *read-out device* which makes it possible to record the measured frequency spectrum directly on preprinted frequency calibrated recording paper, see for instance Figs.5.10

---

[*] Actually ϵ is the relative standard deviation of the RMS fluctuations.

Frequency Analyzer Type	Principle of Operation	Frequency Range	Bandwidth	Type of Frequency Sweep	Remarks
2010	Constant Bandwidth	2 Hz — 200 kHz	3 — 10 — 30 — 100 — 300 — 1000 Hz	Continuous	Heterodyne Analyzer. May be swept automatically by either mechanical or electronic sweep control
2020 + 2606 + 1022 (1024)	Constant Bandwidth	20 Hz — 20 kHz	3 — 10 — 30 — 100 Hz	Continuous	Heterodyne Slave Filter Arrangement. May be swept automatically
2021 + 1025 (1042; 1026)	Constant Bandwidth	5 Hz — 10 kHz	3 — 10 — 30 — 100 — 300 Hz	Continuous	May be swept automatically
2107 (+ 1614) (+ 1615)	Constant Percentage Bandwidth	20 Hz — 20 kHz / 2 Hz — 20 kHz / 25 Hz — 20 kHz	6% — 29% / 1/3 and 1/1 Octave	Continuous / Contiguous Bands	May be swept automatically
2113 2606 + 1615 2114 2607 + 1614	Constant Percentage Bandwidth	25 Hz — 20 kHz / 25 Hz — 20 kHz / 2 Hz — 160 kHz / 2 Hz — 160 kHz	1/3 and 1/1 Octave	Contiguous Bands	May be swept automatically
2203 + 1613 2204 + 1613	Constant Percentage Bandwidth	31,5 Hz — 31,5 kHz	1/1 Octave	Contiguous Bands	Battery Operated No Automatic Sweep
3347	Constant Percentage Bandwidth	25 Hz — 40 kHz	1/3 Octave	Contiguous Bands	Parallel (Real Time) Analyzer. For connection to both Analog Recorders. Digital Computers

Fig.5.36. Table of Brüel & Kjær frequency analysis equipment

and 5.38. When it is used as a read-out device in a vibration measurement the averaging time is normally determined by the writing speed of the recording pen, and certain other internal properties of the Recorder itself.

For the case of the most commonly used input potentiometer (50 dB) and the correspondingly recommended settings of the Recorder control knobs, the resulting averaging times are tabulated in Fig.5.37 as a function of writing speed. In selecting a suitable writing speed the above formula for e should be born in mind.

Writing Speed mm/sec	Approximate Averaging Time*) sec
1000	0.005
800	0.007
630	0.008
500	0.010
400	0.013
250	0.020
160	0.03
100	0.05
63	0.08
40	0.13
25	0.20
16	0.35
8	0.7
4	1.3
2	3

Fig.5.37.   Table of the relationship between the writing speed of the Brüel & Kjær Level Recorder Type 2305 and the resulting effective averaging time. The figures are presently under revision.

When the writing speed (averaging time) has been selected the next problem that arises is in general the selection of an "optimum" sweep rate for the analysis. The sweep rate is, when precalibrated paper is used on the Level Recorder, closely connected to the Recorder's paper drive speed and the Analyzer bandwidth.

A useful formula, which also takes the dynamic range of the measurements into consideration is given by:

111

$$\text{Paper Speed} \lesseqgtr \frac{X}{100} \times \text{Writing Speed}$$

where X *is the distance in mm on the recording paper that corresponds to the Analyzer bandwidth.*

In connection with the use of this formula it should be noted that when other than constant percentage bandwidth analysis and logarithmic frequen-cy scales (or constant bandwidth analysis and linear frequency scales) are used in the measurements, it is necessary to *consider the distance X in various parts of the frequency range.* For instance when using the Brüel & Kjær Frequency Analyzer Type 2107 X is smallest at the highest frequen-
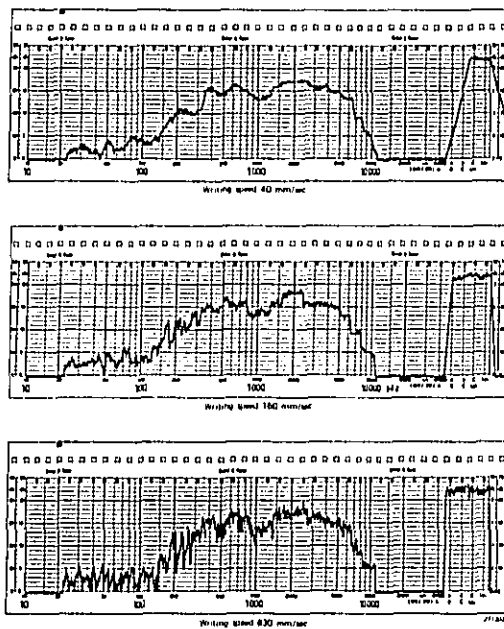
Fig.5.38. *Examples of how the choice of Level Recorder writing speed (averaging time) affects the appearance of frequency analyzed random vibrations*

112

cies, and the value found in this range should be inserted in the formula given above for the paper drive speed.

In concluding the discussion on sequential filtering, averaging time and RMS fluctuations of stationary random vibrations, Fig.5.38 illustrates how the choice of averaging time (writing speed) affects the recording of a particular frequency spectrum.

There is, however, a particular area of measurement where the proper choice of averaging time is of special importance. This is the field of analysis of *non-stationary random vibrations* (see also Chapter 2, section 2.4). If the non-stationarity can be represented by a deterministic function it might, for instance, often be possible (by varying the averaging time) to "separate" the random and the deterministic time trends in the data. Use is, in such cases, commonly made of magnetic tape recording of the original vibration signal. The recording is then dubbed onto an endless tape loop and the loop analysed a number of times, each time with a different averaging time setting on the analyzing equipment. When the analysis averaging time becomes short relative to the deterministic time trend (but still great enough to maintain a reasonable accuracy in the random "portion" of the data) the non-stationarity becomes more or less evident in the recording.

Although sequential filtering and automatic recording of the result is an excellent method of obtaining detailed information on the vibration frequency spectrum, the method may, in many cases be considered too slow, and use has to be made of *parallel analysis* and "instantaneous" read-out of the complete spectrum, see also section 5.2. Also in this case the selected *averaging time* influences the readout. However, the problem of frequency sweep speed is here completely different from the one discussed above in connection with sequential filtering. In the Brüel & Kjær *Real Time Analyzer Type 3347,* for instance, *a complete (electronic) scan of the output from all filter detectors is made in 2 milliseconds,* which is considered "instantaneous", at least when compared to the previously described sequential filtering.

The electronic scanning of the filter outputs is made *after* rectification and averaging, so that each filter is followed by a rectifier and averaging circuit, see Fig.5.15.

This arrangement allows different averaging times to be used on the various filter outputs, whereby similar statistical accuracy characteristics can be obtained over the complete frequency range, even if the absolute filter bandwidth varies. However, unless otherwise specified, certain "Standard"

113
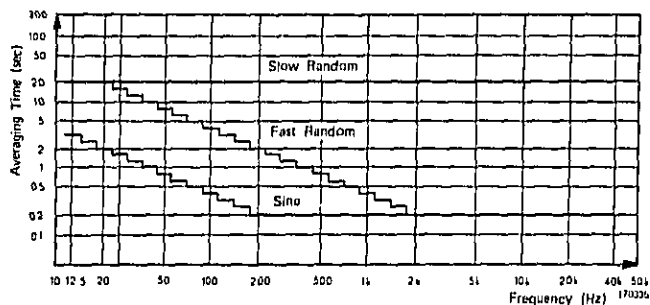
Fig.5.39. *Variation in averaging time with frequency of the Real Time Analyzer Type 3347 (standard version)*

averaging times versus frequency characteristics are available on the instrument. These are shown in Fig.5.39 and are named "Slow Random", "Fast Random" and "Sine", respectively. The corresponding statistical error ε is indicated in Fig.5.40 for 1/3 octave spectrum analysis.

It should be pointed out at this stage that the selection of *appropriate averaging times, and statistical error considerations, are of considerably greater importance when the measured results are to be used directly for further digital processing than when they are used for normal analog recording.* When analog read-outs are utilized the data are, more or less automatically, further averaged by the eye of the observer.
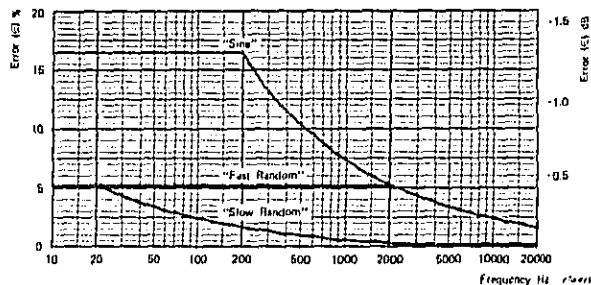
Fig.5.40. *Standard error (ε) in random signal measurements with the Real Time Analyzer Type 3347 as a function of frequency*

114

In the case of digital processing, on the other hand, the outputs from the averaging circuits are sampled periodically, and extreme values may be included among the samples.

Even though the frequency analysis technique may be considered the most important measurement tool that the practicing vibration engineer has at his disposal today, other forms of analysis exist and is of considerable scientific importance. These belong, however, at present to what is commonly termed "more advanced" analysis techniques, see Chapter 8.

5.6. Calibration and Performance Checks

Each instrument produced by Brüel & Kjær has been thoroughly checked and individually calibrated before it leaves the factory. The measurement transducers, in this case the accelerometers, are not only individually calibrated but they are also supplied with a full calibration chart, Fig.5.41. Furthermore a special section in the accelerometer instruction manuals details the procedures utilized for calibration.

The accuracy of the factory calibration is better than ±2% for charge sensitivity, voltage sensitivity. and capacity. Even though the long term stability has been checked and shows less than 2% change in the calibration data per year, the transverse sensitivity may change temporarily when the accelerometer is exposed to large shocks, especially sideways. Normally however, it will return to the original value within the next 24 hours.
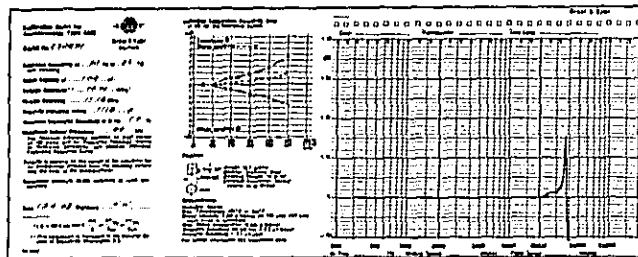
Fig.5.41.   Example of the individual calibration chart supplied with each
            Brüel & Kjær Accelerometer

115

In calibrating a *typical* vibration measuring arrangement this can, in view of the above, be made directly from the figures given in the instrument data sheets. If, on the other hand, some sort of *special* measuring arrangment is used, or it is desired to calibrate a *tape recording* of the vibration signal for later analysis in the laboratory, use can be made of one of the Brüel & Kjær *vibration calibrators.*

One such calibrator is built into the *Preamplifier Type 4292* and consists of a small vibrator operated at the mains frequency, see Fig.5.42. The electromechanical circuit of the vibrator is, by means of a knob, tuned in resonance with the mains frequency, and the amplitude adjusted until its *peak acceleration level corresponds to 1 g* (acceleration of gravity). Because certain difficulties arise in conjunction with the setting of the *exact* vibration level this method of calibration is not recommended for use by un-trained personnel if a calibration accuracy better than some 10% is desired.

Fig.5.42. Photograph of the Brüel & Kjær Accelerometer Calibrator and Preamplifier Type 4292

A second calibrator, Brüel & Kjær Type 4291, is shown in Fig.5.43 and is considerably more sophisticated in its construction. Here the peak *acceler-ation level of 1 g* can be read conveniently and accurately on a built-in meter, and the vibration frequency is *80 Hz*, controlled by an internal Wien bridge type of oscillator. *The accuracy of the calibration will, when*

116
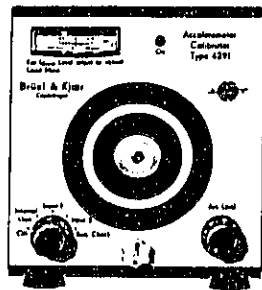
Fig.5.43.   Photograph of the Calibrator Type 4291

this calibrator is correctly used, be better than ±2%. Also, the built-in
oscillator can be disconnected and substituted by an external generator for
calibration in the frequency range 50 to 2000 Hz. Provision is furthermore
made for back-to-back calibration of transducers, reciprocity calibration,
and insert voltage calibration.

   Note: When the calibrator contained in the Preamplifier Type 4292 or
the Calibrator Type 4291 are used for calibration checks the peak acceler-
ation level is adjusted to 1 g. Thus, in order to obtain a correct sensitivity
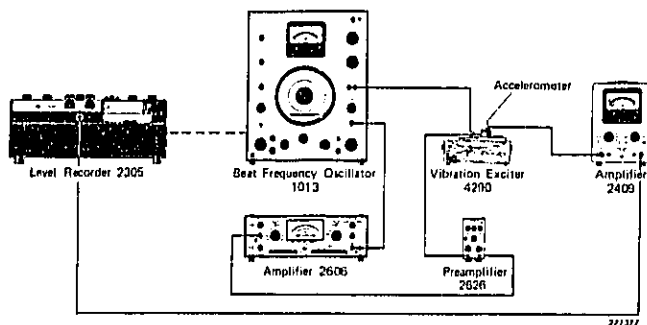

Fig.5.44.   Measuring arrangement suitable for checking the frequency
             response of accelerometers (or complete vibration measurement
             installations) utilizing the Calibrator Exciter Type 4290

117

factor (Electrical peak/Acceleration peak, Electrical RMS/Accel. RMS) the electronic equipment should be switched to measure peak values.

A third Calibrator available from Brüel & Kjær is the *Calibration Exciter Type 4290*. This calibrator has been designed basically to check the frequency response of accelerometers in the frequency range 50 Hz to 30 kHz, utilizing a measuring and control arrangement of the type shown in Fig.5.44. It may also be used for sensitivity calibration by the substitution method. The maximum attainable acceleration level is, however, relatively low (of the order of 0.1 g). Finally, a fourth type of Calibrator allowing the calibration of accelerometers *at acceleration levels up to 100 g* over a limited frequency range is shown in Fig.5.45.

This calibrator is part of a special vibration test system, see also section 7.3 (Vibration Testing), and is basically intended for more permanent laboratory installation.
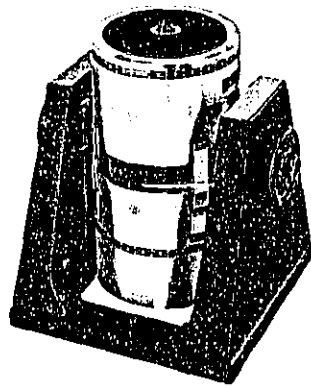
Fig.5.45. *Photograph of a vibration calibrator capable of calibrating vibration pick-ups up to an acceleration level of 100 g (Brüel & Kjær Type 4801 + 4815)*

118

5.7. Some Practical Accelerometer Application Considerations.
   Mounting Techniques

In section 5.1 it was mentioned that the vibration transducer should load the structural member on which it is mounted as little as possible. This requirement, of course, originates from the fact that any "extra" load might change the original motion of the structure and thus invalidate the measurement results. If measurements are made on thin plates use should therefore be made of small, lightweight accelerometers (e.g. Brüel & Kjær Accelerometer Type 4344). To allow an estimate of the influence of accelerometer mass-loading to be made the following formula can be applied:

$$a_r = a_s \frac{m_s}{m_s + m_a}$$

where a_r = acceleration response of structure with accelerometer
       a_s = acceleration response of structure without accelerometer
       m_s = equivalent mass (weight) of that "part" of the structure to which the accelerometer is attached
       m_a = accelerometer mass (weight)

Also, the mass-loading may change the resonant frequencies of the structure. If the mass-loading effects turn out to be no problem the use of a general purpose Accelerometer of the Type 4339 or 4343 may be the best solution in most practical measurement situations.

Having selected the appropriate accelerometer the question arises: *How should it be properly mounted at the measurement point?* Fig.5.46 shows some practical answers to this question. Here *six methods of mounting* are suggested and the merits of each method are briefly described below.

Type 1 mounting is the best solution frequency responsewise, approaching a condition corresponding to the actual calibration curve supplied with the accelerometer. If the mounting surface is not quite smooth it is a good idea to apply a thin layer of silicon grease to the surface before screwing down the accelerometer. This increases the mounting stiffness.
It is essential whenever using a mounting screw, not to screw fully in as it may introduce base bending affecting the sensitivity of the accelerometer.

119
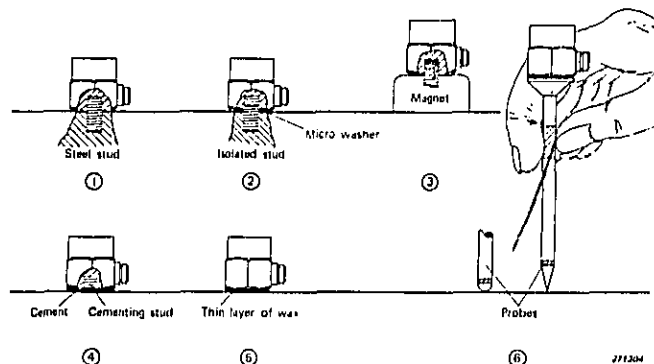
Fig.5.46.   Different methods of mounting of the Accelerometers:
1. With steel stud
2. With isolated stud and mica washer
3. With permanent magnet
4. With cementing stud
5. Accelerometer stuck on with wax
6. Handheld with probe

Type 2 mounting is convenient when electrical isolation between acceler-
ometer and vibrating body is necessary. It employs the
isolated stud and a thin mica washer. Frequency response
is good due to the hardness of the mica. Make sure that
the washer is as thin as possible (it can easily be split up
into thinner layers).

Type 3 mounting employs the permanent magnet which also gives electrical
isolation from the vibrating specimen. A closed magnetic
path is used and there is virtually no magnetic field at the
accelerometer position. This mounting should not be used
for acceleration amplitudes higher than about 200 g.
Max. 150°C short time.
The holding force of the magnet available from Brüel &
Kjær has been investigated for various steel plate thickness
and for various thickness of brass (non-magnetic) between
the magnet and the steel. See Fig.5.47.
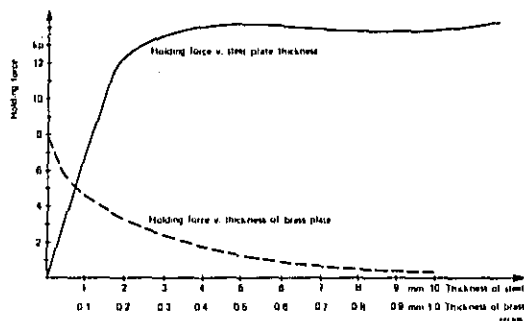
Fig.5.47. *Holding force of the mounting magnet versus thickness of steel*
plate, and versus thickness of intermediate brass plate

Type 4 mounting is convenient when a cementing technique is appropriate,
with the possibility of removing the accelerometer from
time to time.

Type 5 mounting employs a thin layer of wax for sticking the accelerometer
onto the vibrating surface. The wax is delivered with the
Brüel & Kjær Accelerometer Sets. A frequency response
curve is given in Fig.5.48e). It is seen that this method of
mounting gives a very good frequency response due to the
stiffness of the wax. At higher temperatures this will
decrease.
Soft setting glues or gum should be avoided because of
decoupling and bad frequency response.
For minimum weight and optimum performance one may
also recommend the Eastman 910 cement, marketed by
the Armstrong Industry, or Tixo K-1 manufactured by
Tiox-Tinten und Klebstoffwerk G.m.b.H., Vienna. Dental
cement epoxy resins are also very useful, especially in
connection with the cementing stud which is intended for
use in applications where mounting by cementing tech-
niques is preferred while retaining the possibility of
removing the accelerometer itself.

Type 6 mounting employs the probe with interchangeable round and

121
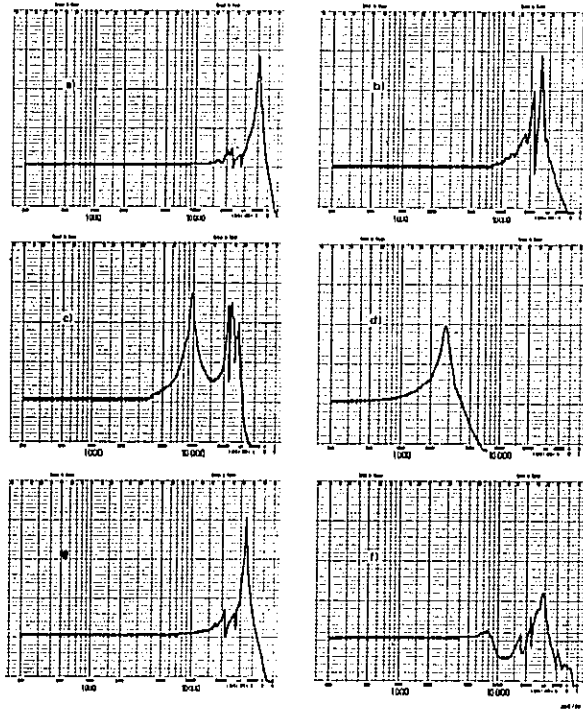
Fig.5.48. Typical frequency response curves for an accelerometer when
mounted according to some of the methods suggested in
Fig.5.46

a) Mounting by means of steel stud
b) Mounting by means of isolated stud and mica washer
c) Mounting by means of permanent magnet
d) Handheld with probe
e) Mounting by means of wax
f) Mounting by means of soft glue (not recommended)

122

pointed tips. The method may be convenient for certain
applications, but should not be used for frequencies much
higher than 1000 Hz, since the natural resonant frequency
in this case is very low.

Fig.5.48 shows some frequency response curves obtained for the various
methods of mounting. The curves may serve as guide-lines when selecting
the most convenient mounting type for a particular measurement problem.
In concluding the discussion on accelerometer mounting technique it should
be mentioned that the mounting torque for threaded screws should be
around 18 kg-cm or 15 lb-in. The accelerometers are not harmed by a larger
torque but the isolated stud may not stand more than 30 lb-in. A mounting
torque of the correct value is applied with a 10 cm (4") spanner with
normal pressure on the handle. A 6" or larger spanner should be used with
care. If a smaller spanner is used, one cannot do any harm to the thread, but
the accelerometer may not be sufficiently well secured. Even though the
selection and mounting of a suitable accelerometer are important problems
to be considered in practical vibration measurements, they are not the only
ones.

Because piezo-electric accelerometers are high impedance devices certain
problems may also arise from *connecting cable noise*. These noises can
originate either from mechanical motion of the cable, or from ground-loop
induced electrical hum and noise. The mechanically caused noises are some-
times called *"tribo-electric effects"*, or simply "microphonic noise". It
originates from local capacity and charge changes due to dynamic bending
or compression and tension of the cable, and may be particularly disturbing
at lower frequencies. The Brüel & Kjær accelerometer cables are designed
and treated for noiseless operation. It is, however, always good policy to
clamp the cables as firmly as possible in order to avoid relative movement,
Fig.5.49. The second noise effect mentioned above, i.e. that of *ground-loop*

Wrong   Correct   The cable should leave the specimen
at the point of lowest vibration

Wax, tape, epoxy or other type of clamping   271316
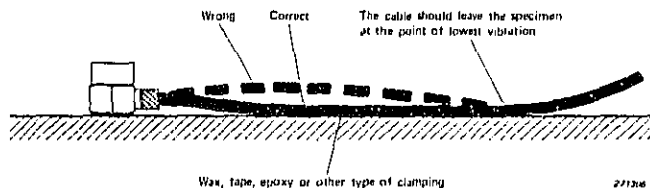
*Fig.5.49.   Clamping of the cable to avoid relative movements (cable
"whip")*

123

induced noise, may, particularly in large vibration measurement installa-
tions, sometimes pose serious problems. Fig.5.50a) illustrates how a ground
loop is formed, and noise introduced (the voltage drop, ΔV adds directly to
the, sometimes very weak signal from the accelerometer). The only way to
avoid the formation of ground loops is to ensure that grounding of the
installation is made only in one point, Fig.5.50b). Where ground loops are
critical the accelerometer should be electrically isolated from the structure
on which it is mounted by means of the isolated stud and mica washer
(Type 2 mounting, Fig.5.46). Grounding should preferably be made at the
analysing or read-out device.
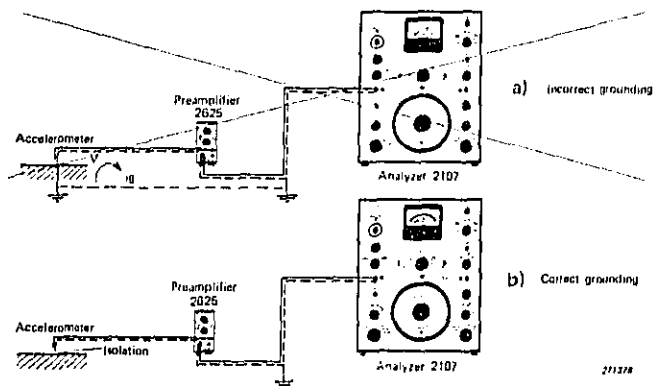
Fig.5.50. Illustration of ground-loop phenomena
            a) This method of connection forms ground loop and should be
            avoided
            b) No ground-loop is formed. Recommended method of con-
            nection

    Finally, an effect which may sometimes be disturbing when measure-
ments are made of *very low frequency, very low level vibration* should be
mentioned. This is the effect of temperature "shocks" or rather temperature
changes. Even by relatively small temperature changes the output from the
accelerometer may under these circumstances vary at a rate determined by
the time constant of the accelerometer-preamplifier input circuit. Normally
this effect will not be noticeable unless the low frequency response of the

124

overall measuring system is adjusted to be linear practically down to DC
(lower limiting frequency of the order of 0.003 Hz). In ordinary vibration
measurements temperature effects as described above need not be con-
sidered.

5.8. A General Measurement Scheme

A careful study of the preceding sections of this chapter should enable
the vibration engineer to select and utilize the measuring equipment
necessary to perform thorough and meaningful vibration measurements in
most of the situations occurring in practice. There is, however, one
important exception, and that is when the "vibrations" to be studied con-
sists of single transients or shocks. The practical measurement of this type
of phenomena is treated in the next Chapter (Chapter 6) of the book. A
further study also of that chapter may thus be required before measure-
ments are made. On the other hand, whether the vibrations consist of steady
(stationary) vibrations or shocks it might be useful at this stage to outline
some sort of a general "measurement scheme". Such a "scheme" is meant as
a help to remember the most important factors in the setting up and use of
a vibration measurement system, rather than as a detailed "turning-of-the-
knobs" type of procedure.

1. *Determine carefully where to place the vibration transducer, and its
   possible mass-loading effects* (Section 5.7).

2. *Estimate what types and levels of vibrations that are likely to be
   present at the transducer mounting point* (periodic vibrations,
   random vibrations, shocks).

3. *Select the most suitable vibration transducer (accelerometer) con-
   sidering items 1 and 2 above as well as environmental factors*
   (temperature, humidity, acoustic and electromagnetic fields). See
   sections 5.3 and 6.2.

4. *Determine what type of measurement would be most appropriate
   for the problem at hand.* (Overall measurement of acceleration,
   velocity or displacement, waveform recording, magnetic tape
   recording, frequency analysis.)

5. *Select the most suitable electronic equipment,* considering frequen-
   cy and phase characteristics, dynamic range, and convenience of
   operation. See sections 5.4, 5.5 and 6.1.

125

6. *Check and calibrate the overall system including accelerometer and connecting cables,* see section 5.6.

7. *Make a sketch of the instrumentation system* with all type numbers and serial numbers included. (Section 5.2).

8. *Select the appropriate accelerometer mounting method,* considering vibration levels, frequency range, electrical insulation problems and ground loops. See section 5.7.

9. *Mount the accelerometer onto the structure, carry out the measurements and record the result.*

10. *Note down the setting of the various instrument control knobs.*

If measurements are to be made in liquids or in very moist environments it is necessary to seal the cable entry into the accelerometer as shown in Fig.5.51. A good sealant for the cable entry is for example Dow Corning Silastic RTV 731 (room temperature vulcanizing silicon rubber) or General Electric equivalent. These sealants show excellent performance for a wide temperature range $-70^{\circ}C$ to $+260^{\circ}C$ ($-100^{\circ}F$ to $+500^{\circ}F$).
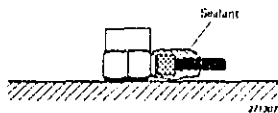
Fig.5.51. Sealing of the accelerometer cable entry

Note: It is good policy always to *check the "back-ground noise" level* of a vibration measurement system. This can be done by mounting the accelerometers on a non-vibrating object and measuring the "apparent" vibration level of this arrangement.

To obtain reasonably good accuracy in the actual vibration measurements the "apparent" vibrations should be less than one third of the measured vibrations. Or said in other words: The noise "floor" of the installation should be at least 10 dB below the vibration levels to be measured.

126

5.9. Selected Bibliography

BECKWITH, T.G. and
BUCK, N.L.:
Mechanical Measurements. Addison-Wesley, 1961.

BOUCHE, R.R.:
Improved Standard for the Calibration of Vibration Pick-ups. Experimental Mechanics Vol. 1, No. 4, April 1961.

BOUCHE, R.R.:
Characteristics of Piezoelectric Accelerometers. Test Engineering. Vol. 8, No. 4, October 1962.

BROCH, J.T.:
Electrical Measurement of Mechanical Vibrations. Brüel & Kjær Tech. Rev. No. 4, 1956.

BROCH, J.T.:
FM Magnetic Tape Recording. Brüel & Kjær Tech. Rev. No. 1-1967.

BROCH, J.T. and
WAHRMANN, C.G.:
Recording of Narrow Band Noise. Brüel & Kjær Tech. Rev. No. 4-1960.

BROCH, J.T. and
WAHRMANN, C.G.:
Averaging Time of Level Recorders. Brüel & Kjær Tech. Rev. No. 1-1961.

CRANDALL, S.H. et al.:
Random Vibrations I and II. The M.I.T. Press and John Wiley and Sons, Inc. 1958 and 1963.

EDELMAN, S., JONES, E.
and SMITH, E.R.:
Some Developments in Vibration Measurements. J.A.S.A. Vol. 27, No. 4. April 1955.

FOSTER, G.B.:
Recent Developments in Machine Vibration Monitoring. IEEE Transactions on Industry and General Applications. Vol. IGA-3, No. 2, March/April 1967.

KEAST, D.N.:
Measurements in Mechanical Dynamics. McGraw-Hill Book Company, Inc. 1967.

KITTELSEN, K.E.:
Vibration Measurements in the Laboratory of Applied Physics at the Technical University of Denmark. Brüel & Kjær Tech. Rev. No. 1, 1967.

127

KÜHL, R.:   A Portable Calibrator for Accelerometers, Brüel & Kjær Tech. Rev. No. 1, 1971.

LEVY, S. and   Calibration of Vibration Pick-ups by the Reci-
BOUCHE, R.R.:   procity Method. Journ. of Research of the N.B.S., Vol. 57, No. 4, October 1956.

LICHT, T.:   Vibration Measurement by a Laser Interferome-
                             ter. Brüel & Kjær Tech. Rev. No. 1, 1971.

MORROW, C.T.:   Averaging Time and Data Reduction Time for Random Vibration Spectra, I and II, J.A.S.A., Vol. 30, Nos. 5 and 6. May-June 1958.

RAMBERG, W.:   Calibration of Shock and Vibration Pick-ups. Noise Control, Vol. 3, No. 5, 1957.

RASMUSSEN, G. and   Accelerometer Configurations. Brüel & Kjær
JENSEN, J.A.:   Tech. Rev. No. 2-1969.

RHODES, J.E.:   Piezoelectric Transducer Calibration Simulation Using Series Voltage Insertion. Environmental Quarterly, Vol. 8, No. 1, March 1962.

ROCKWELL, D.W. and   Measurement of Accelerometer Transverse Sensi-
RAMBOZ, J.D.:   tivity. Shock, Vibration and Associated Environ-
                             ments, Bulletin 35, 1966, Part 4.

SCHLOSS, F.:   Inherent Limitations of Accelerometers for High Frequency Vibration Measurements. J.A.S.A., Vol. 33, No. 4, April 1961.

TUSTIN, W.:   Calibration of Vibration Transducers. Metrology Engineering Center, Bureau of Naval Weapons Representative, Pomona, California, 1965.

WAHRMANN, C.G.:   A True RMS-Instrument. Brüel & Kjær Tech. Rev. No. 3-1958.

WILHJELM, P.:   Vibration Monitoring and Warning Systems. Brüel & Kjær Tech. Rev. No. 2, 1969.

ZAVERI, K.:   Measurements of Lowest Vibration Levels. Brüel & Kjær Tech. Rev. No. 1, 1970.

128

6. SHOCK MEASUREMENTS AND ANALYSES

6.1. General Measurement Considerations

The measurement of mechanical impulses and shocks requires particular care in the selection of measuring and analyzing equipment.

In some cases the only quantity to be measured is the maximum acceleration occurring during the shock, and the measurement instrumentation is selected accordingly. However, very often this information is not considered to be sufficient for a relevant description of the shock motion, and quantities such as the acceleration-time integral (total velocity change), and the spectral content of the shock pulse, must be evaluated. This requires a somewhat different measuring arrangement.

When it is desirable to make measurements on the shock waveform itself, and it normally is, then not only must the *frequency response* of the measurement equipment be linear over the frequency range determined by the spectral content of the shock pulse, but also the *phase response* of the equipment must be such that no phase distortion takes place within this range. The equipment must furthermore be capable of handling large dynamic signals linearly, a requirement which normally manifests itself in a requirement for *large dynamic range.*

As the frequency and phase responses of the equipment are interrelated quantities, the above requirement for no phase distortion may be "transformed" into requirements for the frequency response. Actually, from a theoretical point of view there will always be an error associated with a shock measurement when the measuring system does not have an infinitely wide frequency range. This error is systematic and comes in addition to other errors such as those resulting, for instance, from calibration inaccuracy. The required frequency range for a certain percentage error can be calculated for simple pulse shapes.

To illustrate how an insufficient frequency response influences the result of a shock pulse measurement, it is convenient to separate the effect of a limited low frequency response and the effect of a limited high frequency response.

129

Consider first the effect of a limited low frequency response upon the waveform of an ideal rectangular shock pulse; this is illustrated in Fig.6.1. Because a limitation in low frequency response means that there is no static (DC) transmission through the measurement system, the peak value of the pulse cannot be held, and towards the end of the wave the amplitude has dropped an amount $1 - e^{-T/RC}$ where T is the pulse duration and RC is the low frequency time constant of the measuring system. The undershoot, just after the pulse has occurred, is also equal to this value.
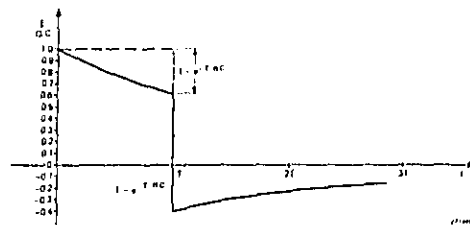
Fig.6.1. Effect of a limited low frequency response upon the measured signal amplitude versus time trace of a rectangular shock pulse

If similar calculations are made for the half sine and the terminal peak sawtooth pulse, their general shapes will be as shown in Figs.6.2 and 6.3. It is found that the reduction of the peak, and the undershoot after the pulse has occurred, are less pronounced with these waveforms.

In order to reduce the error to 5% for example, the factor $e^{-T/RC}$ should be 0.95 or larger for the rectangular pulse. This gives a value T/RC of
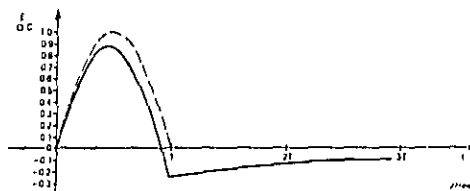
Fig.6.2. Similar to Fig.6.1, the shock pulse in this case being of the half sinetype

130
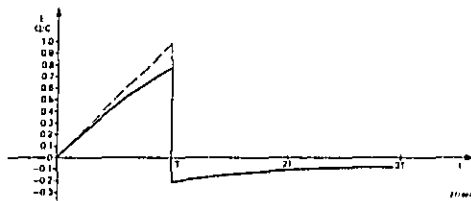
*Fig.6.3. Similar to Fig.6.1, the shock pulse in this case being of the final
peak sawtooth type*

about 0.05, i.e. the time constant, RC, should be twenty times the duration
of the pulse. For the half-sine and final peak sawtooth pulses the RC time
constant should be about twelve and nine times the duration of the pulse
respectively, for the same error.

If the shock pulse does not have its maximum value at the beginning, i.e.
for a half sine or a final peak sawtooth pulse, there will also be a reduction
of the peak value of the output. For the final peak sawtooth pulse the
reduction in peak value is equal to the undershoot, whereas for a sinusoidal
pulse it is approximately equal to half the undershoot (for reasonably small
undershoots) assuming a low-frequency drop-off in the measuring instru-
ment of the simple RC-type.

Whenever the low frequency drop-off is steeper than that corresponding
to the simple RC-type (6 dB/octave) the pulse shape distortion will also
differ from that shown in Figs.6.1, 6.2 and 6.3. It may, for instance, appear
to be of the type illustrated in Fig.6.4.
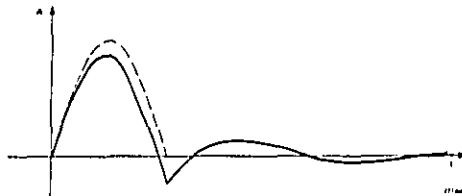
*Fig.6.4   Possible wave shape distortion of a half sine shock pulse when the
low frequency cut-off of the measuring equipment has a roll-off
which differs from the simple 6 dB/octave (RC) type*

131

Effects caused by a limited high frequency response of the measuring system are illustrated in Figs.6.5 and 6.6. Fig.6.5 shows the distortion of a rectangular shock pulse when measured with an arrangement having a high frequency cut-off corresponding roughly to a critically damped system. It is clearly noticed that the major distortion of the pulse here consists in inadequate reproduction of its leading and trailing edges.
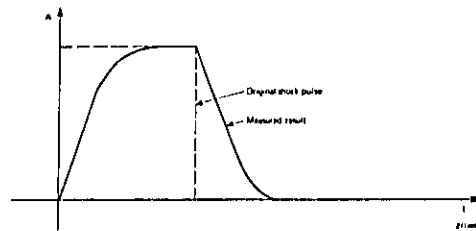
Fig.6.5. Effect of a limited high frequency response upon a rectangular shock pulse. The limitation in high frequency response corresponds in this case roughly to a critically damped system

In Fig.6.6 the effect of a lightly damped resonance type high frequency cut-off is illustrated. This type of cut-off is present when for instance the accelerometer resonance determines the high frequency limit of the measuring system, and the leading (and/or trailing) edge of the pulse is sharp enough to contain frequency components at or around this frequency.
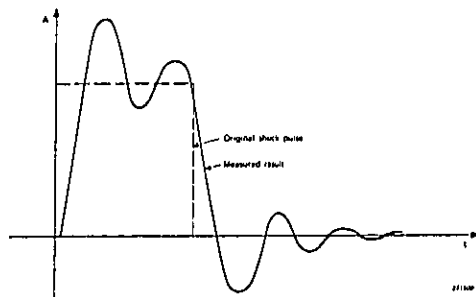
Fig.6.6. Similar to Fig.6.5, the high frequency response of the measurement system in this case corresponding to a lightly damped resonance

132

On the basis of the above theoretical considerations, as well as on the basis of practical experience, it is possible to establish certain "rules of thumb" regarding the frequency range required from a measurement system for faithful reproduction of shock pulses. These "rules of thumb" are graphically illustrated in Fig.6.7.
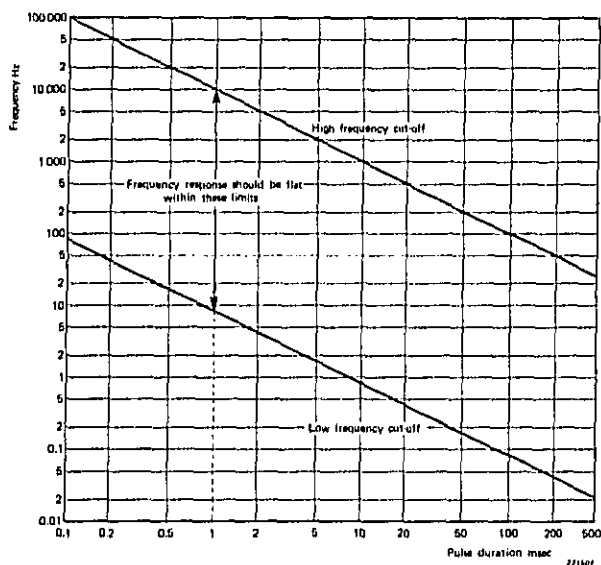
Fig.6.7. Chart allowing the required frequency range of a shock measurement system to be determined when the shock pulse length is known

Before finishing this brief discussion on general considerations in conjunction with shock measurements a special phenomenon termed *zero shift* should be mentioned.

Zero shift, or DC-shift, may be caused by overloading in the electronic circuitry, non-linear amplification, or by a phenomenon known as *accelerometer zero shift.*

133

An exact theory for the *accelerometer zero shift* is, to the author's knowledge, not yet established. It seems reasonable, however, to connect this phenomenon with two physical quantities: 1) A sudden shift in orientation of some of the piezo-electric domains due to stress concentrations, and 2) A slight shift in contact area between the piezo-electric discs and the accelerometer base. Zero shift manifests itself by keeping a slowly decreasing (relatively small) voltage output from the measuring system when the shock pulse has passed. *Note: Zero shift should not be confused with the measuring errors discussed in connection with Figs.6.1, 6.2 and 6.3.*

6.2. Some Basic Shock Measurement Systems

The simplest and most commonly used arrangement for the measurement of mechanical shocks is sketched in Fig.6.8 and consists of an accelerometer, a preamplifier and an oscilloscope. To select the appropriate accelerometer and preamplifier the considerations regarding frequency response and dynamic range discussed in section 6.1 must be taken into account. *Very often, however, use can be made of the Brüel & Kjær Accelerometer Type 4343,* with a sensitivity of 10 pC/g and a free resonant frequency of 75 kHz, together with the *Conditioning Amplifier Type 2626.* The Accelerometer + Conditioning Amplifier combination has a rather low low-frequency cut-off (0.3 Hz) and a selectable (1, 3, 10, 30 kHz) high frequency cut-off.

Accelerometer   Preamplifier   Oscilloscope
    4343   2626   271197
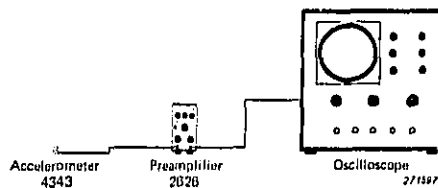
Fig.6.8. A simple shock measurement arrangement

If a measuring arrangement with higher sensitivity is required the Accelerometer Type 4343 may be substituted by Type 4338. This Accelerometer has a sensitivity of 100 pC/g, but its resonant frequency is considerably lower than that of Type 4343. Also the weight of Type 4338 is greater, and it may therefore influence the behaviour of the mechanical system on which it is mounted. On the other hand, if sensitivity is no problem but weight is, use can be made of the light weight Accelerometer Type 4344, see also Fig.5.21.

134

By calibrating the oscilloscope, both with respect to the time axis and with respect to the voltage axis, and photographing the displayed pulse, it is possible to determine not only the maximum acceleration involved in the shock but also the acceleration-time integral. If a *permanent* record of the shock time history is not required use can be made of a so-called *storage oscilloscope.*

In cases where it is desirable to determine the *maximum acceleration only,* the oscilloscope shown in Fig.6.8 may be substituted by the *Measuring Amplifier Type 2607,* Fig.6.9. This instrument has an extremely fast response to pulses, and will *correctly measure and hold the peak value of a signal with a rise time as low as 20 μsec.*

Accelerometer Preamplifier Measuring Amplifier
    4343   2626   2607
                                      271598
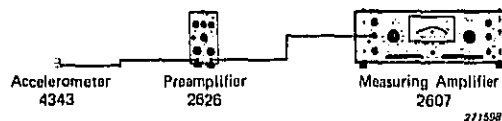
Fig.6.9. *Arrangement suitable for the numerical measurement of maximum shock values (+ peak, −peak, max. peak)*

When the time history of the shock is known for instance in the form of a *photographic oscilloscope record,* it is possible, by means of mathematical approximations, to determine the corresponding Fourier spectrum.

As stated in section 2.3 this kind of information (spectrum) is very important for judging the effects of the shock on the mechanical system in which it occurs. It is, however, normally easier to record the shock pulse on magnetic tape and perform the required frequency analysis electronically rather than to carry out mathematical computations from a graphic record of the time history.

Accelerometer Preamplifier Magnetic Tape Recorder
    4343   2626   7001
                                      271599
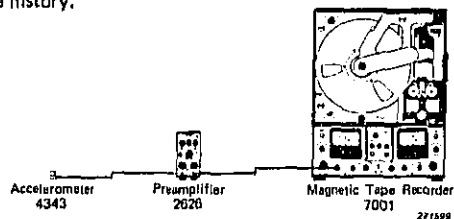
Fig.6.10. *A measuring system allowing the shock pulse to be recorded on magnetic tape for later analysis*

135

A measuring arrangement capable of recording the shock on magnetic tape is shown in Fig.6.10. Use has here again been made of the Conditioning Amplifier Type 2626 and the Accelerometer Type 4343.

The *Tape Recorder Type 7001* is of the F.M. (frequency modulation) type so that no "extra" low frequency limit is introduced due to the magnetic recording system. A further advantage obtained by utilizing the Tape Recorder Type 7001 is the possibility it offers for frequency transformation during later analysis. This will be further discussed in section 6.3.

6.3. Frequency Analysis (Fourier Analysis) of Shock Pulses

By far the most frequently used type of analog shock pulse analysis in practice is based on sequential filtering of a tape recorded signal.

Such an analysis can be made in basically two different ways. However, according to both methods the tape containing the pulse is played back and the signal applied to a tunable *very narrow band filter*.

One method then consists in applying the pulse signal to the analyzing filter *once* per filter position, while the second method consists in *repeating the pulse periodically* by means of, for instance, a very short, closed tape loop.

The first method involves, theoretically, the evaluation of an integral. The second method, on the other hand, involves the time averaging of a periodic signal.

Normally the averaging is made (theoretically) over one period of the (periodically) repeated signal, so that the difference in results obtained by the two methods depends purely upon the period of repetition. This, of course, presupposes that the same type of filters are used in both cases, see also chapter 5, section 5.5.

Assuming first that the analyzing filters are of the *constant bandwidth type* (for instance the Brüel & Kjær Heterodyne Analyzer Type 2010) the two different types of analysis can be exemplified as follows:

The first method is based on the technique discussed in Appendix G, where it is shown that an estimate of the Fourier spectrum (Fourier integral) of the pulse at a particular frequency, can be obtained by measuring the *peak value* of the output of the very narrow band filter tuned to

136
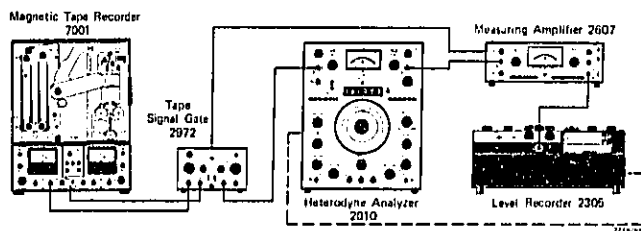
Fig.6.11.   Measuring system suitable for frequency analysis of a tape
recorded shock pulse. Note the electronic gate used to suppress
tape splice noises

that frequency, see Fig.6.11. By shifting the center frequency of the filter
the complete spectrum can be determined.

Fig.6.12b) shows the result of applying this technique to a rectangular
pulse, and recording the data on a graphic Level Recorder Type 2305. The
measuring amplifier used to detect the peak value of the filter output was
here the Brüel & Kjær Type 2607.

To calibrate the recording shown in Fig.6.12b) it should be remembered
(Appendix G) that the Fourier spectrum density at the frequency f_0 is

$$F(f_0) = \frac{[F_{\Delta f}(t)]\ max}{2\Delta f}$$

where $F_{\Delta f}(t)_{max}$ is the peak value measured as described above, and Δf is
the filter bandwidth.

As shown in Appendix G this expression is only correct when $\Delta f \ll \frac{1}{T}$ (T

is the time duration of the pulse). In practice Δf should be of the order of
$\frac{1}{5T}$ (or smaller) to render satisfactory measured results. When the pulse is
recorded on magnetic tape this requirement should, however, pose no
serious problem as it is always possible to transform the time scale of the
pulse by a suitable tape speed transformation.

The method of peak measurements described above may be the simplest
way to obtain a *calibrated* estimate of the pulse Fourier spectrum. However,
also *average absolute or RMS-detection* of the filter output signal can be

137
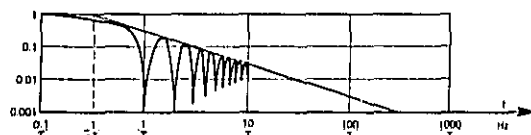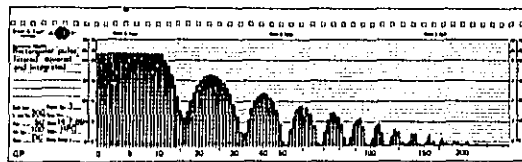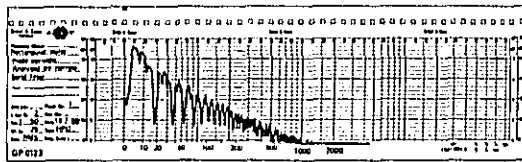
Fig.6.12. Results of frequency (Fourier) analysis of a rectangular shock
pulse
a) Theoretical frequency spectrum
b) Spectrum obtained by measuring the peak value of the out-
put from a sweeping, narrow band filter
c) Spectrum obtained by squaring and integrating the output
from the sweeping filter
d) Spectrum obtained by transforming the single pulse into a
periodic signal and frequency analyzing the resulting periodic
signal

related to the Fourier spectrum value, provided that certain requirements as to the averaging time of the detector circuits are fulfilled (Appendix G). The calibration of the recording is, on the other hand, in this case somewhat more complicated.

Finally, the output from the filter can be *squared and integrated,* theoretically from $-\infty$ to ∞, in practice over the period of time that the filter responds to the pulse. Fig.6.12c) shows an example of a recording obtained by the squaring and integrating method. Note that the values marked on the ordinate therefore represent time integrals of the squared signal magnitudes.

The second method, where the tape is made into a very short closed loop, thereby transforming the single pulse into a periodic signal produces analysis results as illustrated in Fig.6.12d). Here the ordinate values are RMS-values of the filtered signal, and the periodicity of the signal manifests itself in that the measured spectrum consists of discrete components. The distance between the spectral lines is determined by the pulse repetition frequency, which again is determined by the total length of the tape loop and the tape speed used. For the case shown the repetition frequency was 4.2 Hz, corresponding to a tape loop length of 362 mm and a tape speed of 60" per second. This tape loop length was obtained by mounting the Tape Recorder Type 7001 with a special loop adaptor.

In the utilization of a frequency analysis technique of the type just described, and exemplified in Fig.6.12d), there are many practical limitations, some of which are briefly discussed below.

Firstly, to be able to properly frequency analyze a periodic signal it is necessary that *the distance between the discrete spectral lines is larger than the analyzing bandwidth.* In Fig.6.12d) the analysis bandwidth was 3.16 Hz which, with a signal repetition frequency of 4.2 Hz, gives reasonably good results. The signal repetition frequency of 4.2 Hz was the highest repetition frequency which could be obtained on the Tape Recorder 7001 by relatively simple means.

Secondly, if the duration of one period of the repetition frequency is T and the duration of the pulse is T_p then the ratio T/T_p is subject to rather strict limitations. As can be seen from Fig.6.12a) the zeros in the theoretical pulse spectrum occur with frequency intervals of $1/T_p$. To be able to obtain more than one spectral line between successive minima, the ratio T/T_p must therefore be larger than one. Experiments have shown that some 5 lines between minima seem to give a sufficiently good resolution of the spectrum.

139

On the *other hand*, the larger the ratio T/T_p becomes, the smaller becomes the available dynamic range for the analysis. A too large ratio, T/T_p, must also be avoided due to crest-factor limitations in the measuring and analyzing equipment. As a practical compromise a T/T_p ratio between 3 and 5 is recommended. To obtain this value in practice use must often be made of *tape speed transformations.* This immediately brings about a further limitation because the tape speed is closely connected with the available frequency response for recording.

Thirdly, therefore, the frequency response necessary for proper recording of the pulse must be duly considered in conjunction with the tape speed transformations necessary to achieve the required repetition frequency for analysis. As long as recording, tape speed transformations and play back for analysis are made on one and the same tape recorder, frequency response problems are, once solved, automatically taken care of during speed transformations. If, on the other hand, the pulse is recorded on one tape recorder and later transferred onto *another* tape recorder, the two recorders running at different speeds, *then* frequency response requirements must be carefully considered.

One problem which has to be solved before a proper frequency analysis of the above described type can be made in practice is the suppression of unavoidable tape splice noise pulses. When the tape is made into an endless loop the splice will normally cause extraneous noise pulses to occur during playback, and one of the best methods to suppress these undesired pulses is to use a Tape Signal Gate Type 2972 as indicated in Fig.6.11.

In the above discussion on the frequency analysis of pulses (shocks) in practice the analyzing filter was assumed to have *constant bandwidth,* i.e. the bandwidth of the filter was independent of the center frequency to
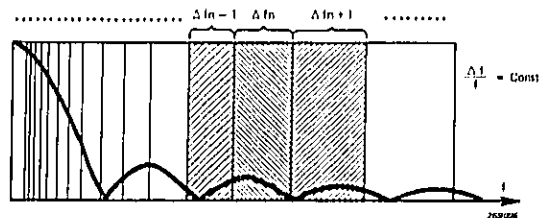
Fig.6.13. Illustration of the effect of using constant percentage band-width type filters in the frequency analysis of shock pulses

Fig.6.14. Typical frequency spectrum of a rectangular shock pulse meas-
ured by means of 1/3 octave filters. (Pulse duration 60 msec)

which it was tuned. Now, what would be the implications if the filter was of
the *constant percentage bandwidth* type, for instance a 1/3 octave filter?
Actually this problem has been touched upon in Chapter 5, section 5.5, and
involves the simultaneous measurement of several spectral components, see
Fig.6.13. If these components, during measurement, are summed on energy-
basis (RMS-measurements) the measured spectrum for a square-shaped pulse
will look as shown in Fig.6.14. By applying a "correction" of the type
indicated in Fig.6.15 (and in Fig.5.33), the spectrum, Fig.6.14, can be trans-
formed into a spectrum of the same overall shape as that measured by
means of constant bandwidth filters and shown in Fig.6.12. If any other
type of measurement than RMS-measurements of the signal components are
made, however, no such transformation is possible and the shape of the
measured spectrum will depend greatly upon the particular measurement
instrumentation used.

Finally, a *special method* of pulse frequency analysis is based on the use
of the Brüel & Kjær Real Time Analyzer Type 3347.

When the pulse is applied, once only, to the input of the Analyzer a
complete frequency spectrum, in terms of 1/3 octave frequency bands, is
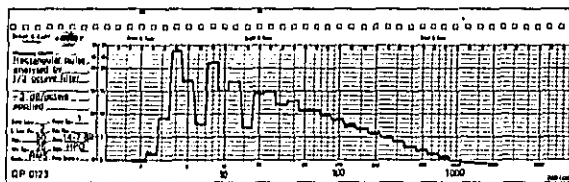
Fig.6.15. Application of the 3 dB/octave correction to the spectrum
shown in Fig.6.14

141

displayed instantly on the screen of the instrument. The built-in analog-to-digital converter also makes a direct digital computer processing on the measured spectrum possible (Chapter 5, section 5.2). There are, however, rather strict limitations as to the pulse duration and frequency range involved when the Real Time Analyzer Type 3347 is used for pulse analysis, and interested readers are referred to the Brüel & Kjær Tech. Rev. No. 1, 1970 for further details.

6.4. Selected Bibliography

ALLNUTT, R.B. and MINTZ, F.:	Instruments for Measuring Vibration and Shock on Ship Hulls and Machinery. Taylor Model Basin Report 563, July 1948.
BRENNAN, J.N.:	Bibliography on Shock and Shock Excited Vibrations. Pennsylvania State University, University Park, September 1957.
BROCH, J.T. and OLESEN, H.P.:	On the Frequency Analysis of Mechanical Shocks and Single Impulses. Brüel & Kjær Tech. Rev. No. 3, 1970.
BROCH, J.T.:	Analog Analysis of Shocks. Proceedings of 7th ICA-Conference. Budapest, August 1971.
FREDERIKSEN, B.:	1/3 Octave Spectrum Readout of Impulse Measurements. Brüel & Kjær Tech. Rev. No. 1, 1970.
GURTIN, M.E.:	The Effect of Accelerometer Low-Frequency Response on Transient Measurements. General Electric, Research and Development Center, Schenectedly, New York, Report No. 58 GL 241, July 1958.
KEAST, D.N.:	Measurements in Mechanical Dynamics. McGraw-Hill Book Company, Inc. 1967.
KITTELSEN, K.E.:	Measurement and Description of Shock. Brüel & Kjær Tech. Rev. No. 3, 1966.
LEVY, S. and KROLL, W.D.:	Response of Accelerometers to Transient Accelerations. Journ. of Research of the N.B.S. Vol. 45, No. 4, October 1950.

LOWE, R.:   Correlation of Shock Spectra and Pulse Shapes
                         with Shock Environment. Environmental
                         Engineering. Vol. 1, No. 1, February 1959.

OLESEN, H.P.:   Frequency Analysis of Single Pulses. Brüel &
                         Kjær Tech. Rev. No. 3, 1969.

RIEDEL, J.C.:   The Accurate Measurement of Shock Phenome-
                         na. Proc. of the Inst. of Environmental Sciences,
                         1962.

VIGNESS, I.:   Instrumentation, Analyses and Problems Con-
                         cerning Shock and Vibration. First Symposium
                         on Naval Structural Mechanics, Stanford Univer-
                         sity, August 1959.

VIGNESS, I.:   Shock Motions and Their Measurements.
                         Experimental Mechanics, Vol. 1, No. 9, Septem-
                         ber 1961.

WOODBURY, R.C.:   Some Instrumentation Requirements of a Non-
                         periodic 6-Millisecond Pulse. Shock, Vibration
                         and Associated Environments, Bulletin 28, 1960,
                         Part 4.

7. SOME METHODS OF SHOCK AND VIBRATION CONTROL

7.1. Isolation of Vibrations and Shocks

Undesired vibrations and shocks may originate from a great variety of sources, such as unbalance and reciprocating motions in mechanical machinery, aerodynamic turbulence, rough sea movements, earthquakes, road and rail transportations, rough handling of equipment, etc.

Even though ideally all undesirable vibrations should be eliminated at the source it is obvious from the above "list" of sources that this may be possible only in very few cases. In other cases, however, it may be possible to *"isolate" the source* by means of shock and vibration isolators, or to reduce the shock and vibration effects by means of effectively designed vibration absorbers, or the use of damping treatments.

On the other hand, "natural" vibration sources like aerodynamic turbulence, rough sea movements and earthquakes cannot be "isolated" in the usual sense of the word. The only way to diminish undesirable vibration effects originating from these types of sources is to *"isolate" the equipment* upon which the vibrations may cause serious damage.

Now, whether it is the source or the equipment that is going to be isolated the physical principles involved are similar.

a) Vibration Isolation

Fig.7.1 shows the "universal" solution to isolation problems, i.e. the proper mounting of the source (machine), Fig.7.1.a, or the equipment, Fig.7.1.b, on springs and dampers. (If the springs consist of cork or rubber-like materials damping is automatically built-into the spring in the form of internal material damping).

Consider first the vibration *isolation of the source*, Fig.7.1.a.

The equation of motion for the mass, m, in the system, Fig.7.1.a, was formulated and solved in Chapter 3, section 3.1 for an arbitrary sinusoidal force, $F_o e^{j\omega t}$:

$$x(\omega) = H(\omega) F_o e^{j\omega t}$$

144
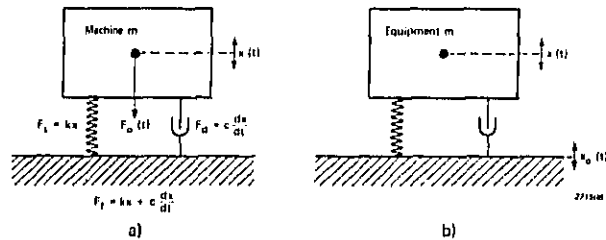
Fig.7.1. Illustration of the basic principles involved in vibration isolation,
i.e. The mounting of the machine (equipment), m, to be isolated
on springs and dampers

where $H(\omega) = \dfrac{1/m}{\omega_o^2 - \omega^2 + j\dfrac{\omega_o}{Q}\omega}$

In the case of vibration isolation one normally is not interested in x (ω)
but rather in the force transmitted to the foundation. This force is the
vectorial sum of the force transmitted through the spring element and that
transmitted through the damper, i.e.:

$$F_f(t) = kx + c\frac{dx}{dt} = kx(\omega) + c\frac{d[x(\omega)]}{dt} = F_f\,e^{j(\omega t + \alpha)}$$

$$F_f\,e^{j(\omega t + \alpha)} = [kH(\omega) + j\omega cH(\omega)]\,F_o\,e^{j\omega t}$$

whereby:

$$\frac{F_f}{F_o}e^{j\alpha} = T = \frac{\dfrac{k}{m} + j\omega\dfrac{c}{m}}{\omega_o^2 - \omega^2 + j\dfrac{\omega_o}{Q}\omega}$$

where T is the *force transmissibility*. A slight manipulation with this
equation results in

$$|T| = \frac{\sqrt{1 + \dfrac{1}{Q^2}(\dfrac{f}{f_o})^2}}{\sqrt{[1 - (\dfrac{f}{f_o})^2]^2 + \dfrac{1}{Q^2}(\dfrac{f}{f_o})^2}}$$

Here f_o is the natural undamped resonant frequency of the spring-mass
system and $\dfrac{1}{Q}$ is a measure of the system damping:

145

$$\frac{1}{Q} = 2\,\xi = 2\,\frac{c}{c_c} = \frac{c}{\sqrt{km}}$$

ξ = damping ratio

c_c = critical damping coefficient $(c_c = 2\,\sqrt{km})$

Fig.7.2 shows a graphical representation of the formula given for $|T|$ for various damping ratios.

The basic principle of vibration isolation now consists in selecting a spring mounting so that the natural frequency, f_o, of the spring-mass system is considerably lower than the lowest frequency component in the forcing spectrum produced by the machine.
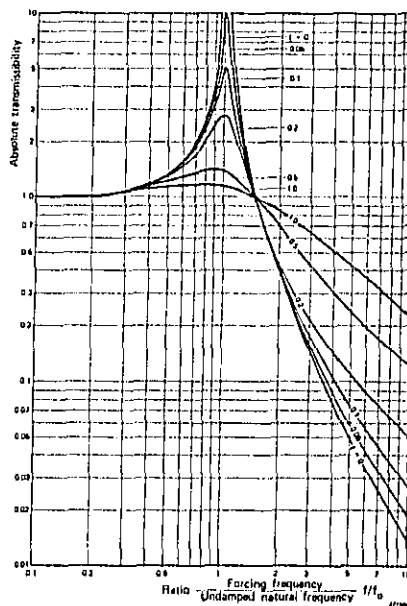
Fig.7.2. Curves showing the absolute transmissibility as a function of the frequency ratio f/f_o for various damping ratios

146

With regard to the choice of *damping ratio* this should be selected with a view *both* to give a relatively low transmissibility amplification at the spring-mass resonant frequency, *and* to give satisfactory isolation (low transmissibility) at frequencies well above resonance.

There are, however, other factors which enter the picture in practice. Some of these are briefly discussed in the following.

A machine which is mounted on four springs as shown in Fig.7.3 may exhibit more than one degree-of-freedom in its motion. Generally speaking it is a *six degrees-of-freedom system*, in that it may have translatory motions in three directions, as well as rotary motions about three mutually perpendicular axes. (see also section 3.3). In selecting a proper isolation mounting the lowest frequency component in the forcing spectrum of the machinery must then be considerably higher than the highest resonant frequency of the (multi-degree-of-freedom) mounting system.
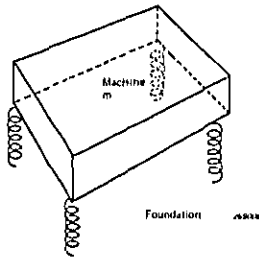
Fig.7.3. Sketch of a machine mounted on four springs

Another factor to be considered is the *lateral stability* of the mounting system. This, in many cases, sets a limit to how soft the mounting springs can be chosen. In practice a resonant frequency of the simple spring-mass system, Fig.7.1 of the order of 5 — 10 Hz is often used.

At high frequencies so-called *"wave" effects* may sometimes occur in the mounting springs. These are due to longitudinal standing waves (chapter 3, section 3.6) in the springs. They seem, however, not to pose too serious problems in practice when the springs are produced from materials with relatively high internal damping. A curve illustrating theoretically the concept of wave-effects is shown in Fig.7.4.

147
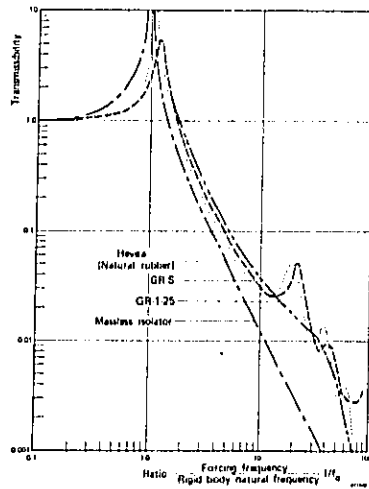
Fig.7.4. Curves showing wave-effects in isolators

Another effect which may be of some concern in the design of practical vibration isolation mountings is *the effect of foundation reaction*. In the above discussion the foundation has been assumed to be infinitely rigid, i.e. the motion of the mass, m, in Fig.7.1.a, is completely taken up by the spring and the damper. This is not always the case, although in many practical situations it may represent a proper approximation.

A somewhat better approximation is to represent the foundation in the form of a mass which is able to move in the X-direction, Fig.7.5. By solving the differential equations of motion for this system one finds that the resonant frequency is now:

$$f'_o = f_o \sqrt{1 + \frac{m}{B}}$$

where f_o is the "original" resonant frequency of the system with mass, m, and spring k ($B = \infty$). If the foundation is best represented by a plate a theoretical treatment of the situation involves the theory of structures (chapter 3, section 3.6) and may become exceedingly complicated.

148
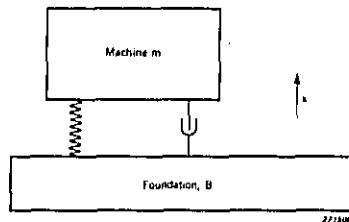
Fig.7.5. Illustration of the approximation of the machine foundation by a mass, B

A *practical approach to vibration problems* of the type sketched in Fig.7.1.a, is to frequency analyse the vibrations produced by the machine. From the measured (or estimated) spectrum the lowest frequency component to be "isolated" can be determined.

By then utilizing the curves, Fig.7.2 the resonant frequency of the mounted system, as well as the damping, necessary to provide sufficient isolation can be estimated.

To find the stiffness required from the isolation mount (spring) when the desired resonant frequency has been determined the formula:

$$k \approx 0.04 \times P \times f_0^2 \text{ kg/cm}$$

can be used. Here P is the weight of the machine to be isolated in kilograms and f_0 is the resonant frequency of the machine and isolation mount system. Figs.7.6, 7.7 and 7.8 illustrate a practical case. In Fig.7.6 the frequency spectrum measured on a rotating electrical machine is shown, while Fig.7.7 shows the measuring arrangement used. From the spectrum, Fig.7.6 it is seen that the major vibrations (accelerations) are found in the frequency range from around 200 Hz to just above some 1000 Hz. Although there are some disturbing vibrations also at frequencies lower than 100 Hz, an effective vibration isolation is relatively easy to obtain in this case.

If the resonant frequency of the isolated system is chosen around 10 Hz the isolation of frequency components higher than 100 Hz will be nearly perfect, and this is taken as a basis for the isolation design. Since, in general it is necessary to use at least four vibration isolators in practice, Fig.7.3, each of the isolators carry only one fourth of the total weight of the

149
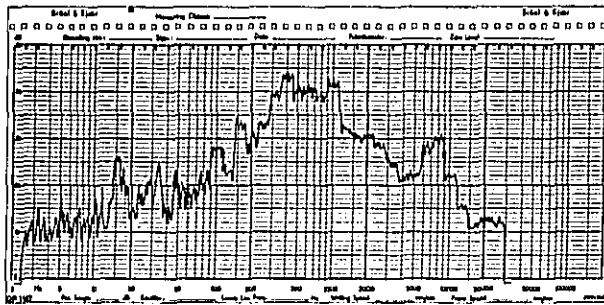
Fig.7.6. *Vibration frequency spectrum produced by a rotating electrical machine*

machine. For the machine in question which has a total weight of 8 kg this means that each isolator will carry a weight of 2 kg. The required isolator stiffness then becomes (see formula above):

$$k = 0.04 \times 2 \times 10^2 = 8 \text{ kg/cm}$$

From the manufacturer's catalog it was found, however, that he did not supply a vibration isolator with exactly this stiffness, and use therefore had to be made of isolators with a stiffness of 1.2 kg/mm.

Actually, it should be mentioned here that most vibration isolator manufacturers do not publish their data in terms of stiffness but rather in terms of the static deflection corresponding to a certain (maximum) static load. If it is assumed that the isolator in question behaves linearly the stiffness can, on the other hand, be readily estimated from the manufacturer's data by means of the simple relationship.
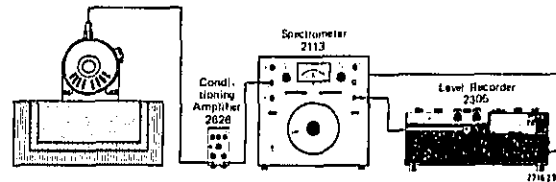
Fig.7.7. *Measuring arrangement used to determine the frequency spectrum shown in Fig.7.6*

150
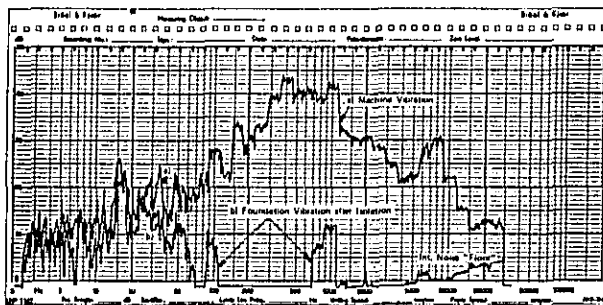
Fig. 7.8. Curves showing the effect of vibration isolation
a) Vibration frequency spectrum produced by the machine
b) Vibration frequency spectrum measured on the foundation after
isolation of the machine

$$k = \frac{P\,(max)}{d\,(max)}$$

where P is the weight of the machine per isolator and d is the static deflection produced by this load. In the above example the maximum weight per isolator was given by the manufacturer to be 3.6 kg, and the corresponding deflection 3 mm thus

$$k = \frac{3.6}{3} = 1.2 \text{ kg/mm} = 12 \text{ kg/cm}$$

It is now necessary to check how this influences the resonant frequency of the isolation system. Rearranging the expression $k = 0.04 \times P \times f_o{}^2$ gives:

$$f_o = \sqrt{\frac{25 \times k}{P}} = \sqrt{\frac{25 \times 12}{2}} = 12.3 \text{ Hz}$$

Considering that the major frequency components to be isolated are considerably higher than 12.3 Hz this change in resonant frequency is quite acceptable. The resulting isolation can be seen from the curves Fig.7.8. Here the curve a) corresponds to that shown in Fig.7.6, while the curve b) was measured on the foundation after isolation of the machine.

Actually, the curves Fig.7.8 have been recorded automatically in terms of *decibels.* The decibel is a logarithmic measure for a ratio, in this case:

$$dB = 20 \log_{10} (\frac{X_1}{X_2})$$

151

where X_1 and X_2 are RMS-values of the vibrational quantities involved. The use of decibels (logarithmic measures) is very often advantageous in technical problems involving large dynamic ranges, due to the *constant relative accuracy obtained* by this method of data presentation. It is widely used in the fields of electronics, communications and acoustic noise measurements, and it is at present becoming more and more popular also in the fields of vibration measurements and technology. A further discussion on the use of decibels is outlined in Appendix I.

Before leaving the subject of vibration isolation of mechanical (or electrical) machinery a few further considerations should be briefly touched upon.

Firstly, it is important that the vibration isolators are placed correctly with respect to the motion of the center of gravity of the machine, see Figs.3.11 and 7.9.
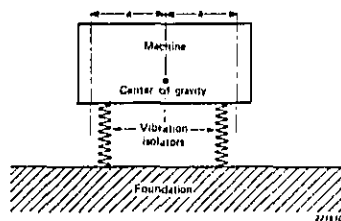
Fig.7.9. *Illustration of proper mounting of the machine. The vibration isolators should be placed symmetrically with respect to the center of gravity of the motion*

Secondly, the center of gravity of the machine should be located as low as possible. If serious "rocking" effects (section 3.3), or other instabilities, become a problem in the mounting, the effective center of gravity may be lowered by first mounting the machine on a heavy mass and then isolating the mass + machine, Figs.7.10 and 7.11. Fig.7.11 actually also illustrates the socalled principle of the "floating" floor.

Thirdly, it is possible, by means of a compound vibration isolation system, Fig.7.12, to obtain a force transmissibility characteristic which gives greater attenuation for frequency components above the (compound) system resonances than does the "simple" system discussed above, see

152
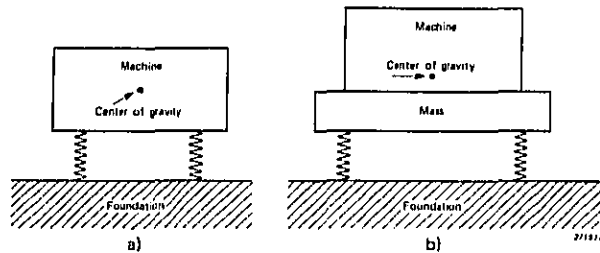
Fig.7.10. Sketch showing how the center of gravity of a machine can be
"artificially" lowered by adding mass (weight) directly onto the
machine
a) Machine
b) Machine with properly added mass (weight)
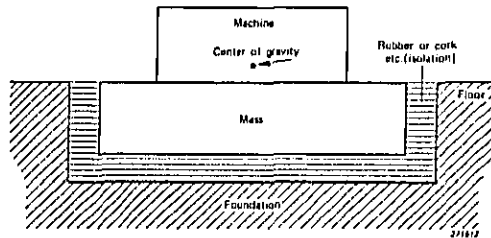
Fig.7.11. Sketch showing how the addition of mass is utilized in the
socalled "floating" floor

Fig.7.13. The design of such compound systems is, on the other hand, more
complicated and critical than the design of a "simple" vibration isolator.

For readers, who are familiar with electrical filter theory and electro-
mechanical analogies the design problems involved may, however, not seem
too formidable.

Returning now to the second "case" of vibration isolation, i.e. the case
where an *equipment* is to be isolated from a vibrating foundation, Fig.7.1.b,
the equation of motion for the mass, m, is:

$$m\frac{d^2x}{dt^2} + c\frac{d(x - x_o)}{dt} + k(x - x_o) = 0$$

153
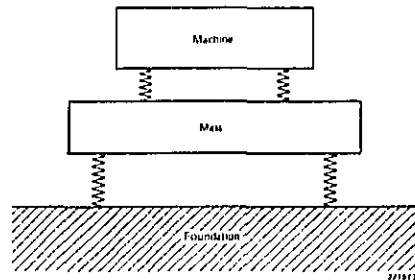
Fig.7.12.   Illustration of a compound system

Again solving the equation for an arbitrary sinusoidal foundation vibration $x_0 = X_0 \, e^{j\omega t}$ results in:

$$x = \frac{\omega_0{}^2 - \omega^2 + j \frac{\omega_0 - \omega}{Q}}{\frac{k}{m} + j\omega \frac{c}{m}} \cdot X_0$$

or

$$\left|\frac{x}{x_0}\right| = \frac{\sqrt{1 + \frac{1}{Q^2} (\frac{f}{f_0})^2}}{\sqrt{[1 - (\frac{f}{f_0})^2]^2 + \frac{1}{Q^2} (\frac{f}{f_0})^2}} = |T|$$

Thus the *displacement transmissibility* is now given by exactly the same relationship, $|T|$, as was the force transmissibility in the case where the vibration source was going to be isolated from the foundation. Simple manipulations with the above formula shows that the same relationship is also obtained for the velocity and acceleration transmissibility of the system Fig.7.1b.

The transmissibility formula (and the curves shown in Fig.7.2) are therefore generally valid in vibration isolation problems. *This again means that the same procedures as outlined in the foregoing are involved in designing a vibration isolation system whether it is the source or an equipment that is going to be isolated.*

There is, however, one significant difference which should be borne in mind. In determining the vibration frequency spectrum of the source Fig.7.1a and Fig.7.6, the effects of internal resonances in the machine are

154
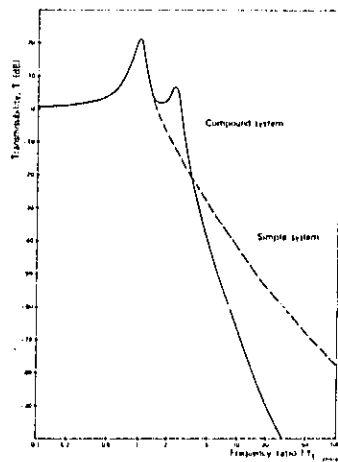
*Fig.7.13. Transmissibility curves illustrating the difference in trans-
missibility between the simple and the compound system*

automatically taken into account. As the foundation on which the machine
(and isolator) is placed is assumed to exhibit no disturbing resonance the
isolation problem consists here simply in selecting an isolator/machine con-
figuration with a resonant frequency, f_o, which is low enough to ensure
sufficient isolation of the forcing frequency components.

When the vibrations originate in the foundation and are transmitted to an
equipment Fig.7.1b, it is not *only* important to know the forcing vibration
frequency spectrum, but also the internal resonances in the equipment.
These may be excited and could cause serious damage, even if the exciting
frequency components are heavily attenuated by the vibration isolation
system. This is due to resonance amplification effects within the equipment
itself. It is therefore necessary when an effective vibration isolation system
is to be designed *also to take such internal equipment resonances into
account.*

If these resonances cannot be predicted theoretically the equipment may
be subjected to a vibration test (see section 7.3) prior to the design of a
proper vibration isolation system. By means of suitable vibration testing,

155

dangerous resonances and their effects can be detected experimentally, and corresponding isolation criteria established.

b) Shock Isolation

Even though the principles involved in shock isolation are very much similar to those involved in vibration isolation some differences exist due to the transient nature of a shock. *The reduction in shock severity, which may be obtained by the use of isolators, results from the storage of the shock energy within the isolators and its subsequent release in a "smoother" form.* However, the energy storage can only take place by deflection of the isolators.

As a shock pulse may contain frequency components ranging from 0 to ∞ it is, generally speaking, not possible to avoid excitation of the isolator/mass resonance. On the other hand, *if the duration of the shock pulse is short in comparison with one half period of the isolation system resonant frequency (f_o), the response of the system may not have serious consequences.* This may be best illustrated by means of Fig.3 1", section 3.5, and the shock response spectrum type of description, also outlined in section 3.5.

In this case the shock response spectrum of greatest interest is the so-called *maximax*, or *overall*, spectrum (section 3.5). Fig.7.14 shows the maximax shock spectra for the three types of shockpulses discussed in section 3.5. From the figure it can be seen that as long as the resonant frequency, f_o, of the isolation system is considerably lower than $\frac{1}{2T}$ where T is the duration of the shock pulse, the shapes of the maximax spectra are quite similar. This is in conformity with the statement made in Chapter 2, section 2.3 that "when the duration of the shock pulse is short compared with the natural period of the mechanical system on which it acts, *the severity of the shock is determined by the area of the shock pulse alone".* In Fig.7.15 the statement may be illustrated even clearer in that here the three maximax shock spectra shown in Fig.7.14 are redrawn to scales where the ordinate is no longer S(f)/F but $S(f)/\frac{1}{T}\int_0^T F(t)\, dt$.

$\int_0^T F(t)\, dt$ is the area of the shock pulse and $\frac{1}{T}\int_0^T F(t)\, dt$ is the "effective pulse height, see Fig.7.16. Fig.7.15 may actually be used as basis for the design and evaluation of an undamped shock isolation system, as described below. Consider first the system shown in Fig.7.17a, which is actually the

156
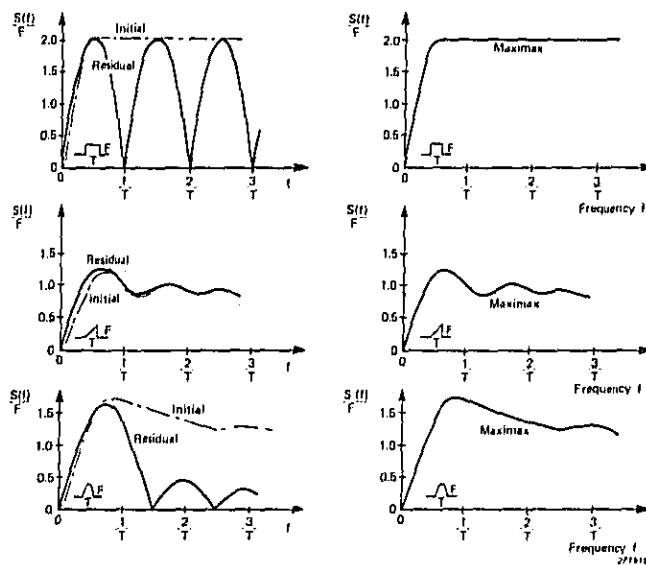
Fig. 7.14. Maximax (overall) undamped shock response spectra for rectangular, final peak sawtooth, and half-sine shock pulses

same system as shown in Fig.7.1a, but without damping. Let the time dependency of the force F (t), in this case be as indicated in Fig.7.18a.

The maximum force acting on the foundation F_r can now be found from Fig.7.18b and Fig.7.15, provided that the resonant frequency, f_o, of the system Fig.7.17 is known. Assuming that this is $f_o = 1/10\,T$ the maximum force acting on the foundation is found from Fig.7.15 to be approximately 0.6 times the "effective" force, Fig.7.18b, i.e.:

Maximum force "response" $= 0.6\ F_o = F_r$

The maximum displacement of the mass, m, is equal to the force divided by the stiffness, k, of the isolator:

$$X_r = \frac{F_r}{k} = \frac{0.6\ F_o}{k}$$

157
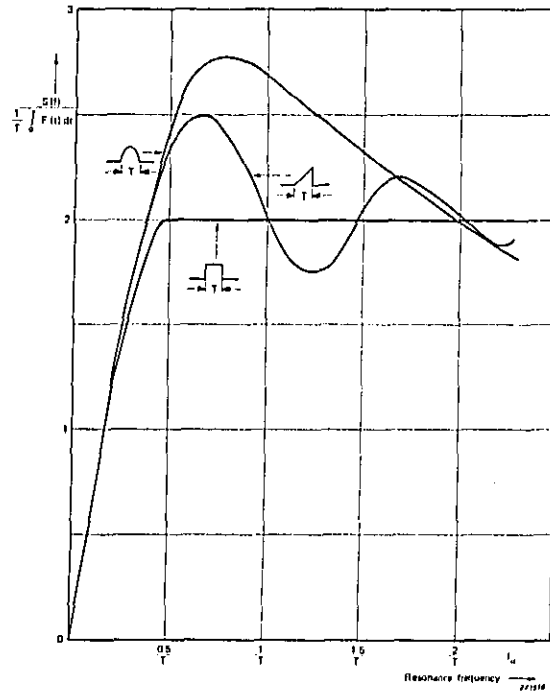
Fig.7.15. *The first part of the maximax shock-response spectra shown in Fig.7.14 redrawn to different scales. Actually the spectra are here normalized to pulses of the same "effective" height*

As the motion of the mass will consist of an oscillation with a frequency equal to the natural frequency (resonant frequency) of the isolation system the maximum velocity and acceleration of the mass, m, can then be found directly from the relationships:

$$v_r = \left|\frac{dx_r}{dt}\right|_{max} = \omega_0\, x_r = 2\,\pi\, f_0\frac{F_r}{k} = 1.2\,\pi\, f_0\frac{F_0}{k}$$

and

$$a_r = \left|\frac{d^2x_r}{dt^2}\right|_{max} = \omega_0^2\, x_r = 4\,\pi^2\, f_0^2\frac{F_r}{k} = 2.4\,\pi^2\, f_0^2\frac{F_0}{k}$$
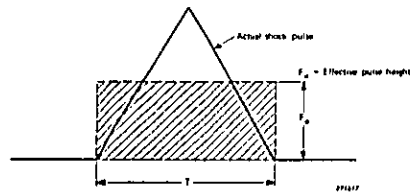
Fig.7.16. Illustration of the concept of "effective" pulse height
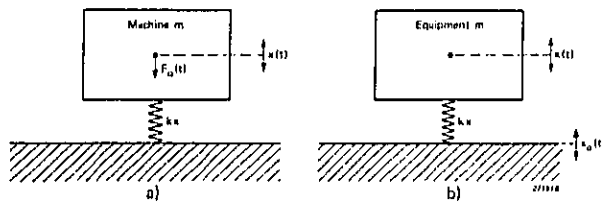
Fig.7.17. Sketch of basic spring-mass systems (without damping)
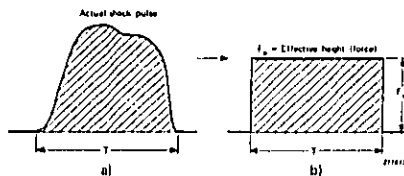
Fig.7.18. Shock force pulse acting upon the system shown in Fig.7.17
a) Actual shock pulse
b) "Effective" shock pulse

When the forcing function, $F(t)$, is unknown, or difficult to measure, it is often convenient by means of an accelerometer to measure instead the acceleration, a_r, of the mass. Calculations may then be performed "backwards" to determine the "effective" force, F_o, as well as other quantities of interest.

159

If viscous damping is included in the isolation system, and it normally is, the above calculations must be modified.

Starting again with the maximax shock spectrum for a damped system, such a "spectrum" is shown in Fig.7.19 for half sine shock pulses. In this case, F_r is found from Fig.7.19, utilizing that curve which corresponds to the damping included in the system. The relationship between F_r and X_r is however, in this case no longer quite so simple because F_r is the vectorial sum of the forces transmitted through both the spring element and the damper (Fig.7.1a).
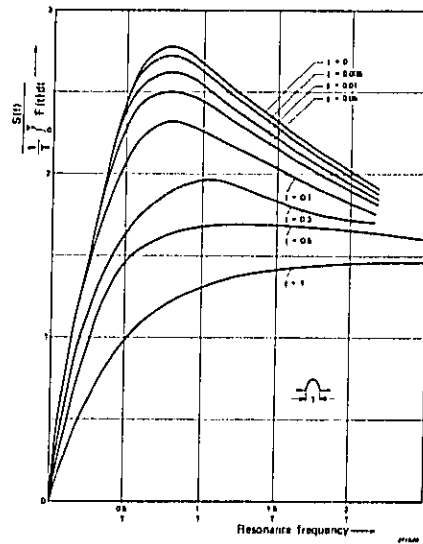
Fig.7.19. Damped shock response spectrum for half sine shock pulses

Also, because of the damping ω_o is no longer simply equal to $\sqrt{\dfrac{k}{m}}$ but rather*):

$$\omega_o = \sqrt{\frac{k}{m}}\sqrt{1 - \xi^2}$$

where

$$\xi = \frac{c}{c_c} = \frac{c}{2\sqrt{km}} = \frac{1}{2Q}$$

Taking these factors into account the maximum displacement, X_r of the mass, m, becomes:

$$x_r = \frac{F_r}{k\sqrt{1 + (2\xi)^2}}$$

Utilizing the relationships between x_r, v_r and a_r one has:

$$v_r = \sqrt{\frac{k}{m}}\frac{\sqrt{1 - \xi^2}}{\sqrt{1 + (2\xi)^2}}\frac{F_r}{k}$$

and

$$a_r = \frac{1 - \xi^2}{\sqrt{1 + (2\xi)^2}}\frac{F_r}{m}$$

When the shock pulse duration is no longer short compared with one half period of the isolation system motion, utilization of the shock spectrum technique becomes somewhat more complicated.

It seems, however, that utilization of the "spectrum" shown in Fig.7.19 and the method of estimation described above for damped systems may result in reasonably good approximations to actual practical problems.

In conjunction with the practical application of shock isolators certain facts should be noted:

Firstly, as mentioned above, reduction in shock force transmissibility can only take place by allowing the isolator to deflect, i.e. by motion. Thus certain space clearances must be allowed for the isolated equipment.

Secondly, if the resonant frequency of the isolation system is chosen incorrectly the isolator may "amplify" the destructive effects of the shock rather than provide the desired isolation.

---

*) Actually this difference in resonant frequency between damped and undamped resonances also applies to *vibration* isolation systems. However, the damping included in these systems in practice is often so small ($\xi \ll 1$) that the resonance shift may be neglected in the calculations.

Thirdly, if the isolator turns out to have unexpected non-linear characteristics (and many practical isolator materials *do* perform non-linearly) a great number of "extra" response effects may take place.

In some cases isolators are, on purpose, designed to be non-linear. If, for instance the space limitations do not allow for the required (linear) motion of the equipment one may be tempted to employ non-linear isolators of the "hardening" spring type (see also Chapter 3, section 3.2, and Appendix C). These kinds of isolators will, when deflecting into the non-linear region, firstly change the resonant frequency of the isolation system (f_o increases with increasing isolator deflection), and secondly produce a number of harmonic force components which may excite internal resonances in the isolated equipment. Also the *peak* acceleration of the equipment may be considerably increased by the use of "hardening" spring type isolators.

On the other hand, *if the isolation system contains a fair amount of damping* the deteriorating effects mentioned above are drastically reduced. Thus, *a heavily damped, "hardening" spring type isolation system may in some cases provide the appropriate solution to a difficult isolation problem.*

Another type of nonlinear shock isolators are those with "softening" spring characteristics. These are found less frequently in practice, but their main advantage is to very effectively reduce the transmitted force on account of large deflections. In cases where equipment is be protected against *one* severe shock only, use may profitably be made of "softening" spring isolators. An example of where "softening" spring isolators are utilized is the landing system of the american Lunar Excursion Module (1969).

It should also be mentioned that, in analogy with vibration isolation systems, also shock isolation may be provided in the form of compound systems (Fig.7.12). This seems, however, to be less frequently utilized in practice than the case is for compound vibration isolation systems.

Finally, to give the reader an idea of some important characteristics and features of commonly used isolators the table given below has been reproduced from R.H. Warring (ed.): "Handbook of Noise and Vibration Control".

162

BASIC TYPES OF ISOLATORS

Material	Frequency Range	Optimum Frequencies	Damping	Limitations	Remarks
Metal Springs: Helical Compression Springs	All (theoretically)	Low frequencies (with high static deflections)	Very low typical	Readily transmit high frequencies	Widely used and easy to produce with required characteristics
Helical Tension Springs	All (theoretically)	Low frequencies	Very low	—	Little used
Leaf Springs	Low	Low	Fairly good (due to friction)	—	Limited to specific applications
Belleville Washers	—	—	High with parallel stacking	Subject to fatigue, more complicated assembly	Compact. Stiffness depends on method of stacking. Controlled non-linear stiffness
Rubber: (i) In Shear (ii) In Compression (iii) Shear-Compression	depends on composition and hardness	High	increases with rubber hardness	limited load carrying capacity	(i) Small energy storage (ii) No change in volume (iii) Has secondary snubbing action
Cork	Depends on density	High	Low (6% of critical)	Practical limit to minimum natural frequency attainable	Highly compressible without lateral expansion
Felt	Depends on density & thickness. Exhibits mid audio frequency range	High (usually above 40 cps)	High	Practical limit to minimum natural frequency dependent on load & thickness	1/2" to 1" thickness normally used
Sponge Rubber	—	Low	Fair	Low stiffness with high compressibility	Used in the form of moulded pads or cut slabs
Steel Mesh	—	Low	Fair to high	Limited load carrying capacity	Used in form of pads, also as inserts
Pneumatic (Cushions, Air Bellows)	Frequency controlled by air volume	—	Low	—	Relatively underdeveloped
Rubber Composites	Depends on design & rubber hardness	High	Depends on design	—	Moulded rubber mounting pads with metallic casings and/or inserts
Spring and Rubber Composites	Wide range depends on design	Depends on design	Low	—	Basically metal springs encased in rubber. May incorporate damping
Rubberised Fabric	—	10–12 cps typical	6–8% typical	—	Properties intermediate between rubber and steel springs
Cork-Rubber	—	High	Low	—	Alternative to rubber or cork
Stuckled or Ribbed Rubber Mats	—	Moderately low	depends on rubber hardness	—	Properties similar to solid rubber but with increased static deflections
Steel Bonded Cork	Depends on density	High	Up to 6% of critical	—	Cork composition with bonded metal faces. Particularly applicable for isolation of concrete mounting blocks

Selected Bibliography

ALLSWAY, P.H.: Antivibration Foundation for Roll Grinding Machine. Noise Control, Vol. 7, No. 1-1961.

CALCATERRA, P.C., CAVANAUGH, R.D. and SCHUBERT, D.W.: Study of Active Vibration Isolation Systems for Severe Ground Transportation Environments. NASA CR — 1464. Clearing-house for Federal Scientific and Technical Information, Springfield, Virginia 22151. Nov. 1969.

163

CREDE, C.E.:	Vibration and Shock Isolation. John Wiley and Sons, Inc. New York 1951 (1962).
DERBY, T.F. and CALCATERRA, P.C.:	Response and Optimization of an Isolation System with Relaxation Type Damping. NASA CR-1542. May 1970.
GERB:	Handbuch über Schwingungsisolatoren und Viscodämpfer. Firma Gerb, Nonnendamm 4/5.1 Berlin 13. B.D.R.
GROOTENHUIS, P.:	The Anti-Shock Mounting of Testing Machine. Proc. Inst. Mech. Engrs. 1965—66.
HIXON, E.L.:	Application of Mechanical Equivalent Circuits to Vibration Problems. Noise Control, Vol. 7, No. 6-1961.
HOUSNER, G.W.:	The Groundshock Problems of Earthquakes and Explosions. Noise Control, Vol. 7, No. 6-1961.
KUNICA, S.:	Servo-controlled Pneumatic Isolators — Their Properties and Applications. ASME Paper No. 65-WA/MD-12. Nov. 1965.
LOWE,R.T.:	Practical Considerations Involved in Shock and Vibration Isolation. Noise Control, Vol. 4, No. 2-1958.
LOWE, R.T. and CREDE, C.E.:	Recent Developments and Future Trends in Vibration Isolation. Noise Control, Vol. 3, No. 6-1957.
LIPPMANN, S.A.:	Tires in Automotive Vibration Problems. Noise Control, Vol. 2, No. 3-1956.
MILLER, L.N. and DYER, I.:	Printing Machine Isolation. Noise Control, Vol. 4, No. 4-1958.
MINDLIN, R.D.:	Dynamics of Package Cushioning. Bell System Tech. Journ., Vol. 24, No.'s 3 and 4-1945.
MUSTER, D.:	Predicting the Vibratory Interaction between a

	Simple Substructure and a Nonrigid Foundation. Noise Control. Vol. 7, No. 3-1961.
MUSTIN, G.S.:	Theory of Cushion Design. Monograph No. SVM-2, Shock and Vibration Information Center Washington, D.C. 1968.
OLESEN, H.P. and DELPY, D.T.:	Shock and Vibration Isolation of a Punch Press. Brüel & Kjær Tech. Rev. No. 1-1971.
OLESEN, H.P.:	Measurements on Resilient Devices for Shock and Vibration Isolation. Proceedings of 7th ICA-Conference Budapest August 1971.
PLANKETT, R.:	Interaction between a Vibratory Machine and its Foundation. Noise Control. Vol. 4, No. 1-1958.
RUZICKA, J.E.:	Resonance Characteristics of Unidirectional Viscous and Coulomb-Damped Vibration Isolation Systems. Trans. ASME, Journ. of Eng. for Industry, 89, Series B, No. 4, Nov. 1967.
RUZICKA, J.E.:	Active Vibration and Shock Isolation. Paper No. 680747, SAE Trans. 77, 1969.
RUZICKA, J.E.:	Passive Shock Isolation. Sound and Vibration, August/Sept. 1970.
SNOWDON, J.C.:	Some Aspects of Package Cushioning Design. Noise Control Vol. 5, No. 5-1959.
SNOWDON, J.C.:	Vibration and Shock in Damped Mechanical Systems. John Wiley and Sons, Inc. New York 1968.
SNOWDON, J.C.:	Rubberlike Materials, Their Internal Damping and Role in Vibration Isolation. Journal of Sound and Vibration. Vol. 2, No. 2, April 1965.
SOLIMAN, J.I. and HALLMAN, M.G.:	Vibration Isolation Between Non-rigid Machines and Non-rigid Foundations. Journal of Sound and Vibration. Vol. 8, No. 2, September 1968.

SPERRY, W.C.:   Analysis of Dynamic Systems Using the
                     Mechanical Impedance Concept. Noise Control,
                     Vol. 7, No. 2-1961.

SUMMERS, A.C.:   Vibration Isolation for Submarine Machinery.
                     Noise Control, Vol. 6, No. 4-1960.

SYKES, A.G.:   Isolation of Vibration when Machine and Found-
                     ation are Resilient and when Wave Effects Occur
                     in the Mount. Noise Control. Vol. 6, No. 3-1960.

THOMAS, J.:   Six-Parameter Seismometer. Paper at the Int.
                     Ass. of Seismology and Physics of the Earth's
                     Interior, Madrid, Sept. 1969.

UNGAR, E.E. and   High Frequency Vibration Isolation, Journal of
DIETRICH, C.W.:   Sound and Vibration. Vol. 4, No. 2, September
                     1966.

WARRING, R.H. ed.:   Handbook of Noise and Vibration Control. Trade
                     and Technical Press, Ltd. Morden, Surrey, Eng-
                     land 1970.

7.2. Dynamic Vibration Control and Vibration Damping

In the previous section the basic aspects involved in the *isolation* of vibrations and shocks have been outlined. There are, however, practical cases where the isolation of the vibrations is not suitable, or difficult to arrange, and other methods of vibration reduction must be sought. One way of reducing the vibration may then be to utilize the principle of the *dynamic vibration absorber*. This principle can, in general, only be used effectively when the "original" vibrations contain one major frequency component only (or they consist of a very narrow band of frequencies such as a lightly damped, randomly excited single resonance).

If vibration reduction is to be achieved in cases of randomly excited multi-degree-of-freedom systems (plates and beams) the application of dynamic vibration absorbers is normally complicated and use is then prefer-ably made of some sort of general *damping treatment*.

a) The Dynamic Vibration Absorber

The basic physical principle of the dynamic vibration absorber is that of attaching to a vibrating structure a resonance system which counteracts the original vibrations. *Ideally such a system would completely eliminate the vibrations of the structure,* on account of its own vibrations.
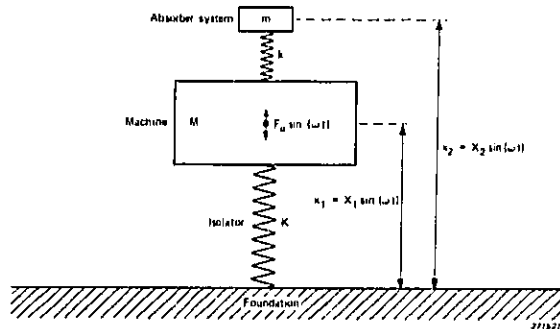
Fig.7.20. Illustration of the principle of the dynamic vibration absorber

Fig.7.20 illustrates these ideas. The mass, M, is here assumed to be the mass of a (rigid) machine structure producing the vibrating force, $F_o \sin (\omega t)$. The machine is mounted on a vibration isolator with a stiffness, K. Attached to the machine is a resonance (dynamic absorber) system consisting of the mass, m, and the spring element, k. It is now a simple matter to write down the equations of motion for the complete system:

$$M\frac{d^2 x_1}{dt^2} + Kx_1 - k (x_2 - x_1) = F_o \sin (\omega t)$$

$$m\frac{d^2 x_2}{dt^2} + k (x_2 - x_1) = 0$$

Assuming that the stationary solutions to these equations can be written

$$x_1 = X_1 \sin (\omega t)$$

and

$$x_2 = X_2 \sin (\omega t)$$

then

$$(1 + \frac{k}{K} - M \frac{\omega^2}{K}) X_1 - \frac{k}{K} X_2 = \frac{P_0}{K}$$

and

$$X_1 = [1 - (\frac{\omega}{\omega_a})^2] X_2$$

where $\omega_a = \sqrt{\frac{k}{m}}$ = resonant angular frequency of the attached (absorber) system.

By setting

$$1 - (\frac{\omega}{\omega_a})^2 = 0 \quad \text{i.e.} \quad f_a = f$$

the motion, X_1, of the machine will be zero, i.e. *the machine will not vibrate at all.* The maximum amplitude of the mass, m, is in this case:

$$- \frac{k}{K} X_2 = \frac{P_0}{K} \quad \text{i.e.} \quad X_2 = - \frac{P_0}{k}$$

This again means that by tuning the absorber system resonant frequency to equal the "disturbing" frequency, the vibration of the machine can be eliminated.

Actually, in practical cases the "disturbing" frequency region often covers the resonant frequency of the machine-isolator system, and both the absorber and the isolation system contain some mechanical damping. The equations of motion for the complete system then become considerably more complex, and so do their solutions.

Figs.7.21, 7.22 and 7.23 illustrate the effects upon the vibration transmissibility of a machine/isolator system when the machine is supplied with a dynamic vibration absorber.

From Fig.7.21 it is seen that when the complete system contains no damping at all and the absorber system is tuned to the resonant frequency of the machine/isolator system the transmissibility at this frequency is zero, in conformity with the above statements and mathematical derivations. However, on both "sides" of the resonant frequency two, theoretically infinitely high, transmissibility "peaks" are found. The shape of the curve is caused by the dynamic coupling between the machine/isolator system and

168
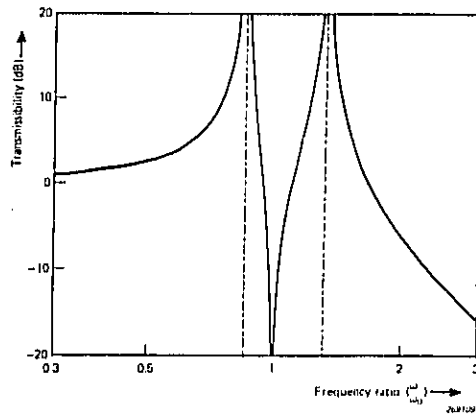
Fig.7.21. Theoretical transmissibility curves for a vibration isolated system supplied with an undamped dynamic vibration absorber, see also Fig.7.20
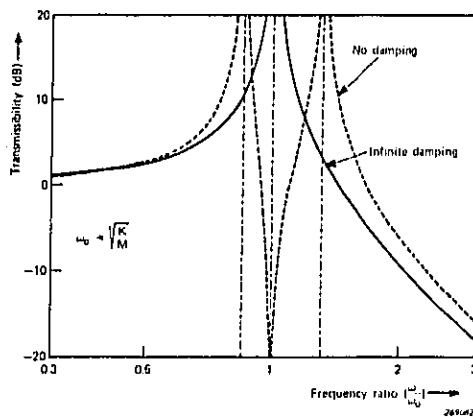
Fig.7.22. Effect of extreme absorber damping upon the transmissibility ratio of an undamped machine/isolator system

169
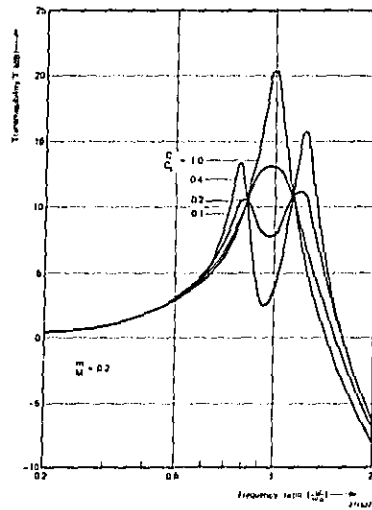
Fig.7.23. *Transmissibility of a machine/isolator system when the machine is supplied with a damped vibration absorber. The degree of damping is indicated on the curves. (Snowdon)*

the absorber system. Coupling effects of this sort is quite common in many branches of physics.

If the absorber damping is infinite the absorber mass is virtually clamped to the machine and the absorber system does not function at all, Fig.7.22. In practice, when a damped vibration absorber is applied to a machine/ isolator system the transmissibility curve must lie between the two extremes sketched in Fig.7.22. This is illustrated in Fig.7.23 for various values of absorber damping ratio.

Theory has shown that when damping is added to the absorber the "optimum" performance conditions*) are, in general, no longer obtained by tuning the resonant frequency of the absorber system to equal the resonant

---

*) "Optimum" conditions are assumed to be those which ensure a maximally "flat" peak-notch region of the transmissibility curve, Fig.7.23, to be obtained.

frequency of the machine/isolator system. Actually the most favourable tuning depends upon the ratio between the absorber mass and the mass of the machine i.e. m/M. It has been found that when the damping is of the viscous type then the ratio between the absorber resonant frequency, f_a, and the machine/isolator resonant frequency f_o, should be:

$$\frac{f_a}{f_o} = \sqrt{\frac{M}{m+M}} = \sqrt{\frac{1}{1+\frac{m}{M}}}$$

From this equation it is noted that when $\frac{m}{M}$ is small the difference between the two resonant frequencies is negligible, while for an increasing mass-ratio the "de-tuning" of the absorber may become very significant. Also the "optimum" viscous damping factor depends upon the mass-ratio, see Fig.7.24. Finally, Fig.7.25 shows some theoretical transmissibility curves calculated for various mass-ratios and "optimum" damping. Note the decrease in resonant amplification with increasing mass-ratios.

As pointed out in section 7.1 the theoretical treatment of the vibration transmissibility from a vibrating source (machine) to its foundation, and that of the vibration transmissibility from a vibrating foundation to a mounted equipment is more or less identical. This, of course, also applies with respect to the use of dynamic vibration absorbers see, Fig.7.26.
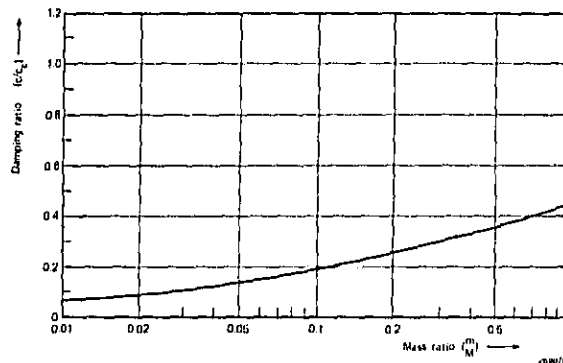
Fig.7.24. Curve showing "optimum" viscous damping factor as a function of the mass ratio $\frac{m}{M}$ (Snowdon)

171
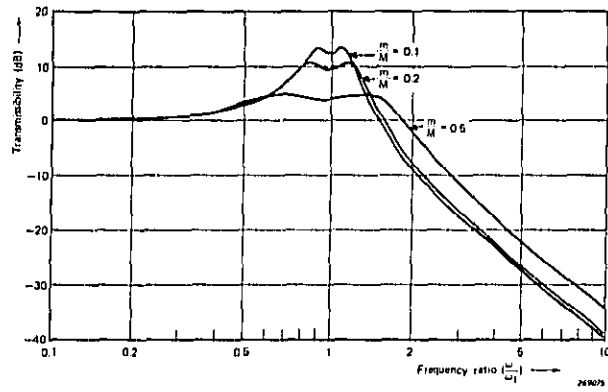
Fig.7.25. Theoretical transmissibility curves for a system of the type shown in Fig.7.20 supplied with a viscously damped dynamic vibration absorber. Optimum absorber tuning and damping for mass ratios of $\frac{m}{M} = 0.1$ $\frac{m}{M} = 0.2$ $\frac{m}{M} = 0.5$. (Snowdon)
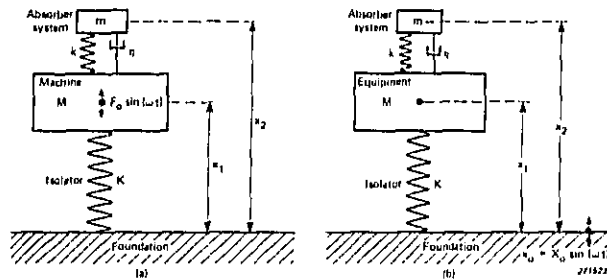
Fig.7.26. Dynamic vibration abosrber applied to:
a) Machine (source)
b) Equipment

172

To illustrate this statement consider a rigid equipment (mass: M) elastically mounted on an electro-dynamic vibration machine (see also section 7.3). The transmissibility curve for this system is measured and automatically recorded on a Brüel & Kjær Level Recorder Type 2305, Fig.7.27a. By attaching a damped dynamic absorber system (mass: m = 0.5 M) to the mass M the transmissibility curve was changed into the one shown in Fig.7.27b. The effect of the absorber is clearly noted. For the sake
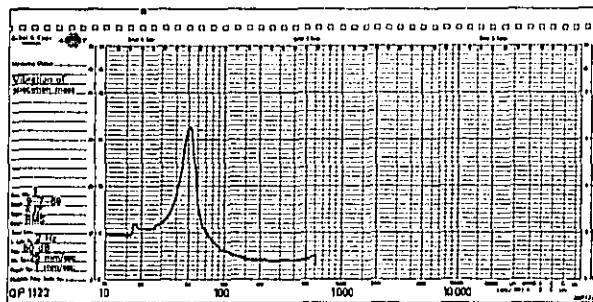
a)
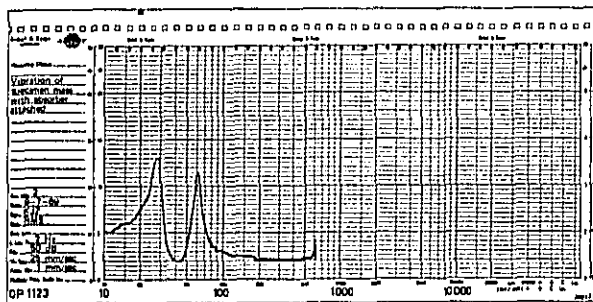
b)

Fig.7.27.   Curves showing a practical example of the effect of applying a
dynamic vibration absorber to a simple vibrating system
a) Transmissibility curve for the system before the dynamic
vibration absorber was applied
b) Transmissibility curve for the system with absorber

173

of completion also the vibration of the absorber mass, m, was measured and
recorded, Fig.7.28. Before finishing this brief discussion of the dynamic
vibration absorber it should be mentioned that the principle of the absorber
may be used not only to reduce resonance effects in vibration and shock
isolation systems, but also to reduce the vibration of beams and plates
vibrating in one of their fundamental modes. Thereby the acoustic radiation
from, for instance, a plate may be reduced making the dynamic vibration
absorber an efficient tool in the "battle" against acoustic noise.
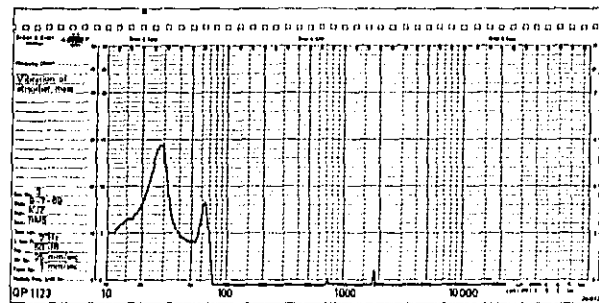
Fig.7.28.   Vibration of the absorber mass, m, in the system used to obtain
             the transmissibility curve shown in Fig.7.27b)

b) Application of Damping Treatments

As pointed out in section 3.6 structural elements like beams and plates
exhibit a, theoretically infinite, number of resonances (normal modes). If
these elements are subjected to vibrations of variable frequency (motor with
variable speed), or to wide band random vibrations, a number of resonances
might be excited and the application of separate dynamic vibration
absorbers becomes impractical. Because most engineering materials like
steel, aluminium, copper, etc. contain little inherent damping, resonant
vibrations must be reduced by some "external" means. In the case of plates
use is sometimes made of some sort of "stiffening" arrangements. These
arrangements do, however, not *damp* the resonances, they merely shift them
towards higher frequencies. If the resonances can be shifted to frequencies
which will not be excited during normal operation of the equipment this
solution to the problem of reducing plate vibrations may be acceptable.*)

*) Actually, because internal material damping often increases with frequency a certain
   "damping" effect may also be achieved by shifting the resonant frequencies.

174

On the other hand, in complicated machinery, the shifting of resonant frequencies in one element *may* cause serious vibration troubles to occur in some other element. The most general solution to the problem will therefore be, in some way or other, to apply some sort of external damping to the elements considered.

External damping can be applied in several ways: (1) By means of interface damping (friction), (2) by spraying a layer of material with high internal losses over the surface of the vibrating element or (3) by designing the critical elements as "sandwich" structures.

Interface damping is obtained by letting two surfaces "slide" on each other under pressure, see Fig.7.29a. If there is no lubricating material between the surfaces the damping effect is produced by dry friction (Coulomb damping). The force versus displacement relationship for this type of damping is shown in Fig.7.29b, and the total dissipated vibrational energy (damping energy) is given by the area enclosed by the curve B — C — D — E — B. Even if dry friction can be a very effective means of damping excessive vibrations it has the disadvantage that it may lead to fretting corrosion of the two surfaces. To avoid the fretting corrosion use is sometimes made of an adhesive separator. The arrangement then, however, turns

a)

b)
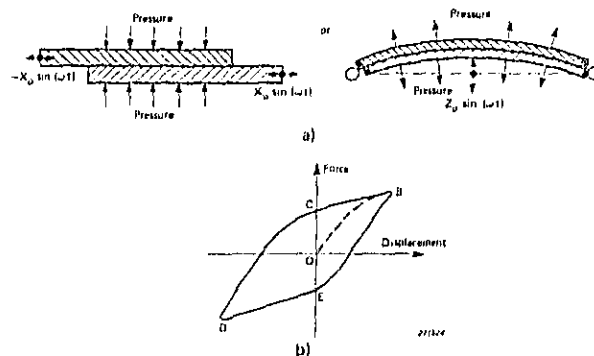
Fig.7.29.   Example of interface damping
            a) Sketch showing a physical system producing dry friction type
            of interface damping
            b) Force versus displacement relationship for this type of
            damping

into what is commonly termed a sandwich structure, a type of damping arrangement which is further discussed later in this section.

One of the "simplest" methods of applying damping to a structural element vibrating in bending is to spray a layer of viscoelastic material with high internal losses over the surface of the element. This kind of damping technique has been widely used in the automotive industry for many years. The most well-known materials, solely made for the purpose are the so-called mastic deadeners made from an asphalt base.

Also other types of "deadening" materials are at present commercially available. Common for all of them are that they are made from high-polymer materials possessing optimum damping properties over certain frequency and temperature regions. These regions may, however, for some mastic materials be rather wide.

To obtain optimum damping of the combination structural element + damping material, not only the internal loss factor of the damping material must be high, but so must also be its modulus of elasticity (Young's modulus).

An approximate formula governing the damping properties of a treated panel in practice is given by the expression:

$$\eta \approx 14 \; (\frac{\eta_2 \; E_2}{E_1}) \; (\frac{d_2}{d_1})^2$$

where (see also Fig.7.30):

$$\eta \quad = \frac{1}{Q} = 2\,\xi = 2\frac{c}{c_c}$$

$\quad\quad$ = Loss factor of the combination structure element (panel) + damping material

η_2 $\quad$ = Loss factor of the damping material

E_1 $\quad$ = Modulus of elasticity (Young's modulus) of the structural element

E_2 $\quad$ = Modulus of elasticity of the damping material

d_1 $\quad$ = Thickness of the structural element (panel)

d_2 $\quad$ = Thickness of the layer of damping material

One fact, which is immediately obvious from the above formula, is that the relative thickness of the layer of damping material, $(\frac{d_2}{d_1})$, plays a very important role for the resultant damping. In practice the ratio is normally
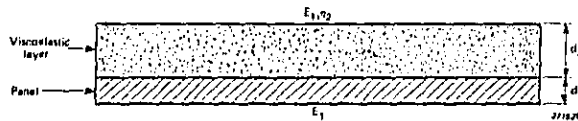
Fig.7.30. Sketch illustrating the use of a single visco-elastic layer to obtain
           the required vibration damped effect

chosen to be of the order of one to three. Also, it can be seen that it is
generally advantageous to apply *one* (thick) layer of damping material
rather than dividing the layer in two by using doublesided coating.

A third method of applying damping to structural elements is the use of
sandwich structures, Fig.7.31. Several types of such constructions exist: The
original structure may be supplied with a constrained viscoelastic layer, i.e.
the damping material is covered with a thin metal sheet, Fig.7.31a; a thin
visco-elastic layer is placed between two equally thick plates (adhesive
separator), Fig.7.31b; or finally use may be made of a thick visco-elastic
layer between the two plates, Fig.7.31c.
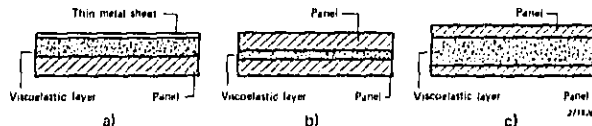
Fig.7.31. Examples of sandwich structures
           a) Use of a constrained visco-elastic layer
           b) Sandwich structure with a thin visco-elastic layer
           c) Sandwich structure with a thick visco-elastic layer

A considerable amount of theoretical and experimental investigations
have, in the later years, been carried out to allow the prediction and com-
parison of damping properties of sandwich structures. The general results of
these investigations indicate that, contrary to the above discussed applica-
tion of mastic deadeners, the thickness of the visco-elastic layer is not a
factor of *prime* importance. It seems, however, that the overall geometry of
the construction (symmetrical, unsymmetrical) is important, the symmetri-
cal construction showing the most favourable overall damping properties.
On the other hand when the thickness of the visco-elastic layer is increased
the temperature and frequency ranges within which optimum damping can
be obtained increases.

177

To illustrate the general difference in damping obtained between a system using one layer mastic deadening and a sandwich construction some measured results (Cremer and Heckl) are reproduced in Fig.7.32.

The measurement of material damping properties is normally carried out according to one of two basic measurement methods:

1. The frequency response method, and

2. The decay-rate (reverberation) method.
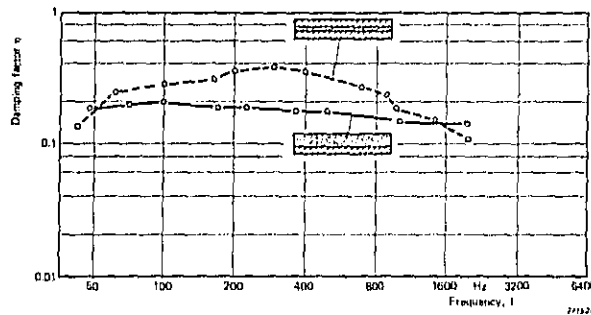
Fig.7.32.   Results of loss factor measurements on a sandwich structure with a thin visco-elastic layer, and on a plate supplied with one layer mastic deadening $(d_2/d_1 \approx 2.5)$. (After Cremer and Heckl)

The practical application of the frequency response method consists normally in cutting a bar-shaped sample from the material to be tested, clamping the sample bar at one end, or both ends, and exciting it into bending vibrations with a variable frequency, sinusoidal force.

The amplitude of the response vibrations is then plotted as a function of frequency, see Fig.7.33. From such a curve, at a resonance peak, the loss factor can be calculated as

$$\eta = \Delta f_n/f_n$$

where Δf_n is the bandwidth at the half power points (3 dB points) and f_n is the resonant frequency. The index n is the order of the resonance, or mode

178
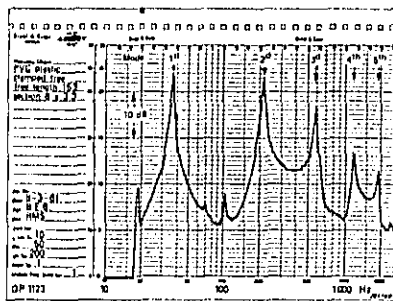
Fig.7.33. Complete frequency response curve obtained from measurements on a sample bar clamped at one end. Measured by means of the arrangement shown in Fig.7.34

number. The modulus of elasticity*) (Young's modulus) can be found from the resonant frequency and the mechanical dimensions of the bar:

$$E = 48 \pi^2 \rho \left(\frac{l^2}{h} \frac{f_n}{K_n^2} \right)^2 \text{ N/m}^2$$

l   is the active length (m) of the bar,
h   is the thickness in the plane of vibration (m)
ρ is the material density (kg/m^3)
K_n depends on the boundary conditions of the bar:

both ends free or clamped:

$$K_1 = 4.73; K_2 = 7.853; K_3 = 10.996$$

$$K_n = (n + \frac{1}{2}) \pi; n > 3$$

one end free, one end clamped:

$$K_1 = 1.875; K_2 = 4.694; K_3 = 7.855$$

$$K_n = (n - \frac{1}{2}) \pi; n > 3$$

*) The modulus of elasticity found according to the described technique actually is the real part of a complex modulus of elasticity (dynamic modulus). In most practical cases, however, the difference between the modulus of elasticity found from the formula given here and Young's modulus is negligible.

This measuring method is suitable for values of η between about 0.6 and 0.001. When the loss factor is large it will be impossible to measure the amplitude because no standing waves will be present, and if it is too small the resonance peaks will be too narrow to allow the bandwidth to be measured with reasonable accuracy.

A measuring arrangement suitable for the frequency response method of measurement is shown in Fig.7.34 and consists of the Brüel & Kjær Complex Modulus Apparatus Type 3930 (Fig.7.35) and associated electronics. Actually the frequency response method has, over the years past, been refined by Dr. H. Oberst et al and constitutes to-day a simple and efficient means of determining complex material damping properties.
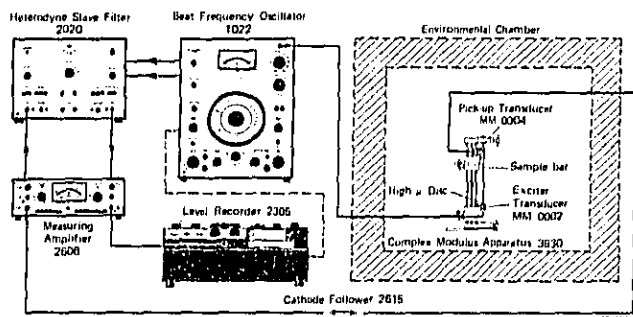
Fig.7.34. Measuring arrangement used to record frequency response curves of the type shown in Fig.7.33 automatically on the Brüel & Kjær Level Recorder Type 2305

The same measuring arrangement as shown in Fig.7.34 may also be used for the second method mentioned above, i.e. the decay rate method. The external exciting force is, in this case tuned to a resonant frequency of the sample which will start a forced oscillation with steady amplitude when equilibrium is reached. If the exciting force is stopped instantly, the vibration amplitude decays exponentially with time. (Thus linearly with time if plotted out logarithmically.) The loss factor η is found from

$$\eta = \frac{D}{27.3\, f_n}$$

180

where D is the decay rate in dB/sec and f_n is the resonant (modal) frequency. The modulus of elasticity, E, is found as described above for the frequency response method.
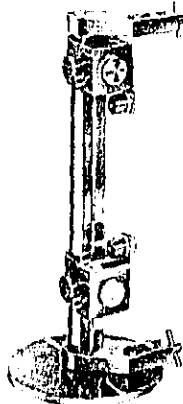
Fig. 7.35. Photo of the Complex Modulus Apparatus Type 3930

In the decay rate method the upper limit for measuring the loss factor depends on the measuring instruments. There is no theoretical lower limit.

A type of decay-rate measurements which has been extensively used in the past, especially in the U.S.A., is the so-called Geiger thick-plate test. The basic principle of this test is the same as already outlined for cut-out sample bars, only that the sample in this case consists of a suspended plate, see Fig. 7.36.

Normally decay measurements according to the Geiger test are made at one frequency only. As this test has been used mainly in conjunction with automotive panels the frequency has commonly been chosen around 160 Hz.

So far the decay-rate type of tests discussed have been based on the interruption of a steady state normal mode (resonant) vibration, i.e. time decay measurements. Also another type of decay-rate measurements are sometimes used: the determination of the decay-rate of progressive waves.
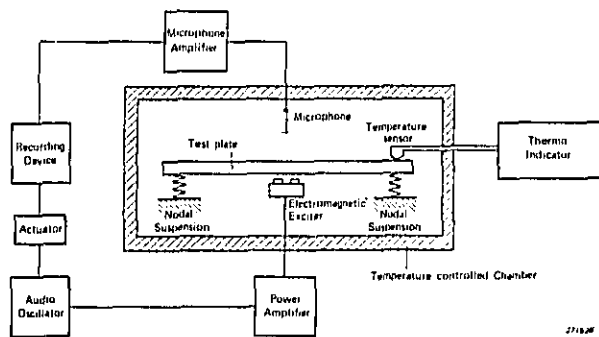
Fig.7.36.   Measuring arrangement suitable for use in conjunction with the
             Geiger thick-plate test

This is based on decay-rate determinations in space rather than in time, as
described below. When a long strip of material is excited to transverse
vibrations at one end, and terminated at the other end in such a way that
practically no reflection takes place, Fig.7.37, one dimensional mechanical
waves progress along the strip. The attenuation of these waves may then be
used as a measure for the damping properties of the strip material:

$$\eta = \frac{D_\lambda}{27.3}$$

where D_λ is the attenuation along the strip in dB per wavelength.
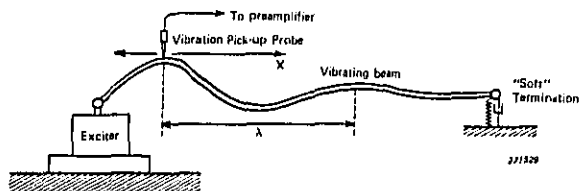
Fig.7.37.   Sketch showing how the attenuation of progressive mechanical
             waves may be measured

182

Selected Bibliography

CHERRY, L.B.:   Electro-Magnetic Induction Damping of Vibratory Motion. Noise Control. Vol. 6, No. 5-1960.

CRANDALL, S.H.:   The Role of Damping in Vibration Theory. J. Sound Vib. Vol. 11. No. 1. 1970.

CREMER, L. and
HECKL, M.:   Körperschall. Springer Verlag. Berlin, Heidelberg/ New York, 1967.

DERBY, T.E. and
RUZICKA, J.E.:   Loss Factor, Resonant Frequency of Viscoelastic Shear Damped Structural Components. NASA Report CR 1269, 1969.

EVANS, L.M.:   Control of Vibration and Noise from Centrifugal Pumps. Noise Control. Vol. 4, No. 1-1958.

EVANS, J.:   Vibration and Acoustical Problems in Missiles. Noise Control. Vol. 4, No. 6-1958.

FREYNIK, H.S.:   Response of Windows to Random Noise. Sound. Vol. 2, No. 3, May-June 1963.

GROOTENHUIS, P.:   Measurement of the Dynamic Properties of Damping Material. Proc. Int. Symp. Assoc. Belge Acoustieus, Leuwen 1967.

GROOTENHUIS, P.:   Sandwich Damping Treatment Applied to Concrete Structures. Trans. R. Soc. A 263, 455. 1968.

GROOTENHUIS, P.:   The Control of Vibrations with Viscoelastic Materials, J. Sound Vib. Vol. 11, No. 4. 1970.

HAGAN, R.D. and
BABCOCK, G.H.:   Shipboard Vibration Problems and their Solutions. Noise Control. Vol. 5, No. 4-1959.

HAMME, R.N.:   Materials and Techniques for Damping Vibrating Panels. Noise Control. Vol. 3, No. 2-1957.

KERWIN, E.M.:   Damping of Flexural Waves by a Constrained
                       Viscoelastic Layer. J.A.S.A., Vol. 31, No. 7, July
                       1959.

KURTZE, G.:   Physik und Technik der Lärmbekämpfung. Ver-
                       lag G. Braun. Karlsruhe, 1964.

McKEE, C.H.:   Selecting Materials for Vibration Control. Mach.
                       Design. Vol. 42, No. 12. May 1970.

MEAD, D.J.:   Criteria for Comparing the Effectiveness of
                       Damping Treatments. Noise Control. Vol. 7,
                       No. 3-1961.

MEAD, D.J.:   The Practical Problems of Assessing Damping
                       Treatments. Journal of Sound and Vibration.
                       Vol. 1, No. 3, July 1964.

OBERST, H. und   Über die Dämpfung der Biegeschwingungen
FRANKENFELD, K.:   dünner Bleche durch fest haftende Beläge.
                       Acustica, (Akustische Beiheft No. 4.)-1952.

OBERST, H.:   Schwingungsdämpfenden   Kunststoffe   aus
                       optimal eingestellten Polymeren. Kolloid-Zeit-
                       schrift. Zeitschrift für Polymere. Band 216-217,
                       S. 64-80, 1967.

OBERST, H.:   Reduction of Noise by the Use of Damping
                       Materials. Trans. R. Soc. A 263, 441, 1967.

OBERST, H. und   Verbundsblechsysteme mit optimal eingestellten
SCHOMMER, A.:   schwingungsdämpfenden   Kunststoff-Zwischen-
                       schichten. Kunststoffe, 55. Jahrg. 1965.

ROSS, D., UNGAR, E.E., Damping of Plate Flexural Vibrations by Means
and KERWIN, E.M.:   of Viscoelastic Laminae. ASME Publ. Structural
                       Damping. Section 3. 1969.

SNOWDON, J.C.:   Vibration and Shock in Damped Mechanical
                       Systems. John Wiley and Sons, Inc. New York,
                       1968.

184

VANCE, D.H.:   The Use of Vibration and Shock Control in
Reducing Noise Levels. Noise Control. Vol. 2,
No. 2-1956.

VON GIERKE, H.E.:   Vibration and Noise Problems Expected in
Manned Space Craft. Noise Control. Vol. 5,
No. 3-1959.

WARRING, R.H. ed: Handbook of Noise and Vibration Control, Trade
and Technical Press, Ltd. Morden, Surrey, Eng-
land 1970.

7.3. Vibration Testing

Vibration testing is a relatively new concept. It originated more or less
with the desire to test parts and equipment for use in airplanes prior to a
first flight. Even though vibration testing, in a sense, was used by Wöhler
some 100 years ago in his experiments on the fatigue of metals, the
intensive use of a more general vibration test technique developed during
and subsequent to World War II.

At this time not only structural mechanical failures due to vibrations
became a problem, but also the use of complicated electronic and electro-
mechanical equipment made control systems and communication
instrumentation sensitive to the vibrations encountered during mobile
operation. Furthermore the speed and maneuvering facilities available in
modern vehicles severely increase the vibrations caused by the overall
environment and complicate theoretical predictions and estimates of
vibration responses.

Even though the development of vibration testing techniques quite
naturally have been closely connected to the aircraft and space vehicle field
it might be worth mentioning that vibration testing, often supplemented by
shock and bump testing, is today also used in many other fields. Typical
examples are the field of packaging and transportation, as well as the auto-
mobile and agricultural machine industry.

Basically two different types of vibration testing are in common usage at
present:

1. The frequency sweep test, and

2. The wide band random vibration test.

185

A third type of test, however, which has gained considerable interest over the last few years is the so-called "sweep random" vibration test. Although in principle a frequency sweep test, this test also retains certain characteristics of random vibration.

Generally speaking the frequency sweep test is an engineering tool which is excellently suited for the investigation of vibration responses of models and prototypes, while the wide band random vibration test is a typical qualification type of test. On the other hand, the cost and complexity of the wide band random test equipment, has often made this test prohibitive for the smaller vibration laboratories, which on many occasions, thus use the frequency sweep test also as a qualification test.

Common for all types of present-day vibration testing is the use of an electrically controlled vibration machine which produces the mechanical motion to which the test object is subjected. The most widely used vibration machine is the *electrodynamic vibrator*, which is basically a large "loud-speaker" system. Another, also frequently used vibrator is based on *electro-*
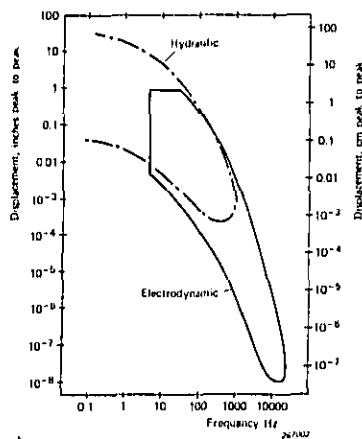
Fig.7.38. *Useful operating regions of modern hydraulic and electro-dynamic vibration machines (G.B. Booth)*

hydraulic principles. While the electrohydraulic vibrator is capable of operating at very low frequencies (theoretically down to DC), allows very large displacement strokes (up to 30 cm), and has a very high force capability (over 50 tons of vibrational force), the electrodynamic vibrator is more generally applicable to most vibration test requirements met in practice to-day. A chart showing the typical regions of operation of the two types of vibration machines is given in Fig. 7.38.

a) The Electrodynamic Vibration Exciter

Fig. 7.39 shows a sketch illustrating the basic design of an electrodynamic vibration machine. It consists of a magnet which produces the required constant magnetic field, a coil which is fed from an AC signal source, the moving element (on which the coil is mounted), and the flexures holding the coil and moving element in position, with respect to the constant magnetic field. The magnetic field strength and the coil diameter, number of turns and current determine the force available. This force is limited by the cooling provided for the coil and the materials and mechanical strength of the moving parts.
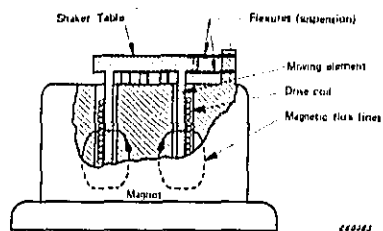
Fig. 7.39.   Basic design of an electrodynamic vibration exciter

Ideally the coil and moving element should be a rigid unit where all points move in phase. Additionally, the ideal suspension of the moving element should be of such a nature that only a one-dimensional movement takes place, and finally the loading of the vibrator by a test specimen should in no way influence the motion. Unfortunately, it is impossible to fulfil these ideal conditions and compromises are therefore necessary.

As all bodies are more or less elastic, the requirement of rigidity must be compromised with the size and design of the moving element. This size is

187

pre-determined by the size and shape of the specimen under test, as this also influences the movement of the moving element. To achieve pure one-dimensional translatory motion, the moving element must either be suspended in such a way that no other modes of movement is possible or forces which may cause such motion, must be eliminated.

To minimize the influence of specimen resonances upon the motion of the moving element the "effective" mass of the moving element should be large. However, this means that to produce a certain acceleration of the specimen a rather high force is necessary. Furthermore adding mass to the moving element normally reduces the useful frequency range of the vibration machine. By intorducing variable compensation networks or servo-control of the moving element motion it is possible to "compensate" for the variation in load, with frequency caused by specimen resonances. Smaller moving masses can then be used for the same test.

If servocontrol is used rather than an increase in mass to minimize influence of resonances, two major advantages are gained:

1. A much greater part of the force produced by the vibration machine is transferred to the test specimen.

2. The useful frequency range of the vibrator can be extended because of the reduction in moving mass.

In Fig.7.40 a typical frequency characteristic for a modern electro-dynamic vibration exciter is shown. The vibrator is driven from a constant
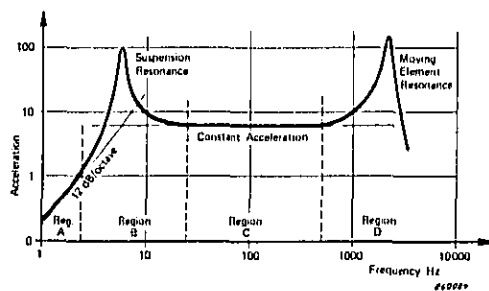
Fig.7.40.   Basic acceleration versus frequency characteristic of electro-dynamic vibration exciters when the input current to the drive coil is kept constant, independent of frequency

188

current level source i.e. constant driving force is delivered to the moving element. The actual acceleration level of the shaker table is then plotted as a function of frequency and the graph divided into different sections A, B, C and D which are described below.

When DC is supplied to the shaker drive coil, a constant force is developed which will cause the moving element to deflect, the magnitude of the deflection being determined by the stiffness of the mechanical suspension arrangement. At very low frequencies the deflection of the moving element will thus be stiffness controlled, i.e. constant displacement level conditions will be present at the shaker table region A in Fig.7.40 (Constant displacement level conditions are represented by a slope of 12 dB/octave in the graph).

If the frequency of the drive signal is increased, the resonance of the overall mass of the moving element assembly and the suspension "spring" will cause a relatively great increase in the table's amplitude, region B in Fig.7.40. Above the suspension resonance the mass of the moving element will control the table motion and a region of constant acceleration is developed, C, in Fig.7.40.

At still higher frequencies the different parts of the moving element itself will resonate and cause major irregularities in the frequency characteristic. In Fig.7.40 only one moving element resonance is shown. These resonances limit the upper end of the useful frequency range.

The acceleration vs frequency characteristic of electrodynamic vibrators is more or less similar for all vibration exciters when the exciter is driven from a constant current level source. However, amplifiers which effectively transform the available electrical power into mechanical force may usually be well approximated by a constant voltage level source. The acceleration vs frequency characteristic of electrodynamic vibration exciters subjected to these conditions varies considerably, depending upon the electrical resistance of the drive coil winding and the mechanical damping of the suspension arrangement. In Fig.7.41 the frequency response of a low rusistance well damped vibration exciter is shown, the drive coil of which was fed from a constant voltage level source (Brüel & Kjær Type 4813).

In the case of the low-resistance, heavy-duty vibration exciter the suspension resonance is completely eliminated due to the electrical damping effect. This damping effect is caused by the low output resistance of the power amplifier which almost short-circuits the back e.m.f. induced in the coil, when it moves in the constant magnetic field of the shaker. As the back

189
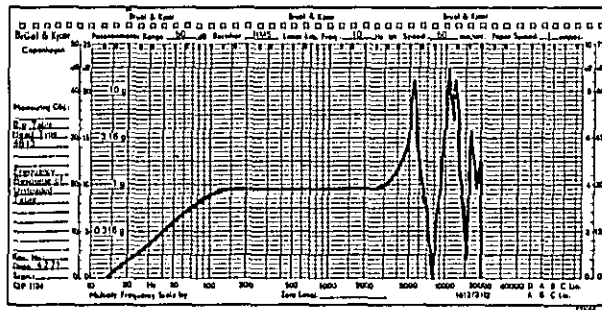
Fig.7.41. Example of acceleration versus frequency response of an electrodynamic vibration exciter driven from a constant voltage source

e.m.f. is proportional to the velocity $(e \sim \frac{dq}{dt})$ the movement of the moving element in this frequency region (corresponding to region B in Fig.7.40) will be velocity controlled, and the acceleration vs. frequency characteristic shows a slope of 6 dB/octave. At higher frequencies, where the movement of the moving element is mass-controlled, the acceleration level of the element will be constant and determined by the formula

$$a = \frac{F}{W + W_0}$$

Here a is the maximum acceleration level achievable in m/sec^2 (g), F is the maximum rated force in newtons (lb force), W is the mass of the test specimen in kg (lb), and W_0 is the mass of the moving element of the vibrator in kg (lb).

Actually, the performance of modern electrodynamic vibration exciters are normally limited as illustrated in Fig.7.42, i.e. by their maximum displacement, velocity and force capabilities, and, at the high frequency end by moving element resonances.

It was mentioned earlier in this section that a number of compromises were necessary in the practical design of electrodynamic vibrators. To minimize the effects of compromises a completely new type of vibration exciter design has been introduced by Booth, Brüel & Kjær. The basic idea in this design is that one vibration exciter *body* can be supplied with

190
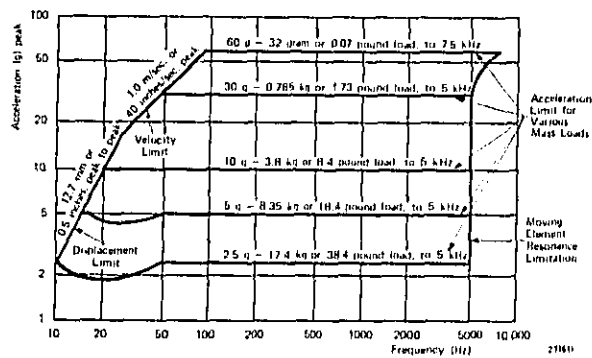
Fig.7.42. Sketch indicating displacement, velocity and acceleration limitations imposed on practical electrodynamic vibration exciters

Fig.7.43. Photograph of an Electrodynamic Vibration Exciter Body together with the relevant set of Vibration Exciter Heads

191

different, interchangeable, vibration exciter *heads*. Each head contains a moving element and its suspension system, and each head is optimized for it's particular field of application. Fig.7.43 shows a photo of an exciter body and it's different heads.

b) The Frequency Sweep Test

The frequency sweep test consists of feeding a vibration exciter with a certain amount of power at a slowly changing frequency. Due to resonances in the test specimen, and in the vibration exciter, the power necessary to subject the test specimen to a certain, constant vibration level will not, however, remain constant during the test, but will be a function of the frequency of the vibrations. This is illustrated in Fig.7.44 which shows a plot of the acceleration of the shaker table as a function of frequency for constant voltage drive of the vibration exciter and a table load consisting of a single degree-of-freedom mechanical system. To keep the vibration level constant the output from a vibration pick-up mounted on the table is used to control the input power to the vibrator, see also Fig.7.45.
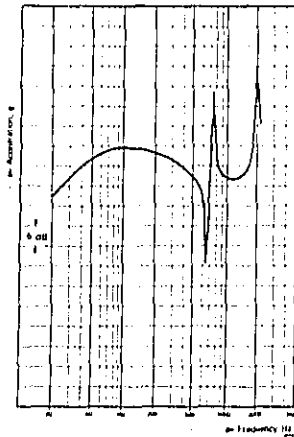
Fig.7.44.   *Typical acceleration level versus frequency curves measured on the shaker table of a vibration machine loaded by a single degree-of-freedom system*

192
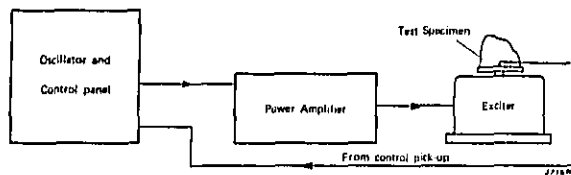
*Fig.7.45.* Block diagram of a typical servo controlled frequency sweep test arrangement

Normally, the control of the vibration level is made in such a way that when the vibration level of the table tends to increase, which would cause the output voltage from the control pick-up to increase, the input power to the vibration exciter is automatically decreased until the same vibration level is regained as was present before the change in vibration level occurred. The automatic decrease in exciter input power will not follow instantaneously when an increase in vibration level is felt by the control pick-up, but it will take a certain amount of time to regain the original level. This time constant of the regulation, or in other words "the regulation speed" should be selected according to the expected Q-values of the system resonances and the sweep-rate chosen for the frequency sweep, i.e. the regulation speed must be greater than the speed with which the system resonances are built up.

In practice this means that the highest regulation speed should be used, the upper limit of the regulation speed being set by interaction between the regulation speed and the actual vibration frequency (causing distortion). To allow for optimum automatic regulation the regulation speed must be variable and preferably provision should be made for programming the regulation as a function of the frequency sweep. A practical arrangement including an electronic generator which allows such programming to be made is shown in Fig.7.46.

The servo system illustrated in Figs.7.45 and 7.46 enables not only a regulation of the exciter frequency response with regard to resonance effects but it is also possible to include in the servo loop certain frequency dependent networks so that various predetermined test programmes can be carried out under controlled conditions.

Also, as reliability, stability and reproducibility are essential factors in vibration testing, the electronic generator shown in Fig.7.46 and 7.47 has been designed to contain no moving mechanical parts. Furthermore,

193
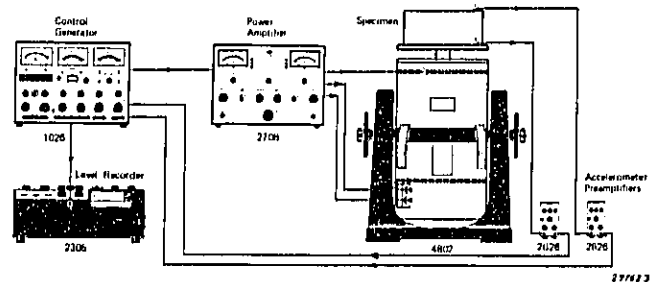
Fig.7.46. A practical frequency sweep vibration test system

accurate reading of the instantaneous test frequency can be made on a built-in 6 digit electronic counter.

Another important factor in vibration testing is the safeguarding of the test specimen, in case by accident (broken cable, etc.) the servo system loses control of the test level. To avoid damage to the specimen in such cases, the generator, Fig.7.47, contains safety circuits which instantaneously shut down the test.

As some test specimens may contain a variety of non-linear devices the control signal may be heavily distorted, even if the signal applied to the vibration exciter is a pure sinusoid. If the distorted signal is used to control
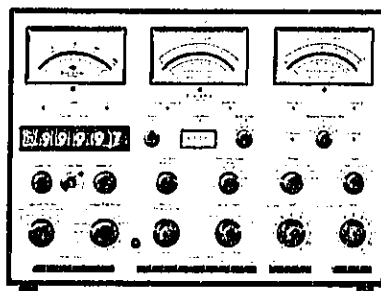
Fig.7.47. Photograph of the Brüel & Kjær Exciter Control Type 1026

194

the test-level directly, undertesting at the fundamental frequency occurs. In cases where undertesting must be avoided use should therefore be made of a so-called *tracking filter* in the control loop. This filter ensures that a signal containing the fundamental frequency component of the control signal only reaches the control circuit. Such tracking filters are also built into the generator shown in Fig.7.47.

Tracking filters may be designed according to different principles. The filters built into the generator are of the constant percentage bandwidth type, having a bandwidth of 6%. In Fig.7.48 the use of another type of tracking filter, the *Heterodyne Slave Filter Type 2021*, is illustrated. This is
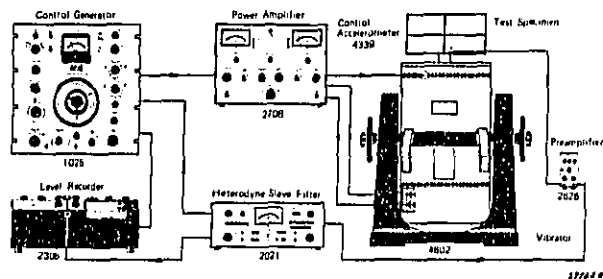

Fig.7.48. Example of the use of a tracking filter in the control loop of a frequency sweep vibration test arrangement

built according to the constant bandwidth principle, and features a number of automatic bandwidth versus frequency programs. Furthermore, it does not only filter out the fundamental frequency component for servo loop control, but, at the same time, measures the overall distortion. *In this way it is possible, during testing, to record automatically the distortion as a function of frequency.* An example of such a recording is shown in Fig.7.49. This kind of tracking filter can also be used as frequency analyzer, for instance for mean square spectral density (power spectral density) measurements.

When large, complex test specimens are bolted to the vibration exciter one finds that feedback control with a single vibration control pick-up, as has been discussed up to this point, is not sufficient. The specimen is not a dead mass, and different parts of the structure resonate at different frequen-
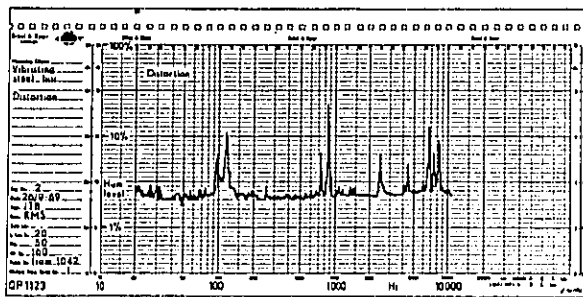
Fig.7.49. Example of an automatically recorded harmonic distortion curve obtained during measurements on a vibrating steel bar

cies, often causing an irregular overall motion. If a single vibration pick-up controls the motion of the shaker table, portions of the test specimen may be severely overtested, while other portions are undertested.

It is therefore often advantageous to use the average of the vibration signals measured at several specimen fixing points as control signal. This kind of control is illustrated in Fig.7.50 and reduces the amount of possible overtesting considerably. Undertesting will only be slightly affected.
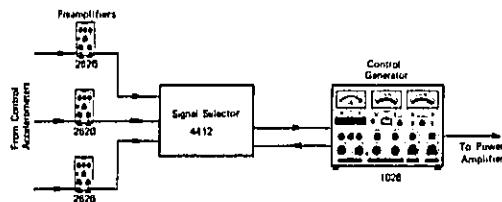
Fig.7.50. Example of a vibration test system allowing test level control from more than a single point

It was mentioned above that the servo loop arrangement also allowed for the inclusion of frequency dependent networks so that various test programmes could be established. Certain networks of this type are included in

196

the electronic control generators produced by Brüel & Kjær, and their insertion in the feedback loop can be controlled by a *Vibration Test Programmer Type 4413*. Fig.7.51 shows a test arrangement utilizing a Vibration Programmer.
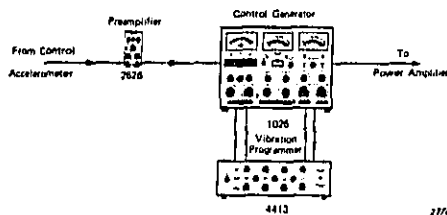

Fig.7.51. Vibration test system utilizing the Brüel & Kjær Vibration Programmer Type 4413

It was stated earlier in this section that the development of vibration testing technique has followed, very closely, the development of aircraft and space vehicles. As the specimens to be tested grew larger and larger so also did the vibration exciter, the largest electro-dynamic exciter available to-day (1971) being capable of producing some fifteen tons of vibrational force. Even though it would be desirable in some cases to have even larger exciters available it has not been found technically realistic to produce electro-dynamic vibration exciters with larger force ratings than the above mentioned fifteen tons machine. One of the reasons for this is that as the test specimen becomes larger, problems in mounting the specimen on the shaker table also become greater. The problem of testing large scale specimens is therefore presently being solved by the use of multiple vibration exciters operated either in series or in so-called master-slave arrangements rather than by trying to build larger vibrators. Fig.7.52 shows the principle involved in the control of a master-slave arrangement. It is seen that while the frequency sweep is governed by the "master" all the "slaves" have separate control signal loops. Also in this case, of course, it is possible to apply the Vibration Test Programmer and Signal Averager technique to each vibration exciter separately. However, in many cases the test specimen might only have one fixing point to each vibration exciter which makes the use of a Signal Averager superfluous. Large test specimens can in this way be tested to high vibration levels. A special feature of the arrangement shown in Fig.7.52 is that the phase relationship between the "master" and "slave" vibration can be adjusted over a full 360° angle, thus producing various kinds of specimen mode excitation.

197

Fig.7.52. Example of a "master-slave" system utilizing three vibration machines to excite the test specimen

c) The Wide Band Random Vibration Test

If a vibration exciter loaded by a resonant specimen is being fed with wideband random noise of constant mean square (power) spectral density, the spectrum of the acceleration at the specimen fixing point might look something like the curve shown on top in Fig.7.53. This means that the excitation of a particular specimen resonance is different from that assumed on the basis of the vibrator input signal spectrum (flat mean square spectrum).

During the course of time various methods have been developed to compensate electronically for these peaks and notches. The first method is fairly straight forward and consists in using a number of "peak-notch" equalizers in cascade. Each such equalizer should exhibit the inverse response of one resonance as measured on the vibration exciter table when the system is

198

Fig.7.53. *Example of ideal equalization of a wide band random vibration test system*

uncompensated. By using as many equalizers as there are resonances it is possible to achieve a response similar to that given in Fig.7.53 botton curve (equalized). This shows the resulting vibration of the shaker table when both the frequency non-linearities of the vibration exciter itself and those due to specimen resonances are ideally compensated for.

The time spent in adjusting for a particular test is, however, rather large and other, more feasible methods of compensation have been sought by the producers and users of random vibration test equipment. One such method is the so-called multiband equalization technique. It involves splitting the test frequency range into a number of discrete filter bands and adjusting the attenuation (or amplification) of each band individually. The adjustment can be performed manually or automatically. In this way it is also a relative- ly simple matter to "shape" the test frequency spectrum according to any given test specification, or for the purpose of further test research. However, the setting-up time of the manual system is still quite considerable.

This time is minimized in automatic multiband systems, where all the bands operate in closed servo loops, see Fig.7.54. Another great advantage gained by the use of automatic equalization is *the automatic correction for*

199
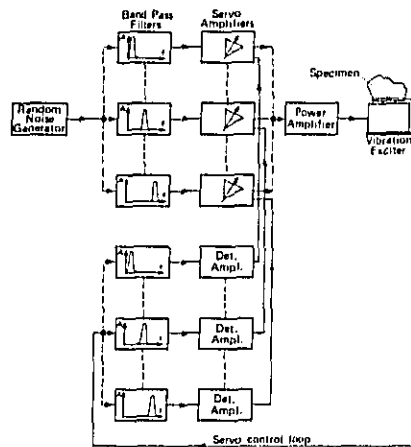
Fig.7.54. *Principle of operation of an automatic multiband random vibra-*
*tion test system*

the effect of frequency response changes which might occur between
setting-up and testing, and during the testing itself.

An automatic equalizer system developed by Booth, Brüel & Kjær is
shown in Figs.7.55 and 7.56. This system has a maximum frequency
coverage from 1 Hz to 10 kHz, and features a very flexible arrangement of
filter channels. Filter sets of 60, 120 and 240 channels are available and one
filter channel in one set may be replaced by two filter channels of the next
larger set. Hereby, it is possible to combine the channels from different sets
in numerous ways and thereby varying bandwidths over the test frequency
range according to specific response requirements.

There are three major reasons why the wide band random vibration test
has become popular as a qualification type of vibration test. These are:

1. The vibration producing mechanisms found in nature are more often
   of a random type than of a sinusoidal type and a random vibration
   test therefore simulates the statistical character of common vibration
   environments better than does a sine wave test.

200
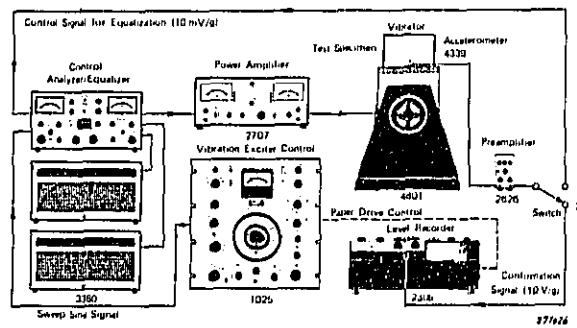
Fig.7.55. Random vibration test utilizing a practical automatic equalizer-
analyzer system (Brüel & Kjær)

2. The wide band random test excites all specimen resonances simultane-
   ously so that possible interaction effects are accounted for.

3. The wide band test-time required for a certain test exposure is orders
   of magnitude smaller than any single frequency sweep test.
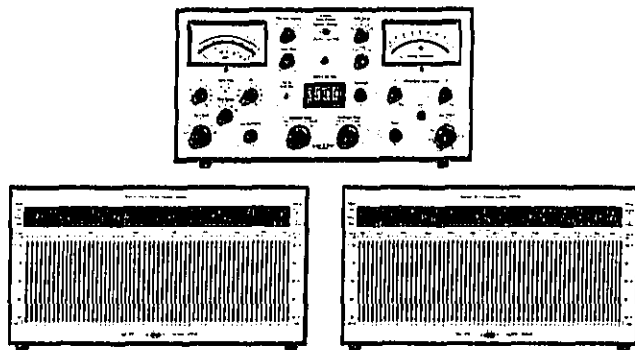
Fig.7.56. Photograph of a 120 channel automatic equalizer-analyzer
system (Brüel & Kjær)

201

Even though the vibrations commonly met in nature have a random amplitude character their mean square (power) spectra vary considerably. This is taken into account (or rather should be taken into account) when random vibration test specifications are developed. It has, however, often proved to be a very difficult task to develop detailed vibration test specifications, partly because the vibration environment is not always known from beforehand, and partly because of insufficient and inaccurate measurement data relating to the particular environment. The lack of exact environmental data has made it a common practice to collect all the measurement results relating to the environment in question and from the collection of data then draw some "estimated envelope" curves. An example of such "estimated envelope" curves are shown in Fig.7.57.
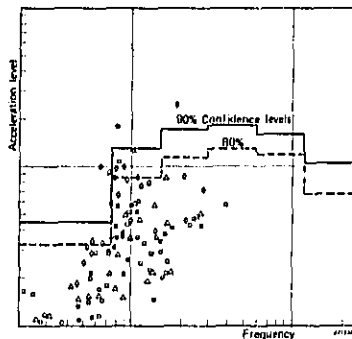

Fig.7.57. Example of the derivation of vibration test level specifications from environmental data

Although the method of "enveloping" seems to be a fairly sound method of developing test specifications, because of the many unknown factors involved in defining a vibration environment, it leaves a lot to be desired with respect to precision. Due to structural filtering effects and "mismatching" of mechanical impedances a test spectrum developed in the way outlined above will often punish the specimen much more severely than will the actual vibration environment encountered during normal operation, Fig.7.58. Also, it generally requires much larger vibration exciters and power amplifiers than might otherwise be necessary. In an attempt to remedy these disadvantages it is not uncommon to specify a certain wide

202
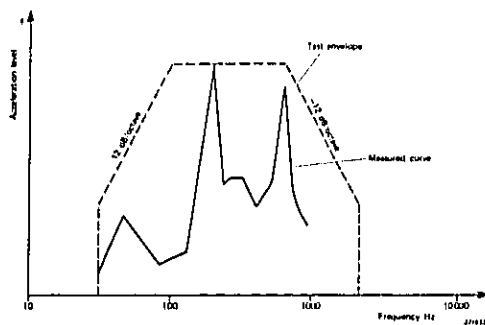
Fig.7.58. Comparison of actually measured vibration data at an instrument fixing point and the corresponding test specification spectrum

band "background" vibration upon which is superimposed a sweeping sine wave or a narrow band of noise. *This method of testing, however, comes close to what is known as the sweep random test technique.*

d) Sweep Random Vibration

In general wide band random vibration testing is very costly and means to substitute this by a less costly test have been sought ever since its first introduction. Various "equivalent" sweep sine tests have been proposed but since the sweep sine test cannot produce the same distribution of acceleration and stress amplitudes within the test specimen no general equivalence between the two types of test is ever likely to be found.

In 1957 M.W. Olesen of the Naval Research Laboratories in U.S.A. suggested the use of a sweeping narrow band random vibration test. This kind of testing is now commonly termed "sweep random" vibration testing. It was originally meant as an "economic" substitute for the wide band random vibration test, and the procedures for setting up the test were based on a wide band "equivalence". There are, however, other methods of setting up a sweep random test as will be discussed later in this section.

There seems to be little doubt that a random vibration test simulates the characteristics of real vibration environments met in sea, road and air transport better than does any kind of pure sinusoidal testing. This is important

203

to consider when a vibration test is specified, as most components and sub-assemblies contain several failure mechanisms. They may contain contact mechanisms, they may be constructed of combinations of ductile and brittle materials, they may show mechanical-electrical modulation effects, etc. Many of these mechanisms will react differently to sinusoidal and random vibration excitation.

Leaving the sweeping sine wave test as more or less a laboratory tool for investigation purposes, the only existing sweep test for practical qualification testing is the sweep random test. This test has the deficiencies that resonances are tested sequentially, and possible interaction effects must therefore be investigated on a prototype development stage prior to qualification testing, – and it takes a longer time than the wide band random test. Both of these deficiencies can, however, be more or less overcome by using a "multiple sweep random technique", and an accelerated test procedure. The main advantages of the sweep random vibration test are:

1. A certain test level can be obtained by the use of much smaller power amplifiers and vibration exciters than if the test was carried out as a "normal" wide band random test.

2. The statistical character of the test signal is retained.

3. The setting-up and control of the test level is simpler and in many cases more accurate than in the case of wide band random testing.

4. It is possible to start with a simple system and add complexity as required.

The original method of setting up a sweep random vibration test consisted in adjusting the test parameters so that the same number of important stress reversals and acceleration peaks were produced at each level as is produced by a wide band test. For a long time the equipment necessary to perform this kind of testing was not commercially available and very little progress was thus made in the use of the method. In 1964, however, the complete control equipment required for sweep random vibration testing was developed and considerable effort has since been made to evaluate and extend the test.

A very important feature of the sweep random vibration test technique is the possibility it offers for "simple" automatic level regulation. The use of a narrow band of noise as test signal makes it possible to utilize a servo regulation technique which is similar to that used in the sweeping sine wave

204
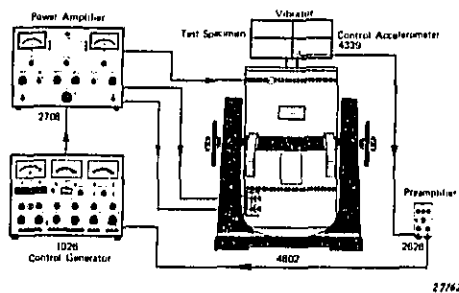
Fig.7.59. A typical sweep random vibration test arrangement using a
single narrow band unit only

test, Fig.7.59. Also the same programming facilities are available for the
sweep random test as for the sweeping sine wave test. This, together with
the trend in the later years to use a sweeping signal superimposed on a low
level wide band background vibration, seem to bring new aspects into the
sweep random test philosophy. Actually, *it is more natural to consider the
sweep random test as a separate type of testing which retains the simplicity
of a sweep test and which adds the feature of a statistically well defined
distribution of amplitude values* rather than trying to establish "equiva-
lence" with wide band tests. It is therefore suggested that sweep random
test specifications should be derived in much the same way as has been usual
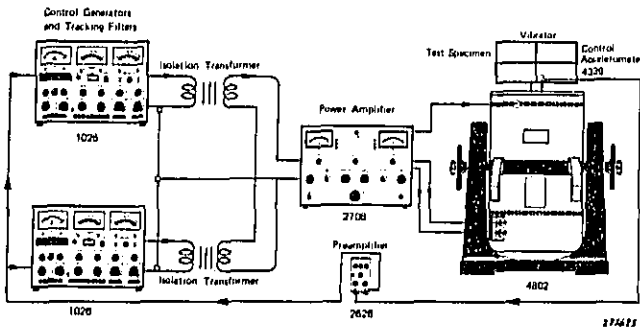
Fig.7.60. Example of a test arrangement suitable for multiple sweep
random testing

205

practice for sweep sine data i.e. directly from the measured or estimated vibration environment and not as previously made by "transforming" a wide band random test specification into an "equivalent" sweep random test.

Furthermore, it seems that one or more narrow bands of noise sweeping (or dwelling) according to more detailed test programmes and emphasizing various important frequency regions would be desirable and convenient. A possible measuring arrangement for this kind of testing is shown in Fig.7.60.

Here one narrow band noise generator with associated tracking filter, sweeps back and forth in one frequency region a second in another frequency region etc. The number of narrow band generators necessary to perform the proper test will then depend upon the number of important frequency regions. In the simple case only one generator is needed. The arrangement can then be extended to include more generators whenever required. In this way the capital investment required to perform adequate random vibration testing is reduced to a minimum and a very flexible test system is obtained.

Selected Bibliography

BOOTH, G.B.:   Random Motion. Product Engng. November 1956.

BOOTH, G.B.:   Random Motion Test Techniques. Proc. Inst. Env. Engrs. April 1958.

BOOTH, G.B.:   Sweep Random Vibration. Proc. Inst. Env. Sci. April 1960.

BOOTH, G.B. and BROCH, J.T.:   Analog Experiments Compare Improved Sweep Random Tests and Wide Band Random and Sweep Sine Tests. Shock and Vibr. Bull. 34, No. 5, and Brüel & Kjær Tech. Rev. No. 3-1965.

BOOTH, G.B.:   Interchangeable Head Vibration Exciters. Brüel & Kjær Tech. Rev. No. 2-1971.

BROCH, J.T.:   Automatic Level Regulation of Vibration Exciters. Brüel & Kjær Tech. Rev. No. 2-1958.

BROCH, J.T.:   Vibration Exciter Characteristics. Brüel & Kjær Tech. Rev. No. 3-1960.

BROCH, J.T.:   Non-Linear Amplitude Distortion in Vibrating Systems. Brüel & Kjær Tech. Rev. No. 4-1963.

BROCH, J.T.:   An Introduction to Sweep Random Vibration. Brüel & Kjær Tech. Rev. No. 2-1964.

BROCH, J.T.:   Some Aspects of Sweep Random Vibration. J. Sound Vibr. Vol. 3, No. 2. 1966.

BROCH, J.T.:   Some Experimental Tests with Sweep Random Vibration. Brüel & Kjær Tech. Rev. No. 2-1966.

BROCH, J.T.:   Vibration Testing — The Reasons and the Means. Brüel & Kjær Tech. Rev. No. 3-1967.

BROCH, J.T.:   Peak Distribution Effects in Random Load Fatigue. Brüel & Kjær Tech. Rev. No. 1-1968.

BROCH, J.T.:   On the Damaging Effects of Vibration. Brüel & Kjær Tech. Rev. No. 4-1968.

BROCH, J.T.:   Some Aspects of Vibration Testing. Proc. of Anglo Dutch Symposium on Environmental Engineering. Delft, April 1970.

CRANDALL, S.H. et al.:   Random Vibration. John Wiley and Sons, Inc. New York 1959.

CRANDALL, S.H. et al.:   Random Vibration II. MIT. Press, Cambridge, Mass. 1963.

CREDE, C.E. and LUNNEY, E.J.:   Establishment of Vibration and Shock Tests for Missile Electronics as Derived from the Measured Environment. WADC Tech. Report No. 56-503. ASTIA Doc. No. 1183. 1956.

GRANICK, W. and TOLLE, E.A.:   Simulated, Combined Vibration, Sustained Acceleration, and Extreme Temperature Environments. Noise Control. Vol. 7, No. 1-1961.

HALL, B.M. and WATERMAN, L.T.:   Correlation of Sinusoidal and Random Vibrations, Shock and Vibr. Bull. 29, Number 4, 1961.

KARTMAN, A.E.:   Empirical Prediction of Missile Flight Random Vibration, Shock and Vibr. Bull. 41, Part 2, 1970.

LUEBKE, R.W.:   The Box Car Dynamic Environment. Shock and Vibr. Bull. 41, Part 2, 1970.

MAHAFFEY, P.T. and SMITH, K.W.:   Methods for Predicting Environmental Levels in Jet Powered Vehicles. Noise Control. Vol. 6, No. 4, 1960.

IEC: Vibration Test for Electronic Equipments and Components. Recommendation Publication 68-2-6. Test F: Vibration.

JACKMAN, K.R.:   Cross-Axis Vibration Test Facility Evaluation. General Dynamics, Pomona Division, 1967.

MONROE, J.:   A Problem of Sinusoidal vs. Random Vibration. Proc. Inst. Env. Sci. April 1961.

MORROW, C.T. and MUCHMORE, R.B.:   Shortcomings of Present Methods of Measuring and Simulating Vibration Environments. J. Appl. Mech. 1955.

MORROW, C.T.:   Should Acoustic Noise Testing of Missile Equipment Be Made Routine? Noise Control. Vol. 5, No. 4, 1959.

MORROW, C.T.:   Application of the Mechanical Impedance Concept to Shock and Vibration Testing. Noise Control. Vol. 6, No. 4, 1960.

MORROW, C.T.:   Significance of Power Spectra and Probability Distributions in Connection with Vibration. Noise Control. Vol. 6, No. 5-1960.

MORROW, C.T.:   Shock and Vibration Engineering. John Wiley and Sons, Inc. 1963.

MØLLER PETERSEN, P.E.:   Problems in Feedback Control of Narrow Band Random Noise. Brüel & Kjær Tech. Rev. No. 4-1962.

OLESON, M.W.:	A Narrow Band Vibration Test. Shock and Vibr. Bull. 25, No. 1, 1957.
OTTS, J.V.:	Methods Used to Realistically Simulate Vibration Environments. Shock and Vibr. Bull. 41. Part 2. 1970.
PIERSOL, A.G.:	Generation of Vibration Test Specifications. Measurement Analysis Corp. 1965.
PIERSOL, A.G.:	Investigation of Statistical Techniques to Select Optimal Test Levels for Spacecraft Vibration Tests. Report 10909801 — F, Digitek Corporation, Marina del Rey, California. October 1970.
REGIER, A.A. and HUBBARD, H.H.:	Response of Structures to High Intensity Noise Noise Control. Vol. 5, No. 5. 1959.
SMITH, P.W. Jr.:	Sound-Induced Vibration. Noise Control. Vol. 4. No. 6. 1958.
SPENCE, H.R.:	Random-sine Vibration Equivalence Tests on Missile Electronic Equipment. Proc. Inst. Env. Sci. April 1960.
TROTTER, W.D.:	An Experimental Evaluation of Sinusoidal Substitutes for Random Vibration. Shock and Vibr. Bull. 29. No. 4. 1961.
TRULL, R.V.:	Sweep Speed Effects in Resonant Systems. Shock and Vibr. Bull. 41. Part 2. 1970.
USHER, TH. Jr.:	AEROS: A Generalized Vibration Control System. Brüel & Kjær Tech. Rev. No. 2-1971.
WITTE, A.F.:	Specification of Sine Vibration Test Levels Using A Force-acceleration Product Technique. Shock and Vibr. Bull. 41. Part 2. 1970.
WITTE, A.F.:	Dual Specifications in Random Vibration Testing, an Application of Mechanical Impedance. Shock and Vibr. Bull. 41. Part 2. 1970.

7.4. Shock Testing

The basic philosophy behind shock testing of delicate equipment is essentially the same as that underlying vibration qualification testing: to ensure that the tested equipment will operate satisfactorily under estimated practical shock environments. Nearly all equipment experience some sort of shock in practice in the form of handling and transportation shocks, — and some equipment, mounted in vehicles, may be exposed to a great variety of shock conditions during operation.

It is clear that to try and duplicate exactly in a test the actual shock environment to be expected in practice would only be possible in a few, selected cases. Shock testing therefore in general try to ensure that the *effects* of the test shock upon the equipment are similar to the effects of the shock(s) occurring in practice, rather than utilizing an exact duplication of any particular service shock.

In the course of time various shock test machines have been developed which allow certain shock effects to be produced and, which is very impor- tant, furnish *completely reproducible results.* The latter is of prime impor- tance in judging the results from tests made at various institutions, and in comparing the shock "resistivity" of various equipment designs.

Different methods may be used to specify a shock test: It may be specified in terms of the acceleration vs. time trace of the shock pulse (IEC Recommendation 68 — 2 — 27), it may be specified in terms of a shock (response) spectrum[*]) or it may be specified in terms of the type (possible also manufacture) of the shock test machine to be used.

The specification in terms of an acceleration vs. time trace also requires the specification of rather strict tolerances on the pulse shape, as well as tolerances on the total velocity change produced by the pulse (time integral of the acceleration pulse trace). Fig.7.61 shows the preferred pulse shapes recommended by the I.E.C. (International Electrotechnical Commission) together with the specified tolerances. One of the major reasons why prefer- ence is given to the pulse-shapes shown in Fig.7.61 is that they produce relatively flat overall (maximax) shock spectra.

In specifying a shock test certain requirements are normally also laid down with regard to mounting of the test specimen onto the shock machine, the maximum transverse motion to be allowed during testing ($<$30% of the

---

*) See Section 3.5.

Reference line corresponding
to pre-pulse conditions

1.15 A
A
0.85 A
0.2 A
-0.2 A
0.1 D
0.4 D
D
D
T

Reference line corresponding
to pre-pulse conditions

1.15 A
A
0.85 A
+0.15 A
+0.15 A
0.2 A
-0.2 A
0.4 D
D
D
T

Reference line corresponding
to pre-pulse conditions

1.2 A
A
0.8 A
0.2 A
-0.2 A
0.1 D
0.1 D
D
D
0.4 D
T

T = Minimum time during which the pulse should be monitored
D = Duration of nominal pulse
A = Peak acceleration of nominal pulse

– – – Nominal pulse ———— Tolerance boundaries

Fig.7.61.   I.E.C. preferred pulse shapes for shock testing

nominal peak value), and the number of test shocks to be applied in each
direction of three mutually perpendicular axes.

Furthermore, the frequency characteristic of the measuring and monitor-
ing equipment must be linear over a relatively wide frequency range to
ensure correct phase relationship between the various frequency com-
ponents of the measured pulse, see Fig.7.62 (I.E.C.).
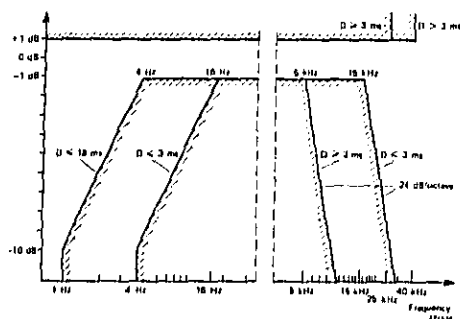
Fig.7.62.   Frequency characteristics required from shock measurement
           systems (I.E.C.)

It was mentioned above that the acceleration versus time trace of the test
pulse was subject to rather strict tolerances. This is due to the fact that very
often in practical testing a certain ripple (caused for instance by undesirable
resonance effects in the shock machine and test fixture) is super-imposed
upon the test pulse, Fig.7.63. Even if the ripple may look relatively
insignificant when studying the pulse shape itself, it may cause a very
significant change in the shock response spectrum related to the pulse,
Fig.7.64. As the shock spectrum provides an efficient measure of the
damage potential of the shock motion the ripple may actually invalidate the
test results!

From a technical point of view it therefore seems more appropriate to
specify shock tests on the basis of shock spectra rather than on the basis of
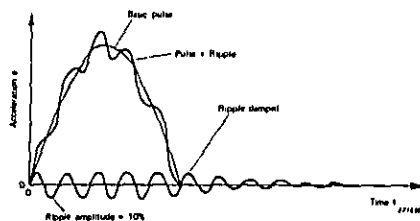
Fig.7.63.   Example of a shock pulse upon which a certain amount of
           ripple (10%) is superimposed

212
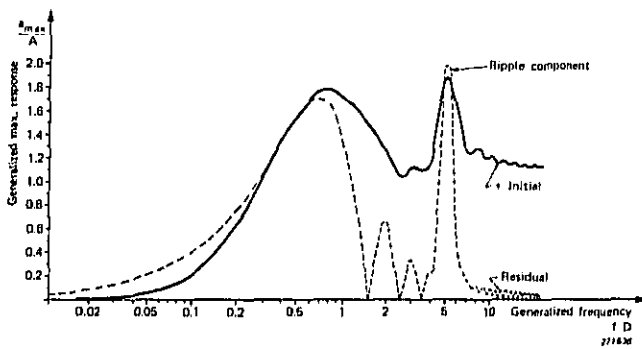
Fig.7.64. Shock response spectrum of the pulse shown in Fig.7.63. Note the effect of the 460 Hz ripple component

test pulse shapes. On the other hand, because a certain overall shock spectrum may be produced by a variety of shock pulse shapes, there is no single unique time function associated with a specified shock spectrum. Damage due to the accumulation of stress cycles (mechanical fatigue) *may* therefore differ between two tests even if the shock spectrum was the same in both tests. However, the *peak* acceleration levels and the *peak* stress levels of the equipment resonance responses will usually be approximately the same in the two cases. As a shock test is normally applied to test the *"resistivity"* of an equipment *against short duration peak stresses and accelerations,* the shock spectrum method of specifying the test still seems to be superior to the acceleration versus time method of specification.

An interesting, practical aspect of specifying a shock test in terms of its shock spectrum has appeared in recent years in that this kind of testing may be advantageously performed by means of ordinary electrodynamic vibration exciters combined with special electronic control equipment. Fig.7.65 shows an example of such an arrangement utilizing a set of 1/3 octave shock spectrum shaping filters. Here a short duration impulse from the pulse generator ("unit" impulse) excites a bank of 1/3 octave filters simultaneously. The time function of the summed output from the filters then looks somewhat like the time trace shown in Fig.7.66a). If this time function is analyzed by a damped shock spectrum analyzer the response at a particular analyzer frequency has a shape as recorded in Fig.7.66b). One of the essential features of this type of testing can be seen from Fig.7.66 in that

213
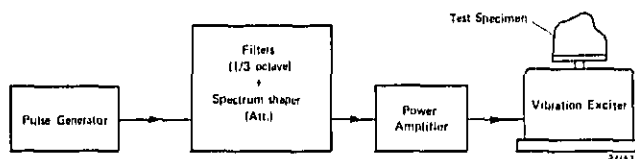
Fig.7.65. *Block diagram of a 1/3 Octave shock spectrum synthesis system*

the peak shock response, Fig.7.66b), is here roughly five times larger than
the peak of the exciting transient, Fig.7.66a). Thus to produce a certain
shock response in a test specimen a considerable lower "input" force is
required by the test method, Fig.7.65, than is the case when testing is
performed with a more conventional type of shock test machine. Physically
this is due to the fact that the "input" to the test specimen from the
vibration exciter (Fig.7.65) takes the form of an oscillating transient while
the "input" from a conventional shock machine normally consists of a
single impulse.
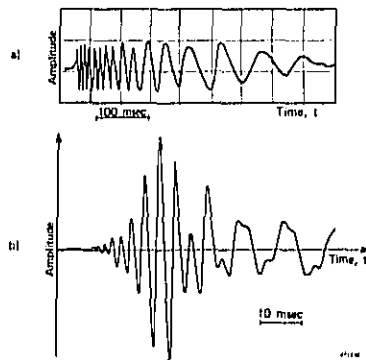
Fig.7.66. *Time function of a 1/3 octave synthesized shock*
a) Overall vibration table motion (summed output from the 1/3
octave filter bank of Fig.7.65)
b) Shock spectrum analyzer (narrow band) output of the signal
shown in a)

214

A further argument in favour of the above technique is that *most shock motions observed in service have waveforms that are generally oscillatory in character.* Also, their Fourier spectra are distributed over a reasonably wide range of frequencies. Quite possibly these observed shocks are the result of simpler shock waveforms having undergone time-spreading and general spectral filtering by being transmitted through complex structures and/or dispersive media. It still remains true, however, that simple shock motions of the kind shown in Fig.7.61, occur only rarely in practice, if ever, at the mounting points of an equipment.

The kind of shock vibration testing discussed above is commonly termed *shock synthesis.* Although the system shown in Fig.7.65, which was used to illustrate the features of the shock synthesis test, consists of a set of manual-ly adjustable 1/3 octave filters, it is not very suitable for practical testing purposes.

Firstly, the bandwidth of the filters of 1/3 octave (23%) is far too wide to provide adequate equalization for narrow-band test specimen resonances. Actually, the equalization requirements for a shock synthesis test are just as severe as those for random vibration testing (see section 7.3c).

Secondly, the manual adjustment of the filter channels is, also in this case, prohibitively time consuming.

These draw-backs have been eliminated in the Booth, Brüel & Kjær auto-matic equalizer system mentioned in section 7.3c. Here special electronic
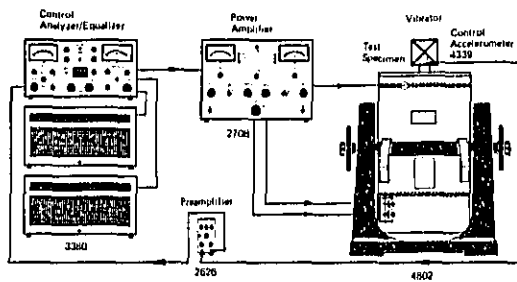
Fig.7.67.   Example of a narrow band shock spectrum synthesis system with automatic spectrum equalization in 120 channels (Brüel & Kjær)

215

circuitry has been incorporated in the instrumentation so as to also allow adequate shock synthesis testing, with automatic spectrum equalization, to be performed. While earlier the use of two different electronic control systems were necessary to carry out random and shock vibration testing with the same power amplifier and vibration exciter, this is no longer so, see Fig.7.67 (and 7.55).

Oscillatory shock motions, such as described above, are often termed *complex shocks.* While the possibility of producing a large variety of complex shocks is offered by a shock synthesis system, some "simpler" machines do exist which produce specific complex shocks. These are in general, designed according to the pendulum principle shown in Fig.7.68a). Fig.7.68b) shows a typical acceleration versus time trace of the impulse delivered by such a machine.
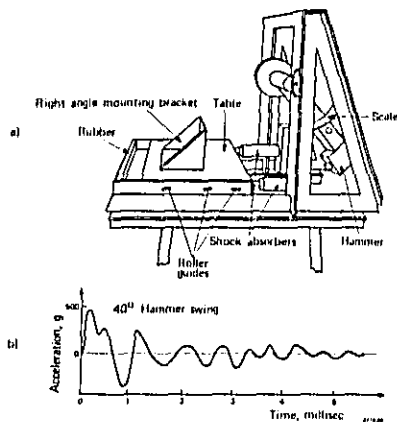
Fig.7.68. Shock testing by means of a pendulum type shock machine
a) Sketch of the machine
b) Typical acceleration versus time trace produced by the machine

Finally some typical designs used in conventional shock machines should be briefly mentioned. The simplest of these machines may be the so-called drop-test machine, Fig.7.69. Here the test specimen is bolted onto a carriage

216
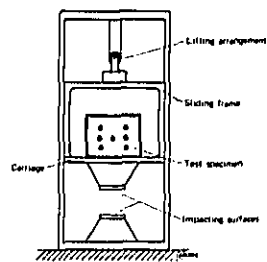
Fig.7.69.   Sketch of a drop test machine

which is dropped from a certain height. The shape of the shock pulse is
mainly determined by the properties of the material upon which the
carriages falls, or rather upon *the material and shape of the impacting
surfaces.* Shock pulses with magnitudes up to 80,000 g have been obtained
by this method. Further types of single pulse shock testing machines utilize
hydraulic or *pneumatic* principles and their operation do not depend upon
gravity for production of the desired shock force. The basic operation of a
machine built on pneumatic principles is sketched in Fig.7.70. By letting air
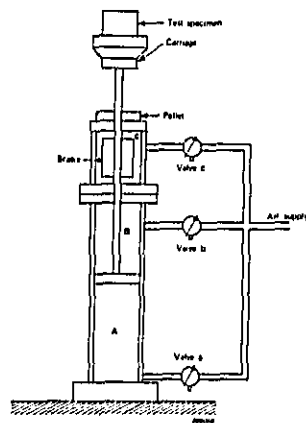
Fig.7.70.   Principle of operation of a pneumatic shock test machine

217

into the cylinder, A, through the valve, a, the carriage containing the test specimen is lifted. When it has reached a certain height the brakes are activated through the valve, c, and clamp the carriage in position. Air is now ·forced into cylinder, B, through valve, b, until a substantial overpressure has been built up in, B. The air pressure in cylinder, A, is then released via valve, a. By releasing the brakes the carriage is forced downwards due to the overpressure in cylinder, B, until it hits the pellet. The shape and material of the pellet controls the waveform of the shock pulse. Normally, the brakes are again actuated immediately after the impact so that rebouncing of the carriage, and thereby distortion of the shock pulse does not take place.

Selected Bibliography

ASTM: Symposium on Impact Testing. Special Technical Report, American Society for Testing and Materials. 1916 – 1918 Race Street, Philadelphia, Pa. 19103.

BELSHEIM, R.O.:   Response Motions of a Submarine – like Cylinder Caused by Underwater Explosions. Noise Control, Vol. 6, No. 2-1960.

BROOKS, G.W. and CARDEN, H.D.:   A Versatile Drop Test Procedure for the Simulation of Impact Environments. Noise Control, Vol. 7, No. 5-1961.

CREDE, C.E.:   Criteria of Damage from Shock and Vibration. Shock, Vibration and Associated Environments, Bulletin 25, 1957. Part 2.

FRANKLAND, J.M.:   Effects of Impact on simple Elastic Structures. Proceedings of the SESA, Vol. 6, No. 2-1949.

GOLDBERG, A.:   Shock Studies for Fire Control Material Response Analysis of the Jan – S – 44 Type Shock Test Machine. Frankfort Arsenal Report R–1169. August 1954.

IEC: Basic Environmental Testing Procedures for Electronic Components and Electronic Equipment. Recommendation Publication 68 – 2 – 27. Test Ea: Shock.

218

IEC:

Basic Environmental Testing Procedures for Electronic Components and Electronic Equipment. Recommendation Publication 68 – 2 – 27 Eb: Bump.

JACOBSEN, L.S. and AYRE, R.S.:

A Comparative Study of Pulse and Step-Type Loads on a Simple Vibratory System. Technical Report 16, Structural Dynamics, Contract N6 – ORI 154, Task 1, Stanford University, 1952.

JACOBSEN, L.S. and AYRE, R.S.:

Engineering Vibrations. McGraw-Hill Book Company, Inc. 1958.

JORDAN, J.C.:

Shock Response Spectrum Synthesis and Analysis. Proc. of the Inst. of Environmental Sciences 1967.

KEEFFE, R. E. and BATHKE, E.A.:

Shock Pulse Shaping Using Drop Test Techniques. Shock and Vibr. Bull. No. 41, Part 5, 1970.

KITTELSEN, K.E.:

Measurement and Description of Shock. Brüel & Kjær Tech. Rev. No. 3-1966.

LEVENSON, M. and SUSSHOLZ, B.:

The Response of a System with a Single Degree of Freedom to a Blast Load, Taylor Model Basin Report No. 572. 1947.

McGRATH, M.B.:

A Discussion of Pyrotechnic Shock Criteria. Shock and Vibr. Bull. No. 41, Part 5, 1970.

METZGAR, K.J.:

Test Oriented Appraisal of Shock Spectrum Analysis and Synthesis. Proc. of the Inst. of Environmental Sciences 1967.

MORROW, C.T. and SARGEANT, H.I.:

Sawtooth Shock as a Component Test. J.A.S.A. Vol. 28, No. 5. September 1956.

MORROW, C.T.:

The Shock Spectrum as a Criterion of Severity of Shock Impulses. J.A.S.A. Vol. 29, No. 5. May 1957.

MORROW, C.T.:

The Shock Spectrum – A Means of Stating

	Mechanical Shock Requirements. Electrical Manufacturing. Vol. 64. No. 2. August 1959.
MORROW, C.T.:	Shock and Vibration Engineering. John Wiley and Sons, Inc. New York 1963.
MORROW, C.T.:	Measures of Blast Wave Damage Potential. Shock and Vibr. Bull. No. 41. Part 5. 1970.
PAINTER, G.W. and PARRY, H.J.:	Simulating Flight Environment Shock on an Electrodynamic Shaker. Shock, Vibrations and Associated Environment. Bulletin 33. Part 3. 1964.
SPANG, K.:	The Advantages of Using Initial Sawtooth Pulse Shapes in Shock Testing. Environmental Engineering No. 23 1966.
USHER, TH. Jr.:	AEROS: A Generalized Vibration Control System. Brüel & Kjær Tech. Rev. No. 2-1971.
VIGNESS, I.:	Some Characteristics of Navy "High Impact" Type Shock Machines. Proceedings of the SESA, Vol. 5, No. 1, 1947.
VIGNESS, I.:	The Fundamental Nature of Shock and Vibration. Electrical Manufacturing. June 1959.
VIGNESS, I.:	Navy High-Impact Shock Machines for Lightweight and Mediumweight Equipment. NRL Report 5618. U.S. Naval Research Laboratory. June 1961.
VIGNESS, I.:	Elementary Considerations of Shock Spectra. Shock, Vibrations and Associated Environments. Bulletin 34, 1965, Part 3.

7.5. Balancing of Rotating Machines

In Chapter 4, section 4.2 it was stated that unbalance in rotating machinery may be of basically two different kinds: "Static" unbalance (in one plane), and "dynamic" unbalance (in two or more planes).

220

While the simple cases of static unbalance could be corrected by placing the stationary disc with its axis of rotation horizontally, and adding weight "on top" of the disc until it is brought into indifferent equilibrium, dynamic balancing requires that the rotor (disc) rotates.

It should be noted, however, that the above described method of static balancing will only work when the rotor consists of a rigid disc, mounted on a rigid axle (or the disc during normal operation is rotating at a speed far below the critical speed*) of the disc-axis-bearing system), and the axle moves in frictionless bearings.

If the speed of rotation is not far below the critical, the original residual unbalance will cause a still further displacement of the center of gravity away from the center of rotation, and the relationship between the centrifugal forces of the unbalance and those required for balance becomes (see also Fig.7.71b).

$$\omega^2 M (e + \delta) = \omega^2 m' \times r$$

Thus:

$$m' \times r = M (e + \delta)$$

where m' is the correction weight (balancing mass) required.
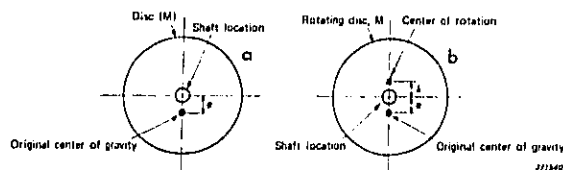
Fig.7.71.   Example of a disc mounted on a flexible axis and rotating at a speed not too far from the "critical" speed

One method of determining the size and position of m' is in this case to use a Motion Analyzer Type 4911 in combination with normal vibration measuring equipment, see Fig.7.72. The accelerometer is here placed on (or near) the bearing and the frequency analyzer is set to a frequency corresponding to the speed of rotation of the disc (grinding machine).

---

*) Critical speed = first resonant frequency of the disc-axis-bearing system.

221
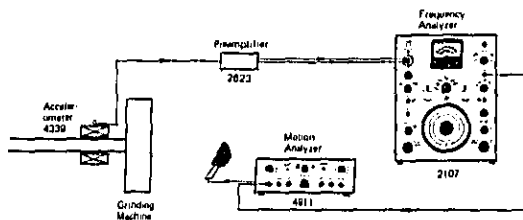
Fig. 7.72. Measuring arrangement utilizing a Motion Analyzer (strobo-
scope) Type 4911 and the Frequency Analyzer Type 2107 for
determination of unbalance during operation of a grinding
machine
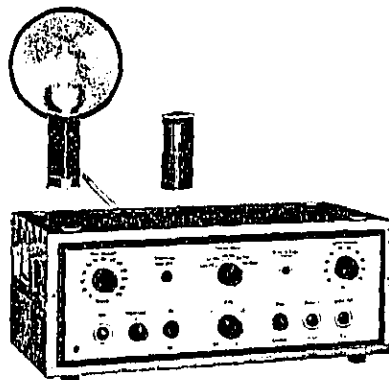
Fig. 7.73. Photograph of the Brüel & Kjær Motion Analyzer Type 4911

The output from the frequency analyzer is used to trigger the Motion
Analyzer ensuring a reasonably clean triggering waveform. At the same time
the vibration signal caused by the unbalance can be read off the frequency
analyzer indicating meter.

Before starting the test reference marks should be set on the rotor as well
as on the stator, Fig.7.74a). When the machine is running at the desired

222
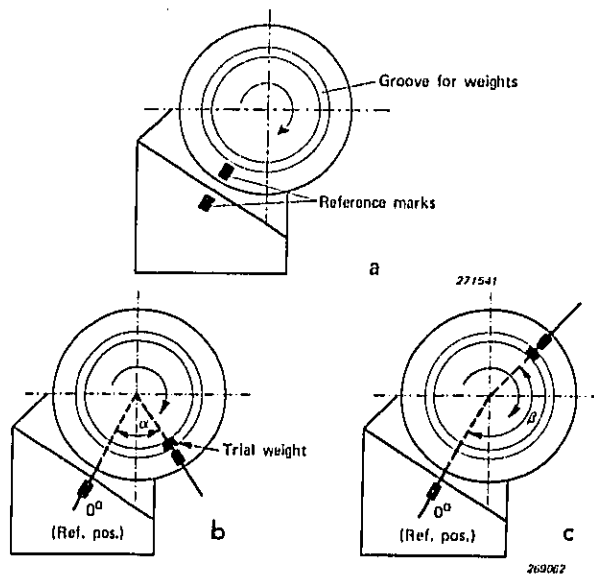
Fig.7.74. Method of unbalance determination utilizing the arrangement
shown in Fig.7.72
a) Marking of the stator as well as the rotor of the machine
b) Stroboscopic picture of the mark on the rotating machine
c) Stroboscopic picture of the rotating machine with the trial
weight in position

speed the mark on the rotor appears stationary under the stroboscopic light
from the Motion Analyzer but will normally not be positioned directly
opposite to the original mark on the stator, Fig.7.74b). Both the angle, α in
Fig.7.74b) and the meter reading, a, on the frequency analyzer should be
noted. (The angle, α can be found directly in degrees by utilizing the phase
control knob of the Motion Analyzer).

The machine is then stopped and a trial weight of known mass, m_x, is
fixed to the rotor at the angular position of the rotor reference mark.

Repeating the above procedure with the machine running at the same

speed as before and the trial weight in position, the reading on the frequency analyzer will be, b, and the new angular position of the rotor mark is, β, Fig.7.74c). It is now possible to construct a vector diagram, Fig.7.75, from which both the required amount and the location of the proper correction mass can be deduced. In the vector diagram the length of the vector v_1 is arbitrary, and so is its direction. However the length *represents* the meter reading, a, as shown. The vector, v_2 is then drawn at an angle, $\beta - \alpha$, from

the direction of v_1, and its length is $\dfrac{b}{a}$ x v_1.
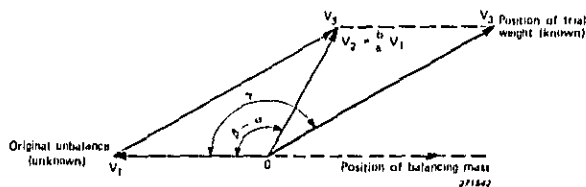
Fig.7.75. Vector diagram illustrating how both the magnitude and the direction of the original unbalance during operation can be found

These two vectors (v_1 and v_2) represent the original unbalance force vector (v_1) and the combined original plus trial weight unbalance force vector (v_2). The *difference* in unbalancing force obtained by introducing the trial weight, m_x, is given by the vector, v_3. Since both the weight, m_x, causing the difference in unbalance between the two tests, and the direction of the difference force vector, v_3, are known, the magnitude and the direction of the original unbalance can be found: Its direction must be at an angle, γ, away from the actual position of the trial weight, Fig.7.76, and its magnitude can be represented by a mass, $M = \dfrac{v_1}{v_3}$ x m_x, located the same distance away from the center of rotation of the rotor as the mass, m_x. By utilizing the relationship between unbalancing and balancing centrifugal forces stated in Chapter 4 section 4.2 (m x r = M x e) it is possible to place the amount of correction weight necessary to obtain proper balance at its correct location.

Usually the application of the above described procedure once only is not sufficient to obtain complete balance, due to non-linearities and

224

Trial weight.

Direction of
original
unbalance
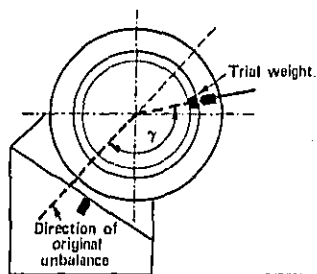
269061

Fig.7.76.   Sketch illustrating how the direction of the original unbalance is
found on the machine

inaccuracies in the practical test arrangement. It is therefore often necessary
to repeat the procedure (adjust the correction weight and its position) until
an acceptable level of balance is reached.

A second method of balancing the disc, which only requires the use of a
"simple" Vibration Meter Type 2510, Fig.7.77, is described below. This
method does, however, require four test runs of the disc. In three of the test
runs an experimental test weight is attached. To illustrate the use of the
method consider Fig.7.78. In Fig.7.78a) an x-y-coordinate system has been
laid out perpendicular to the axis of rotation of the disc, and Fig.7.78b)
shows the same coordinate system with the positions of the test weight
indicated by circles. The length of the vectors, Fig.7.78b), represent the
magnitudes of the measured vibrations, and the angles represent their
mutual phase relationships.

Accelerometer 4338   Vibration Meter

Bearing   2510

271671
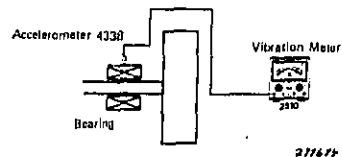
Fig.7.77.   Example of a "simple" balancing arrangement

225

The vibration vectors are produced by the following unbalances:

Vector $\vec{U}$:   Original unbalance.

Vector $\vec{M}_1$:   Unbalance resulting from mounting the test weight "m_x" on a radius "r" in position 1.

Vector $\vec{M}_2$:   Unbalance resulting from mounting the test weight "m_x" on radius "r" in position 2.

Vector $\vec{M}_3$:   Unbalance resulting from mounting the test weight "m_x" on radius "r" in position 3.

Vector $\vec{A}$:   Resultant unbalance of $\vec{U}$ and $\vec{M}$
$$\vec{A} = \vec{U} + \vec{M}_1$$

Vector $\vec{B}$: $\vec{B} = \vec{U} + \vec{M}_2$

Vector $\vec{C}$: $\vec{C} = \vec{U} + \vec{M}_3$

Vector $\vec{D}$:   The calculated balance.

By first running the disc without the test weight the *magnitude* of the original unbalance ($|$vector $\vec{U}|$) can be found. The locus of the endpoint of

(a)   (b)
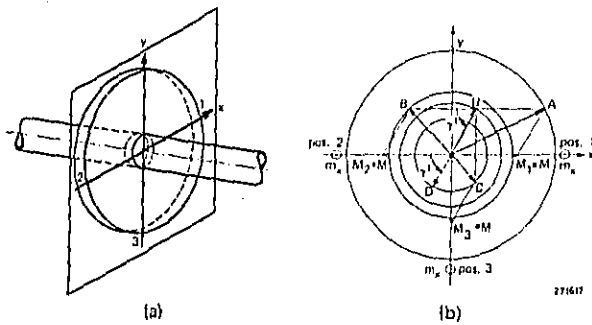
Fig.7.78.   *Graphical analysis of the results obtained by measurements carried out by means of the arrangement shown in Fig.7.77*
a) Position of the hypothetical coordinate system
b) Vectorial representation of the measured vibration levels

226

this vector must be a circle around zero with radius equal to the magnitude value of $|\vec{U}|$.

A second run of the disc is then made with the test weight, m_x, mounted in an unspecified position on the disc at a distance, r, from the center of rotation (position 1, Fig.7.78b)).

The addition of the test weight to the disc will in itself produce an unbalance, $\vec{M}_1$.

By means of this test run the magnitude of the unbalance produced by a combination of the original unbalance and that caused by the test weight, m_x, can be determined, i.e. the magnitude of the vector $\vec{A}$.

Before a third test run is made the test weight, m_x, is moved to a position 180° relative to its first position, and at the same distance, r, away from the center of rotation (position 2, Fig.7.78b)). This will cause the same amount of additional unbalance $|\vec{M}_2|$, to the disc, i.e.:

$$|\vec{M}_2| = |\vec{M}_1| = |\vec{M}|$$

and a resultant unbalance magnitude equal to the magnitude of the vector $|\vec{B}| = (|\vec{M}_2 + \vec{U}|)$ is measured.

From Fig.7.78b) the following relationships can now be deduced:

$$B^2 = M^2 + U^2 - 2 MU \cos (\gamma')$$

$$A^2 = M^2 + U^2 + 2 MU \cos (\gamma')$$

where γ' is the angle between the horizontal axis of the coordinate system and the balance vector, $\vec{D}$.

Thus:
$$M = \sqrt{\frac{A^2 + B^2 - 2 U^2}{2}}$$

and
$$\cos (\gamma') = \frac{A^2 - B^2}{4 \, MU}$$

As $\cos (\gamma') = \cos (-\gamma')$ it is not immediately evident whether the vector D is located below or above the x-axis (connection line between test weight position 1 and test weight position 2). It is therefore, in general, necessary to undertake a fourth measurement with the test weight attached at position 3 (Fig.7.78b)).

227

The result of this measurement will be the magnitude of the vector $|\vec{C}|$.

Then if $C^2 < M^2 + U^2 \, \gamma'$ lies *below* the x-axis, while if $C^2 > M^2 + U^2 \, \gamma'$ lies *above* the x-axis.

Finally, if the balancing weight, m, is placed at the same distance, r, from the center of rotation of the disc as was the test weight, the necessary weight for proper balancing can be determined from the relationship:

$$m = \frac{|\vec{U}|}{|\vec{M}|} \, m_x$$

The methods described above may be used for balancing in one plane, i.e. for the balancing of rigid disc types of rotors. If the rotor consists of an elongated rigid body, such as the one shown in Fig.7.79 *dynamic* unbalance may be present (see also Chapter 4, section 4.2). In this case it is then not sufficient to carry out the balancing in one plane only, and balancing is normally done in two planes (I, II) as indicated in Fig.7.80.

Bearing   Bearing

Rigid Rotor   271618
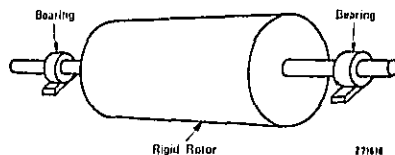
Fig.7.79.   Example of an elongated, rigid rotor in its bearings

Special dynamic balancing machines (centrifugal balancing machines) have been developed for the purpose. When using these machines, however, the rotor to be balanced has to be placed in the balancing machine, and the machine operated according to prescribed procedures.

If it is not possible to disconnect the rotor and place it in a proper balancing machine, or if it is desirable to balance the rotor in its own bearings, field balancing in two planes may be carried out according to the following procedure.

Using a measuring arrangement of the type shown in Fig.7.72, and making three test runs at the nominal operating speed of the machine (rotor), the magnitudes and locations of the correction masses can be determined.

228
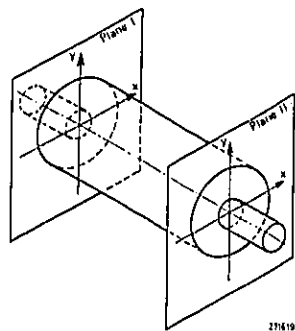
Fig. 7.80.   *Sketch indicating the two balancing planes with the correspond-ing hypothetical coordinate systems*

During each test run, measurements are made of the vibration level (at the bearings) and the angle of maximum vibration level, referred to a reference mark on the rotor, is found. The results are plotted in the form of vectors in the two planes of balancing. Note that the phase angles are marked out *clockwise* from the x-axis (Figs. 7.81 and 7.82).

The test runs are made in accordance with the scheme tabulated below.

Test Run	Test Mass Position		Notation of Vibration Vectors	
	Plane I	Plane II	Plane I	Plane II
0	—	—	$\vec{M}_{1,0} : M_{1,0} ; \angle \gamma_{1,0}$	$\vec{M}_{2,0} ; M_{2,0} ; \angle \gamma_{2,0}$
1	$\vec{R}_1 ; R_1 : \angle r_1$	—	$\vec{M}_{1,1} : M_{1,1} ; \angle \gamma_{1,1}$	$\vec{M}_{2,1} ; M_{2,1} ; \angle \gamma_{2,1}$
2	—	$\vec{R}_2 ; R_2 ; \angle r_2$	$\vec{M}_{1,2} : M_{1,2} ; \angle \gamma_{1,2}$	$\vec{M}_{2,2} ; M_{2,2} ; \angle \gamma_{2,2}$

In run 0 the vibration vectors $\vec{M}_{1,0}$ (in plane I) and $\vec{M}_{2,0}$ (in plane II) are found with no test mass attached to the rotor:

$\vec{M}_{1,0}$: Vibration level $M_{1,0}$; phase angle $\angle \gamma_{1,0}$

$\vec{M}_{2,0}$: Vibration level $M_{2,0}$; phase angle $\angle \gamma_{2,0}$

229
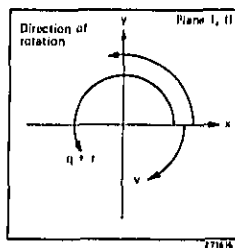
Fig.7.81. *Sketch indicating the directions in which phase angles are drawn in the described balancing procedure*

In run 1 a test mass, m_x, is mounted on the rotor end I (plane I) at radius R_1 and phase angle $\angle r_1$ (re. reference mark). Again the vibration vectors are determined in both balancing planes.

In run 2 the same test mass, m_x, is mounted on the rotor end II (plane II) at radius R_2 and phase angle $\angle r_2$, and the vibration vectors determined as before.

The above scheme is then completed, and the results are illustrated graphically in Fig.7.82.

It can, furthermore, be seen that:

$\vec{M}_{1,1} - \vec{M}_{1,0}$: Effect of m_x at rotor end I in plane I

$\vec{M}_{2,1} - \vec{M}_{2,0}$: Effect of m_x at rotor end I in plane II

$\vec{M}_{1,2} - \vec{M}_{1,0}$: Effect of m_x at rotor end I in plane I

$\vec{M}_{2,2} - \vec{M}_{2,0}$: Effect of m_x at rotor end II in plane II

To properly balance the rotor weights should be added at both rotor ends so that they produce vibration vectors which are equal in magnitude to $|\vec{M}_{1,0}|$ and $|\vec{M}_{2,0}|$, respectively, but point in the opposite directions of $\vec{M}_{1,0}$ and $\vec{M}_{2,0}$.

In mathematical terms the problem consists of finding two vector operators $\vec{Q}_1 : Q_1 ; \angle q_1$ and $\vec{Q}_2 : Q_2 ; \angle q_2$

230
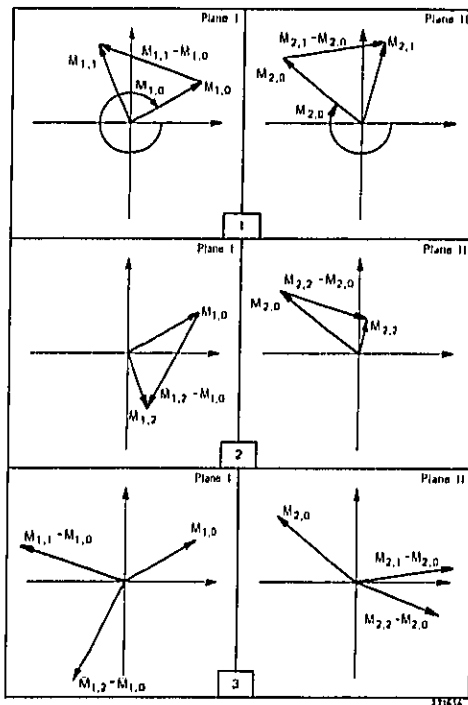
Fig. 7.82.   Vectorial representation of the vibration levels

which satisfy the equations:

$$(\vec{M}_{1,1} - \vec{M}_{1,0}) \times \vec{Q}_1 + (\vec{M}_{1,2} - \vec{M}_{1,0}) \times \vec{Q}_2 = -\vec{M}_{1,0}$$

$$(\vec{M}_{2,1} - \vec{M}_{2,0}) \times \vec{Q}_1 + (\vec{M}_{2,2} - \vec{M}_{2,0}) \times \vec{Q}_2 = -\vec{M}_{2,0}$$

A computer program in BASIC language, which will give the values of Q_1; $\angle q_1$ and Q_2; $\angle q_2$ is shown in Fig. 7.83.

```
LIST
DYNBAL    10:06    KBH MA 01/06/70

10 DIM C (2, 2), D (2, 2), E (2, 2), F (2, 2), G (2, 2), H (2, 2), I (2, 2), J (2, 2)
12 DIM K (2, 2), L (2, 2), M (2, 2), N (2, 2), O (2, 2), P (2, 2), Q (2, 2), R (2, 2)
14 DIM S (2, 2), T (2, 2), U (2, 2), V (2, 2), X (2, 2)
20 FOR Y = 1 TO 6
30 READ A (Y), B (Y)
40 NEXT Y
50 LET C (1, 1) = A (1) * COS (B (1)/57)
60 LET C (1, 2) = A (1) * SIN (B (1)/57)
62 LET C (2, 1) = C (1, 2)
65 LET C (2, 2) = C (1, 1)
70 LET D (1, 1) = A (2) * COS (B (2)/57)
75 LET D (1, 2) = A (2) * SIN (B (2)/57)
80 LET D (2, 1) = -D (1, 2)
85 LET D (2, 2) = D (1, 1)
90 LET E (1, 1) = A (3) * COS (B (3)/57)
95 LET E (1, 2) = A (3) * SIN (B (3)/57)
100 LET E (2, 1) = -E (1, 2)
105 LET E (2, 2) = E (1, 1)
110 LET F (1, 1) = A (4) * COS (B (4)/57)
115 LET F (1, 2) = A (4) * SIN (B (4)/57)
120 LET F (2, 1) = -F (1, 2)
125 LET F (2, 2) = F (1, 1)
130 LET G (1, 1) = A (5) * COS (B (5)/57)
135 LET G (1, 2) = A (5) * SIN (B (5)/57)
140 LET G (2, 1) = -G (1, 2)
145 LET G (2, 2) = G (1, 1)
150 LET H (1, 1) = A (6) * COS (B (6)/57)
155 LET H (1, 2) = A (6) * SIN (B (6)/57)
160 LET H (2, 1) = -H (1, 2)
165 LET H (2, 2) = H (1, 1)
200 MAT I = E - C
205 MAT J = F - D
210 MAT K = G - C
215 MAT L = F - D
220 MAT M = H - D
225 MAT N = E - C
230 MAT O = D * I
235 MAT P = C * J
240 MAT Q = K * L
245 MAT R = M * N
250 MAT S = O - P
255 MAT T = Q - R
260 MAT U = INV (T)
265 MAT V = S * U
270 MAT I = C * M
275 MAT J = D * K
280 MAT K = I - J
285 MAT X = K * U
290 LET Y1 = SQR (V (1, 1) ↑ 2 + V (1, 2) ↑ 2)
300 LET Y2 = SQR (X (1, 1) ↑ 2 + X (1, 2) ↑ 2)
310 IF V (1, 1) < 0 THEN 340
320 LET Y3 = 0
330 GO TO 350
340 LET Y3 = 180
350 IF X (1, 1) < 0 THEN 380
360 LET Y4 = 0
370 GO TO 390
380 LET Y4 = 180
390 LET Y5 = Y3 + ATN (V (1, 2)/V (1, 1)) * 57
400 LET Y6 = Y4 + ATN (X (1, 2)/X (1, 1)) * 57
410 PRINT "MODULUS AND ARGUMENT OF Q1:", Y2, Y6
420 PRINT "MODULUS AND ARGUMENT OF Q2:", Y1, Y5
500 DATA 170, 112, 63, 78, 235, 94, 58, 68, 185, 116, 77, 104
510 END
RUN
DYNBAL    10:09    KBH MA 01/06/70

MODULUS AND ARGUMENT OF Q1:   1.71758      236.077
MODULUS AND ARGUMENT OF Q2:   .927035      121.92
USED      3.83 SEC.
```

Fig.7.83. The computer program used in conjunction with dynamic balancing according to Figs.7.80, 7.81 and 7.82

232

Dynamic balancing according to the above described procedure has been carried out at Brüel & Kjær on an experimental rotor arrangement. The results of the balancing, in terms of frequency analyses of the bearing vibrations, are given in Fig.7.84.

(a)

(b)   271630
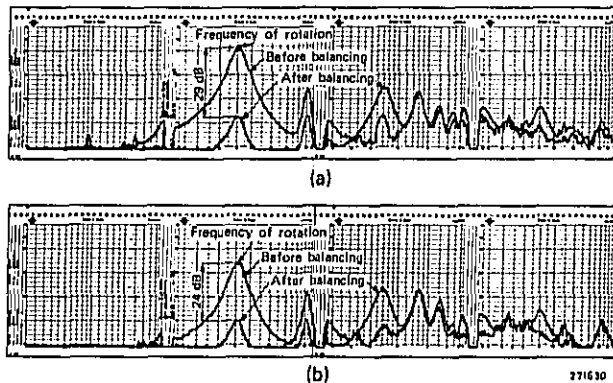
Fig.7.84.   Frequency analysis of bearing vibrations before and after balancing
            a) Frequency spectra obtained from measurements on the rotor pedestal at balancing plane I
            b) Similar to a) Measured on the rotor pedestal at balancing plane II

Selected Bibliography

ADKINS, F.E. and   Dynamic Balancing at Heaton Works, Parsons,
GRAY, A.:   Newcastle upon Tyne, 1960.

BISHOP, R.E.D. and   The Vibration and Balancing of an Unbalanced
GLADWELL, G.M.L.:   Flexible Rotor. J. Mech. Eng. Sci., Vol. 1, No. 1.
                        June 1959.

EL-HADI, I.:   Zusammenstellung, kritische Untersuchung und
                        Weiterentwicklung der Verfahren zum Aus-
                        wuchten betriebsmäßig aufgestellter Maschinen
                        mit starren und mit elastischen Läufern. Diss.
                        Darmstadt 1962.

FEDERN, K.:

Grundlagen einer systematischen Schwingungs-
entstörung wellenelastischer Rotoren. VDI
Berichte, Band 24, 1957.

FEDERN, K. und
JAKUBASCHKE, O.:

Wie Wuchtet man werkstückgerecht aus? Carl
Schenck Maschinenfabrik Mitteilungen, Heft 5,
Darmstadt 1957.

GUINS, S.B. and
BURMIST, J.:

Precision Balancing of Rotating Machine Parts.
Machine Design. Vol. 24, No. 12, December
1952.

JUDGE, A.W.:

The Testing of High Speed Internal Combustion
Engines with Special Reference to Automobile
and Aircraft Types, Including Gas Turbines.
Chapman & Hall, 4. ed., London, 1955.

KOLBE, W.:

Wuchten großer Induktoren. Elektrizitätswirt-
schaft, 57. Jahrg. Heft 1, Februar 1958.

LAWRIE, G.C.:

Precision Production Balancing. Tool Engineer,
Vol. 3, No. 4, April 1953.

LUND, J.W. and
TØNNESEN, J.:

Experimental and Analytic Investigation of High-
Speed Rotor Balancing. Research Report
No. FR8. Dept. of Mach. Design. Tech. Univ. of
Denmark. December 1970.

MACDUFF, J.N.:

A Procedure for Field Balancing Rotating
Machinery. Sound and Vibration. July 1967.

PETERMANN, J.E.:

Balancing Heavy Shafts and Rotors. Allis
Chalmers Electrical Review. Vol. XXIII,
No. 1 – 1958.

STISEN, B.:

Dynamic Balancing of Rotating Machinery in-
Situ. Brüel & Kjær, June 1970 (Unpubl. Report).

THEARLE, E.L.:

Dynamic Balancing in the Field. Trans. ASME,
56 (10). 1935.

WILCOX, J.B.:

Dynamic Balancing of Rotating Machinery.
Pitman, London 1967.

234

8. SOME ADVANCED MEASUREMENT METHODS

8.1. Mechanical Impedance and Mobility

The concepts of mechanical impedance and mobility are very important in modern vibration analysis for two major reasons:

1. They enable predictions to be made of the overall performance of a complex mechanical system from a knowledge of the characteristics of the system "components".

2. They allow estimations to be made of the force acting at a certain point in the system from the measurement of a motional quantity, and vice versa.

The concepts are not new, actually they seem to have been introduced theoretically already in the nineteen-twenties (impedance) and nineteen-thirties (mobility). However, the practical application of the concepts are of a considerably newer date, and their experimental determination may still (1971) be regarded as "advanced mechanical measurements".

They connect the motion at a point in a vibrating system with the force causing the motion in that:

$$\bar{Z} = \frac{\bar{F}}{\bar{V}} \qquad \text{(Mechanical Impedance)}$$

and

$$\bar{M} = \frac{\bar{V}}{\bar{F}} \qquad \text{(Mechanical Mobility)}$$

Here $\bar{F}$ is the complex force vector and $\bar{V}$ the complex velocity vector*). From the above definitions it can be seen that mechanical impedance may be described as "resistance against being set into motion", while mobility is the converse ("willingness" to be set into motion).

---

*) Because $\bar{F}$ and $\bar{V}$ are not only complex *time* vectors, but also *space* vectors, mechanical impedances and mobilities are actually complex space *tensors*. This fact sometimes complicates the practical use of the concepts considerably. In this text, however, the space relationships have been "neglected", and only time relationships have been considered.

The concept of mechanical impedance has grown out of the similarity between the differential equations governing the behaviour of linear mechanical and electrical systems. Since about 1900 electrical engineers have with great success utilized the concept of electrical impedance for the analysis of electrical circuits. It therefore seemed quite reasonable that introducing the concept of mechanical impedance into the analysis of vibratory systems should turn out to be equally successful. There are, on the other hand, several reasons why such a success could not be achieved immediately.

First of all, while electrical circuits normally consist of lumped parameters (R, L, C) mechanical systems are, in general, of the distributed parameter type. Secondly, it turns out that the impedance "analogy" is not so straight forward to apply to mechanical systems because parallel electrical elements "transform" into mechanical series elements when this type of analogy is used.

The second type of analogy, utilizing the concept of mechanical mobility, overcomes this difficulty. Here parallel electrical elements is analogous to parallel mechanical elements. This may be easiest to understand in considering the following: In the "impedance analogy" mechanical force is taken to be analogous to electrical voltage and mechanical velocity to electrical current. In the "mobility analogy", on the other hand, *force is taken to be analogous to current and velocity to voltage.*

Now, just as the total force acting at a point in a mechanical system is equal to the sum of the partial forces acting at the same point so is the total current flowing through a point in an electrical circuit equal to the sum of the partial currents, thus:

$$\sum_i F_i = F \quad \Leftrightarrow \quad \sum_i I_i = I$$

Similarly, the point in the mechanical system where the force, F, acts is, due to the action of F, given a certain velocity, v, while the partial electrical current I_i produces the same voltage drop, E, across all the elements in the circuit where the total current is I. These facts are illustrated in Fig.8.1, and show that from knowledge of electrical circuit theory it is a relatively simple matter to construct the mechanical mobility "circuit".

If the impedance analogy was used on the system, Fig.8.1, the result would be the circuit shown in Fig.8.2. Here, however, confusion may sometimes arise with respect to reference points when the system considered contains both series and parallel elements.

236
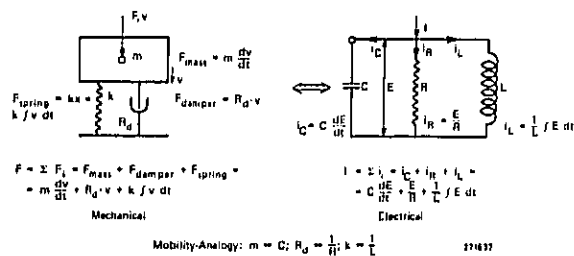
Fig.8.1. Example of a mobility type analog circuit
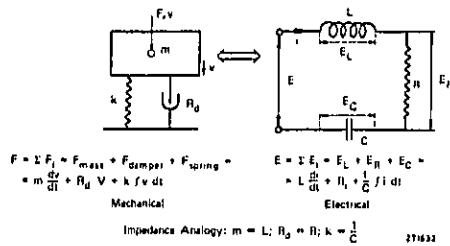
Fig.8.2. Example of an impedance type analog circuit

To allow numerical values to be assigned to mechanical impedances and mobilities consider the various lumped parameters of a mechanical system, i.e. masses, springs and dampers. The motion of a mass is governed by Newton's second law, i.e.:

$$F_m = m\frac{dv_m}{dt}$$

For an arbitrary sinusoidal component of the force, $F_{mo} = F_o\, e^{j\omega t}$ then

$$\frac{dv_{mo}}{dt} = \frac{F_o}{m}\, e^{j\omega t}$$

and

$$V_{mo} = \int\frac{F_o}{m}\, e^{j\omega t}\, dt = \frac{F_o}{j\omega m}\, e^{j\omega t}$$

237

whereby the mechanical impedance of the mass is:

$$Z_m = \frac{F_{mo}}{V_{mo}} = \frac{F_o \, e^{j\omega t}}{\dfrac{F_o \, e^{j\omega t}}{j\omega m}} = j\omega m$$

and the mechanical mobility

$$M_m = \frac{1}{Z_m} = \frac{1}{j\omega m}$$

Similarly, the impedance and mobility of a spring are:

$$Z_s = \frac{k}{j\omega} \text{ and } M_s = \frac{j\omega}{k}$$

and of a damper

$$Z_d = C \text{ and } M_d = \frac{1}{c}$$

Thus, summarizing the lumped parameter mechanical-electrical analogies the following table can be laid out:

Impedance Analogy		Mobility Analogy	
Mechanical	Electrical	Mechanical	Electrical
Force	Voltage	Force	Current
Velocity	Current	Velocity	Voltage
Parallel Elements	Series Elements	Parallel Elements	Parallel Elements
Mass	Inductance	Mass	Capacity
Spring	Capacity (inverse)	Spring	Inductance (inverse)
Damper	Resistance	Damper	Resistance (conductance)

Furthermore, mechanical impedances and mobilities can be represented vectorially in the complex plane. This is illustrated in Fig.8.3, while Fig.8.4 shows the frequency dependency of the different lumped parameter impedance and mobility elements.

238
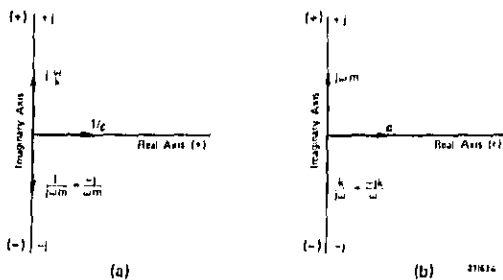
Fig.8.3. Vectorial representation of mechanical mobility and impedance:
   a) Mobility type vector diagram
   b) Impedance type vector diagram
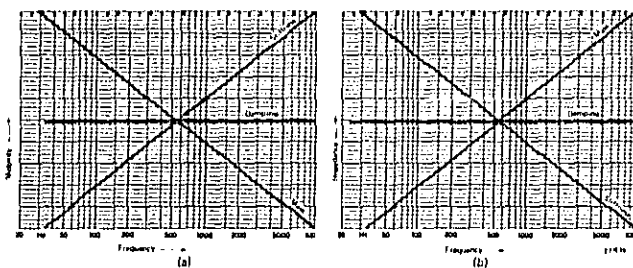
Fig.8.4. Frequency dependency of lumped mobility and impedance parameters
   a) Mobility lumped parameters
   b) Impedance lumped parameters

   An example of the use of analog analysis is given in Fig.8.5. Here the lumped parameter representation of a so-called Artificial Mastoid (B & K Type 4930) is shown in Fig.8.5a), while Fig.8.5b) shows the mobility analog and Fig.8.5c) the impedance analog circuit (The Artificial Mastoid is used in the field of technical audiology for the objective calibration of bone conduction hearing aids).

239
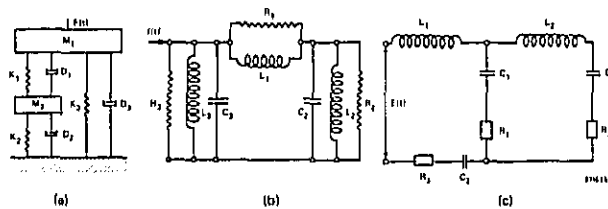
Fig.8.5. Lumped parameter representation of an Artificial Mastoid and its
electrical analog circuits
a) The mechanical system
b) The electrical mobility analog circuit
c) The electrical impedance analog circuit

Before discussing the more practical aspects of mechanical impedance
and mobility measurement it should be mentioned that other quantities
than "velocity" mobility and "velocity" impedance are sometimes used to
characterize the connection between the driving force and a motional
quantity. For instance, when the force is measured relative to the accelera-
tion one obtains the acceleration impedance, or the *apparent mass*. Similarly
a displacement impedance, or dynamic *stiffness*, may be defined. The
corresponding mobility concepts would be the acceleration mobility or
inertance, and the displacement mobility, often termed *compliance or
receptance*.

Also, the various impedance and mobility concepts may be defined as
point impedances and *point mobilities*, or as *transfer impedances* and *trans-
fer mobilities*, see Fig.8.6.
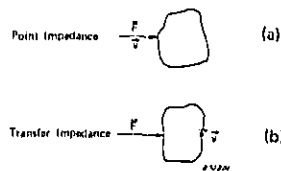
Fig.8.6. Illustration of the concepts of point impedance and point mobility,
and of transfer impedance and transfer mobility
a) Point impedance, point mobility
b) Transfer impedance, transfer mobility

240

When the mechanical system being studied can no longer be considered a lumped parameter system, i.e. a system consisting of individual masses, springs and dampers, electro-mechanical analogies may still be applicable in the form of transmission line theory. This does, however, to certain extent complicate the use of analogies in theoretical treatments.

In practice mechanical point impedances or point mobilities can be determined by means of measuring arrangements of the type shown in Fig.8.7. Here a vibration exciter is connected to the mechanical system being studied via a so-called Impedance Head.
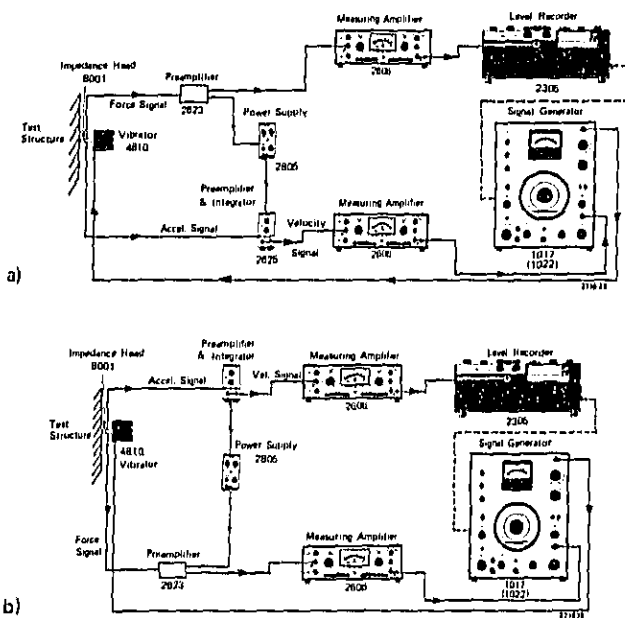
Fig.8.7. Measuring arrangements used to determine point impedance and point mobilities
a) Arrangement for point impedance measurements
b) Arrangement for point mobility measurements

An Impedance Head is an electro-mechanical device which contains two types of electro-mechanical transducers. One of the transducers measures the force which is applied to the structure being investigated while the second measures the motion of the point to which the force is applied. Normally, the motion is measured in terms of acceleration, and the output from the transducer is electronically integrated to obtain a signal proportional to velocity.

The actual construction of an Impedance Head can be seen from Fig.8.8. It contains basically as mentioned above, an accelerometer and a force gauge. These are made up of pairs of lead zirconate titanate piezoelectric discs with conductors sandwiched between them and leading out to output sockets in the housing. A seismic mass of tungsten alloy is mounted above the accelerometer discs. The driving platform below the force gauge is machined from beryllium to obtain high stiffness and low mass (weight 1.0 gram). It can be fastened to the test specimen in various ways, see also Chapter 5, section 5.7.
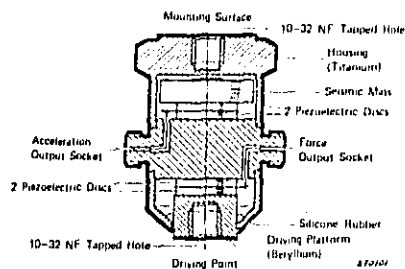
Fig.8.8. Cut away schematic view of an Impedance Head

The measuring arrangements shown in Fig.8.7 are capable of recording the measured results automatically. If the desired end result of the measurements is the point impedance the arrangement shown in Fig.8.7a) should be used, while the one shown in Fig.8.7b) is intended for point mobility measurements.

In the case of impedance measurements the velocity level of the measuring point is kept constant, whereby a recording of the force level immediately indicates the absolute value (modulus) of the impedance as $|Z| = |F| / |V|$.

242

Similarly, if it is desired to record the mobility of the measuring point the driving force level should be kept constant and the velocity level recorded $|M| = |V|/|F|$.

Fig.8.9 shows the result of impedance measurements on a lathe's cutting tool made by means of an arrangement of the type shown in Fig.8.7a). Here only the modulus of the impedance ($|Z|$) is given as a function of frequency.

a)

1. Cutting tool in normal position

b)

2. Cutting tool in outer position
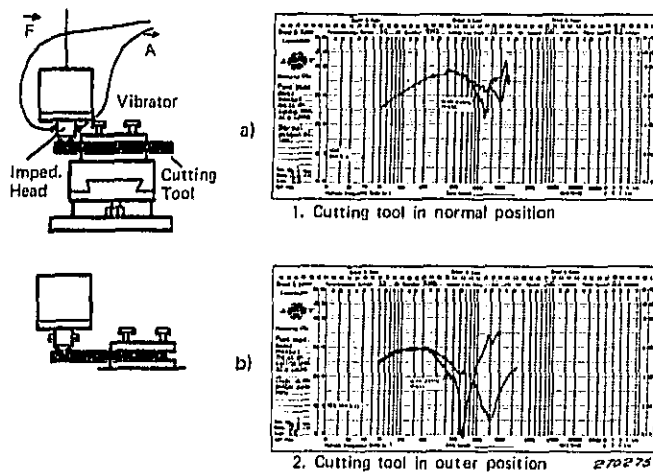
Fig.8.9. Point impedance measurements on a lathe's cutting tool
a) Measurements with the cutting tool in its normal position
b) Measurements with the cutting tool in its outer position

In some cases of impedance and mobility measurements it is found that signal harmonics and extraneous noises interfere with the measurements. To overcome this problem use can be made of two Heterodyne Slave Filters as indicated in Fig.8.10.

When measurements are carried out on large structures, or when it is desired to determine transfer impedances, or transfer mobilities, separate force gauges and accelerometers should be used, see Fig.8.11.

243
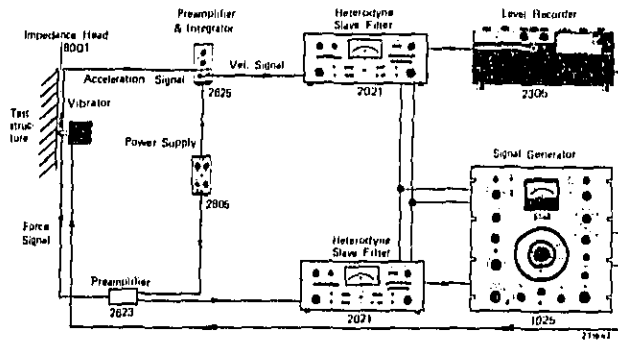
Fig.8.10. *Measuring arrangement suitable for frequency selective measurements of point impedances and point mobilities*
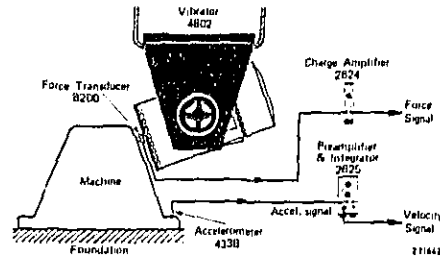
Fig.8.11. *Use of separate force gauge and accelerometer for the determination of transfer impedance and transfer mobilities*

Fig.8.12. *Photograph of the Brüel & Kjær Force Transducer and Impedance Heads*

Finally Fig.8.12 shows a photograph of two Impedance Heads and a Force Transducer produced by Brüel & Kjær.

Selected Bibliography

BALLARD, W.C., CASEY, S.L. and CLAUSEN, J.O.:	Vibration Testing with mechanical Impedance Methods. Sound and Vibration. January 1969.
BANNISTER, R.L. and THOMAN, R.J.:	An experimental Mechanical Impedance Technique. Sound and Vibration March 1968.
BARUCH, M.J. and TELLES, S.:	A Steady State Response Analysis of Complex Structures Using Impedance Coupling Techniques. Shock and Vibr. Bull. 34, part 3, 1965.
BELSHEIM, R.O.:	Application of Mechanical Impedance Concepts to Rocket Motor Vibration. Shock and Vibr. Bull. 29, part 4, 1961.
CANT, D.:	Model Method for Finding the Stress Areas. The Engineer. January 1970.
COMSTOCK, T.R., TSE, F.S. and LEMON, J.R.:	Application of Controlled Mechanical Impedance for Reducing Machine Tool Vibrations. Journ. of Engineering for Industry. November 1969.
FIRESTONE, F.A.:	A New Analogy Between Mechanical and Electrical Systems. J.A.S.A., Vol. 4, 1933.
KERLIN, R.L. and SNOWDON, J.C.:	Driving-Point Impedances of Cantilever Beams-Comparison of Measurement and Theory. J.A.S.A., Vol. 47, No. 1, 1970.
MAINS, R.M.:	The Application of Impedance Techniques to Shipboard Vibrations. Shock and Vibr. Bull. 33, part 4, 1963.
OBERST, H.:	Schwingungsdämpfung von Blechen. Klepzig Fachberichte, November 1968.

OSGOOD, C.C.:   Mechanical Impedance of Spacecraft Structures.
                       Shock and Vibr. Bull. 34, part 3, 1964.

PLUNKETT, R. (ed):   Mechanical Impedance Methods. A.S.M.E.,
                       December 1958.

SCHWARTZ, J.I.:   Vibration Analysis of an Ideal Motor Using
                       Mechanical Impedance. Shock and Vibr. Bull. 33,
                       part 4, 1963.

STISEN, B.:   Introduction to Structural Response Measure-
                       ments and Their Applications. Brüel & Kjær
                       1970. (Unpubl. Report).

TIPTON, H.:   Vibration Measurements. Machine Tool Re-
                       search. July 1963.

8.2. Cross-Correlation and Cross-Spectral Density Measurements

There are several methods of relating measurement data observed at a certain point in a system to data obtained at some other observation point within the same system. The most straight forward method may simply be to compare the data directly by eye.

However, even if the human eye is an amazingly sensitive and selective measuring device, situations occur where such comparison is extremely difficult. Also, although a qualitative measure of the relationship between data may be obtained by merely looking at the time records, it is not possible in general to obtain a quantitative measure of the relationship by means of this "method".

Mathematical physicists have therefore introduced the so-called cross-correlation function which actually gives a quantitative measure of the relationship

$$\psi_{xy}(\tau) = \lim_{T \to \infty} \frac{1}{T} \int_0^T f_x(t)\, f_y(t + \tau)\, dt$$

Here $f_x(t)$ is the magnitude of a signal observed at the point x at an arbitrary instant of time, t, and $f_y(t + \tau)$ is the magnitude of a signal observed at a point y a time τ later. By varying τ the relationship between the signals at x and y as a function of time delays is obtained.

246

Fig.8.13 shows a "classic" example of such a correlation function. It can be seen that when τ is zero practically no relationship exists between the two signals. By increasing τ it becomes evident, however, that a certain relationship does exist. At a certain delay-time, τ_0, this relationship reaches a maximum, whereafter the relationship again decreases to zero for large values of τ.

A relationship of the kind indicated in Fig.8.13 is typical for a system which is frequency independent and contains some sort of time delay mechanism. If the maximum value of ψ_{xy} (τ) is equal to unity the signal at y is exactly the same signal as that at x, but delayed a time τ. On the other hand, if ψ_{xy} (τ) is less than unity only a certain part of the signal observed at x is present at y.
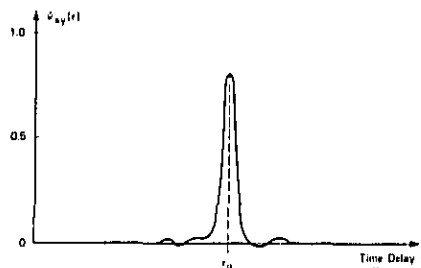
Fig.8.13. *Sketch indicating the cross-correlation function for a hypotheti-cal frequency independent random process*

The case illustrated in Fig.8.13 is an idealized case and this kind of correlation function is found rather rarely in practice because normally the system within which observations are made is frequency dependent. To investigate the frequency dependency use may be made of Fourier transform methods. The result of applying the Fourier transform to the cross correlation function is the cross-spectral density function (see also chapter 2, section 2.2):

$$W_{xy} \ (f) \ = \int_{-\infty}^{\infty} \psi_{xy} \ (\tau) \ e^{-j2\pi f \tau} \ d\tau$$

This function is, in general, complex, containing both real and imaginary terms, a fact which is readily seen in that both magnitude and phase

247

measures should be preserved. (Time delays, for instance represent phase differences in the frequency domain).

From the theory of Fourier integrals it is known that $\psi_{xy}\,(\tau)$ can also be found by inversion.

$$\psi_{xy}\,(\tau) = \int\limits_{-\infty}^{\infty} W_{xy}\,(f)\,e^{j2\pi f\tau}\,df$$

writing

$$W_{xy}\,(f) = |W_{xy}\,(f)|\,e^{-j\varphi_f}$$

and considering the fact that $\psi_{xy}\,(\tau)$ is always a real quality one obtains:

$$\psi_{xy}\,(\tau) = \int\limits_{-\infty}^{\infty} |W_{xy}\,(f)|\,e^{j(2\pi f\tau - \varphi f)}\,df = \int\limits_{-\infty}^{\infty} |W_{xy}\,(f)|\,\cos\,(2\,\pi\,f\,\tau - \varphi_f)\,df$$

This can also be written:

$$\psi_{xy}\,(\tau) = \int\limits_{-\infty}^{\infty} |W_{xy}\,(f)|\,\cos\varphi_f\,\cos\,(2\,\pi\,f\,\tau)\,df + \int\limits_{-\infty}^{\infty} |W_{xy}\,(f)|\,\sin\varphi_f\,\sin\,(2\,\pi\,f\,\tau)\,df$$

Consider now that an ideal analog frequency analyzer will allow only that part of the signal to be measured which has frequency components within a narrow frequency band, Δf, see Fig.8.14.
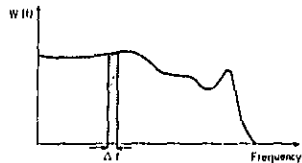
Fig.8.14.   Illustration of an "ideal" frequency analysis

When no attenuation or amplification of these frequency components takes place in the analyzer, and both analyzer channels used have equal phase shifts then the cross-correlation between the two measurement channels is given by the expression:

$$\psi_{xy\,\Delta f}\,(\tau) = \int\limits_{f}^{f+\Delta f} 2\,|W_{xy}\,(f)|\,\cos\varphi_f\,\cos\,(2\,\pi\,f\,\tau)\,df + \int\limits_{f}^{f+\Delta f} 2\,|W_{xy}\,(f)|\,\sin\varphi_f\,\sin\,(2\,\pi\,f\,\tau)\,df$$

The reason for introducing $2\,|W_{xy}\,(f)|$ instead of $|W_{xy}\,(f)|$ is that in physically realizable systems only positive frequencies are involved, while

248

$W_{xy}(f)$ was introduced for mathematical convenience where both positive and negative frequencies were considered.

When $\Delta f \to 0$:

$$\psi_{xy_{\Delta f}}(\tau) \approx 2\,|W_{xy}(f)|\cos\varphi_f \cos(2\pi f \tau)\,\Delta f + 2\,|W_{xy}(f)|\sin\varphi_f \sin(2\pi f \tau)\,\Delta f$$

Setting $\tau = 0$ and utilizing the original definition of $\psi_{xy}(\tau)$ then

$$2\,|W_{xy}(f)|\cos\varphi_f\,\Delta f = \lim_{T \to \infty} \frac{1}{T} \int_0^T f_{x_{\Delta f}}(t)\,f_{y_{\Delta f}}(t)\,dt$$

Rearranging this equation and setting $2\,|W_{xy}(f)|\cos\varphi_f = C_{xy}(f)$ gives

$$C_{xy}(f) = \lim_{\Delta f \to 0}\ \lim_{T \to \infty}\ \frac{1}{T\,\Delta f} \int_0^T f_{x_{\Delta f}}(t)\,f_{y_{\Delta f}}(t)\,dt$$

Furthermore setting $\tau = \frac{1}{4f}$ (90° phase shift) in the above expression for $\psi_{xy_{\Delta f}}(\tau)$ gives:

$$Q_{xy}(f) = \lim_{\Delta f \to 0}\ \lim_{T \to \infty}\ \frac{1}{T\,\Delta f} \int_0^T f_{x_{\Delta f}}(t)\,f^*_{y_{\Delta f}}(t)\,dt$$

where $Q_{xy}(f) = 2\,|W_{xy}(f)|\sin\varphi_f$ and $f^*_{y_{\Delta f}}(t)$ is equal to $f_{y_{\Delta f}}(t)$ shifted 90° in phase. $C_{xy}(f)$ is denoted as the co-spectral density function while $Q_{xy}(f)$ is the quadrature (quad) spectral density function.

From the derivation outlined in the preceeding text it is seen that:

$$W_{xy}(f) = C_{xy}(f) - j\,Q_{xy}(f)$$

or

$$|W_{xy}(f)| = \sqrt{C_{xy}^2(f) + Q_{xy}^2(f)}$$

and

$$\varphi_f = \varphi_{xy}(f) = \tan^{-1}\left[\frac{Q_{xy}(f)}{C_{xy}(f)}\right]$$

where $|W_{xy}(f)|$ is the absolute magnitude (modulus) of the cross spectral density function at the frequency f and $\varphi_{xy}(f)$ is the phase difference between the signal at x and the signal at y.

As the cross-correlation function and the cross-spectral density function constitute a Fourier transform pair the same amount of information is contained in $W_{xy}(f)$ as in $\psi_{xy}(\tau)$. Whether one or the other of the two

249

functions should be used to solve a particular practical problem is therefore basically a matter of convenience, as will be discussed to some extent in the following.

Because the cross-correlation function $\psi_{xy}(\tau)$ is a function which depends on time (or rather on time delays), τ, it seems obvious that when systems containing time delay mechanisms are studied use should preferably be made of this function directly. This statement is, however, a "truth" with considerable limitation.

In Fig.8.13 it was shown that a cross-correlogram clearly showed both the time delay, τ_o, and the magnitude of the correlation $\psi_{xy}(\tau_o)$ involved in a particular hypothetical process. It was also stated that in this case the transmission paths within the system were frequency independent. Now, what happens if the transmission paths (or the signals) are frequency dependent? Fig.8.15 gives an indication of the answer to this question. The system on which this correlogram was measured consisted of a mechanical framework with two tightly coupled resonant modes in the transmission path. If more resonant modes and/or reflections had been present the correlogram would have become still more complicated.

Correlation
Coefficient

Tightly coupled modes — one mode predominant
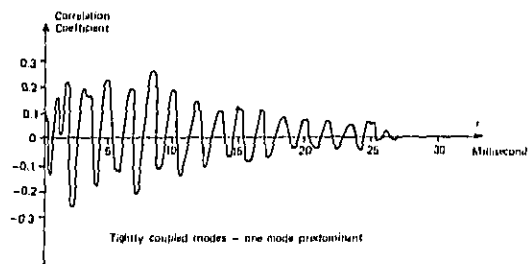
Fig.8.15. Cross-correlation function measured on a mechanical framework with two tightly coupled resonant modes. (I.S.V.R.)

Theoretical analogies (and practical experiments) have pointed at the fact that a bandwidth-reflection time limitation of the kind:

$$\Delta f_{min} \times \tau_s \gtrsim C_1 \frac{\psi_{xy}(\tau_1)}{\psi_{xy}(\tau_2)}$$

exists in correlation function measurements. Here $\psi_{xy}(\tau_1)/\psi_{xy}(\tau_2)$

represents the ratio between two successive correlation maxima and $\tau_s = \tau_2 - \tau_1$, see also Fig.8.16. Δf_{min} is the *minimum* bandwidth involved in the correlation process (and measurement) and the constant c_1 may be taken in the range $2 - 3$.
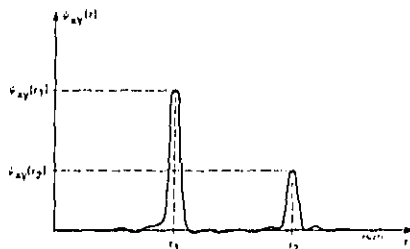
Fig.8.16. Sketch illustrating cross-correlation maxima and time delays in a hypothetical random process

This limitation in bandwidth-reflection time makes the use of correlation function techniques in the time domain seem a quite unrealistic proposition for vibration studies on complex mechanical structures. On the other hand, the cross-spectral density techniques (in the frequency domain) seems to offer considerable possibilities.

The basic principle involved in cross-spectral density measurements is illustrated in Fig.8.17. From the figure it can be seen that the measurement of co- and quad spectral density functions is a rather straight forward matter. Also in this case, however, certain practical restrictions regarding filter bandwidths and signal time delays are imposed upon the measurements, in that here a limitation of the kind

$$\Delta f_{max} \times \tau_{max} \lesssim C_2$$

can be shown to exist. Δf_{max} is now the *maximum* bandwidth involved in the measurements and τ_{max} is the maximum delay time between the signals to be correlated. A suitable value for C_2 is 0.3.

From the above discussion it is seen that the restrictions imposed upon practical correlation time function measurements and those imposed upon cross spectral density measurements actually oppose each other.

251
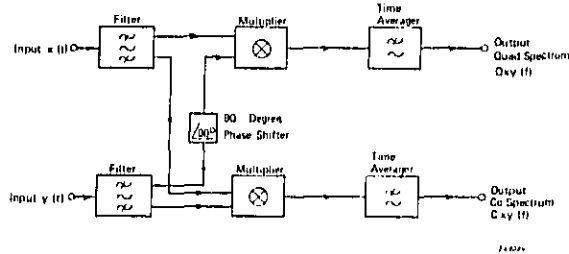
Fig.8.17. *Principle of operation of an analog cross-spectrum analyzer*

In correlation time function measurements a certain *minimum* measure-
ment bandwidth is required to allow for proper determination of the
correlation function maxima while proper cross-spectral density measure-
ments require the measurement bandwidth to be *smaller* than a value given
by the relationship C_2/τ_{max}.

One of the most interesting applications of the cross-spectral density
technique in the field of mechanical vibration studies might be the
possibility it offers to determine complex transfer characteristics in a system
without interfering with the system's normal operation. This kind of
measurement is of particular importance in the fields of shipboard, aircraft
and space vehicle vibration but has also been utilized in vibration studies on
automobiles and special machinery.
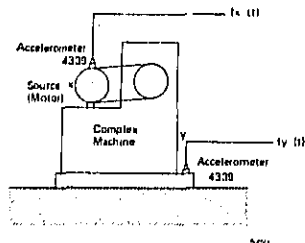
Fig.8.18. *Illustration of transfer characteristic measurements on a*
complex machine without interfering with the machine's normal
operation

252

The relation between the cross-spectral density measured between the point x and the point y in the system sketched in Fig.8.18, the ordinary mean square spectral density, W_{xx} (f), measured at x and the (complex) transfer characteristic between x and y, H_{xy} (f) is:

$$W_{xy} \text{ (f)} = H_{xy} \text{ (f)} \, W_{xx} \text{ (f)}$$

Thus, the function H_{xy} (f) can be completely determined from measurements of the co- and quad spectral density functions between x and y, and the mean square spectral density function at x.
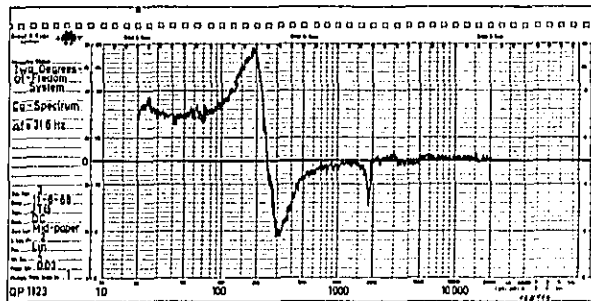
(a)
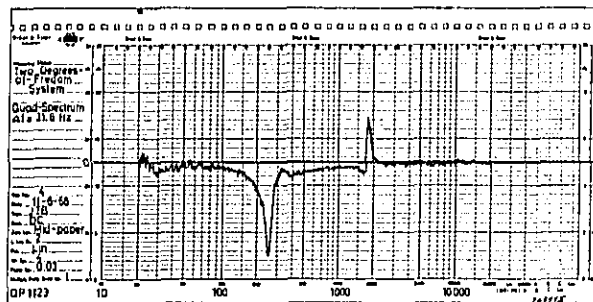
(b)

Fig.8.19. Cross-spectral density curves obtained from measurements on a two degrees-of-freedom system excited by "white" random noise
a) Co-spectral density curve   b) Quad spectral density curve

253

To demonstrate the use of this technique a simple experiment has been made at Brüel & Kjær on an electrical analog model consisting of a two degree-of-freedom system. The resulting co- and quad spectral density functions are shown in Fig.8.19. Because the input to the system in this case consisted of random noise with constant mean square spectral density $(W_{xx} (f) = \text{constant})$ the graphs shown in Fig.8.19 at the same time represent $H_{xy} (f)$.

The practical experiments were carried out by means of the measuring arrangement shown in Fig.8.20, which consists of a control oscillator (Brüel & Kjær Type 1025) two Heterodyne Slave Filters Type 2021, a Graphic Level Recorder Type 2305, and an electronic multiplier. It might be mentioned, in this connection, that the Heterodyne Slave Filters have been designed to include a phase-shift of 90°, specifically for use in cross-spectral density measurements.
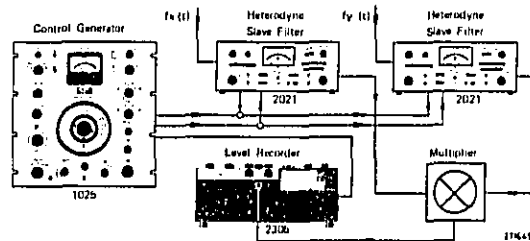
Fig.8.20. Practical measuring arrangement used for cross-spectrum analysis and utilizing two Brüel & Kjær Heterodyne Slave Filters Type 2021

Finally, it should be pointed out that by measuring both the cross spectral density between the signals observed at the points x and y in a physical system and the ordinary mean square spectral density at *both* points the *correlation coefficient* R_{xy} between the two signals can be calculated from the formula:

$$R_{xy} = \sqrt{\frac{|W_{xy}|^2}{W_{xx} \, W_{yy}}}$$

As this coefficient depends on frequency it is normally termed *coherence function* (to distinguish it from the correlation function which is defined in the time domain). The coherence function is often denoted by γ_{xy} (f) whereby the above equation takes the form:

$$\gamma_{xy}\ (f)\ =\ \sqrt{\frac{|W_{xy}\ (f)|^2}{W_{xx}\ (f)\ W_{yy}\ (f)}}$$

Selected Bibliography

BENDAT, J.S.:

Principles and Applications of Random Noise Theory. John Wiley & Sons. Inc. New York 1958.

BENDAT, J.S.,
ENOCHSON, L.D.,
KLEIN, G.H. and
PIERSOL, A.G.:

The Application of Statistics to the Flight Vehicle Vibration Problem. ASD TR 61 – 123. Wright-Patterson AFB, Ohio, December 1961. (AD 271913).

BENDAT, J.S. and
PIERSOL, A.G.:

Measurement and Analysis of Random Data. John Wiley & Sons. Inc. New York 1966.

BROCH, J.T.:

On the Measurement and Interpretation of Cross-Power-Spectra. Brüel & Kjær Techn. Rev. No. 3 – 1968.

BROCH, J.T.:

On the Application and Limitations of the Cross-Correlation and the Cross-Spectral Density Techniques. Brüel & Kjær Techn. Rev. No. 4 – 1970.

CLARKSON, B.L. and
MERCER, C.A.:

Note on the Use of Cross-Correlation in Studying the Response of Lightly Damped Structures to Noise. I.S.A.V. Memorandum No. 116, November 1964. University of Southampton.

ENOCHSON, L.D.:

Frequency Response Functions and Coherence Functions for Multiple Input Linear Systems. Washington D.C. NASA CR – 32, April 1964.

LANGE, F.H.:

Korrelationselektronik. VEB-Verlag Technik. Berlin 1959.

GOODMAN, N.R.:   On the Joint Estimation of the Spectra, Co-
                   Spectrum and Quadrature Spectrum of a Two
                   Dimensional Stationary Gaussian Process. Scien-
                   tific Paper No. 10. Engineering Statistics Labora-
                   tory. New York Univ. New York 1957.

GOODMAN, N.R.:   Measurement of Matrix Frequency Response
                   Functions and Multiple Coherence Functions.
                   AFFDL TR — 65 — 56. Research and Tech-
                   nology Division AFSC. Wright-Patterson AFB,
                   Ohio. February 1965.

TICK, L.J.:   Conditional Spectra, Linear Systems, and
                   Coherency. Chapter 13, Time Series Analysis, M.
                   Rosenblatt(ed) John Wiley & Sons Inc. New
                   York 1963.

URBAN, P. and   Cross Spectral Density Measurements with
KOP, V.:   Brüel & Kjær Instruments. Part I, Brüel & Kjær
                   Techn. Rev. No. 3 — 1968, and Part II, Brüel &
                   Kjær Techn. Rev. No. 4 — 1968.

8.3. Probability Density Measurements and Description

A great variety of probability density functions can be derived and used for the description of random processes. One of the most important of these functions is the probability density function for the instantaneous ampli- tude values of the process also designated as the *first order probability density* function (see Chapter 2, section 2.2). The reason for designating this function will be clear from the discussion later in this section where also higher order probability density functions are introduced.

The importance of the first order probability density function may be better appreciated by considering a special class of random processes, name- ly Gaussian (normal) random process. This type of random processes occur relatively frequently in nature and it has been shown by Rice and others that if the process behaves linearly and has a Gaussian first order probability density function then *the process is more or less completely described by means of its mean square (power) spectral density function* (or its correla- tion function). It is therefore of considerable practical interest in the study of random processes to be able to measure the first order probability density function. If this turns out to be Gaussian, only very few further

256

measurements are necessary for a satisfactory description (assuming, of course, that the process being investigated is stationary).

In cases where one knows that the process behaves linearly, i.e. where no selective amplitude non-linear element (non-linear resonance) is present, a measurement of the mean square spectral density function only, will normally suffice.

Should it not be possible, however, from beforehand to judge whether or not the process behaves linearly, a check on this may be obtained for instance by simply integrating the time function once and repeating the measurement of the first order probability density function, in this case on the integrated time function. An example of such a case is a randomly excited resonant system containing a non-linear stiffness element (see also Chapter 3, section 3.2).

From measurements on these kinds of systems, it is found that the first order probability density function of the relative velocity, v_r in Fig.8.21a), has a perfect Gaussian shape, Fig.8.22a). (This can also be confirmed theoretically). However, if the velocity signal is integrated once with respect to time, i.e. turned into a relative displacement signal, the non-linearity will show itself clearly in the probability density characteristic, Fig.8.22b).
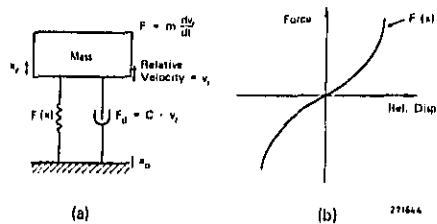
Fig.8.21. *Example of a single degree-of-freedom system containing a non-linear suspension element of the hardening spring type*
a) Mechanical model
b) Static force versus displacement characteristic of the spring element

Although the non-linearity may also be detected by other means, for instance by probability density measurements on the differentiated velocity signal, integration has been chosen here, because it is a relatively simple operation to perform electronically, see Appendix E.

257
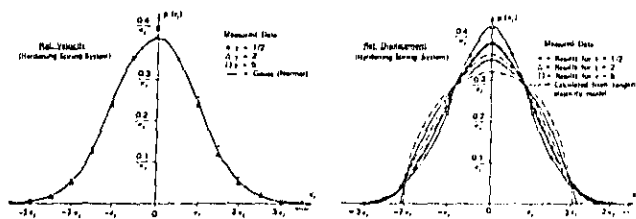
Fig.8.22. Examples of first order probability density functions
          a) Probability density plot for the instantaneous relative
          velocity of the mass
          b) Probability density plot for the instantaneous relative dis-
          placement of mass

An instrument which allows the measurement of probability density
functions is shown in Fig.8.23 and Fig.8.24 shows the schematic block
diagram of its operation when switched to measure first order probability
densities. Briefly, the functioning of the arrangement is as follows. The
signal to be analyzed is fed to the input of the instrument, whereafter its
actual level is "normalized" (to 1 Volt RMS) by means of the input
potentiometer. A variable DC signal is then added in the input amplifier and
the resulting signal (input + DC) led to two measuring "window" detector
circuits (electronic flip-flops). The measuring "window" is here adjusted to
0.1 σ (0.1 times the normalized input signal RMS-value = 0.1 Volt).

By letting the outputs of the "window" detectors control a gating
circuit, it is possible to measure the time intervals during which the input
signal stays within the "window" (re. also Fig.2.8).
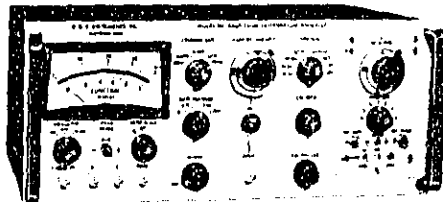
Fig.8.23. Photograph of an analog probability density analyzer
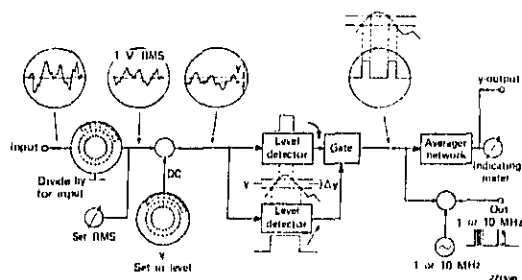
Fig.8.24. Block diagram illustrating the principle of operation of the probability density analyzer shown in Fig.8.23 when switched to measure first order probability densities

The signal from the gating circuit is either used to control a 1 MHz (or 10 MHz) built-in oscillator, or fed to an averaging circuit and instrument meter. When properly calibrated the instrument meter indicates directly the probability density, and by varying the DC added to the signal in the input amplifier the probability density can be measured at various amplitude levels (from -5σ to $+5\sigma$). If the gating circuit is used to control one of the built-in precision oscillators a digital output is also obtained.

The DC-signal can be varied either manually or by means of a built-in stepping motor whereby automatic recording of the measurement data is possible. An example of such a recording is shown in Fig.8.25 and the corresponding measuring arrangement in Fig.8.26. As the recording instrument, a Brüel & Kjær Level Recorder Type 2305 was used, switched for DC recording and supplied with a 50 dB logarithmic range potentiometer. The use of logarithmic recording bears some advantage in that the same relative accuracy is obtained in the recording over the full amplitude range and the very low probability densities obtained from measurements of high amplitude levels are more easily read from the curve.

It should in this connection be mentioned that very long averaging times are required to obtain a reasonable measurement accuracy at very low probability density levels. This may in some cases (narrow band random signals and sharp infrequent pulses) make measurements at these probability density levels rather tedious, because the "built-in" averaging time may not be sufficiently long to produce the required accuracy. It is therefore often convenient to automatically record the probability density curve with a

259
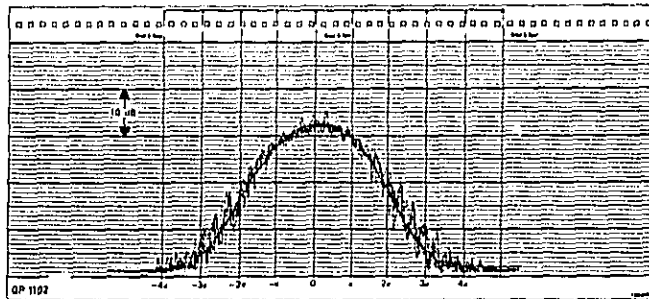
Fig.8.25.   Example of automatically recorded probability density data

relatively short averaging time and then specifically investigate regions of low probability density by manual measurements using the digital output from the instrument in conjunction with an electronic counter.

The instrument shown in Fig.8.23 is capable of measuring several other statistical quantities apart from the first order probability density of random time functions. This will be explained below.

In cases where the results of first order probability density measurements indicate that the process being investigated is non-Gaussian, an experimental determination of its mean square spectral density function is normally *not* sufficient for an adequate description.
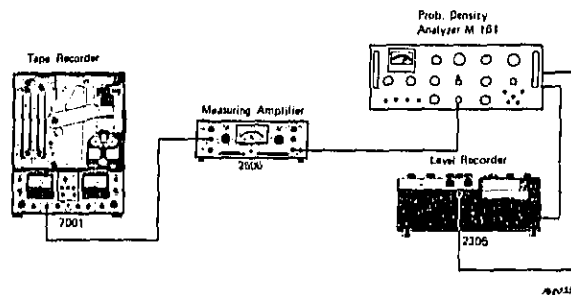
Fig.8.26.   Measuring arrangement used to record the curves shown in Fig.8.25

260

One way of obtaining further relevant information about the statistical behaviour of the process is then to determine some higher order probability characteristics. A higher order probability characteristic is a characteristic which does not depend only upon the average behaviour of a random signal when it is inside a narrow amplitude window, Δx in Fig.2.8, but it defines certain restrictions as to the behaviour of the signal also when it is outside Δx. A great variety of higher order probability characteristics can be formulated, among which is the probability density function for the process maxima, Fig.8.27.
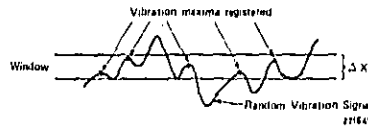
Fig.8.27. Sketch illustrating the principles involved in measurement of the probability density of random vibration maxima (peak probability densities)

That this is a higher order probability density function is clear because it restricts the observations on the signal inside Δx to cases where the magnitude of the signal is smaller than x both immediately before the signal enters the window and immediately after it leaves it again. By plotting the number of maxima inside Δx per unit time as a function of signal level, x, a curve proportional to the probability density curve for the process maxima is obtained. When this curve is normalized to unit area it is commonly termed the *peak probability density curve*.

To illustrate the use of peak probability density data consider first a completely linear, single degree-of-freedom system excited by Gaussian random vibrations. The peak probability density curve for the relative displacement of the mass can in this case be shown, both theoretically and experimentally, to follow a so-called Rayleigh distribution function (Fig.8.28a):

$$p(x) = \frac{x}{\sigma^2} e^{-\frac{x^2}{2\sigma^2}}$$

If now the single degree-of-freedom system contains a non-linear stiffness element of the hardening spring type, Fig.8.21, the shape of the peak probability density function of the relative displacement of the mass will depend upon the level of excitation. The limitation in displacement caused by the hardening of the spring is clearly noticed.

261
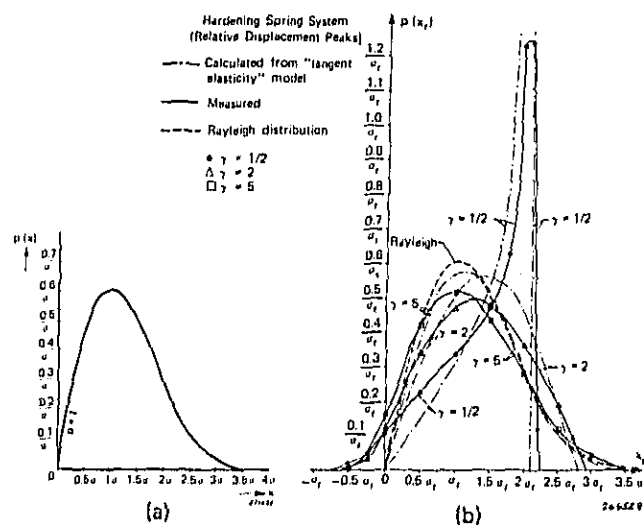
Fig.8.28.   Example of peak probability density data
            a) Peak probability density curve valid for the relative displace-
            ment of the mass in a linear single degree-of-freedom system
            excited by Gaussian random vibrations
            b) Peak probability density curves valid for the relative displace-
            ment of the mass in a single degree-of-freedom system, contain-
            ing a non-linear suspension element of the hardening spring
            type, excited by Gaussian random vibrations

   To further illustrate the displacement limiting effect of the hardening
spring Fig.8.29 shows some oscillographic samples of the displacement
waveshape. (The oscilloscopic record has been obtained from analog model
studies made at Brüel & Kjær).

   Even though the records shown in Fig.8.29 are very illustrative, they do
not lend themselves easily to quantitative descriptions. On the other hand,
probability density data, such as shown in Figs.8.22 and 8.28, do allow for
quantitative descriptions of the vibrations being studied. These data are
therefore of considerable value in obtaining measures for, for instance, the
damaging effects of vibrations, see also Chapter 4, section 4.1.

262

Fig.8.29. Samples of the relative displacement signal in a single degree-of-freedom system containing a hardening spring type non-linearity. (See also Appendix C)

It was mentioned above that the instrument shown in Fig.8.23 is capable of measuring other statistical quantities apart from the first order probability density function. One of these quantities is the peak probability density function, and Fig.8.30 illustrates the principle utilized. The "normalization" of the input signal level as well as the setting of the "window" level (DC) are exactly the same as described earlier in connection with Fig.8.24. However, to produce an output proportional to the number of peaks (signal maxima) which occur inside the measuring "window" it is necessary to "block" the detecting circuit when the signal
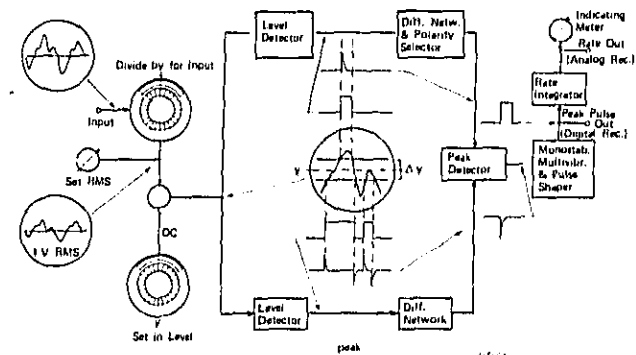
Fig.8.30. Block diagram illustrating the principle of operation of an analog probability density analyzer switched to measure peak probability densities

263

passes *through* the "window". This is accomplished by means of electronic
logic circuitry and can be basically understood by a study of Fig.8.30. If the
signal passes the upper limit of the "window" a pulse is produced which
blocks the peak detector circuitry so that no output is obtained.

On the other hand, if the signal passes the lower limit of the "window"
but *does not* pass the upper limit before it leaves the "window" again, the
peak detector circuitry produces an output pulse. The pulses produced by
the peak detecting circuitry can either be measured as such (digital record-
ing) or they are fed to an integrating and averaging circuit which produces
an analog output proportional to the peak rate (maxima per second).

Automatic recording of the analog data can be made in the same way as
shown in Fig.8.26. If desired the measured peak "rate" can also be read off
the instrument meter.

By combining two of the instruments, Fig.8.23, higher order probability
densities other than the peak probability density function may be measured,
such as the function commonly termed the *joint probability density
function.*
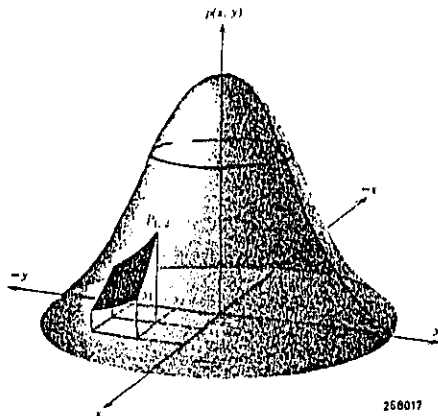
Fig.8.31.   Illustration of joint probability density data presentations

The joint probability density function describes the probability that the data at two points of observation assume values within some defined pairs of amplitude "windows" at any instant of time, divided by the product of the "window" widths:

$$p(x;y) = \lim_{\Delta x \to 0} \lim_{\Delta y \to 0} \frac{[P(x) - P(x+\Delta x); P(y) - P(y+\Delta y)]}{\Delta x \, \Delta y}$$

This is a much more complicated function than the other probability density functions discussed in this section of the book and although it contains a rather large amount of information it has, to the author's knowledge, very rarely been used in practical applications.

A very important reason for this might be the time required for its analog measurements. That the time required to measure the joint probability density function is rather large, follows from the fact that all combinations of amplitude values, x and y, must be considered. *The result of such measurements is therefore no longer a curve, but a surface, Fig.8.31.*

The first order probability density curve and the peak probability density curve, are on the other hand relatively easy to measure, and are, therefore, especially attractive to use in the description of complex random vibration.

Selected Bibliography

ARIARATNAM, S.T.:   Random Vibration of Non-Linear Suspensions. J. Mech. Eng. Sci. 2, 3. Sept. 1960.

ARIARATNAM, S.T.:   Response of a Loaded Non-Linear String to Random Excitation. J. Appl. Mech. Sept. 1962.

BENDAT, J.S.:   Principles and Applications of Random Noise Theory. John Wiley & Sons Inc. New York 1958.

BENDAT, J.S. and   Measurement and Analysis of Random Data.
PIERSOL, A.G.:   John Wiley & Sons, Inc. New York 1966.

BROCH, J.T.:   Automatic Recording of Amplitude Density Curves. Brüel & Kjær Techn. Rev. No. 4 — 1959.

BROCH, J.T.:   Effects of Spectrum Non-Linearities upon the Peak Distribution of Random Signals. Brüel & Kjær Techn. Rev. No. 3 — 1963.

BROCH, J.T.:   Random Vibration of Some Non-Linear Systems. Brüel & Kjær Techn. Rev. No. 3 – 1964.

CAUGHEY, T.K.:   Derivation and Application of the Fokker-Planck Equation to Discrete Non-Linear Dynamic Systems Subjected to White Random Excitation. J.A.S.A., Vol. 35. Nov. 1963.

CHUANG, K.:   A study of Non-linear Systems with Random Inputs. Ph. D. Thesis. University of Michigan, U.S.A. 1958.

CRANDALL, S.H. et al.: Random Vibration II. The M.I.T. Press, U.S.A. 1963.

CRANDALL, S.H.:   Random Vibration of Systems with Non-linear Restoring Forces. Presented at the International Symposium on Non-linear Oscillators. Kiev, U.S.S.R. Sept. 1961.

CRANDALL, S.H.:   The Envelope of Random Vibration of a Lightly-Damped Non-linear Oscillator. A.F.O.S.R. – M.I.T. – 201.

CRANDALL, S.H.:   Random Vibration of a Non-linear System with Set-up Spring. J. Appl. Mech. Vol. 29. Nov. 1962.

CRANDALL, S.H.:   Zero Crossings, Peak and other Statistical Measures of Random Responses. J.A.S.A., Vol. 35. Nov. 1963.

KHABBAZ, G.R.:   On Random Vibrations of Systems with Non-linear Damping. Sc. D. Thesis, Dept. of Mech. Engrg. M.I.T. U.S.A. July 1962.

KLEIN, G.H.:   Random Excitation of a Non-linear System with Tangent Elasticity Characteristics. Master's Thesis, School of Engineering U.C.L.A., U.S.A. 1963.

266

LYON, R.H.:   On the Vibration Statistics of a Randomly
                     Excited   Hard-Spring   Oscillator.   J.A.S.A.,
                     Vol. 32. 1960.

LYON, R.H.:   On the Vibration Statistics of a Randomly Hard
                     Spring Oscillator II J.A.S.A., Vol. 33. 1961.

POWELL, A.:   On the Fatigue Failure of Structure Due to
                     Vibrations Excited by Random Pressure Fields.
                     J.A.S.A., Vol. 30. 1958.

RICE, S.O.:   Mathematical Analysis of Random Noise. Bell
                     System Techn. Journal 23 (1944) and 24 (1945).
                     Also contained in N. Wax: Selected Papers on
                     Noise and Stochastic Processes. Dover Publica-
                     tions 1954.

APPENDICES

Appendix A

On the Statistical Interpretation of the RMS-value

In conjunction with the brief discussion carried out in Chapter 2, section 2.2, on the probabilistic description of random vibration signals it might be of considerable interest to relate the concept of the signal RMS-value to this kind of data.

The definition of *probability density* given in section 2.2

$$p(x) = \lim_{\Delta x \to 0} \frac{P(x) - P(x + \Delta x)}{\Delta x}$$

immediately leads to the following expression for the *probability* of finding instantaneous amplitude values within the (small) amplitude interval, Δx:

$$P(x) - P(x + \Delta x) = P(x; x + \Delta x) = \int_{x}^{x + \Delta x} p(x) \, dx$$

When x is a function of time as indicated in Fig.A.1, then

$$P(x; x + \Delta x) = \int_{x}^{x + \Delta x} p(x) \, dx = \frac{\Sigma \Delta t_n}{T} = \frac{\Delta t}{T}$$

Defining now the statistical quantity

$$\sigma^2 = \int_{-\infty}^{\infty} x^2 \, p(x) \, dx$$

this may be expressed as follows:

$$\sigma^2 = \int_{-\infty}^{\infty} x^2 \, p(x) \, dx = \lim_{\Delta x \to 0} \sum_{-\infty}^{\infty} x^2 \, P(x; x + \Delta x) =$$

$$= \lim_{\Delta t \to 0} \sum_{o}^{T} x^2 \frac{\Delta t}{T} = \int_{o}^{T} \frac{x^2}{T} \, dt = \frac{1}{T} \int_{o}^{T} x^2 \, dt$$

σ^2 is, in the literature on statistics, commonly termed *variance* and the square-root of the variance is called the *standard deviation*, σ. However,
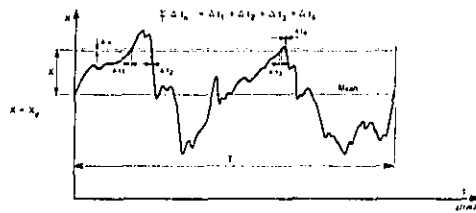
Fig.A.1. Example of a stationary random time function (vibration)

when the statistical phenomenon being studied is a stationary time-function
as shown in Fig.A.1, then

$$\sigma = \sqrt{\frac{1}{T} \int_0^T x^2 (t) \, dt}$$

which is nothing but the expression used in engineering dynamics for the
signal *RMS-value*. Thus, besides being related to the power involved in the
process, the RMS-value is also directly related to the process statistics. This
may be best appreciated by considering the fact that most probability
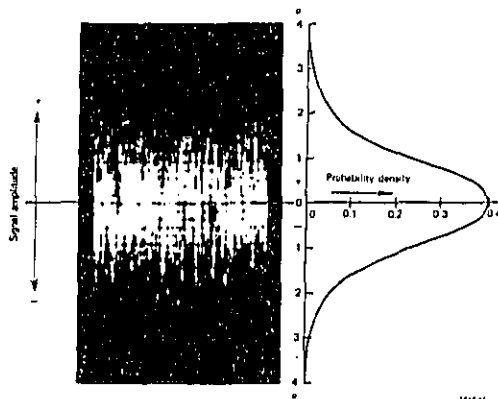
Fig.A.2. Illustration of the relationship between the instantaneous magnitude values in a Gaussian random vibration signal and the Gaussian probability density curve

269

density curves are expressed in terms of standard deviations (RMS-devia-tions), see also Fig.2.9.

Finally, Fig.A.2 illustrates the relationship between the instantaneous amplitude values in a Gaussian random vibration signal and the Gaussian probability density curve.

Appendix B

Response versus Excitation Characteristics for Linear Single Degree-of-Freedom Systems

In Chapter 3, section 3.1, the differential equation of motion for a *force-excited*, linear, single degree-of-freedom system was formulated (see also Fig.3.1b) and Fig.B.1a) below):

$$m \frac{d^2x}{dt^2} + c \frac{dx}{dt} + kx = f(t)$$
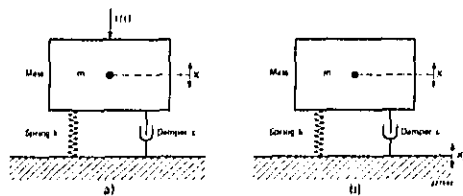
Fig.B.1. Models of a single degree-of-freedom system
   a) System excited by a force acting upon the mass
   b) System excited by motion of the foundation

By Fourier transformation it was shown, furthermore, that the displace-ment response, x, of the mass, m, to a sinusoidal exciting force can be written:

$$x = H(\omega) F_0 e^{j\omega t}$$

where

$$H(\omega) = \frac{1/m}{\omega_0^2 - \omega^2 + j \frac{\omega_0}{Q} \omega}$$

$H(\omega)$ was termed the *complex frequency response function.*

Remembering that $\omega_o = \sqrt{\dfrac{k}{m}} = 2\pi f_o$ the complex frequency response function can be rearranged to yield

$$H(f) = \frac{1}{k\left[1 - (\frac{f}{f_o})^2\right] + \frac{j}{Q}(\frac{f}{f_o})}$$

or

$$|H(f)| = \frac{1}{k\sqrt{\left[1 - (\frac{f}{f_o})^2\right]^2 + \frac{1}{Q^2}(\frac{f}{f_o})^2}}$$

$$\varphi(f) = \tan^{-1}\frac{1}{Q(\frac{f_o}{f} - \frac{f}{f_o})}$$

where $|H(f)|$ is the absolute value of the displacement frequency response function and

$\varphi(f)$ is the *phase lag* between the displacement of the mass, m, and the exciting force.

By utilizing the relationships

$$v(t) = \frac{dx}{dt} \text{ and } a(t) = \frac{d^2x}{dt^2}$$

the velocity and acceleration frequency response functions can be readily found. The results are tabulated below and the corresponding functions are graphically illustrated in Fig.B.2.

Force-excited, linear, single degree-of-freedom system	
Response quantity	Frequency response function
Displacement of mass, m, Fig.B.1a)	$H_x(\omega) = \dfrac{1}{m(\omega_o{}^2 - \omega^2 + j\frac{\omega_o}{Q}\omega)}$
Velocity of mass, m, Fig.B.1a)	$H_v(\omega) = \dfrac{j\omega}{m(\omega_o{}^2 - \omega^2 + j\frac{\omega_o}{Q}\omega)}$
Acceleration of mass, m, Fig.B.1a)	$H_a(\omega) = \dfrac{-\omega^2}{m(\omega_o{}^2 - \omega^2 + j\frac{\omega_o}{Q}\omega)}$

271

If the excitation of the system is not a force, but a *motion of the foundation* Fig.B.1b) a large number of response versus excitation functions can be formulated. The response of interest may, for instance, be the absolute motion of the mass, m, or it may be the relative motion between the mass and the foundation (the loading on the spring element).

Response versus excitation functions for the absolute *motion of the mass* are tabulated below.

Response Quantity, Fig.B.1b)	Excitation Quantity Fig.B.1b)		
	Displacement	Velocity	Acceleration
Displacement $x(t)$	$\|H(f)\| = \dfrac{D_1}{D_2}$	$\|H(f)\| = \dfrac{D_1}{2\pi f D_2}$	$\|H(f)\| = \dfrac{D_1}{4\pi f^2 D_2}$
Velocity $v_x(t)$	$\|H(f)\| = \dfrac{2\pi f D_1}{D_2}$	$\|H(f)\| = \dfrac{D_1}{D_2}$	$\|H(f)\| = \dfrac{D_1}{2\pi f D_2}$
Acceleration $a_x(t)$	$\|H(f)\| = \dfrac{4\pi f^2 D_1}{D_2}$	$\|H(f)\| = \dfrac{2\pi f D_1}{D_2}$	$\|H(f)\| = \dfrac{D_1}{D_2}$

where
$$D_1 = \sqrt{1 + \frac{1}{Q^2}\left(\frac{f}{f_0}\right)^2}$$

and
$$D_2 = \sqrt{\left[1 - \left(\frac{f}{f_0}\right)^2\right]^2 + \frac{1}{Q^2}\left(\frac{f}{f_0}\right)^2}$$

Similarly response versus excitation functions for the *relative motion between* the mass and the foundation can be tabulated:

Response Quantity, Fig.B.1b)	Excitation Quantity Fig.B.1b)		
	Displacement, $x_0(t)$	Velocity, $v_{x0}(t)$	Acceleration, $a_{x0}(t)$
Relative Displacement $x(t) - x_0(t)$	$\|H(f)\| = \dfrac{4\pi^2 f^2}{4\pi^2 f_0^2 D_2}$	$\|H(f)\| = \dfrac{2\pi f}{4\pi^2 f_0^2 D_2}$	$\|H(f)\| = \dfrac{1}{4\pi^2 f_0^2 D_2}$
Relative Velocity $v_x(t) - v_{x0}(t)$	$\|H(f)\| = \dfrac{8\pi^3 f^3}{4\pi^2 f_0^2 D_2}$	$\|H(f)\| = \dfrac{4\pi^2 f^2}{4\pi^2 f_0^2 D_2}$	$\|H(f)\| = \dfrac{2\pi f}{4\pi^2 f_0^2 D_2}$
Relative Acceleration, $a_x(t) - a_{x0}(t)$	$\|H(f)\| = \dfrac{16\pi^4 f^4}{4\pi^2 f_0^2 D_2}$	$\|H(f)\| = \dfrac{8\pi^3 f^3}{4\pi^2 f_0^2 D_2}$	$\|H(f)\| = \dfrac{4\pi^2 f^2}{4\pi^2 f_0^2 D_2}$

where D_2 has the same meaning as before.

By studying the above tables it is readily noticed that *when one of the desired response versus excitation functions, |H (f)|, has been formulated the other follows immediately by manipulating with the quantity $\omega = 2\pi f$, see also the curves,* Fig.B.2. That this must be so follows immediately from the mathematical relationships between the displacement, velocity and acceleration.[*]
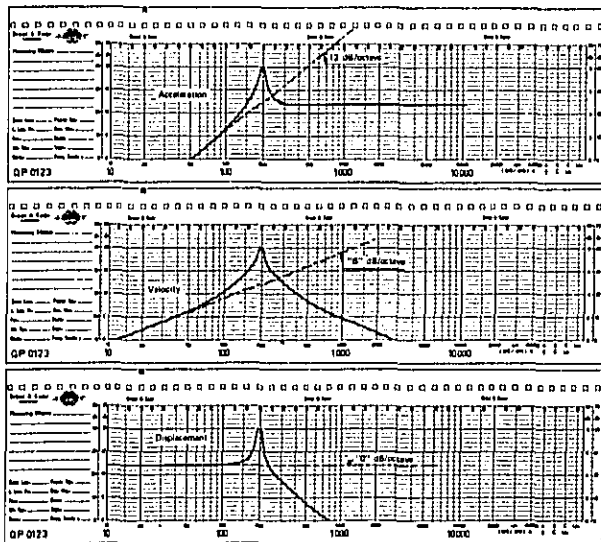
Fig.B.2. *Curves showing the displacement, velocity and acceleration response of a force-excited single degree-of-freedom system. Note that the curves for velocity and acceleration response can be found simply by adding respectively 6 and 12 dB/octave to the displacement response*

---

[*] For the special case $|H (f)| = \dfrac{D_1}{D_2}$. See also Fig.7.2 of the text.

Appendix C

On the Wave-Shape Distortion in Non-Linear Mechanical Systems

While a linear resonance system may act as a signal "wave filter" suppressing possible harmonic distortion *a non-linear resonance system actually produces waveform distortion.* The degree of distortion depends on the type of non-linearity and upon the excitation of the system.

As a first example consider a non-linear, single degree-of-freedom system of the *hardening spring* type, Fig.C.1 (see also Chapter 3, section 3.2). Assume further that the foundation of the system moves sinusoidally at a frequency close to the system resonance. The waveform of the displacement of the mass may then look as shown in Fig.C.2a).
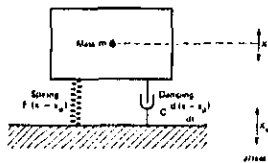
Fig.C.1. Model of a single degree-of-freedom system containing a non-linear spring element

By differentiation of the displacement signal with respect to time one finds that the corresponding velocity of the mass will have a wave-shape as indicated in Fig.C.2b). Finally, a second differentiation yields the acceleration wave-shape shown in Fig.C.2c).

As a second example of non-linear resonance distortion, assume that the system, Fig.C.1 is of the *softening spring* type. Under the same excitation conditions as stated above the motion of the mass then produces wave-shapes as shown in Fig.C.3. Although the wave-shape distortion is here not nearly as heavy as in the hardening spring case it can be clearly noticed.

Wave-shape distortion will also be produced when the non-linearity is situated in the damping element of the system. It seems, however, that *the most pronounced distortion effects are produced by the hardening spring type resonant non-linearities.* This is important to remember as the use of

274

a)

b)

c)   269113
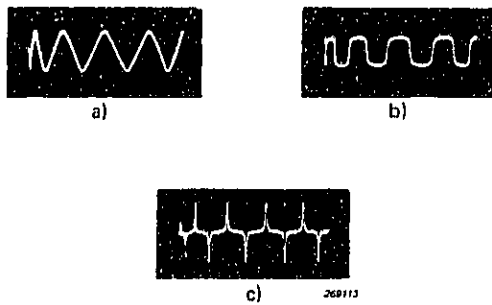
Fig.C.2. Typical resonant wave-shapes for the motion of the mass in a single
degree-of-freedom system containing a hardening spring type stiff-
ness element
a) Displacement
b) Velocity
c) Acceleration

a)

b)

c)   269114
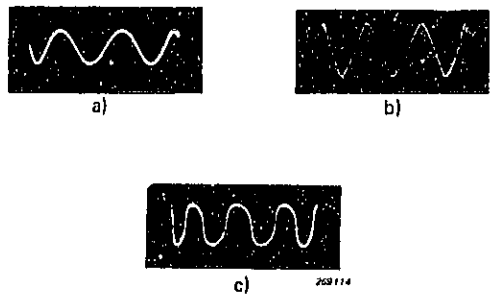
Fig.C.3. Similar to Fig.C.2, the stiffness element in this case being of the
softening spring type
a) Displacement
b) Velocity
c) Acceleration

275

hardening springs in practice is not at all uncommon (Chapter 7, section 7.1).

Before closing this brief discussion on wave-form distortions in mechanical systems it should be mentioned that non-linearities in one or more elements in a multi degree-of-freedom system may cause many "unexpected" effects in the response. As an example of such effects the response of the second mass in a two degree-of-freedom system, Fig.C.4, to
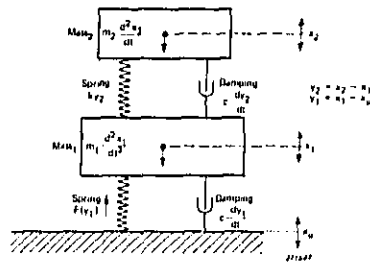
Fig.C.4. Model of a two degrees-of-freedom system containing one non-linear stiffness element of the hardening spring type
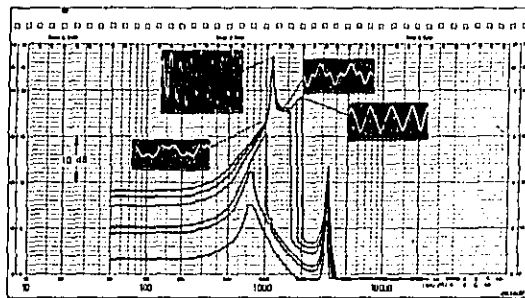
Fig.C.5. Frequency response curves for the motion of the second mass in the system sketched in Fig.C.4. Curves are shown for different levels of excitation of the foundation

276

a sweeping sinusoidal excitation of the foundation is illustrated in Fig.C.6. The sweep was here carried out with increasing frequency and both the change in wave-shape and the "jump" phenomenon, described in section 3.2, are demonstrated.

Appendix D

Connection Between the Fourier Spectrum of a Shock Pulse and the Residual Shock Spectrum

To demonstrate the relationship between the Fourier spectrum of a shock pulse and the undamped residual shock spectrum consider the following.

Fig.D.1 shows an arbitrary acceleration shock amplitude as a function of time.
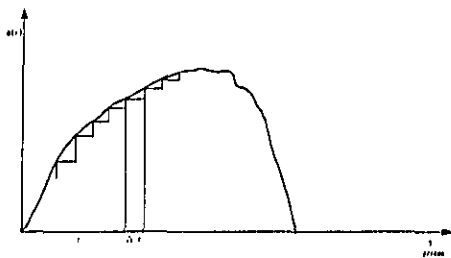
Fig. D. 1. Example of a shock excitation waveform illustrating the principle of superposition in the time domain

Assuming a linear resonance system, its response to such a shock can be calculated as the superposition of the responses to a number of *step* functions approximating the shock pulse.

The change in *excitation velocity* per step is

$$\Delta v \ = a(\tau)\, \Delta \tau$$

where $a(\tau)$ is the value of the acceleration excitation at time τ and $\Delta \tau$ is the width of the step.

277

The partial velocity response at some time t after the step has occurred is

$$\Delta v_R = h(t-\tau)\, a(\tau)\, \Delta\tau$$

where $h(t-\tau)$ is the *velocity response to a unit velocity step*. The total response at a time t after the shock has occurred is then

$$v_R = \Sigma\, h(t-\tau)\, a(\tau)\, \Delta\tau$$

Letting the width of the steps, $\Delta\tau$, approach zero, the sum turns into an integral

$$v_R = \int_{-\infty}^{t} h(t-\tau)\, a(\tau)\, d\tau$$

Now, the velocity response to a unit velocity step can be found by solving the linear differential equation for the system under consideration (single degree-of-freedom, undamped system), utilizing the boundary conditions given by the unit velocity step. The solution is simply:

$$h(t-\tau) = 1 - \cos\left[2\pi f(t-\tau)\right]$$

thus:

$$v_R = \int_{-\infty}^{t}\left[1 - \cos\left(2\pi f(t-\tau)\right)\right]a(\tau)\, d\tau$$

$$= \int_{-\infty}^{t} a(\tau)\, d\tau - \int_{-\infty}^{t}\cos\left[2\pi f(t-\tau)\right]a(\tau)\, d\tau$$

$$v_R = v(t) - \int_{-\infty}^{t} a(\tau)\cos\left[2\pi f(t-\tau)\right]d\tau$$

Letting $t \to \infty$ (residual spectrum) then $v(t) = $ Const. (see Fig.D.1) and

$$v_R = -\int_{-\infty}^{\infty} a(\tau)\cos\left[2\pi f(t-\tau)\right]d\tau + \text{Const.}$$

This is also the expression for the Fourier spectrum of the *acceleration* shock pulse except for the phase (see Chapter 2, section 2.3). Thus

$$\text{Max. } v_R = |F_a(f)|$$

For each frequency component in the response "spectrum" the relationship $a_R = 2\pi f\, v_R$ is valid, whereby

$$S_a(f) = 2\pi f\, |F_a(f)|$$

Appendix E

Electronic Integration of Accelerometer Output Signals

It was stated in Chapter 5, section 5.1 that it does not normally matter which of the three quantities acceleration, velocity or displacement is actually measured in an experimental vibration study, because they are all interrelated by simple differentiating and integrating operations. It was furthermore mentioned that these operations can be readily performed electronically on the output signal from the transducer.

There are, however, certain practical restrictions imposed upon these statements.

Firstly, as will be obvious from the succeeding description of electronic integration, this cannot include zero frequency (D.C), and a certain *low* frequency does therefore always exist in practice below which no integration takes place. Similarly, electronic differentiators must exhibit a certain *upper* frequency limit.

Secondly, electronic differentiators are very sensitive to high frequency noise, and to the high frequency performance of the transducer used for the actual measurement.

Due to the preference given to-day to acceleration sensitive transducers only the problem of electronic *integration* is considered in detail in the following.

If an arbitrary Fourier component, $a = A_0 e^{j\omega t}$, of an acceleration signal spectrum is integrated the result will be the corresponding Fourier component of the corresponding velocity signal spectrum:

$$v = \int a\, dt = \int A_0\, e^{j\omega t}\, dt = \frac{A_0}{j\omega} e^{j\omega t} = V_0\, e^{j\omega t}$$

Thus:

$$V_0 = \frac{A_0}{j\omega} \tag{1}$$

Similarly, a second integration of the acceleration signal component yields the displacement signal component:

$$x = \iint a\, dt\, dt = \int v\, dt = \int V_0\, e^{j\omega t}\, dt = \frac{V_0}{j\omega} e^{j\omega t} = -\frac{A_0}{\omega^2} e^{j\omega t} = X_0\, e^{j\omega t}$$

279

Thus:

$$X_0 = \frac{V_0}{j\omega} = -\frac{A_0}{\omega^2}$$ (2)

Now, if the output signal from an accelerometer (or rather accelerometer + preamplifier), e_a, is fed to an electronic circuit of the type shown in Fig.E.1, the voltage across the capacitor C, i.e. the circuit output voltage, e_c, is:

$$e_c = \frac{1}{1 + j\omega RC}\, e_a$$

Thus when $\omega RC \gg 1$ then

$$e_c \cong \frac{1}{RC} \times \frac{e_a}{j\omega}$$ (3)

By comparing the expressions (1) and (3) it is readily seen that when e_a represents a particular acceleration signal component then e_c must represent the corresponding velocity signal component, i.e. *an electronic integration has taken place in the network*, Fig.E.1. (The multiplying factor 1/RC is taken care of in the internal calibration of the integrator).
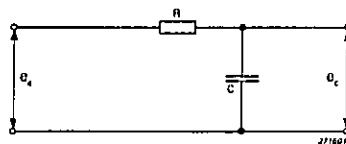
Fig.E.1. Typical electrical integration network of the simple RC-type

The absolute value of the expression

$$\left|\frac{e_c}{e_a}\right| = \left|\frac{1}{1 + j\omega RC}\right|$$

is plotted in Fig.E.2 and demonstrates clearly the meaning of the condition $\omega RC \gg 1$ stated above. It also illustrates the fact that a certain low frequency limit, f_L exists below which no integration takes place. Between f_L and f_T, i.e. in the frequency region around $f_n = 1/2\pi RC$, the signal is only "partly" integrated.

The low frequency limit for "true" integration, f_T, is in the integrators produced by Brüel & Kjær taken to be the frequency at which an integra-

280
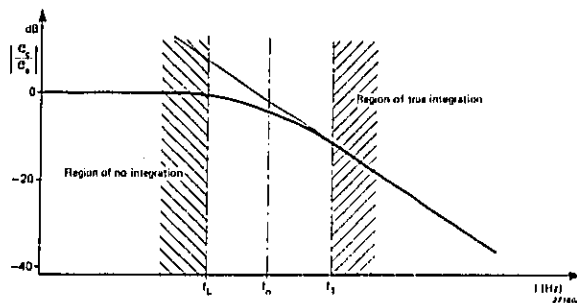
Fig.E.2. Graphical illustration of the function $\left|\dfrac{e_c}{e_a}\right| = \left|\dfrac{1}{1 + j \, \omega \, R_c}\right|$ indicating the frequency region where true integration of the input signal, e_a, takes place

tion error of 1.5 dB ($\approx$ 15%) exists. To ensure true integration of the signal it must therefore not contain frequencies below f_T.

If frequency components lower than f_T exist in the signal to be inte-grated the problem can sometimes be solved by the use of magnetic tape recording and tape speed transformations, see also Chapter 5, section 5.2.

Appendix F

Lowest Measurable Vibration Levels

The lowest vibration signal level that can be usefully detected by a particular measurement system is determined by randomly varying voltages and currents existing in the circuits of the preamplifier. Here the major source of noise is normally the amplifying element, i.e. the transistor (or tube) in the first stage. However, in the measurement of low level signals picked up by accelerometers, additional noise may be introduced, either due to pick-up from nearby electrical or magnetic fields, or by internal noise generation due to cable motion. The primary cause of generated cable noise is the "triboelectric effect" which is, however, minimized by a special treat-ment of the coaxial cables.

281

LOWEST MEASURABLE VIBRATION LEVELS (WORST CASE)

ACCELEROMETERS Type No.	2616 Gain 0 dB L.L.F. 0.13 Hz mg	2623 L.L.F. 0.16 Hz mg	2624 Sensitivity 0.1 mV/pC L.L.F. 0.003 Hz mg	1 mV/pC L.L.F. 0.03 Hz md	10 mV/pC L.L.F. 0.3 Hz ng	2625 Acc 10 m/sec² L.L.F. 1 Hz mg	3 m/sec L.L.F. 1 Hz mm/sec	Velocity 0.3 m/sec L.L.F. 10 Hz μm/sec	0.03 m/sec L.L.F. 100 Hz μm/sec	1000 mm L.L.F. 1 Hz μm	100 mm L.L.F. 3 Hz μm	Displacement 10 mm L.L.F. 10 Hz μm	1 mm L.L.F. 30 Hz nm
WITH 1/3 OCTAVE FILTER 1616 FREQUENCY RANGE 2 Hz – 10 kHz						**POSITION 20 dB GAIN**							
4339 4343 8301 8302	0.6	0.4	7	1	0.7	0.4	0.2	10	1.6	30	4	0.2	20
4332 4334	0.13	0.08	1.8	0.2	0.18	0.08	0.05	2	0.3	6	0.8	0.04	4
4333 4335 4340	0.4	0.3	5	0.6	0.5	0.3	0.16	6	0.8	20	2.5	0.13	13
4338	0.06	0.04	0.7	0.1	0.07	0.04	0.02	1	0.15	3	0.4	0.02	2
4344 8303	3	2.2	55	8	5.5	2.2	1.3	50	7	170	20	1	100
4345 8304 8305	1.5	1	18	3	1.8	1	0.6	25	4	80	10	0.5	50
			70	6	1.8								
8306						0.002	0.001	0.2	0.01	0.3	0.03	0.001	0.2
8307	6	6	130	13	6.0	4.5	2.5	100	14	350	40	2	200
LINEAR FREQUENCY RANGE 2 Hz – 42 kHz						**POSITION 0 dB GAIN**							
4339 4343 8301 8302	4	3	35	4	1.5	4	3	300	30	1000	100	10	1000
4332 4334	0.8	0.6	8	1	0.35	1	0.7	70	7	220	22	2.2	220
4333 4335 4340	2.5	2	26	3	1	3	2.3	210	23	720	72	7.2	720
4338	0.4	0.3	3.5	0.4	0.15	0.4	0.3	30	3	100	10	1	100
4344 8303	20	17	280	36	10	25	19	1900	100	6000	600	60	6000
4345 8304 8305	10	8	80	10	4	10	8	800	80	3000	300	30	3000
			320	22	4								
8306						0.008	0.01	1	0.10	25	0.3	0.04	45
8307	35	30	650	50	12	50	40	4000	400	12.000	1200	120	12.000

L.L.F. = Lower Limiting Frequency.
*With 20 Hz High Pass Filter Values are possibly better.
$m = 10^{-3}$
$\mu = 10^{-6}$
$n = 10^{-9}$
$\frac{Signal}{Noise} > 6\ dB$

LOWEST MEASURABLE VIBRATION LEVELS (WORST CASE)

		PREAMPLIFIERS											
		2626	4292 POSITION 20 dB GAIN										
		Sensitivity	Acc.		Velocity					Displacement			
0.1 mm L.L.F. 100 Hz nm	0.01 mm L.L.F. 300 Hz nm	1 V/g L.L.F. 0.3 Hz mg	10 m/sec² L.L.F. 1 Hz mg	3 m/sec L.L.F. 1 Hz mm/sec	0.3 m/sec L.L.F. 10 Hz µm/sec	0.03 m/sec L.L.F. 100 Hz µm/sec	1000 mm L.L.F. 1 Hz µm	100 mm L.L.F. 3 Hz µm	10 mm L.L.F. 10 Hz µm	1 mm L.L.F. 30 Hz nm	0.1 mm L.L.F. 100 Hz nm	0.01 mm L.L.F. 300 Hz nm
2	0.2	0.16	0.6	0.3	15	2.3	45	6	0.3	30	3	0.3
0.4	0.04	0.04	0.12	0.08	3	0.45	10	1.2	0.06	6	0.6	0.06
1.3	0.13	0.12	0.45	0.23	10	1.2	30	3.6	0.2	20	2	0.2
0.2	0.02	0.016	0.06	0.03	1.5	0.23	4.5	0.6	0.03	3	0.3	0.03
10	1	1.2	3.3	20	75	10	750	30	1.5	150	15	1.5
5	0.5	0.4	1.5	0.8	40	6	120	15	0.8	60	8	0.6
		0.4										
0.02	0.003	0.002	0.002	0.001	0.2	0.01	0.3	0.03	0.003	0.2	0.02	0.003
20	2	1.1	0.6	4	150	20	600	60	3	300	30	3
POSITION 0 dB GAIN												
100	10	0.9	6	4.5	450	45	1500	150	15	1500	150	15
22	2.2	0.23	1.5	1.0	100	10	330	33	3.3	330	33	3.3
72	7.2	0.84	4.5	3.4	340	34	1100	110	11	1100	110	11
10	1	0.09	0.6	0.45	45	4.5	150	15	1.5	150	15	1.5
600	60	6.6	33	30	3000	300	0000	900	90	9000	900	90
300	30	2	15	11	1100	110	4500	450	45	4500	450	45
		2										
0.9	0.05	0.006	0.006	0.01	1	0.16	2.5	0.3	0.04	4.5	0.5	0.05
1200	120	6	80	60	6000	600	18 000	1800	180	18 000	1800	180

VELOCITY AND DISPLACEMENT VALUES ARE REFERRED TO INPUT AS IF
INTEGRATION WAS CARRIED OUT BEFORE THE AMPLIFIER.

283

The lowest measurable vibration levels have been determined experimentally at Brüel & Kjær for a number of measurement configurations and the results are tabulated above. It should be noted that the figures given represent the "worst cases" and are 5 dB above the "noise floor" (IEC Recommendation 179).

Further details as to the measured spectra are given in "K. Zaveri: Measurements of Lowest Vibration Levels, Brüel & Kjær Techn. Rev. 1 – 1970, p. 31 – 38".

Appendix G

Frequency Analysis of Shock Pulses

In Chapter 2, section 2.3 the frequency (Fourier) spectra of various shock pulses were illustrated. These spectra were obtained theoretically by applying the Fourier transform

$$F(f) = \int_{-\infty}^{\infty} f(t)\, e^{-j\omega t}\, dt$$

to the shock pulse time function. Now, how could such spectra be measured experimentally?

To obtain an answer to this question let the pulse considered be applied to a very narrow band filter centered at the frequency f_o, Fig.G.1. If the filter is "ideal" it will only transmit frequency components inside the filter pass-band, Δf, as indicated in the figure. (Here the Fourier Spectrum of a rectangular pulse is used as example).

It is clear that what is measured at the output of the filter must be directly related to that part of the pulse frequency spectrum which is inside Δf, i.e. it must be a measure of the pulse Fourier transform (spectrum) value at the frequency f_o. To obtain the appropriate analytical relationship between the filter output signal and the Fourier spectrum value use can be made of the inverse Fourier transform:

$$f(t) = \int_{-\infty}^{\infty} F(f)\, e^{j\omega t}\, df$$

For the case of a rectangular pulse and an "ideal" very narrow band filter the following expression is then obtained for the filter output signal:

284
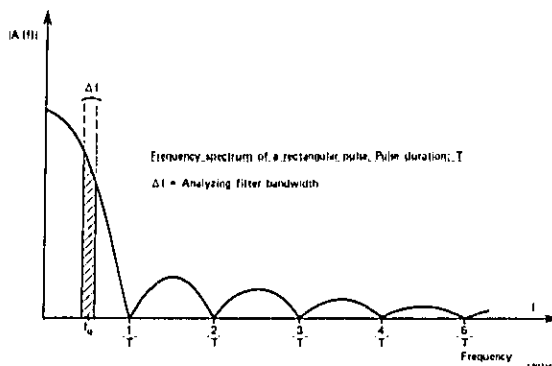
Fig.G.1. Ilustration of narrow band filtering of the Fourier spectrum produced by a rectangular pulse

$$F(t) \approx 2AT \frac{\sin(\pi f_o T)}{\pi f_o T} \Delta f \frac{\sin[(\pi \Delta f (t - t_L)]}{\pi \Delta f (t - t_L)} \cos(2\pi f_o t)$$

where

A = Height of the rectangular pulse
T = Impulse duration
f_o = Center frequency of the narrow filter
Δf = Filter bandwidth
t_L = Transmission time of the filter (depends on the filter phase-shift).

This expression is plotted graphically in Fig.G.2.

From the figure it can be seen that as long as the filter center frequency, f_o, remains unchanged the output signal consists of a rapidly varying "carrier signal" ($\cos 2\pi f_o t$) enveloped by the function:

$$2AT = \frac{\sin(\pi f_o T)}{\pi f_o T} \Delta f \frac{\sin[(\pi \Delta f (t - t_L)]}{\pi \Delta f (t - t_L)}$$

The maximum of this function occurs when $t = t_L$ and is:

$$F(t)_{max} = 2AT \frac{\sin(\pi f_o T)}{\pi f_o T} \Delta f$$

285
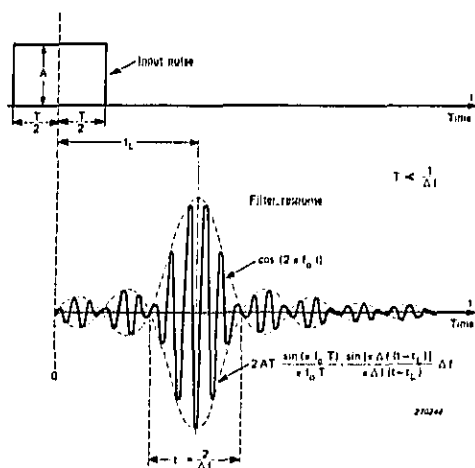
Fig.G.2. Response of an "ideal" narow band filter to a rectangular pulse

As the analytical expression for the Fourier transform (spectrum) value of a rectangular pulse at the frequency is:

$$F(f_o) = AT \frac{\sin(\pi f_o T)}{\pi f_o T}$$

then

$$F(t)_{max} = 2 F(f_o) \Delta f$$

Thus by measuring the maximum (peak) value of the filter output signal $(F(t)_{max})$ this is related to the theoretical Fourier spectrum by the simple relationship:

$$F(f) = \frac{F(t)_{max}}{2 \Delta f}$$

It is therefore a simple matter to obtain an estimate of the Fourier spectrum by measuring the peak value of the output signal from a set of very narrow band filters, centered at closely spaced frequencies (or use may be made of repetitive application of the pulse to a continuously tunable filter).

286

However, not only *peak* measuring devices can be used to relate the output signal from the filter, Fig.G.2, to the Fourier spectrum. Also *average absolute* and *RMS* detection circuits can be utilized provided that their averaging (integration) time and crest-factor capabilities fulfill certain requirements:

Firstly, their averaging (integration) time, T_a, must be longer than the response time of the filter, i.e. $T_a > 2/\Delta f$, see also Fig.G.2. This is necessary to ensure full integration of the filter response.

Secondly, the averaging time must not be *too* long, otherwise limitations in the crest-factor capability of the detector circuit will distort the measured result, as the crest-factor may be defined as $\sqrt{T_a/T_R}$, where T_R is the response time of the filter.

For normal practical detector circuits a requirement of the order of

$$T_a \, \Delta f \approx 3 - 10$$

would constitute a reasonable compromise.

The problem of relating the measured value to the Fourier spectrum is, however, somewhat more complicated in the case of average absolute and RMS measurements than in the use of peak measurements.

A further method of obtaining an estimate of the Fourier spectrum of the pulse is to square and integrate the output from the filter, i.e.:

$$E_{\Delta f} = \int_{-\infty}^{\infty} F^2(t) \, dt$$

By some mathematical computation it can be shown that this integral, for the case of the rectangular pulse, is:

$$E_{\Delta f} = 2 A^2 T^2 \left[\frac{\sin(\pi f_0 T)}{\pi f_0 T} \right]^2 \Delta f$$

That is

$$E_{\Delta f} = \int_{-\infty}^{\infty} F^2(t) \, dt = 2 |F(f)|^2 \Delta f$$

Now, what happens if the filter is no longer a very narrow band filter? Such a case is illustrated in Fig.G.3, and the corresponding filter input and output signals are sketched in Fig.G.4. It is seen that instead of one (oscillating) response transient the filter output signal here consists of two oscillat-
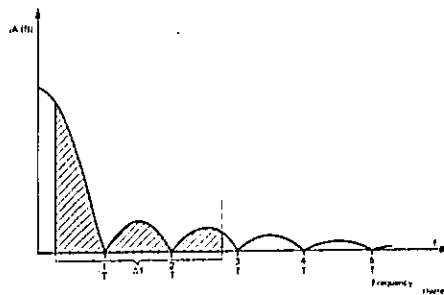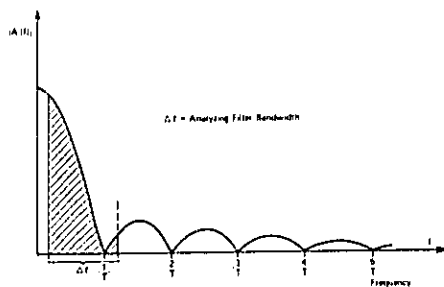
Fig.G.3. Illustration of the effect of broad band filtering
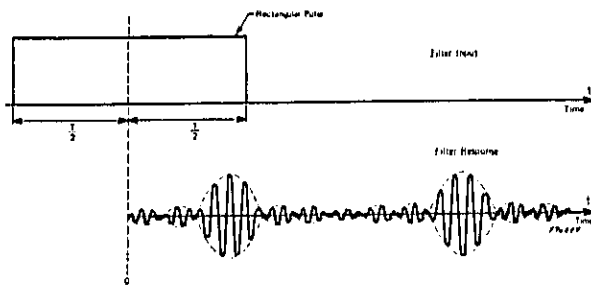
Fig.G.4. Broad-band filter response to a rectangular pulse

ing transients. One of these transients is caused by the response of the filter to the "start" of the original (input) pulse and the other is due to its sudden ceasation. In other words: the filter responds no longer to a pulse, but more or less to two step functions, the distance between the two steps being equal to the original pulse duration. It is also readily seen from Fig.G.3 that the detailed shape of the analytical Fourier spectrum cannot be obtained from measurements with such wide band filters. On the other hand, the squared and integrated output from the filter still gives an indication of the "energy" spectrum value in that:

$$E_{\Delta f} = \int_{-\infty}^{\infty} F^2(t)\, dt = 2 \int_{f_o - \frac{\Delta f}{2}}^{f_o + \frac{\Delta f}{2}} |F(f)|^2\, df$$

The exact shape of the measured "energy" spectrum will, however, in this case depend upon the absolute bandwidths used in the measurements.

Appendix   H

CONVERSION CHARTS, TABLES etc.

Conversion of Length

m	cm	mm	ft	in
1	100	1000	3.281	39.37
0.01	1	10	0.0328	0.3937
0.001	0.1	1	0.00328	0.03937
0.3048	30.48	304.8	1	12
0.0254	2.54	25.4	0.0833	1

Conversion of Velocity

m/s	km/h	ft/m	mph
1	3.6	196.85	2.2369
0.2778	1	54.68	0.6214
$5.08 \cdot 10^{-3}$	$1.829 \cdot 10^{-2}$	1	$1.136 \cdot 10^{-2}$
0.4470	1.6093	88	1

Conversion of Acceleration

g	m/sec^2	cm/sec^2	ft/sec^2	in/sec^2
1	9.81	981	32.2	386
0.102	1	100	3.281	39.37
0.00102	0.01	1	0.0328	0.3937
0.03109	0.3048	30.48	1	12
0.00259	0.0254	2.54	0.0833	1

Conversion of Area

m^2	cm^2	sq ft	sq in	sq yd
1	10^4	10.764	1550	1.196
10^{-4}	1	$1.0764 \cdot 10^{-3}$	0.1550	0.0011
$9.29 \cdot 10^{-2}$	929	1	144	0.1111
$6.452 \cdot 10^{-4}$	6.452	$6.944 \cdot 10^{-3}$	1	0.0008
0.8361	8361	9	1296	1

Conversion of Volume

m³	l = dm³	cu ft	gal (brit)	gal (USA)	cu yd
1	10³	35.315	219.98	264.28	1.308
10^{-3}	1	0.035315	0.21998	0.26428	0.0013
$2.8317 \cdot 10^{-2}$	28.317	1	6.2290	7.4805	0.0370
$4.546 \cdot 10^{-3}$	4.546	0.1605	1	1.2011	0.0059
$3.785 \cdot 10^{-3}$	3.785	0.13368	0.8326	1	0.0050
0.7646	764.56	27	168.16	201.97	1

Conversion of Weight (Mass)

kg	tekma	gram	lbs	oz
1	0.102	1000	2.2046	35.274
9.807	1	9807	21.6205	345.93
10^{-3}	$1.02 \cdot 10^{-4}$	1	$2.205 \cdot 10^{-3}$	$3.527 \cdot 10^{-2}$
0.45359	$4.625 \cdot 10^{-2}$	453.59	1	16
$2.835 \cdot 10^{-2}$	$2.8908 \cdot 10^{-3}$	28.35	$6.25 \cdot 10^{-2}$	1

Conversion of Specific Weight (Mass)

kg/m³	lb/ft³
1	$6.243 \cdot 10^{-2}$
16.0185	1

Conversion of Force

N	kp	lb ft/s²
1	0.102	7.2329
9.807	1	71.0
0.1379	$1.405 \cdot 10^{-2}$	1

Conversion of Pressure

N/m²	mbar	mm H₂O	atm	in WG	psi
1	10^{-2}	0.102	$9.869 \cdot 10^{-6}$	$4.02 \cdot 10^{-3}$	$1.4504 \cdot 10^{-4}$
100	1	10.917	$9.869 \cdot 10^{-4}$	0.402	$1.4504 \cdot 10^{-2}$
9.807	$9.807 \cdot 10^{-2}$	1	$9.678 \cdot 10^{-5}$	$3.937 \cdot 10^{-2}$	$1.4223 \cdot 10^{-3}$
$1.013 \cdot 10^5$	1013	$1.0332 \cdot 10^4$	1	406.77	14.696
249.10	2.491	25.4	$2.453 \cdot 10^{-3}$	1	$3.605 \cdot 10^{-2}$
6908.9	69.089	704.49	$6.805 \cdot 10^{-2}$	27.736	1

Conversion of Work, Energy and Heat

J = Ws	kWh	kpm	kcal	Btu	ft lb
1	$2.778 \cdot 10^{-7}$	0.1020	$2.39 \cdot 10^{-4}$	$9.48 \cdot 10^{-4}$	0.7376
$3.6 \cdot 10^6$	1	$3.6710 \cdot 10^5$	860	3413	$2.655 \cdot 10^6$
9.807	$2.7241 \cdot 10^{-6}$	1	$2.3423 \cdot 10^{-3}$	$9.2948 \cdot 10^{-3}$	7.233
4187	$1.163 \cdot 10^3$	427	1	3.9685	3087.4
1.055	$2.93 \cdot 10^4$	107.59	0.25198	1	777.97
1.3558	$3.766 \cdot 10^{-7}$	0.1383	$3.239 \cdot 10^{-4}$	$1.285 \cdot 10^{-3}$	1

Conversion of Power

kW	kpm/s	hk	kcal/h	ft lb/s	hp
1	102	1.36	860	738	1.34
$9.81 \cdot 10^{-3}$	1	$1.33 \cdot 10^{-2}$	8.44	7.23	$1.32 \cdot 10^{-2}$
0.735	75	1	632	542	0.986
$1.16 \cdot 10^{-3}$	0.119	$1.58 \cdot 10^{-3}$	1	0.858	$1.56 \cdot 10^{-3}$
1.36	0.138	$1.84 \cdot 10^{-3}$	1.17	1	$1.82 \cdot 10^{-3}$
0.745	76	1.014	642	550	1
$2.93 \cdot 10^{-4}$	$2.99 \cdot 10^{-2}$	$3.99 \cdot 10^{-4}$	0.252	0.216	$3.93 \cdot 10^{-4}$
3.52	35.9	0.479	3024	259	0.471

Temperature:

$$F = \frac{9}{5}C + 32 \qquad C = \frac{5}{9}(F - 32)$$

Single Degree of Freedom System

M = mass (kg)
K = Stiffness (Newt/m)

$$\omega_o = \sqrt{\frac{K}{M}} = 2\pi \times \text{resonant frequency}$$

$$\omega_o = \sqrt{\frac{g}{\Delta_{st}}} \text{ where } \Delta_{st} = \text{static deflection of the mass.}$$

For Single Frequency (Sinusoidal) Vibration

Acceleration	Velocity	Displacement
$a \cos \omega t$	$\frac{1}{\omega} a \sin \omega t$	$-\frac{1}{\omega^2} a \cos \omega t$
$-\omega v \sin \omega t$	$v \cos \omega t$	$\frac{1}{\omega} v \sin \omega t$
$-\omega^2 d \cos \omega t$	$-\omega d \sin \omega t$	$d \cos \omega t$

RMS Values

A	A/ω	A/ω^2
ωV	V	V/ω
$\omega^2 D$	ωD	D

293

Frequency, Acceleration, Velocity, Displacement Nomograph (RMS-values)

Velocity, Displacement and Acceleration, RMS values

Frequency
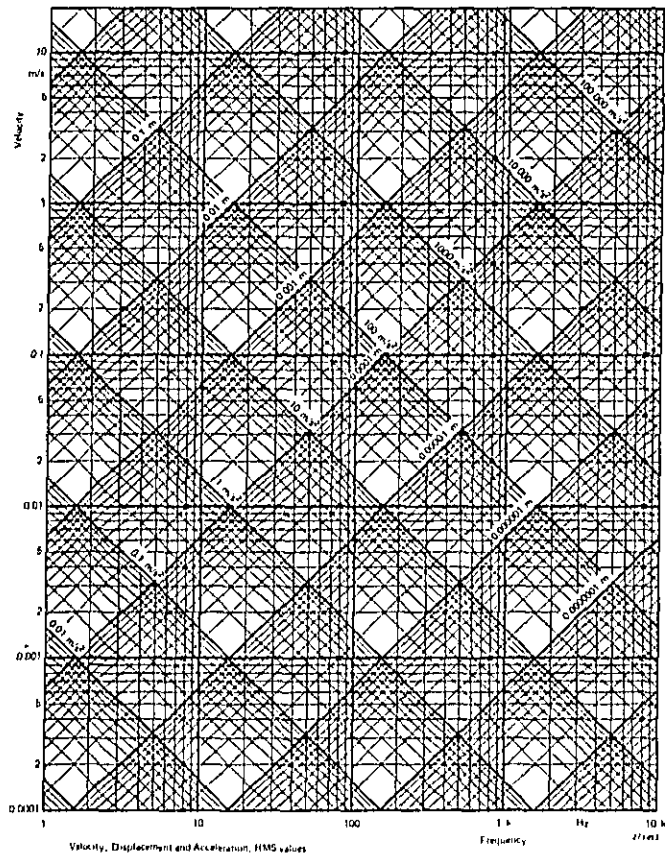
Appendix I

On the Use of Decibels

Modern day engineering requires that accurate measurements are made over wide dynamic ranges.

When the dynamic range considered covers more than one or two decades the graphical presentation of the measured results to linear scales often becomes impractical. The major reason for this is that the accuracy of the graph near the zero axis becomes extremely difficult to interprete. A commonly used solution to the problem is then to present the data in terms of *logarithmic scales*. One such logarithmic scale which is becomming increasingly popular in various fields of engineering is the *decibel (dB) scale*. Although the decibel scale originates from transmission line theory and telephone engineering it is at present widely used not only in the general field of electronic engineering but also in the fields of sound and vibration engineering.

The original definition of the decibel is based on *power ratios:*

$$dB = 10 \log_{10} \left(\frac{W}{W_o}\right)$$

where W_o is a reference power. However, as the power measured across a certain impedance is related to the square of the force acting upon this impedance, Z, a more commonly used definition is

$$dB = 10 \log_{10} \left(\frac{F^2/Z}{F_o^2/Z}\right) = 20 \log_{10} \left(\frac{F}{F_o}\right)$$

where F and F_o are the RMS (root mean square) values of the forces.

Actually, *as long as the measurements are related to one and the same impedance the decibel-notation in the form* $20 \log_{10} (X/X_o)$ *may be used as a conveninet relative magnitude scale for a variety of quantities*, not only forces. X may, for instance, be an RMS displacement, a velocity or an acceleration. X_o, however, must always be a reference quantity of the same type as X. That is when X represents a displacement then X_o represents a reference displacement, and when X represents an acceleration then X_o represents a reference acceleration.

A useful application of the decibel scale is evident in the frequency analysis of mechanical vibrations where large changes in amplitudes occur at

295

,resonance. The use of decibels (dB) compresses a range of displacement or acceleration magnitudes of $1:1000$ to $0-60\,dB$, at the same time attaining constant relative accuracy in the graphical presentation. A further consequence that arises from the decibel scale is that multiplicative factors become additive terms in their logarithmic equivalents.

Also, when the ratio X/X_o is smaller than 1.0 the logarithm to the base ten of the ratio, and thus the decibel value, becomes negative. In the table given below only ratios X/X_o larger than one have been considered. The same table can, however, also be used in cases where X/X_o is smaller than one remembering that $20\log_{10}(\frac{X}{X_o}) = 20\log_{10}(\frac{1}{X_o/X}) = -20\log_{10}(\frac{X_o}{X})$

i.e. by finding the decibel value for the *inverse ratio* $(\frac{X_o}{X})$ and assigning to it a negative value.

Example

$$\frac{X}{X_o} = 0.5$$

As $\frac{X}{X_o}$ is smaller than one it is necessary to calculate the inverse ratio:

$$\frac{X_o}{X} = \frac{1}{0.5} = 2$$

From the table the corresponding decibel value is found to be 6.021 dB, and because of the inverting operation the actual decibel value is −6.021.

To find X/X_o when the decibel value is given, the nearest dB-value is sought in the table and the corresponding ratio read off the left hand and top columns.

Examples

a) *Find the ratio corresponding to 3.5 dB.*
   From the table it is seen that the nearest dB-value tabulated is 3.522, corresponding to a ratio of 1.5.

b) *Find the ratio corresponding to −3 dB.*
   The nearest dB-value given in the table is 2.984 corresponding to a ratio of 1.41. However, as the dB-value stated above has a negative sign it is necessary to invert the ratio 1.41, i.e. −3 dB corresponds to a ratio of $\frac{1}{1.41} = 0.706$.

Table of Ratio-to-Decibel Conversion

$\left(\dfrac{x}{x_0}\right)$	.00	.01	.02	.03	.04	.05	.06	.07	.08	.09
1.0	.000	.086	.172	.257	.341	.424	.506	.588	.668	.749
1.1	.828	.906	.984	1.062	1.138	1.214	1.289	1.364	1.438	1.511
1.2	1.584	1.656	1.727	1.798	1.868	1.938	2.007	2.078	2.144	2.212
1.3	2.279	2.345	2.411	2.477	2.542	2.607	2.671	2.734	2.798	2.860
1.4	2.923	2.984	3.046	3.107	3.167	3.227	3.287	3.346	3.405	3.464
1.5	3.522	3.580	3.637	3.694	3.750	3.807	3.862	3.918	3.973	4.028
1.6	4.082	4.137	4.190	4.244	4.297	4.350	4.402	4.454	4.506	4.558
1.7	4.609	4.660	4.711	4.761	4.811	4.861	4.910	4.959	5.008	5.057
1.8	5.105	5.154	5.201	5.249	5.296	5.343	5.390	5.437	5.483	5.529
1.9	5.575	5.621	5.666	5.711	5.756	5.801	5.845	5.889	5.933	5.977
2.0	6.021	6.064	6.107	6.150	6.193	6.235	6.277	6.319	6.361	6.403
2.1	6.444	6.486	6.527	6.568	6.608	6.649	6.689	6.729	6.769	6.809
2.2	6.848	6.888	6.927	6.966	7.008	7.044	7.082	7.121	7.159	7.197
2.3	7.235	7.272	7.310	7.347	7.384	7.421	7.458	7.495	7.532	7.568
2.4	7.604	7.640	7.676	7.712	7.748	7.783	7.819	7.854	7.889	7.924
2.5	7.959	7.993	8.028	8.062	8.097	8.131	8.165	8.199	8.232	8.266
2.6	8.299	8.333	8.366	8.399	8.432	8.465	8.498	8.530	8.563	8.595
2.7	8.627	8.650	8.691	8.723	8.755	8.787	8.818	8.850	8.881	8.912
2.8	8.943	8.974	9.005	9.036	9.066	9.097	9.127	9.158	9.188	9.218
2.9	9.248	9.278	9.308	9.337	9.367	9.396	9.426	9.455	9.484	9.513
3.0	9.542	9.571	9.600	9.629	9.657	9.686	9.714	9.743	9.771	9.799
3.1	9.827	9.855	9.883	9.911	9.939	9.966	9.994	10.021	10.049	10.076
3.2	10.103	10.130	10.157	10.184	10.211	10.238	10.264	10.291	10.317	10.344
3.3	10.370	10.397	10.423	10.449	10.475	10.501	10.527	10.553	10.578	10.604
3.4	10.630	10.655	10.681	10.706	10.731	10.756	10.782	10.807	10.832	10.857
3.5	10.881	10.906	10.931	10.955	10.980	11.005	11.029	11.053	11.078	11.102
3.6	11.126	11.150	11.174	11.198	11.222	11.246	11.270	11.293	11.317	11.341
3.7	11.364	11.387	11.411	11.434	11.457	11.481	11.504	11.527	11.550	11.573
3.8	11.596	11.618	11.641	11.664	11.687	11.709	11.732	11.754	11.777	11.799
3.9	11.821	11.844	11.866	11.888	11.910	11.932	11.954	11.976	11.998	12.019
4.0	12.041	12.063	12.085	12.106	12.128	12.149	12.171	12.192	12.213	12.234
4.1	12.256	12.277	12.298	12.319	12.340	12.361	12.382	12.403	12.424	12.444
4.2	12.465	12.486	12.506	12.527	12.547	12.568	12.588	12.609	12.629	12.649
4.3	12.669	12.690	12.710	12.730	12.750	12.770	12.790	12.810	12.829	12.849
4.4	12.869	12.889	12.908	12.928	12.943	12.967	12.987	13.006	13.026	13.045
4.5	13.064	13.084	13.103	13.122	13.141	13.160	13.179	13.198	13.217	13.236
4.6	13.255	13.274	13.293	13.312	13.330	13.349	13.368	13.386	13.405	13.423
4.7	13.442	13.460	13.479	13.497	13.516	13.534	13.552	13.570	13.589	13.607
4.8	13.625	13.643	13.661	13.679	13.697	13.715	13.733	13.751	13.768	13.786
4.9	13.804	13.822	13.839	13.857	13.875	13.892	13.910	13.927	13.945	13.962
5.0	13.979	13.997	14.014	14.031	14.049	14.066	14.083	14.100	14.117	14.134
5.1	14.151	14.168	14.185	14.202	14.219	14.236	14.253	14.270	14.287	14.303
5.2	14.320	14.337	14.353	14.370	14.387	14.403	14.420	14.436	14.453	14.469
5.3	14.486	14.502	14.518	14.535	14.551	14.567	14.583	14.599	14.616	14.632
5.4	14.648	14.664	14.680	14.696	14.712	14.728	14.744	14.760	14.776	14.791
5.5	14.807	14.823	14.839	14.855	14.870	14.886	14.902	14.917	14.933	14.948
5.6	14.964	14.979	14.995	15.010	15.026	15.041	15.056	15.072	15.087	15.102
5.7	15.117	15.133	15.148	15.163	15.178	15.193	15.208	15.224	15.239	15.254
5.8	15.269	15.284	15.298	15.313	15.328	15.343	15.358	15.373	15.388	15.402
5.9	15.417	15.432	15.446	15.461	15.476	15.490	15.505	15.519	15.534	15.549
6.0	15.563	15.577	15.592	15.606	15.621	15.635	15.649	15.664	15.678	15.692
6.1	15.707	15.721	15.735	15.749	15.763	15.778	15.792	15.806	15.820	15.834
6.2	15.848	15.862	15.876	15.890	15.904	15.918	15.931	15.945	15.959	15.973
6.3	15.987	16.001	16.014	16.028	16.042	16.055	16.069	16.083	16.096	16.110
6.4	16.124	16.137	16.151	16.164	16.178	16.191	16.205	16.218	16.232	16.245

Ratio $\left(\frac{x}{y_t}\right)$	.00	.01	.02	.03	.04	.05	.06	.07	.08	.09
6.5	16.258	16.272	16.285	16.298	16.312	16.325	16.338	16.351	16.365	16.378
6.6	16.391	16.404	16.417	16.430	16.443	16.456	16.469	16.483	16.496	16.509
6.7	16.521	16.534	16.547	16.560	16.573	16.586	16.599	16.612	16.625	16.637
6.8	16.650	16.663	16.676	16.688	16.701	16.714	16.726	16.739	16.752	16.764
6.9	16.777	16.790	16.802	16.815	16.827	16.840	16.852	16.865	16.877	16.890
7.0	16.902	16.914	16.927	16.939	16.951	16.964	16.976	16.988	17.001	17.013
7.1	17.025	17.037	17.050	17.062	17.074	17.086	17.098	17.110	17.122	17.135
7.2	17.147	17.159	17.171	17.183	17.195	17.207	17.219	17.231	17.243	17.255
7.3	17.266	17.278	17.290	17.302	17.314	17.326	17.338	17.349	17.361	17.373
7.4	17.385	17.396	17.408	17.420	17.431	17.443	17.455	17.466	17.478	17.490
7.5	17.501	17.513	17.524	17.536	17.547	17.559	17.570	17.582	17.593	17.605
7.6	17.616	17.628	17.639	17.650	17.662	17.673	17.685	17.696	17.707	17.719
7.7	17.730	17.741	17.752	17.764	17.775	17.786	17.797	17.808	17.820	17.831
7.8	17.842	17.853	17.864	17.875	17.886	17.897	17.908	17.919	17.931	17.942
7.9	17.953	17.964	17.975	17.985	17.996	18.007	18.018	18.029	18.040	18.051
8.0	18.062	18.073	18.083	18.094	18.105	18.116	18.127	18.137	18.148	18.159
8.1	18.170	18.180	18.191	18.202	18.212	18.223	18.234	18.244	18.255	18.266
8.2	18.276	18.287	18.297	18.308	18.318	18.329	18.340	18.350	18.361	18.371
8.3	18.382	18.392	18.402	18.413	18.423	18.434	18.444	18.455	18.465	18.475
8.4	18.486	18.496	18.506	18.517	18.527	18.537	18.547	18.558	18.568	18.578
8.5	18.588	18.599	18.609	18.619	18.629	18.639	18.649	18.660	18.670	18.680
8.6	18.690	18.700	18.710	18.720	18.730	18.740	18.750	18.760	18.770	18.780
8.7	18.790	18.800	18.810	18.820	18.830	18.840	18.850	18.860	18.870	18.880
8.8	18.890	18.900	18.909	18.919	18.929	18.939	18.949	18.958	18.968	18.978
8.9	18.988	18.998	19.007	19.017	19.027	19.038	19.048	19.056	19.066	19.075
9.0	19.085	19.094	19.104	19.114	19.123	19.133	19.143	19.152	19.162	19.171
9.1	19.181	19.190	19.200	19.209	19.219	19.228	19.238	19.247	19.257	19.266
9.2	19.276	19.285	19.295	19.304	19.313	19.323	19.332	19.342	19.351	19.360
9.3	19.370	19.379	19.388	19.398	19.407	19.416	19.426	19.435	19.444	19.453
9.4	19.463	19.472	19.481	19.490	19.500	19.509	19.518	19.527	19.536	19.545
9.5	19.554	19.564	19.573	19.582	19.591	19.600	19.609	19.618	19.627	19.636
9.6	19.645	19.654	19.664	19.673	19.682	19.691	19.700	19.709	19.718	19.726
9.7	19.735	19.744	19.753	19.762	19.771	19.780	19.789	19.798	19.807	19.816
9.8	19.825	19.833	19.842	19.851	19.860	19.869	19.878	19.886	19.895	19.904
9.9	19.913	19.921	19.930	19.939	19.948	19.956	19.965	19.974	19.983	19.991

Ratio $\left(\frac{x}{x_e}\right)$	0	1	2	3	4	5	6	7	8	9
10	20.000	20.628	21.584	22.279	22.923	23.522	24.082	24.609	25.105	25.575
20	26.021	26.444	26.848	27.235	27.604	27.959	28.299	28.627	28.943	29.248
30	29.542	29.827	30.103	30.370	30.630	30.881	31.126	31.364	31.596	31.821
40	32.041	32.256	32.465	32.669	32.869	33.064	33.255	33.442	33.625	33.804
50	33.979	34.151	34.320	34.486	34.648	34.807	34.964	35.117	35.269	35.417
60	35.563	35.707	35.848	35.987	36.124	36.258	36.391	36.521	36.650	36.777
70	36.902	37.025	37.147	37.266	37.385	37.501	37.610	37.730	37.842	37.953
80	38.062	38.170	38.276	38.382	38.486	38.588	38.690	38.790	38.890	38.988
90	39.085	39.181	39.276	39.370	39.463	39.554	39.645	39.735	39.825	39.913
100	40.000	--	--	--	--	--	--	--	--	--

Appendix J

Standards Related to Vibration and Shock Measurements

Country	Identification of Standard	Contents of Standard	Issuing Institution
C.S.S.R.	CSN 01 1390	Methods of Measurements of mechanical vibrations.	Office for Standards and Measurements. Václavské Námesti 19, Praha 1-Nové Mesto.
	CSN 01 1391	Mechanical vibration measuring equipment. General terminology.	
	CSN 01 1401	Balancing of rotating machine elements. Terminology.	
	CSN 01 1410	Permitted limits for unbalanced solid machine elements.	
	CSN 02 8902	Characteristic data for design of elastic bearing elements.	
	CSN 12 3062	Measurement of noise and vibration from ventilators.	
France	E 90-200	Graph for plotting the characteristics of vibration generator systems.	L'Association Française de Normalisation 19, rue du 4. Septembre, Paris 2ᵉ.
	E 90-210	Characteristics of electro-dynamic vibration generator systems.	
	E 90-211	Characteristics of electro-dynamic vibration generators.	
	E 90-213	Characteristics of power amplifiers for use with electrodynamic vibration generators.	

299

Country	Identification of Standard	Contents of Standard	Issuing Institution
Germany (D.B.R.)	DIN 1311	Schwingungslehre, Bl. 1 Kinematische Begriffe.	Beuth-Vertrieb GmbH. Berlin W 15 und Köln.
	DIN 45661	Schwingungsmessgeräte, Begriffe, Kenngrössen, Störgrössen.	
	DIN 45662	Eigenschaften von Schwingungsmessgeräten. Angaben in Typenblättern.	
	DIN 45664	Ankopplung von Schwingungsmessgeräten und Überprüfung auf Störgrössen.	
	DIN 45665	Schwingstärke von rotierenden elektrischen Maschinen der Baugrössen 80 bis 315. Messverfahren und Grenzwerte.	
	DIN 45666	Schwingstärkemessgerät. Anforderungen.	
	DIN 45667	Klassierverfahren für das Erfassen regelloser Schwingungen.	
	DIN 45668 (Entwurf)	Ankopplung für Schwingungsaufnehmer zur Überwachung von Grossmaschinen.	
	DIN 40046	Klimatische und mechanische Prüfungen für elektrische Bauelemente und Geräte der Nachrichtentechnik. Bl. 7: Prüfung, e: Stossen. Bl. 8: Prüfung, f: Schütteln.	
	DIN 50100	Dauerschwingversuche. Begriffe Zeichen, Durchführung, Auswertung.	

Country	Identification of Standard	Contents of Standard	Issuing Institution
	DIN 51228	Dauerschwingprüfmaschinen. Begriffe, allgemeine Forderungen.	
	DIN 52214	Bauakustische Prüfungen. Bestimmung der dynamischen Steifigkeit von Dämmschichten für schwimmende Böden.	
	VDI 2056	Beurteilungsmasstübe für mechanische Schwingungen von Maschinen.	
	VDI 2057	Beurteilung der Einwirkung mechanischen Schwingungen auf den Menschen.	
Germany (D.D.R.)	TGLO – 1311	Schwingungslehre. 1. Benennungen. 2. Einfache Schwinger. 3. Schwingungssysteme mit endlich vielen Freiheitsgraden.	Amt für Standardisierung der D.D.R. Mohrensstr. 37a, 108 Berlin.
	TGL 22747	Geräte und Einrichtungen zur Messung nichtelektrischer Grössen, Schwingungsmessgeräte.	
Great Britain	BS 2011	Methods for the environmental testing of electronic components and electronic equipment. Part 2 Ea: Shock. Part 2 Eb: Bump. Part 2 F: Vibration.	British Standards Institution, 2 Park Street, London W.1.
	BS 3015	Glossary of terms used in vibration and shock testing.	

Country	Identification of Standard	Contents of Standard	Issuing Institution
	BS 4675	A basis for comparative evaluation of vibration in machinery.	
Japan	JIS C0911 (1960)	Vibration Testing procedures for electric machines and equipment.	Japanese Institute of Standards, Hitotsugi-cho, Akasaka, Minato-ku, Tokyo.
	JIS C0912 (1960)	Shock testing procedures for electric machines and equipment.	
	JIS 1601 (1959)	Vibratile testing methods for automobile accessories.	
	JIS W 6053 (1955)	Shock testing methods for aeronautical instruments.	
Roumania	STAS 7536-66 (1966)	Measurement of vibration from electrical rotating machines.	Oficiul de stat pentru Standarde. Str. Edgar Quinet 6, Bucarest 1.
	STAS 8048-67 (1967)	Measurement of dynamic stiffness of vibration absorbing materials in building acoustics.	
U.S.A.	S2.1-1961	Design, construction and operation of variable-duration, medium-impact, shock testing machine for light-weight equipment.	United States of America Standards Institute, 10 East 40th Street, New York, N.Y. 10016.
	S2.2-1959	Methods for the calibration of shock and vibration pick-ups.	
	S2.4-1960	Method of specifying the characteristics of auxiliary equipment for shock and vibration measurements.	

Country	Identification of Standard	Contents of Standard	Issuing Institution
	S2.5-1962	Recommendations for specifying the performance of vibrating machines.	
	S2.6-1963	Nomenclature and symbols for specifying the mechanical impedance of structures.	
	S2.7-1964	Terminology for balancing rotating machinery.	
	Z 24.21-1957	Methods for specifying the characteristics of pick-ups for shock and vibration measurements.	
U.S.S.R.	GOST 13731-68	Mechanical vibration. General requirements for measurement performances.	Komitet Standartov, Leninsky Prospekt 9b, Moskva M-49.
International	IEC 68-2	Basic Environmental testing Procedures. 68-2-6: Test F_c: Vibration (Sinusoidal) Draft: Test F_d: Random Vibration (wide band). 68-2-27: Test E_a: Shock. 68-2-29: Test E_b: Bump.	International Organization for Standardization, 1. Rene de Varambé, Geneva, Switzerland.
	IEC 184	Methods for specifying the characteristics of electromechanical transducers for shock and vibration measurements.	
	IEC 222	Methods for specifying the characteristics of auxiliary equipment for shock and vibration measurements.	

Country	Identification of Standard	Contents of Standard	Issuing Institution
	Draft ISO No. 1925	Balancing terminology.	
	Draft ISO No. 1940	Balance quality of rotating rigid bodies.	
	Draft ISO No. 2017	Vibration and shock-isolators — specifying characteristics. (Guide for selecting and applying resilient devices).	
	Draft ISO No. 2041	Vibration and shock-terminology.	

Index

307

310